Processing to valorise green biomass side streams to create new food ingredients

Thesis submitted to the University of Nottingham for the degree of Doctor of Philosophy

By Jade Phillips

3/8/2019

Abstract

The aim of the work presented in this thesis was to investigate differing conversion routes on pea biomass in order to make it a functional food ingredient with differing properties than it has in its native form. These would then have differing microstructures and properties to enable the pea biomass to have alternative structures and functions, which mirror starch functions. These modifications were made to formulate a powder-like material similar to that of a flour and to make a dispersion with added fibre, which is to be used within a composite model system. Thereby replacing a high calorific ingredient with a zero digested calorific one.

Firstly the composition of pea biomass was assessed in order to understand the complexity of the compositional matrix.

Then pea biomass was successfully ball milled for different periods of time. Ball milled pea biomass, which had a reduced crystallinity, degree of polymerisation and degradation temperature, was rehydrated and re-crystallised. No glass transitions were determined through thermodynamic measurements. Upon swelling amorphous ball milled pea biomass particulates doubled in hydrated volume. Rheological measurements showed that with various methods of swelling, the rehydrated ball milled pea biomass (at solid contents of 25 % and 33 %), provided visco-elastic properties similar to starch but at much higher solid contents. Methods of swelling showed that once the powder was successfully mixed with water for a period of time, more coherent pastes were apparent, rather than the alternative method of subsequently quenching the powders in water for a 24 hour period, without continuous mixing.

Fibrillated pea biomass was created through a combination of various conversion routes. Fibrillated pea biomass with a mixed diameter of fibrillated masses were engineered through hydrothermal and various chemical/mechanical treatments. The mechanical methods showed that microfluidisation was advantageous for creating a high NFC:MFC, and that sonicated fibres were advantageous for creating a mainly MFC system with larger macro-fibres still present. The chemical pre-treatment of a sodium hydroxide wash successfully reduced the amount of hemicellulose content, however this did not have advantageous yields of MFC/NFC and or properties in terms of rheology and microstructure than without the treatment. Ethanol washes had no effect in reducing the concentrations of polysaccharides and lignin proportionally to the overall composition. These results indicated that other polymers and lignin within plant cell wall materials may have a synergistic effect on the fibrillation of cellulosic materials, with ethanol washed samples having the most desired fibrillated properties, for example producing the greatest expanded structure to be used in a model snack product. As a control Solka floc was successfully fibrillated through the mechanical means, without heat and chemical pre-treatments. These fibrillated masses provided stable dispersions with visco-elastic properties at low solid concentrations of 1 %, within an aqueous dispersion and were shown to be stable. Furthermore, fibrillated samples showed a strong network structure with suspected high reinforcement capabilities through the creation of new structures with varying levels of crystalline fractions.

Ratios of all starch commodities in model snack products were replaced by using modified pea biomass in the form of a ball milled powder and

fibrillated masses, which contained a mixture of fibre diameters and lengths. Results showed that up to 30 % starch commodities could be replaced by pea biomass and the resulting composite would have similar properties of texture, viscosity, fried expansion and structure, but visually aesthetic aspects of the resulting product such as colour were different, with low added biomass concentrations of as much as 10 % starch replacement.

Thereby indicating that valorised pea biomass can successfully be utilised and partially replace starch commodities, benefiting the nutritional content of a composite snack product and provide advantageous health benefits over the traditional snack product.

This thesis is dedicated to my mother and father (Tina and Carl Edwards), who have taught me “The unconceivable is not unachievable”.

Acknowledgements

Firstly, I would like to thank Bill MacNaughtan especially for his help across each section of my thesis in the form of analytical equipment or expertise knowledge. I would also like to thank Joanne Gould, Clive Ford, Charfedinne Ayed and Deepa Agarwal for their aid in both knowledge and use of equipment in these works to do with general food science and fibrillation. I would specifically like to thank Khatija Nawaz, Christine Grainger-Boultby, Dennise Mclean and Craig Sturrock for their expertise and aid in microscopy techniques. Moreover, to thank Val Street and Steven Johnson for their aid in experimentations of TGA and using the Microfluidiser. For statistics assistance, I would like to thank Robert Linforth. For my first initial year of my PhD I would like to thank David Gray, my main supervisor at that time, for his help in nutritional assessments. For general assistance across the course of my PhD in terms of general requirements, I would like to greatly thank Dawn Beatson who has constantly shown to be the most helpful and kind co-worker I could have asked for.

I would also like to thank my best friends within the department also known as the Food Sci Crew for their support and friendship. As well as, many other individuals within the department that I have come across and that have been an imperative support network. As well as other family members and pups.

Lastly and most importantly I would like to thank PepsiCo for sponsoring me and my supervisor Tim Foster who with his knowledge, expertise and patience to teach me, enabled me to accomplish this PhD and gained the understanding of the area that I have today.

List of Publications and Conferences

R. Ibbett, J. Phillips, D. Gray, T.J Foster, Enzyme digestion of pea halum pulp as an approach for upgrading for improved textural and nutritional qualities for food and feed applications. Journal (under review).

J. Phillips, G. Tucker, T.J Foster, D. Gray, Breaking open cells from green waste: An initial step to recover novel ingredients, Centre for Innovative Manufacturing conference, Loughborough. UK, March 30-31, 2016 (Poster presentation).

J. Phillips, W. MacNaughtan, Z. Umar and T.J Foster, The effect of ball milling on the de and re-crystallisation of valorised green biomass, Centre for Innovative Manufacturing conference, Birmingham, UK, March 30-31, 2017 (Oral Presentation).

J. Phillips, W. MacNaughtan, Z. Umar and T.J Foster, Functionalising cellulose waste as a functional food ingredient, L'Oreal and Unesco women in science award ceremony, London, UK, May 04, 2017 (Poster Presentation).

J. Phillips, W. MacNaughtan, Z. Umar and T.J Foster, Functionalising cellulose waste as a functional food ingredient, The 19th Gums and Stabiliser conference for the Food industry, Berlin, Germany, June 27-30, 2017 (Poster Presentation).

J. Phillips, S. Holland, W. MacNaughtan, Z. Umar and T.J Foster, Mechanical amorphisation of cellulosic materials and subsequent recrystallization. EPNOE 5th International Polysaccharide Conference, Jena, Germany, August 20-24, 2017 (Oral Presentation).

J. Phillips, W. MacNaughtan, Z. Umar and T.J Foster, Functionalising cellulose waste as a replacement for high-energy dense ingredients, NYAS/PepsiCo journey through science, New York, America, September 18, 2017 (Poster Presentation).

J. Phillips, W. MacNaughtan, Z. Umar and T.J Foster, Identification and characterisation of Micro-fibrillated cellulose (MFC) from pea fibre food waste, Centre for Innovative Manufacturing conference, Nottingham, UK, March 26-27, 2018 (Oral Presentation).

J. Phillips, W. MacNaughtan, Z. Umar and T.J Foster, Micro-fibrillated cellulosic systems of Pisum sativum, 3rd International EPNOE Junior Scientist, Maribor, Slovenia, May 14-15, 2018 (Oral Presentation).

Table of Contents

Abstract I

Acknowledgements V

List of Publications and Conferences VI

List of Abbreviations and Symbols XIII

Chapter 1 General Introduction 1

1.1 The Food Crisis 1

1.1.1 Food security/sustainability 1

1.1.2 Obesity 6

1.2 Ready to eat snacks 8

1.2.1 Market value/cost efficiency 9

1.2.2 Obtaining and processing of raw ingredients 10

1.3 Potential use of Plant Cell Wall Materials (PCWM) 11

1.3.1 Cellulose 12

1.3.2 Hemicellulose 16

1.3.3 Lignin 18

1.3.4 Pectin 21

1.4 Introduction to the thesis: 23

Chapter 2 Techniques 25

2.1 ^{13}Carbon Cross Polarisation Magic-Angle Spinning Nuclear Magnetic Resonance (^{13}C CP-MAS NMR) 25

2.2 Wide-Angle X-Ray Diffraction (WAXD) 26

2.3 Dynamic Mechanical Analysis (DMA) 27

2.4 Oscillatory Rheology 29
2.5 Micro-Computed Tomography (Micro-CT) 30
2.6 Turbiscan Stability Index (TSI) 30
2.7 Thermogravimetric Analysis (TGA) 31
2.8 Dynamic Vapour Sorption (DVS) 32
2.9 Differential Scanning Calorimetry (DSC) 32
2.10 Statistics used in the experimentation 33
Chapter 3 Composition of raw materials 35
3.1 Introduction 35
3.1.1 Cellulose 38
3.1.2 Hemicellulose 40
3.1.3 Lignin 40
3.1.4 Pectin 42
3.1.5 Starch 43
3.1.6 Protein 44
3.1.7 Lipids 46
3.1.8 Chlorophyll and carotenoids 47
3.1.9 Ash content 48
3.1.10 Aims of this chapter 50
3.2 Materials and methods 51
3.2.1 Materials preparation: 51
3.2.2 Drying and storage 52
3.2.3 Analytical methods 52

3.2.4 Statistics 60
3.3 Results 61
3.3.1 Composition of Pea biomass 61
3.3.2 Cellulose 62
3.3.3 Hemicellulose 64
3.3.4 Lignin 65
3.3.5 Pectin 66
3.3.6 Starch 67
3.3.7 Protein 68
3.3.8 Lipids 69
3.3.9 Chlorophyll and carotenoids 70
3.3.10 Ash 71
3.3.11 Composition of Solka floc 900 72
3.4 Conclusion 73
Chapter 4 Design of Pea Powder Biomass 74
4.1 Introduction 74
4.1.1 Ball milling 74
4.1.2 Properties of Cellulose: Crystallinity, glass transitions and re-crystallisation. 75
4.1.3 Aims of this chapter 80
4.2 Materials and methods 81
4.2.1 Materials 81
4.2.2 Drying and storage 81

4.2.3 Processing methods 82

4.2.4 Analytical methods 83

4.3 Results 89

4.3.1 Water content of Pea Biomass and Ball Milled Pea Biomass… 89

4.3.2 The effects of Ball Milling on Pea Biomass morphology 90

4.3.3 The effects of Ball Milling on the crystallinity of Pea Biomass …… 94

4.3.4 Thermal analysis and DVS of Ball Milled Pea Biomass 99

4.3.5 The effects of rehydration on an amorphous Ball Milled Pea Biomass 107

4.4 Conclusion 119

Chapter 5 The production of Micro-fibrillated cellulose from Pea Biomass……..... 121

5.1 Introduction 121

5.1.1 Introduction to fibrillation 121

5.1.2 Properties of fibrillated materials 125

5.1.3 Treatments to enable/facilitate or improve properties of fibrillated masses 127

5.1.4 Aims of this chapter 132

5.2 Materials and methods 134

5.2.1 Materials 134

5.2.2 Processing methods 134

5.2.3 Storage of MFC/NFC samples 138

5.2.4 Analytical methods 138

5.3 Results 144

5.3.1 Chemical composition of polysaccharides after thermal and chemical treatments 144

5.3.2 Impact of chemical treatment and mechanical disruption method of sonication 148

5.3.3 Impact of differing mechanical disruption methods (Sonication and Microfluidisation) on chemically pre-treated PB (ethyl alcohol washed) 164

5.3.4 Crystallinity of MFC comparing Sonication and Microfluidisation mechanical disruption methods. 178

5.3.5 Impact of different mechanical disruption methods on the rheological properties of MFC/NFC dispersions 180

5.4 Conclusion 188

Chapter 6 Application of Pea Biomass powder and fibrillated mass to model system. 190

6.1 Introduction 190

6.1.1 Starch 190

6.1.2 Potato Starch (PS) and Potato Flakes (PF) 192

6.1.3 Rice Starch (RS) 194

6.1.4 Tapioca Starch (TS) 195

6.1.5 Manufacturing of Snacks 196

6.1.6 Aims of this chapter 200

6.2 Materials and methods 201

6.2.1 Processing parameters chosen to convert Pea Biomass to a functional food ingredient 201

6.2.2 Manufacture of pellet and expanded snack..... 202

6.2.3 Analytical methods 205

6.3 Results..... 211

6.3.1 Rheological measurements of raw materials and composite mix……..... 211

6.3.2 Intermediate and expanded snack product properties..... 225

6.3.3 Rheological properties of Pellets and Expanded Snack Product…..... 240

6.3.4 Calorific content..... 248

6.4 Conclusion..... 251

Chapter 7 Conclusions and Future work 254

Chapter 8 References..... 258

Chapter 9 Appendix 285

List of Abbreviations and Symbols

AOAC	Association of Analytical Chemists
ANOVA	Analysis of Variance
BM	Ball Milling
BMPB	Ball Milled Pea Biomass
BS	Back Scattering
CNS	Cellulose Nano-Crystals
CP-MAS NMR	Cross Polarised Magic Angle Spinning NMR
CLSM	Confocal Laser Scanning Microscopy
CuKα	Copper K alpha -1
DF	Dietary Fibre
DMA	Dynamic Mechanical Analysis
DSC	Differential Scanning Calorimetry
DP	Degree of Polymerisation
DVS	Dynamic Vapour Sorption
E*	Complex modulus
ER	Expansion Ratio
FIB PB	Fibrillated Pea Biomass
G	Guaiacyl

G'	Storage Modulus
G''	Loss modulus
GHG	Greenhouse gas
H	Coumaryl alcohol units of lignin
Hr	Hour
HPB	Hydrothermal treated Pea Biomass
HPLC	High Performance Liquid Chromatography
GS	Gelatinised Starch
K	Geometry constant
LS	Life Sciences
LVE	Linear Viscoelastic
MF	Microfluidiser
MFC	Micro-Fibrillated Cellulose
Micro-CT	Micro-Computed Tomography
n	Number of monomers
η^*	Complex Viscosity
Native PB	Native Pea Biomass
NCW	Cellulose Nano-Whiskers
NFC	Nano Fibrillated Cellulose
NS	Native Starch

2P	2 Passes
4P	4 Passes
6P	6 Passes
PCW	Plant Cell Walls
PCWM	Plant Cell Wall Materials
PF	Potato Flakes
PS	Potato Starch
PSD	Particle Size Distribution
RF	Radio Frequency
RH	Relative Humidity
RO	Reverse Osmosis
RS	Rice Starch
RVA	Rapid Visco Analyser
S	Syringyl
S*	Stiffness Indirect Viscosity
S’	Stiffness Storage Modulus
S’’	Stiffness Loss Modulus
SEM	Scanning Electron Microscopy
SF	Solka Flock
SM	Stir Mixed

Son	Sonication
T	Transmission
TA	Texture Analysis
TEM	Transmission Electron Microscopy
T_g	Glass Transition
TGA	Thermogravimetric Analysis
TS	Tapioca Starch
TSI	Turbiscan Stability Index
UN	Un-stirred
WAXD	Wide Angle X-Ray Diffraction

Chapter 1 General Introduction

1.1 The Food Crisis

We are in a time where food security is threatened by the increasing amount of mouths to feed and future predictions foresee a challenge to produce enough food to feed over 9 billion people by 2050 (Godfray *et al.*, 2010). The planet's population has increased by more than 400 % over the 20th century. Countries currently with the largest populations (over 1 billion) are China and India (The World Bank, 2017) and developed countries are also increasing rapidly. This means growing food demand is set to still escalate for at least another 40 years (Godfray *et al.*, 2010). These calculated assumptions pose the question, "how are we going to feed everyone? ". Moreover, there is an increasing demand from governments and consumers to do this in an environmentally, sustainable manner (European Commission, 2015). There is now a significant need for scientific research focused on how we can sustainably feed this ever-growing population with what we already produce, whilst reducing environmental costs, which greatly impact on the ecosystem of the planet.

1.1.1 **Food security/sustainability**

Food security, is defined as - "when all people, at all times, have access to sufficient, safe, nutritious food to maintain a healthy and active life" (FAO, 2002). The current recommendations for improving food security are to: grow/produce more food; while doing this more efficiently, improving distribution and storage and lastly reduce food waste. However, in the last 50 years alone, world crop production has increased by threefold (FAO,

2013). Over the past few centuries, across the globe, companies and individuals are constantly adapting new techniques and methods, for producing higher quantities of food (Carvalho, 2006). For example, in Kansas (USA) a particular farm is currently harvesting up to 25 acres of wheat an hour and is set to increase this amount (Foley, 2014). Nevertheless, agriculture is one of the largest contributors to global warming via greenhouse gas (GHG) emissions (Foley, 2014). At the world environment summit meeting, in Paris 2015, governments decided to actively reduce GHG emissions and other detrimental, environmental effects worldwide. Therefore, this is a concept that creates a requirement for new manufacturing of the future (European Commission, 2015).

The need for increasing the production of food can also lead to a requirement for an increase in land use, to comply with this. Foley (2014) states that we have already used land roughly the size of South America in order to grow crops and an area the size of Africa to grow livestock. This begs the question: Will we be able to afford to increase food production through agricultural expansion forever? With a worldwide population increase, there will also be a need for more land for housing, schools, fuel production, work/companies and so on. Currently there is 46.5 % of undeveloped land in the world, this includes forests, high mountains, deserts and Tundra (Foley, 2014). Then 38.6 % is currently used for agriculture such as pastureland and cropland than another 14.9 % is occupied by urban area, erosion, logging and other detrimental effects to the planet, that also means it can now not be used for agriculture production (Foley, 2014). The use of fertilisers, pesticides, irrigation and more efficient machines/equipment has all increased in recent years (Carvalho, 2006; Boye and Arcand, 2013). There is only so much that can be done naturally and still be called organic farming. Similarly,

developing countries currently do not have the infrastructure to make amendments, by which to employ such technologies to their crops/livestock production thus improving efficiency of increasing yields (Boye and Arcand, 2013). As a result the answer of growing more, and more efficiently, leads to a lack of confidence to appropriately match foreseeable demands.

Transportation increases the carbon footprint of produce, which is exacerbated by the high demand from the consumer for the produce all year round, instead of it being seasonally sold in supermarkets. As many countries are subjected to specific temperature and climate conditions, we must source particular foods from other countries to meet large-scale needs of the consumer. If, these countries have a particularly low socioeconomic status and poor infrastructure, then this makes it difficult to not waste any produce through transportation/distribution methods (Gustavsson *et al.*, 2011). By means of decay and physical damage (i.e bruising) through the processing and transport stage (Gustavsson *et al.*, 2011), post-harvest loss literature suggests that gentler handling of produce, better conditioning, faster transportation and sufficiently improved storage is required in developing nations (FAO, 1981, Rolle, 2006). Choudhury (2006), highlighted the importance of loss rates in India, with a lack of packing houses and stated examples whereby food was packed in a field and some transported without any packaging at all, excessively damaging the products (Choudhury, 2006). These losses in India equate to 30 % of fresh produce production being lost or wasted through lack of a cold chain (low-cost energy efficient cool storage system). Figure 1 shows a previous (2011) breakdown of food system losses across all sectors of the food chain of all continents and vary in socio-economic status.



***Figure 1 Breakdown of food system losses across all sectors of the food chain of continents with varying socio-economic status* (Gustavsson *et al.*, 2011).**

Previous figures estimated that $\frac{1}{3}$ of all food produced is wasted annually (Gustavsson *et al.*, 2011). Therefore, the most sustainable method of future food production is utilising what we already produce. Food waste and loss occurs across all processes of the Food Supply Chain (FSC). Some losses are unavoidable for example due to climate conditions (such as frost or dry heat) (Gustavsson *et al.*, 2011). On the other hand, most are avoidable for example mainly at a consumer level (such as consumers throwing edible food away due to it surpassing its recommended date of consumption) (Lipinski *et al.*, 2013; Girotto and Alibardi, 2015). When discussing food waste/loss in this literature it will be defined by using a combination of the two following terms:

1) Wholesome edible material intended for human consumption, arising at any point in the FSC that is instead discarded, lost, degraded or consumed by pests (FAO, 1981).

2) As (1), but including edible material that is intentionally fed to animals or is a by-product of food processing diverted away from the human food chain (Stuart, 2009).

Food loss and spoilage are another set of terminologies, which usually refers to a decrease in food quality or quantity, which is deemed unfit for human consumption (Grolleaud, 2002). With such high quantities of produced food being wasted it is clearly the simplest current solution/method of providing enough food to sustain the growing population. Through utilisation and valorisation methods of what we already produce there is potentially no need to produce more and grow more efficiently as a short-term fix for the growing population. As a result optimising what land space we already use, requiring no need to exacerbate more and unnecessarily increase further detrimental

environment impacts. Waste foods, which are nutrient-rich, are potential nutritious sources to be valorised and thereby utilised for those who are malnourished/nutrient deficient. Moreover, for those who are not malnourished the valorised ingredient may additionally provide added health benefits, through consumption, over consuming less nutritious materials. However, in order to transform wasted/lost produce in the form of Plant Cell Wall Materials (PCWM) for the purpose of ingredients they must firstly be converted into having a function within a food matrix. Foster, 2013, suggested four main conversion routes which include; the use of enzymes, thermal, mechanical and chemical treatments, or a combination thereof (Foster, 2013). In which all give differing properties and functionalities, which may also add beneficial factors to a product if used as an ingredient within a formulation/matrix system (Foster, 2013).

1.1.2 **Obesity**

Certain agronomists believe that in order to guarantee food security, nations should aim to supply 130 % of the nutritional requirements, set by the current standards of differing government agencies (Stuart, 2009).This equates to around 2,600-2,700 kcal per person per day. The current recommendations for adults in the United Kingdom (UK) are around 2,000 kcal and 2,500 kcal for women and men per day, respectively (Public Health England, 2016). With these recommendations in mind, it was estimated that consumers within Europe in the year 2000 had over 3,300 kcal available per capita per day (Alexandratos, and Bruinsma, 2012). This, in relevance to the previous statistics mentioned, means that Europe is producing and providing up to 20 % more of what is demanded and 40-50 % more than an individual physically needs (Alexandratos, and Bruinsma, 2012). Having food in such

high quantities and being so readily available, can create easy access of high calorific foods due to competition through companies and of the type of ingredients used.

Table 1 Current and projected calorie intake per day of individuals from differing socio-economic status continents/countries, modified from (Alexandratos and Bruinsma, 2012).

	New historical data			Projections		
	1989/1991	1990/1992	2005/2007	2015	2030	2050
Developing Countries	2429	2433	2619	2740	2860	3000
Developing excluding South Asia	2497	2504	2754	2870	2970	3070
Sub-Saharan Africa	2051	2068	2238	2360	2530	2740
Near East/North America	3003	2983	3007	3070	3130	3200
Latin America and Caribbean	2664	2672	2898	2990	3090	3200
South Asia	2254	2250	2293	2420	2590	2820
East Asia	2487	2497	2850	3000	3130	3220
Developed countries	3288	3257	3360	3390	3430	3490
Average Global intake	2634	2627	2772	2860	2960	3070

Table 1 provides projections for future consumption rates around the globe. The future predictions claim that, per capita, across all continents the amount of calories consumed will escalate. With certain developing regions, for instance East Asia, Caribbean and North Africa, appear to increase at a higher rate than that of developed countries and approach an equivalent amount of calories consumed per capita. Obesity can be linked to an increase in calorie intake on a regular basis and to the types of food commodities consumed for differing socioeconomic statuses (Drewnowski and Specter, 2004; Pickett *et al.*, 2005). An increased consumption of

snacks has repeatedly been shown to cause obesity and excess weight gain in individuals (Zizza, Siega-Riz and Popkin, 2001; Appelhans *et al.*, 2012). Snacks are classed as high-energy dense products due to high and rich starch and fat content, whereas diets that are low-energy dense include the consumption of fruits and vegetables (Martí-Henneberg *et al.*, 1999). Many studies focusing on dietary choices leading to obesity have focused on the sugar and fat content of snacks (Drewnowski and Specter, 2004; Appelhans *et al.*, 2012). With many studies finding a link with obesity to those with low socio-economic status and found high-energy foods to be more affordable (Reidpath *et al.*, 2002; Drewnowski and Specter, 2004). This inverse relationship between energy density and affordable cost suggests “obesity promoting” foods to be prolific across the food supply chain (Drewnowski and Specter, 2004). Considering this difference in energy cost between low and high-energy density foods, an advice to manufacturers and consumers is to replace salty/sweet and fatty foods with fresh vegetables. Though consequently this may come as an unintended economic consequence to the consumer (Drewnowski and Specter, 2004). Therefore, if some of the high-energy dense commodities were replaced with low-energy dense materials in a product, then this would be advantageous to consumers’ health. Moreover, if this was carried out by valorisation of a wasted low-energy dense product, then it would thereby not impinge economically to the consumer or the manufacturer. Moreover, it would be sustainable and advantageous for the environment as it is a by-product.

1.2 Ready to eat snacks

Ready to eat snacks are a food product in a form that is edible without the consumer needing to additionally prepare anything (Collins English Dictionary, 2018) and typically consumed in-between meals (Brennan *et al.*,

2013). Trends have shown a large increase in the consumption of salty snacks over the past two/three decades (Piernas and Popkin, 2010a and 2010b). Crisps have become a large proportion of the salty savoury snack market, which consists of either potato slices, classed as 1st generation crisps, which are either deep fried or baked or, 2nd and 3rd generation crisps, known to be extruded and have an intermediate pellet form (Mishra, 2013); the later savoury snacks are used as the model system snack in this study. Further information on each individual starch commodity and the manufacturing methods used in this study can be found in Chapter 6: Application of Pea Biomass and Fibrillated mass to model system.

1.2.1 **Market value/cost efficiency**

In the last 20 years consumer awareness on the importance of functional foods has increased (Gilbert, 1998; Bogue and Ryan, 2000; Annunziata and Vecchio, 2011, 2013). With the global market of functional foods worth €17.7 billion in 2013 (Sivam *et al.*, 2010) (CAGR U.S. 2017 Statistic, 2017). The global snack food market is projected to grow by 5.8 % between 2017 and 2021 according to CAGR. The latest reports suggest that the growth is mainly from developing countries in the Asia-Pacific (13.7 %) and Eastern European (7.3 %), whilst Latin America is only foreseen to increase by a mere 3.2 % in comparison (FoodExecutive, 2017). Therefore, showing that there is great opportunity and need to improve and create innovative products that allow industry to compete strongly. Moreover, functional foods containing high levels of dietary fiber (DF) and antioxidants are of high demand due to their associative health benefits and protection against non-communicable diseases. This immense increase in demand from developing nations compared to developed nations, leads to a high demand

to manufacturers, as developing nations additionally have the largest populations across the world. Furthermore, food waste and loss can have many negative economic impacts. They represent a wasted investment that can reduce a farmer's or manufacturer's income and increase consumer expenses (Lipinski *et al.*, 2013). There is a surplus of economic benefits to utilisation of a wasted crop for direct human consumption.

1.2.2 **Obtaining and processing of raw ingredients**

As previously stated, in section 1.1, transportation and storage creates an abundance of wasted/lost fresh produce in developing nations. In order to obtain a material for modification, firstly it must be acknowledged that an indication of processing of the produce in a developing country has been envisioned to meet with the infrastructure requirements. Secondly, the processing of the produce, which is currently a by-product, will be proposed to be used for the purpose of valorisation into a functional ingredient. Whereby the ingredient will have similar functionalities to already used expensive high proportion based commodities within a model system product. Therefore, a raw material ingredient (once processed and modified) is required to have the ability of being stable and does not readily permit physical changes to its system through poor infrastructure of transport and handling mechanisms. Whether the material/ingredient be in a dry or wet state, as long as it is appropriate to carry out its newly founded properties, which have been adapted through conversion routes as explained earlier.

1.3 Potential use of Plant Cell Wall Materials (PCWM)

It is fundamental to understand the function and material properties of a matrix within an ingredient for application, as this may denote how the material will potentially behave within a composite. However, in the case of PCWM some of these functional properties can be modified and be enhanced through aforementioned conversion routes described by Foster (2011). PCWM typically consist of cellulose, hemicellulose, lignin and pectin as well as, other components in smaller amounts such as protein, starch, lipids and micro-nutrients (Gilbert, 2010). The major macromolecules formed in the plant (cellulose, hemicellulose and lignin) as fibrous material are formed in the walls of the supporting cells in the plant tissues (Gilbert, 2010). These cell walls are made up of polymeric composite materials conveying tensile and pressure resistant components with each described in sections 1.3.1 to 1.3.4 and the structure of the PCW is depicted by Figure 2. The main components being that of polysaccharides, which consist of one type of sugar structural unit (known as a homoglycan) or several types of units (known as heteroglycans). Polysaccharides can be linear such as cellulose, or they can be in a branched such as amylopectin and hemicellulose (Belitz, Grosch and Schieberle, 2004).

The chain conformation of polysaccharides are determined by the monosaccharide structural unit conformation and the positions/types of linkages in the chain.

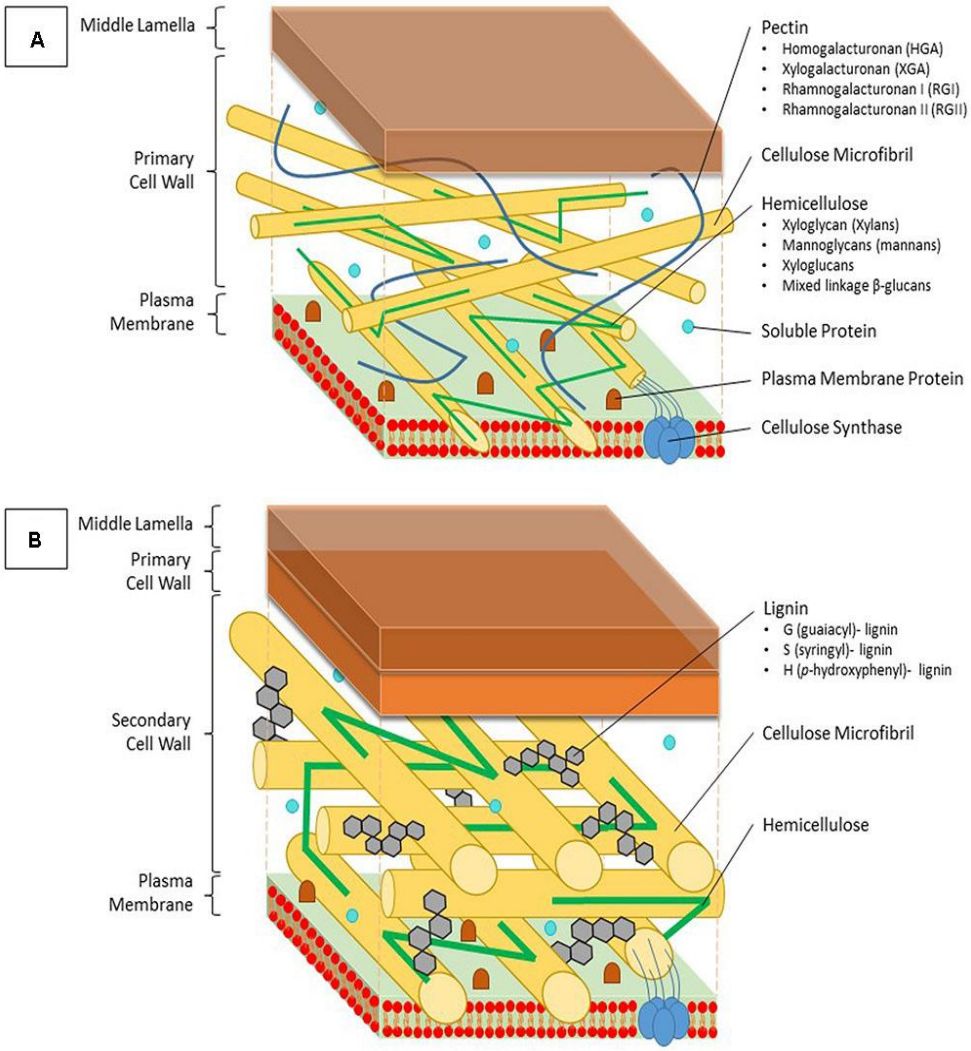


Figure 2 The structure of the primary and secondary cell walls of plants. (A) Shows the the primary cell wall, which is located outside the plasma membrane and consists of cellulose microfibrils, hemicellulose, pectin's and soluble proteins. Hemicellulose binds to the surface of cellulose microfibrils and the varying hemicellulose types are listed. Pectins then form a gel between cellulose and hemicellulose network. (B) Shows the secondary cell wall which is found between the primary cell wall and the plasma membrane. Here cellulose microfibrils are more arranged still with hemicellulose complexes, but lignin is present instead of pectin. Taken from (Loix et al., 2017).

1.3.1 **Cellulose**

Cellulose is the most abundant polymer found on Earth. It is a natural building block of the cell wall structure of higher plants and used to build tensile plant tissues (Wüstenberg, 2014). It has been estimated that nature produces (through photosynthesis) 500-1000 billion tons of pure cellulose

per year (Wüstenberg, 2014). In general cellulose constitutes to around 40-50 % of a PCWM (McKendry, 2002). Its role in the plant is to reinforce and therefore has high tensile strength (Wüstenberg, 2014).

Cellulose is a hierarchical structure formed of linear polymers containing D-glucopyranosyl residues, which are linked entirely in a β - (1→4) configuration (Wüstenberg, 2014). Cellulose is an isotactic β -1, 4 - polyacetal of cellobiose (4 -*O*- β-glucopyranosyl-D-glucose). The base unit of cellobiose consists of two molecules of glucose. Therefore for this reason cellulose is considered as a (syndiotactic) polyacetal of glucose (Wüstenberg, 2014). The cellobiose unit is repeated and Figure 4 depicts the most basic building block of cellulose in the inset, with an example of two rings joined by a β - (1→4) linkage of cellobiose (shown in brackets, but with -OH groups in equatorial positions in place of glycosidic bonds). The hierarchical structure of cellulose starts with micro-fibrils and elementary fibrils, which consist of around 36 individual cellulose molecules, packed together into large units (Habibi, Lucia and Rojas, 2010). These are then assembled into common cellulose fibres (Lavoine *et al.*, 2012). Micro-fibrils are formed during the biosynthesis of cellulose; one can consider each micro-fibril like a flexible strand whose cellulose crystals link along the micro-fibril axis varying in amorphous domains (see Figure 3). Crystalline domains with their strong and complex network of hydrogen bonds (Habibi, Lucia and Rojas, 2010) resemble nano-crystalline rods when subjected to chemical and physical treatment (Lavoine *et al.*, 2012).

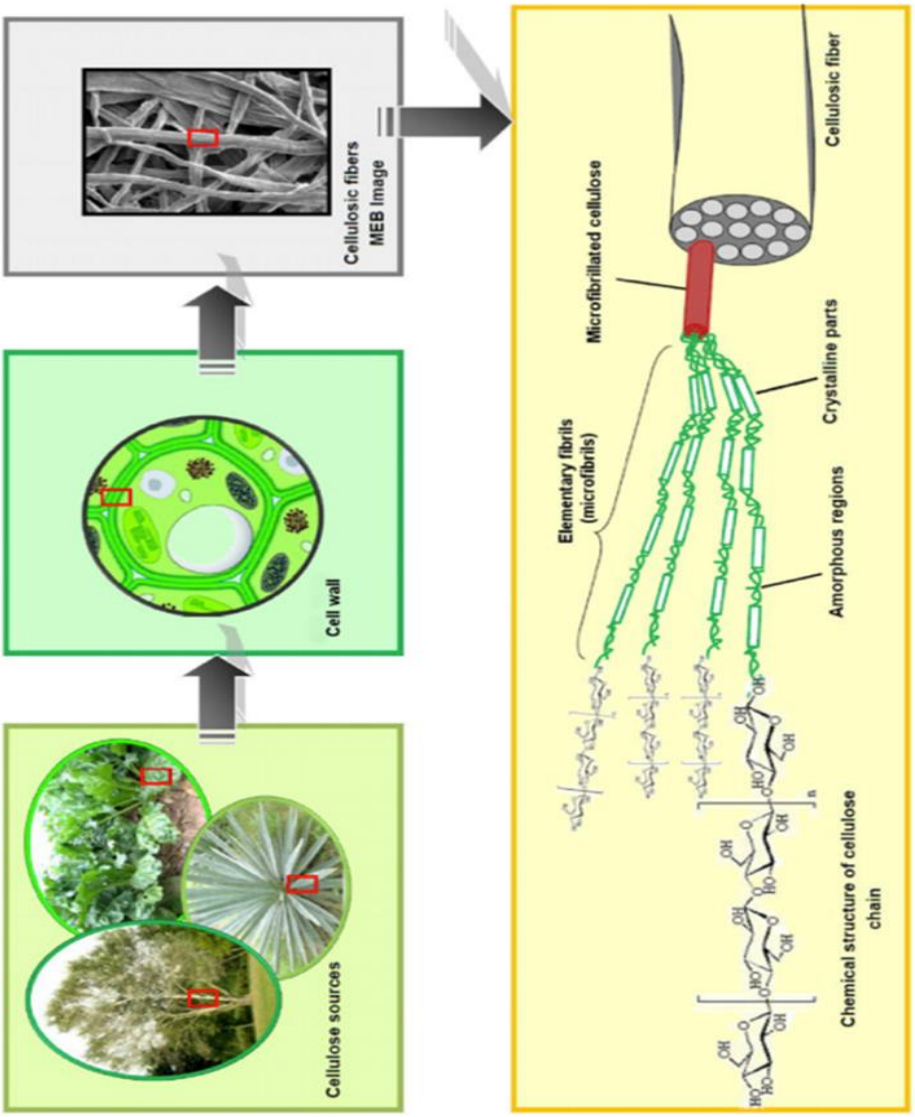


Figure 3 Cellulose hierarchical structure found in nature taken from (Lavoine et al., 2012).

As an industrial raw material cellulose generally has had two purposes, construction materials including the use of paper and textile fibres and as a versatile starting material for chemical conversions, which may be used to produce artificial, cellulose-based threads, films and cellulose derivatives (Belitz, Grosch and Schieberle, 2004), and is currently used in many industries including that of the food industry (Wüstenberg, 2014). There are

many ways of adapting cellulose in order to achieve functionality especially in food systems, in which case it needs to be converted to being more water soluble, by a means of physicochemical modification (Foster, 2013). In current food applications native cellulose is partially depolymerised, the resulting products are; microcrystalline cellulose and powdered cellulose. Moreover, highly purified cellulose can be used in the form of pulps for producing functional cellulose ethers such as cellulose gum; methylcellulose, hydroxypropylcellulose and ethyl cellulose (Wüstenberg, 2014). There are various chemical, physical and thermal methods of adapting cellulose in order to produce cellulose derivatives (Wüstenberg, 2014). In this study milling and fibrillation techniques are explored, in order to adapt cellulose for later functional properties as a food ingredient.

The cellulose structure depicts stretched chain conformation due to a zigzag geometry of monomer linkages involving oxygen bridging (Belitz, Grosch and Schieberle, 2004). This chain has the ability to be somewhat shortened or compressed to enable the formation of hydrogen bonds between neighboring residues, which contributes to neighbouring stabilisation. The term “n” is given to the number of monomers typically found in the structural conformation to accurately state the required amount to form a polymer (Belitz, Grosch and Schieberle, 2004).

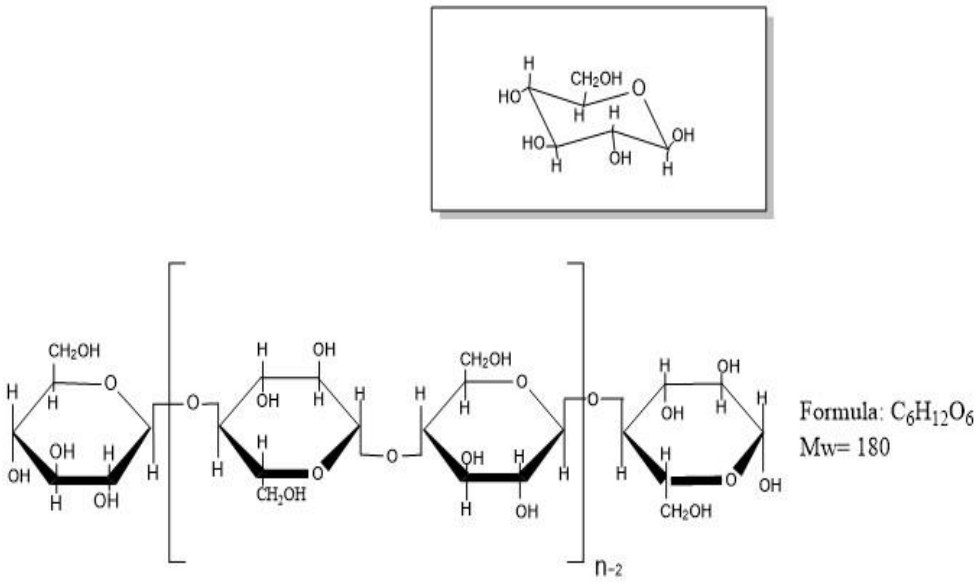


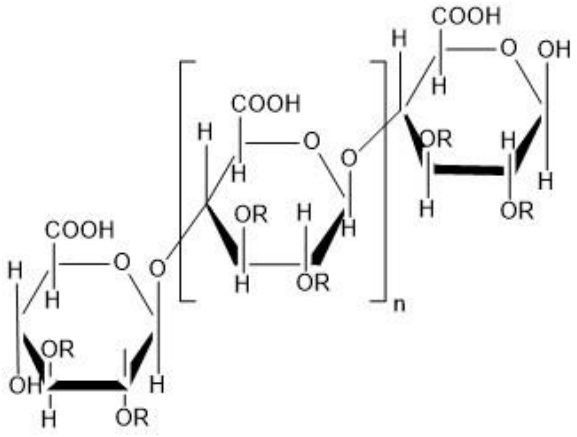
Figure 4 The structural conformation of general native cellulose. The smallest building block is a single β-D-glucose ring (inset). There are two rings joined by a β-(1→4) linkage, which is cellobiose (as shown within brackets but with the -OH groups in equatorial positions in place of glycosidic bonds). The standard formula and Mw in Daltons for cellulose in general is disclosed.

1.3.2 **Hemicellulose**

Hemicelluloses also known as polyose are a heterogenous polysaccharides with the most abundant component being either xylan, mannan or glucan, which is determined by the main sugar residue backbone (Brunner, 2014). Hemicelluloses are often branched polymers with many short side chains, consisting of pentose (β-D-xylose and α-L-arabinose), hexose sugars (β-D-mannose, β-D-glucose and α-D-galactose) and uronic acids (β-D-glucuronic acid, α-D-4-O-methylglucuronic acid and α-D-galacturonic acid), additionally in smaller amounts α-L-rhamnose and α-L-fucose may appear (Pereira, 2007; Hayes, Mylotte and Swift, 2017). The short side chains composed of the differing sugars do not form aggregates, even when co-crystallisation occurs with cellulose chains. Hemicelluloses also contains a range of structural linkages such as α or β- linkages (1→2, 1→3, 1→4, 1→6) (Hayes,

Mylotte and Swift, 2017). These compositional differences depend on their origins, typically hardwood hemicelluloses contain more amounts of xylan, whereas softwoods contain mostly glucomannans. In this study it is expected, as others have found, that xyloglucan configurations are the type of hemicellulose for the plant based material used (Fry, 1989; Talbott and Ray, 1992). The typical structural conformation of a xyloglucan derivative can be found in Figure 5 taken from (Muhd Julkapli, Akil and Ahmad, 2011) and will have slight variations from differing plant origins and species regarded by OR on figure 5. The backbone of xyloglucan is chemically identical to that of cellulose, such that it is a ridged straight chain polymer of β-(1→4) linked D-glucopyranose residues (Fry, 1989).

Hemicellulose is the dominant carbohydrate in the compound middle lamella (Caballero, Trugo and Finglas, 2003). The role of hemicellulose in plants is to fill voids around cellulose fibrils and provide couplings/flexible adhesions to lignin as well as, influencing aggregation of cellulose during the formation of the cell wall (Wüstenberg, 2014; Hayes, Mylotte and Swift, 2017). As hemicelluloses are closely linked to lignin they constitute around 30-40 % of the dry weight of the plant cell wall (Ansell and Mwaikambo, 2009), though xyloglucan has been reported to make up about 20-25 % (dry weight) of the primary cell wall in dicotyledons (Fry, 1989). Compared to cellulose, hemicelluloses are amorphous and more reactive (Pereira, 2007), but have a higher solubility and readily hydrolysed (Wang, 2003). The degradation of hemicellulose proceeds via endo- and exo-hydolysis. This substrate specificity is dependent on the monosaccharide building blocks and on the type of binding. For example, endo β-1-4-D-xylanase, which occurs frequently in plants just like cellulase enzymes obtained naturally from cellusomes.



Formula: $C_{45}H_{76}O_{38}$
Mw = 1224

Figure 5 A structural conformation of a generalised xyloglucan derivative, there is one ring depicting the singular unit typically present observed in brackets. However, chain length and side chains vary depending on the origin of the source and this is just an indication of the structure, which can join to OR regions. However, COOH groups are always present. The formula and Mw is depicted in Daltons for xyloglucan when it is in its full form and not for the conformation example depicted in these works. Drawn from (Muhd Julkapli, Akil and Ahmad, 2011).

1.3.3 **Lignin**

Lignin is a complex and highly cross-linked structure. The highest proportions of lignin are found in the middle lamella of the plant cell wall whereby cellulose microfibrils are encased in lignin (Belitz, Grosch and Schieberle, 2004). Lignin concentrations tend to be higher in hardwood based materials rather than softwood.

Lignin as a matrix material in the PCW and contains little flexibility, and therefore can be described as being brittle, extremely strong, hydrophobic and has slow biological degradation. Therefore its role in the plant is to strengthen the walls of plant tissues (Wüstenberg, 2014). This strength and rigidity enables contribution to resistance for the plants to impact of bending and compressive deformation. Lignin constitutes to around 15-30 % of the PCW (Xu and Ferdosian, 2017).

Compared to cellulose's well–defined structure, lignin has a three-dimensional structure that depends on the vegetal species, location, season produced and other environmental factors. Lignin is a phenolic polymer formed by the dehydrogenative (radical coupling) polymerisation of three monolignols, coniferyl (G), sinapyl (S) and *p*-coumaryl (H) alcohols (Xu and Ferdosian, 2017). An example of each of these structures is given in Figure 6, which is catalyzed by a peroxidase and requires water. Each alcohol is produced from either phenylalanine or tyrosine for H units predominantly, or they can be converted into C, G and S units. Moreover, ferulic acid and caffeic acid produce C, G and S units, this is demonstrated in Figure 7. In hardwood species, lignin's dominating monomer is both Syringyl (S) and Guaiacyl (G) units, whilst in softwood species it is just the Guaiacyl monomer (Xu and Ferdosian, 2017). The Syringyl are made up of Sinapyl alcohols and therefore both classed as S units, whereas Guaiacyl units are made up of Coniferyl alcohols (Serk, 2015). There is additionally small amounts of hypdroxyphenyl (H) units consisting of *p*-coumaryl alcohol (Serk, 2015). Lastly, it is extremely rare in nature to observe any Caffeyl alcohol (C) units. Figure 6 depicts the conversion of amino acids into alcohols, to then particular units (G, S, H and C) found in the secondary cell wall (Serk, 2015). These are linked mainly by ether linkages for example α-O-4, 5-O-4 and β-O-4, and condensed linkages for example (5-5, β-β, β-5 and β-1 linkages) (Xu and Ferdosian, 2017). Though around 40-60 % of the total intermolecular linkages consist of ether bonds and the β-O-4 bond is a predominant linkage (Xu and Ferdosian, 2017). The reactivity of lignin is dependent upon the form and composition of reactive functional groups within each specific monomer unit, there are three types of functional groups

including: p- hydroxyl-phenyl, aliphatic hydroxyl and carboxylic (Xu and Ferdosian, 2017).

Lignin is amorphous (Wüstenberg, 2014) and has many applications based on some unique properties such as being an antioxidant, biodegradability and reinforcement capabilities. Therefore it has been applied to a wide range of systems such as reinforcing fillers, natural rubbers, adhesives, surfactants, emulsifier and dispersants to name a few (Xu and Ferdosian, 2017).

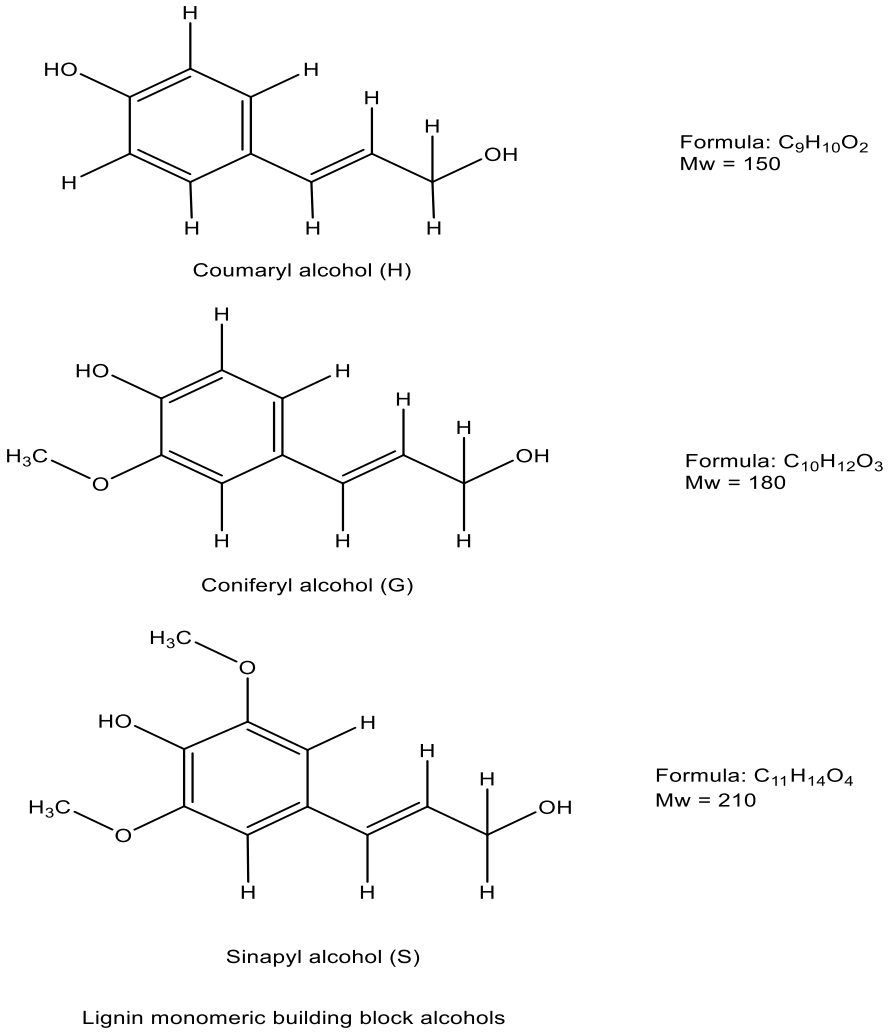


Figure 6 Individual standard lignin monolignols p-Coumaryl, Coniferyl and Sinapyl alcohols found in abundance, also known as the lignin monomeric building blocks, which build units of Guaiacyl (G), Syringyl (S) and hydroxyphenyl (H) (capitilised letters represent which alcohol builds with which units). Structures drawn and adapted from (Xu and Ferdosian, 2017) with each individual formula and Mw given for each particular alcohol in Daltons.

1.3.4 **Pectin**

Pectin is a polysaccharide consisting of α-D-galacturonic structural units joined by α-1→4 linkages (Belitz, Grosch and Schieberle, 2004). With additional rhamnose residues in the main chain, where rhamnose units may be in adjacent to or alternating positions. Moreover, pectin contains small amounts of D-galactan and arabinose in extended side chains. Lastly, in minimal extents fucose and xylose sugars are found in the short side chains (Belitz, Grosch and Schieberle, 2004). Though these short side chains are not regarded as typical pectin constituents. Therefore the term pectin covers a number of polymers that vary in molecular weight, chemical configuration and content of neutral sugars depends on the plant base source (Flutto, 2003). A standard configuration can be found in Figure 8 with linear homogalacturonan (α-1,4-galacturonic acids) chains interspersed with branched rhamnogalacturonan (α-1,4-galacturonic acid to α-1,2-rhamnose) chains, in which the neutral sugar branches are connected through rhamnose residues.

Pectin plays a vital role in the PCW by contributing and regulating cell growth/expansion and cell differentiation, which thereby determines the integrity and rigidity of plant tissues. Furthermore, pectin contributes a role in defending against plant pathogens and wounding (Voragen *et al.*, 2009).

Pectin is an amorphous material with no crystalline fractions (Belitz, Grosch and Schieberle, 2004; Wüstenberg, 2014) and whose importance in the food sector mainly lies in its ability to form a gel in the presence of Ca^{2+} ions or in the presence of high amounts of soluble solids at low pH (Thakur *et al.*, 1997). Within the food industry pectin extracts are used in jams, jellies, frozen foods and in low-calorie foods as a fat and/or sugar replacer (Thakur

et al., 1997). Though other non-food applications include edible films, paper substitutes, foams and plasticizers (Thakur *et al.*, 1997).

The degradation of pectin also occurs in plants by enzymatic action: firstly pectin methyl esterases, which occur widely in plants and microorganisms, secondly polygalactosidases, which attack the glycosidic bond in polygalact-uronides as do pectin lyase enzymes (Belitz, Grosch and Schieberle, 2004).

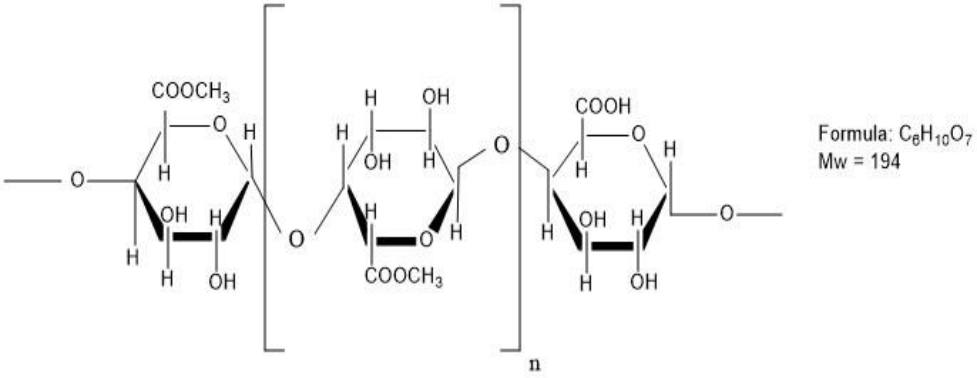


Figure 7 Generalised structural conformation of pectin with linear homogalacturonan (α-1,4-galacturonic acids) chains interspersed with branched rhamnogalacturonan (α-1,4-galacturonic acid to α-1,2- rhamnose) chains, in which the neutral sugar branches are connected through rhamnose residues. Mw given in Daltons and the molecular structure was drawn from (Hassan et al., 2018).

It is imperative to know the constituents, their types (for example which hemicellulose complexes) and their amounts within a wasted agricultural produce, as these will ultimately determine differing functions and properties, as an ingredient, within a composite. This is due to large variations of differing structures across plant species. Moreover, understanding the fundamental structure of plant species in this case pea plants, in their raw form, will enable further understanding of process functionality on the modification and adaptation of the then processed structures. This will be able to infer hypotheses by which structural transformations may be designed.

1.4 Introduction to the thesis:

In recent years there has been an increase for the business world to operate competitively but with a sustainable footprint. Moreover, to achieve this, in combination with improving the nutritional quality of the product and without the consumer noticing large adverse changes. Therefore, this means that sustainable food manufacturing options will need to be achieved without compromise to nutrition. A starting concept of this was described in section 1.1, whereby utilisation of what is already produced is an environmentally sound argument against current environmental crises. Furthermore, utilisation of valorised by-products that are nutrient rich, compete against those that are energy dense, for inclusion in products. Mainly due to their advantageous health benefits as aforementioned, over adverse and negative ones permitted through the consumption of energy dense commodities. Lastly, in developing countries the increased demand of snack products typically consumed in western diets has grown in interest. Though the demand cannot be met by manufacturers unless formulations are suited for production and for a cost effective market. Therefore, replacement materials are sought after and to be obtained through valorisation of manufacturing by-products (in the case of this study pea halum/biomass, after harvest of pea seeds), for use as an ingredient within a dough formulation of a ready to eat expanded savoury snack product. It was proposed for developing countries that a different formulation is required that enables; both cost efficiency and stabilisation of materials, due to lack of infrastructure and poorly equipped transportation methods for previously mentioned developing nations. Therefore, the inclusion of the biomass must be adapted to suit transportation mechanisms, be cost effective and also have added value to the current formulation i.e. reduce calorific content. The

newly formatted product must have similar properties that are not significantly different from the control formulation, due to that particular formulation showing consumer approval.

Thus, the target of this study was to reduce the amount of starch in the overall product. There are differing starch commodities within the product formulation including potato, tapioca and rice. Potato being an expensive commodity would have been an obvious starting point for partial or complete replacement. However, the functionality of each individual starch within the product/dough formulation, as a combination, within a food matrix are not fully understood by the manufacturer. With each individual starch-based commodity having different functionality for example (texture, sensory or taste, appearance and expansion), but in combination the starches work effectively to produce the ideal product for the current market, for that particular formulation recipe. However, as the formulation needs to be adapted to better suit the production in a developing country, an initial study on proportional replacement of all starch commodities was undertaken, which then will provide targets and concepts for replacement in the future.

Chapter 2 Techniques

2.1 ^{13}Carbon Cross Polarisation Magic-Angle Spinning Nuclear Magnetic Resonance (^{13}C CP-MAS NMR)

NMR spectroscopy measures the properties of nuclei with an uneven number of subatomic particles (neutrons and protons) within the nucleus, in this case ^{13}C. NMR is well recognised to be an insensitive technique when using ^{13}C. In addition to relaxation effects, two major influences (di-polar broadening and lack of local molecular motion) influence the ability to obtain high-resolution ^{13}C signals from solids. Solid state CPMAS ^{13}C NMR was used in this study to determine the composition of materials and the relative crystalline/amorphous content. The practical solution to these two difficulties in obtaining NMR-spectra for solids is to use 'magic-angle' spinning. A simulated motional average as well as high-power decoupling using powerful radio frequency (RF) amplifiers is used to minimise dipolar interactions. Spinning at this 'magic angle' requires frequencies greater than the anisotropy of the chemical shift of carbons in particular chemical groups; for many solids, using a 600 MHz spectrometer 10-12 kHz is considered sufficient for most but not all (carbonyl for example) carbons in chemical groups. Moreover, cross-polarisation allows magnetisation to be transferred from ^{1}H nuclei to ^{13}C nuclei via dipolar coupling. A combination of both magic angle spinning and cross-polarisation enables an increase in the inherent sensitivity. As well as increases in the speed of the experiment due to a reduced T_1 relaxation time through the rapid ^{1}H pathway, over the alternative slower ^{13}C path. However, a reduced acquisition time may lead to an increase in signal to noise ratio. This methodology is used for systems lacking in molecularly mobility. It can approximately be viewed as giving the solid a liquid-like character. The specific resonant frequency of the energy

transition is portrayed as a chemical shift in parts per million (ppm). The effect of neighbouring nuclei on a considered nucleus of the same type, which may also be affected by the magnetic field, known as spin-spin coupling and can be measured by the T_2 value.

2.2 Wide-Angle X-Ray Diffraction (WAXD)

A diffraction peak is produced when each object in a periodic array scatters radiation producing constructive interference at specific angles. The electrons within an atom coherently scatter x-rays when the electrons interact with the oscillating electric fields of the x-ray waves. Therefore diffraction occurs when these wavelengths are of the order of the distance between atoms (distance between 0.1 Å and 100 Å), which is similar to the inter-atomic distances in a crystal.

WAXD can be used to measure the crystallinity content of samples. Powder diffraction is commonly used, whereby the powder is randomly packed to ensure a random crystal orientation, which ensures attainment of all possible orientations of the lattice. Amorphous materials have no order, whereas crystalline materials have an ordered structure. Therefore, when amorphous materials are hit by x-rays the lack of order results in x-ray beams reflecting at all angles and results in destructive interference. This is due to waves being out of phase with one another. Whereas, when crystalline materials are hit by x-rays, the incoherent scattering patterns in the crystals results in the waves being in phase and causes constructive interference resulting in an intensified pattern measured by the detector. The amorphous material will still produce a signal but this produces a lack of structure (peaks) and results in what is called an amorphous halo.

In order to produce a measurement, the smallest repeating part of the unit cell, which has a fixed arrangement, reflects the x-ray beams at certain angles of incidence known as 2 theta (θ) as shown in Figure 9. This angle is dependent on the distance between the atomic layers and the wavelength of the incident x-ray beam (λ) and this relationship is defined by Bragg's Law:

Equation 1 $$n\lambda = 2d\ sin\ \theta$$

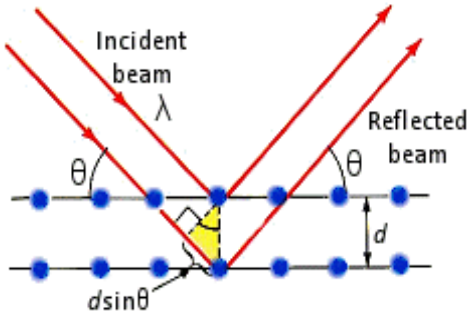


Figure 8 Bragg diffraction in a crystal showing constructive interference of reflected waves, taken from (ChemViews, 2012).

Lastly, Miller indices describe the orientation of a plane within a lattice, in relation to the unit cell. These are imperative for denoting crystalline arrangements of atoms in semi-crystalline solids such as cellulose, and therefore can be used to determine and calculate the cellulose allomorph type which are present, due to the establishment of the symmetry of the crystal in question and the intensity signal that is produced (Hunter and Dweltz, 1979).

2.3 Dynamic Mechanical Analysis (DMA)

DMA is a measurement of oscillatory rheology, and additionally thermal analysis, which refers to the mechanical properties or flow of a solid-like

material. This can give information of the Complex Modulus (Equation 2 where E * = Complex Young's modulus , S* = Stiffness modulus and K = the geometry constant), melting and/or softening point and finally the glass transition of a material. This information provides fundamental details of properties of the composite material. DMA is performed by applying a force of known magnitude and phase, which allows for measurement of the displacement amplitude with reference to the force signal i.e. one is slightly bending the material back and forth if using a single cantilever geometry, as used in this study. Material pockets can be used to assess powders of a material if they are of an irregular shape for the clamps (Figure 10). In doing so, the Complex Modulus (E*) (Equation 2) cannot be determined due to lack of information required of the geometry constant and therefore domination of the metal pocket. Therefore the Stiffness Modulus (S*) is calculated and assessed, which provides information on the flow properties of a material as an indirect complex viscosity measurement, which was used in this study (the equation is further described in DMA results within Chapter 6).

Equation 2: $$E^* = S^*/K$$



Figure 9 Materials pocket (stainless steel) were used instead of a solid bar of material. The material must be ground to a fine powder with the smaller the particulates the more sensitive the equipment is to measuring. The material is then placed in the pockets and the pocket is folded with the ends additionally folded and sealed.

2.4 Oscillatory Rheology

Rheology is the measurement of material flow, which can either be purely viscous and thereby Newtonian, visco-elastic or solid-like as ascribed by Hooke's law, of a material under applied forces. Oscillatory tests are used to examine visco-elastic materials from low-viscosity liquids to polymer solutions and dispersions. Viscosity is the resistance of a fluid to flow as a function of differing frequencies (therefore deformation) at an applied stress and can be measured through a frequency sweep. However, in order to perform a frequency sweep on a material, first an amplitude sweep (varying amplitude whilst frequency is kept at a constant) must be performed. The amplitude sweep is required to obtain a linear visco-elastic (LVE) region, which indicates the range in which the test (frequency sweep) can be carried out without destroying/deforming the structure of the sample. This LVE region can then be used for a frequency sweep (varying frequency with a constant amplitude) in order to obtain a complex viscosity of a given sample. There are many geometries used in oscillatory tests, however, here a serrated or smooth parallel plate (Figure 11) was used. Having a serrated plate reduces the slip of the material. The gap size (the distance between the plates) is often larger with a parallel plate geometry than that of a cone and plate for example, but the gap size should be about 10 x the mean particle size diameter. However, due to larger gap sizes, sample drying can incur. If that is the case or seen in practice runs, then in those particular experiments pure mineral oil (Sigma-Aldrich, UK) could be used as a barrier around the geometry (ensuring no contact with the sample), in order to try and prevent water loss.

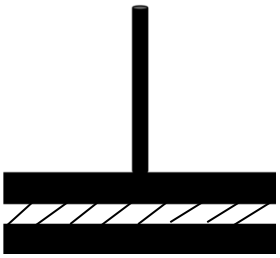


Figure 10 Schematic of a smooth parallel plate geometry with an example of a sample.

2.5 Micro-Computed Tomography (Micro-CT)

Micro-CT can be used to quantify the structure and function relationships of materials. It is a non-destructive imaging tool, which is used to produce a high-resolution (details given in methods Chapter 6) three-dimensional (3D) series of images, composed of two-dimensional (2D) slices of a target sample. 3D imaging is performed by rotating the sample or the detector, whilst x-rays pass through it. In this study it was used to look at the internal structure of a material composite and provides quantifiable data within the structure such as voids/voxels.

2.6 Turbiscan Stability Index (TSI)

Turbidity is a measurement, which assesses suspended solids, within a suspension/dispersion. A dispersion containing dissolved molecules and ions, can be coloured but not necessarily turbid. Over time turbid dispersions can sediment. Therefore, turbidity can be simply defined as the cloudiness of a material in a solvent e.g water. Colloids contribute to water turbidity if in a dispersion, similar to the fibrillation dispersions found later in Chapter 5. Therefore, to assess fibrillated dispersions, turbidity and destabilisation kinetics were performed and gave a value of Turbiscan Stability Index (TSI). TSI is a function computed by the Turbiscan (Formulaction, France) and it

uses Back Scattering (BS) and Transmission (T) percentages (%) in order to generate a number which reflects the destabilisation of a given sample. A higher TSI (%) score equates to a stronger destabilisation of the sample; equally the lower the TSI (%) score the more stable the sample/system is. TSI is defined by the following equation:

Equation 3 $$TSI = \sum_i \frac{\sum h \left| scan_i(h) - scan_{i-1}(h) \right|}{H}$$

2.7 Thermogravimetric Analysis (TGA)

Thermogravimetric analysis refers to a group of techniques in which a property of a sample is monitored against time or temperature, whilst the temperature of the sample (in a specified atmosphere), is changed. Additionally, it allows for analysis of a change in a property of a sample, which is related to an imposed temperature alteration.

A constant rate temperature change programme was used here. The mass change of a sample is measured by a balance, whilst the heating is carried out in either inert (nitrogen) or reactive atmospheres (oxygen). An inert atmosphere was used here. This allows one to determine calorimetric effects such as thermal stability, degradation of, in this case, polymers. It also allows one to assess the water content of a sample. Such physical changes of a sample were assessed in this study to predict the behaviour of a modified material, as a new functional food ingredient within a product and/or composite material.

2.8 Dynamic Vapour Sorption (DVS)

DVS is the measurement of absorption or adsorption kinetics of a solvent (water in this case). This can be done through mechanisms of physisorption (physical attraction i.e. Van der Waals) or chemisorption (chemical bonds i.e. covalent). DVS uses a reference and a sample holder, with both being attached to a very sensitive balance, which is purged under pure nitrogen. Once the weight has stabilised, the relative humidity (RH) is raised in steps of 10 %, until it reaches 95 % RH, including desorption which returns the sample to 0 % in steps (a full cycle). Samples are classed as equilibrated once the change in mass per unit time is less than 0.0005 mg min^{-1}, or once the equilibration time has reached 1500 min. In the case of this study DVS was used to assess re-crystallisation and measure sorption isotherms. This gives fundamental information of a sample's properties as an ingredient and the stability with changing environmental water contents.

2.9 Differential Scanning Calorimetry (DSC)

DSC is a thermal analysis technique, which describes the difference between a reference and a sample (Differential), whilst changing/measuring the temperature (Scanning) upon heat changes (Calorimetry). DSC measures heat flow into or from a sample, defined as endothermic/exothermic respectively as it is heated/cooled at a controlled rate. The standard mode, and used here, involves either constant heating or cooling ($dT/dt=\beta$). Heat flow (Mw) is measured and plotted against time or temperature. DSC allows one to look at the melting, re-crystallisation and glass transition of polymers. In this study it has been used to observe these physical phenomena of the PCWM. Furthermore, it can observe chemical changes such as degradation and interactions between components, which

was analysed in this study. Both physical and chemical changes observed can then give insight into the structure of the material such as whether it is in an amorphous or crystalline form. It can also give characteristics of the material such as its melting point. Such characteristics are fundamental when assessing an ingredient and how it is likely to act within a composite material or product.

2.10 Statistics used in the experimentation

For all statistical assessments Graph Pad Prysm software was used for performing Standard Regression, ANOVA and/or a Paired ANOVA. All experiments were performed in triplicate within this study apart from the following exceptions:

- Results Chapter 3: Composition of raw materials. Pectin assessments were not performed in this study but were used as found in a collaborative paper (attached).
- Results Chapter 4: Design of Pea Biomass powder; ^{13}Carbon Cross Polarisation Magic-Angle Spinning Nuclear Magnetic Resonance (^{13}C CP-MAS NMR) assessments were only performed once due to availability of the equipment. TGA and NMR assessments were performed by trained specialists.
- Results Chapter 5: The production of Micro-Fibrillated cellulose from *Pisum sativum* (Pea) Biomass; Wide Angle X-ray Diffraction assessments of chemically treated Pea Biomass with varying mechanical disruption via microfluidisation were only performed once (Rigaku, Sevenoaks,UK) due to lack of equipment at that particular time (in-house equipment failure).

- Results Chapter 6: Application of Pea Biomass powder and fibrillated mass to a model system; textural analysis samples were done in sets of six in order to gain a full perspective of the hardness of newly formatted structures within examined composites. Variation between sample replicates occurred due to sample preparation using a customised, non-commercial piece of equipment. Similarly, due to these variations, expansion ratio assessments were performed in sets of five across multiple random batches completed on different days, these were done in order to gain a true representation of the sample characteristics investigated.

Chapter 3 Composition of raw materials

3.1 Introduction

Pisum sativum more commonly known as the pea crop belongs to the family Leguminosea, also known as Fabaceae biomass (Royal Botanic Gardens Kew Science, 2003). Like many legumes, peas are nitrogen- fixing with a symbiotic relationship co-existing between bacteria housed within root nodules of the plant biomass (Royal botanic gardens kew science, 2003). The origin of pea plants is not fully understood. Evidence suggests that humans have been cultivating peas since 8,000 BC in Western Asia. Now, cultivars have spread to Europe, China and India. The pea plant is mainly cultivated for its edible seeds. There are three main types of varieties of pea grown for consumption, which are: field peas for their dry seeds, garden peas for immature green seeds and sugar peas for immature pods. Pea pods contain up to eleven seeds, which are known as the fruit of the plant. They are commonly green (crinkled garden pea), occasionally yellow (sugar pea) and less commonly purple or a cream-ish white. The seeds themselves are spherical and the pods are oblong-shaped. The pea crop additionally comprises leaves and flowers. The leaves arranged alternately along the stem, comprise four pairs of leaflets and end in a tendril, which is typically branched. Stipules are found at the base of each leaf and petioles connect leaves with stems. The flowers are arranged along a raceme, which each contain one to three flowers and axils, which are white to purple in colour. Flowers occur before seed setting and therefore mature crops do not have them (Royal botanic gardens kew science, 2003).

Pea crops thrive in cooler and higher altitude environments with maturity of cultivars in main crops taking around 16 weeks. Peas have both low growing

and vining cultivars. The vines grow thin tendrils from leaves that coil around and provide support. The annual height is up to 3 meters (Royal botanic gardens kew science, 2003). The pea crops used in this study are vining cultivars of shelling peas. Pea harvest in the UK mainly occurs from June until August, with the crop in these works being harvested in July at optimum yield time for that particular farm.

In the UK around 153 kt of pea seeds are produced on 25000 acres of land (Briars, 2018). It has been estimated that $\frac{3}{4}$ to $\frac{7}{8}$, of the pea crop is not utilised as an edible source for human consumption, with an untapped source of nutrients (Briars, 2018). The leaves, pods, tendrils and stems (entire crop after harvest without roots) are often used for either; compost to recycle nutrients back into the soils (only $\frac{1}{4}$ to $\frac{1}{8}$ is estimated to be necessary for nitrogen fixation) (Briars, 2018), animal feed (in some cases), or left to decompose. Therefore, this waste streamside crop has the potential to be valorised due to the enormous volumes of production not being utilised.

Pea seeds themselves provide great sources of fibre, protein and starch. Additionally, peas contain many micro-nutrients including potassium, magnesium, calcium, iron, zinc, molybdenum, copper vitamin A, vitamin B6, vitamin C, vitamin K, phosphorous, magnesium, iron, zinc and lutein. They have many human benefits such as the fibre from the seed coat and the cell walls of the cotyledon, which have shown to decrease the amount of starch digested from the pea seed and furthermore aid in gastrointestinal functions (Dahl, Foster and Tyler, 2012). Dahl *et al*. (2003) and Flogan and Dahl, (2010), found pea fibre to increase bowl movement by between 7.5 and 24 % (Dahl *et al.*, 2003; Flogan and Dahl, 2010). Additionally pea protein has the ability, when hydrolysed, to yield peptides with bioactive activity including

angiotensin I-, which is an enzyme inhibitor and antioxidant (Dahl, Foster and Tyler, 2012). Furthermore, vitamin and mineral constituents help to aid in the prevention of deficiency-related diseases. Such health benefits are derived from the relative concentration and properties of starch, protein, fibre, vitamins, minerals and phytochemicals. Concentrations and properties of protein have shown to vary significantly and be influenced by both environmental conditions and genetic factors (Dahl, Foster and Tyler, 2012). Similarly, these factors may also influence other nutrient compositions within pea seeds. Studies and suppliers of peas (such as supermarkets) have performed assessments of the nutritional composition of peas (Reichert and MacKenzie, 1982) and (Gdala, Buraczewska and Grala, 1992). Fewer studies have looked into the nutritional composition of the entire crop and even fewer as a total crop, once harvested and mixed as one biomass (Åman and Graham, 1987).

Therefore, the crop, when mature and harvested, is explored in this study, in order to develop nutritional valorisation strategies and to provide dietary requirements for those malnourished, as well as improve the nutritional index of a ready to eat snack. Therefore, in order to assess nutritional composition, differing analytical and quantification techniques were explored for each macronutrient, PCW sugars and lignin, as well as, protein, ash and chlorophyll. No individual micro-nutrients were assessed only as a total ash volume. Extraction methods vary between macro- and micro-nutrients. Furthermore, many extraction methods exist for each component and it is not an objective of this work to reviewcomparisons of them. Firstly, it should be noted that extraction techniques, in order to retrieve 100 % of a particular nutrient, are extremely difficult, as one needs to account for human error and reactivity of particular compounds.

3.1.1 Cellulose

As aforementioned cellulose is the most abundant polymer source on Earth. This is due to cellulose being the principal structural component of plants. Structural and functional information of cellulose can be found in Chapter 1. In hardwoods cellulose composition is around 43-47 %, whereas in wheat straw cellulose composition is about 30 % (Wüstenberg, 2014).

Due to cellulose being hygroscopic, yet referred to as an inert substance, it shows only minimal swelling in water. It is additionally insoluble in most organic solvents/dilute acids but swells more readily and is more soluble in concentrated acids. However, solubility through these means leads to considerable degradation of the cellulose chain through acetalic (glycosidic) hydrolysis. Alkaline solutions can additionally be used to extract cellulose though these advertently dissolve hemicellulose (Wüstenberg, 2014). Suitable solvents used for extracting cellulose usually include dimethylacetamide/lithium chloride; dimethyl sulfoxide/tetrabutyl ammonium fluoride and aqueous copper (II) tetra-ammonium hydroxide solution (Schweitzer's reagent). A novel approach to extracting cellulose is by dissolving a source in a physical manner within ionic liquid, as patented by BASF (Swatloski, Rogers and Holbrey, 2002). Though, in order to fractionate and purify polysaccharide components within a pulp- like material, a concentrated sodium hydroxide solution can be used. Hemicelluloses are soluble in 17.5 % sodium hydroxide though α-cellulose is insoluble (Wüstenberg, 2014). The β-component is able to be separated from the ɣ-fraction by subsequent neutralisation. The β-fraction then precipitates whilst the ɣ-fraction goes into solution (Wüstenberg, 2014).There are two methods for hydrolysis to monomers which are acid or autohydrolysis. Garrote *et al*.

(2001), described autohydrolysis (which proceeds through acid-catalysed reactions) as being advantageous over acid hydrolysis due to:

(i) Corrosion problems are avoided, since no mineral acid is added to the reaction media,

(ii) No neutralisation sludges are required to be handled,

(iii) The mild operational conditions allow excellent selectivity towards cellulose degradation,

(iv) Limited concentrations of unwanted sugar-degradation products are found in the media,

(v) The soluble reaction products are useful for a variety of purposes,

(vi) Autohydrolysis can improve the susceptibility of the solid residues to further processing (including enzymatic hydrolysis of the cellulosic fraction or chemical delignification), owing to the improvements in cellulose accessibility and to the partial hydrolytic degradation of lignin (Garrote, Domínguez and Parajó, 2001).

Ibbett *et al*. (2011), used a full acid hydrolysis to assess the cellulose and other varying PCW polysaccharides of wheat straw. Extraction of hemicellulose and solid residues was carried out in 1 M sulfuric acid, for 2 hours (Hr) at 98 °C. Then, analysis of sugar monomers in all hydrolysates was determined by high-performance anion exchange chromatography with pulsed amperometric detection (Dionex, UK). They also compared autohydrolysis at 200 ºC and found no significant differences in cellulose content between auto and acid hydrothermal residues (59 % and 58 % respectively). Due to the nature of the current study such methodologies are

similarly used for modification (i.e. hydothermal) in Chapter 5 and necessary subsequent evaluation of biomass after said modification.

3.1.2 Hemicellulose

As aforementioned hemicellulose can be found intertwined with cellulose within PCWM. Its structural and functional information can be found in Chapter 1. Hemicellulose usually comprises xylose, glucose, arabinose and galactose (Ibbett *et al.*, 2011). This is species dependent and are either xyloglucans or galactoglucomannans. Hemicellulose can be extracted at the same time as cellulose using the same aforementioned method for cellulose (Ibbett *et al.*, 2011). Ibbett *et al*. (2011) found differing amounts of hemicellulose between auto- and acid- hydrolysis methodologies (6 and 2 %, respectively). The acid hydrolysis method was employed in this study, in order to assess hemicellulose within pea biomass. However, it is noted that in order to obtain a high degree of knowledge from each cellulose and hemicellulose, separate extractions are necessary (Preece, 1944), especially due to studies showing that delignification facilitates hemicellulose extraction (Norman and Shrikhande, 1935; Norman, 1937).

3.1.3 Lignin

Lignin is the second most abundant polymer found on Earth (Xu and Ferdosian, 2017). It is found within PCWM and provides strength and support. Further information regarding structural and functional properties can be found in Chapter 1.

There are three main methods of extracting lignin from plant-based materials which include (Hatfield and Fukushima, 2005):

I) thioglycolic acid,

II) acetyl bromide,

III) The Klason method (gravimetric assay).

The first two are associated with solubilising lignin then reading the solubilised sample at an absorbance wavelength of 280 nm (Moreira-Vilar *et al.*, 2014). The acetyl bromide method can provide an over estimation due to oxidative degradation of other polysaccharides (namely components of hemicellulose) (Hatfield *et al.*, 1999). The thioglycolic acid method can under estimate lignin content based upon specificity of the reaction with ether bonds of lignin (Brinkmann *et al.*, 2002). During precipitation using this method soluble lignin may remain in solution (Hatfield and Fukushima, 2005). Finally, the Klason method is a direct method of analysing both soluble and insoluble (through digestion in 72 % sulfuric acid) fractions of lignin (Moreira-Vilar *et al.*, 2014). However, other fractions of a mixed PCWM may be solubilised such as proteins and other polysaccharides not intended to be extracted, thereby increasing the supposed lignin content. In some instances, the Klason method under-estimates the lignin content due to a considerable amount of the soluble lignin fraction not being measured (Bunzel, Schüßler and Tchetseubu Saha, 2011). Moreira-Villar *et al*. (2014), compared all three methods on three differing plant tissues with contrasting lignin compositions. They found that although all the methods produced a high amount reproducibly, they found major inconsistencies between them. The thioglycolic acid under estimated the lignin content compared to others and the Klason method was similar to that of the acetyl bromide but only for samples with a high concentration of lignin. They suggested that acetyl bromide was the best method for recovering lignin. Therefore, acetyl bromide was used in this study to extract lignin with the assumption that it may overestimate the amount found.

3.1.4 Pectin

Pectin was first discovered as a gelling agent in the 1820's (Wüstenberg, 2014) and acts in combination with cellulose as an intracellular matrix substance. Previous statements on functionality and properties of pectin can be found in Chapter 1. Pectin consists of D-galactouronic acid, L-rhamnose, L-arabinose, D-galactose, xylose and small amounts of fucose. There can also be two types of pectin depending on their degree of methylation, which are high or low methoxy pectin (Sandarani, 2017). In investigating the amount of pectin within a sample one usually refers to the amount of galacturonic acid found within the sample, as FAO regulations currently state that pectin must contain at least 65 % galacturonic acid (Liew, Chin and Yusof, 2014).

The conventional method of extracting pectin is one which involves hydrolysis of proto-pectin into pectin using acids and then subsequently precipitated by ethanol (Pagán *et al.*, 2001; Djilas, Čanadanović-Brunet and Ćetković, 2009; Kanmani *et al.*, 2014; Sandarani, 2017). Other novel methods including microwave assisted, enzymatic, supercritical water and ultrasound extractions have been reported (Ros, Schols and Voragen, 1996; Liew, Chin and Yusof, 2014). In a review of pectin extraction by Sandarani (2017) a number of methods were evaluated. Sandarani (2017) stated that microwave extractions do not differ in yield of pectin in comparison to the conventional acid methods. Particular enzymatic extractions using cellulase and polygalaturonase provide higher quantities of pectin. The supercritical water method is conventionally used as a commercial process for extracting pectins. Wang *et al*. (2015) compared supercritical water with ultrasound extractions of pectin from grapefruit peel. They found that the ultrasound extraction provided higher yields of pectin by 16.34 % (Wang *et al.*, 2015).

Therefore, one can deduce that higher yields of pectin may be extracted from either using enzymes or ultrasound extractions.

Pectin concentrations were not assessed in this study but assessed in a collaborative study whereby the results (galacturonic acid content) are presented in this study, additionally to the paper currently under review and attached in the appendix (Ibbett *et al*., 2019).

3.1.5 Starch

Starch is produced by most green plants and cultivated as agricultural crops which are considered to be staple foods. Starch provides plants with energy storage, further information regarding structural and functional properties can be found in Chapter 6.

Starch is usually extracted using an enzymatic method or acid hydrolysis (Anon, 1987). Acid hydrolysis procedures are only feasibly accurate for samples which contain just starch (Knudson, 1997). Before, the A.O.A.C method 920.40 required the use of Rhozyme-S though this since has been discontinued (Hall, 2009). New enzymatic methods were necessary to be sought after, for the total analysis of starch within a sample. The main enzymatic colourimetric method uses two stages for determination of total starch, a thermostable α-amylase and amyloglucosidase enzymatic extraction at a low pH of 5, A.O.A.C method 996.11 (A.O.A.C., 2006).

Zhu *et al*. (2016), evaluated the A.O.A.C international method 996.11 with a modified glucoamylase method and found that the glucoamylase method provided an overall greater extent of hydrolysis and therefore total starch determination. However, both methods overestimate total starch concentration in a feedstock, which has multiple components. Furthermore,

Hall. (2009) determined starch, including maltooligosaccharides, in various animal feeds and they found that the acetate buffer method developed by Knudesen (1997), provided higher amounts of total starch. McCleary *et al*. (1997) performed collaborative studies in order to test the reliability of Megazyme's total starch assay kit, which investigated biomass including green peas. This study then prompted an adoption of improvements of the assay kit from Megazyme to include an acetate buffer (McCleary, Gibson and Mugford, 1992). Based on these findings, the improved/adapted method of A.O.A.C 996.11 used by Megazyme is a total starch assay kit, used to calculate the total starch within mixed pea biomass in this study**.**

3.1.6 Protein

Proteins are a class of nitrogenous organic compounds. They have molecules comprising one or more long chains of amino acids and are essential for growth and repair of structural components within biological organisms. *Pisum sativum* have been ascribed as being a protein-high crop, which in recent years is being increasingly grown as a replacement of expensive protein supplements in animal feeds (Åman and Graham, 1987). Protein content of pea seeds appears to be highly variable, so the content in the remaining mature crop biomass (after harvest) may also vary. Utilisation of the entire crop has been recorded to raise protein quality, although it reduces protein content and digestibility of feeds overall (Lund and Håkansson, 1986).

Standard operating procedures for protein content use nitrogen content, peptide bonds, dye binding capacity based on isoelectric point, U-Vis absorptivity and light scattering, which may all give differing protein contents

of the same sample (Hill, 2014). In order to prepare samples for such techniques, differing chemical solvent-based extractions are used (Mitra *et al.*, 2009) including:

I) Bicinchoninic acid on materials having already had their chlorophyll and lipids extracted by using tricholoroacetic acid (TCA) – acetone (Santoni, Bellini and Caboche, 1994),

II) Phenol based extractions followed by methanol and ammonium acetate precipitation (Hurkman and Tanaka, 1986; Meyer *et al.*, 1988; Mijnsbrugge *et al.*, 2000; Isaacson *et al.*, 2006),

III) Hybrid techniques such as a combination of TCA–acetone/phenol (Wang *et al.*, 2006),

Accordingly, no single protocol captures the entire proteome (Abdullah, Chua and Rahmat, 2017). Overall, most analytical methods can overestimate protein contents (Mæhre *et al.*, 2018). Inaccuracies can be linked to nitrogen determinations and subsequent conversion to protein, as well as interference from other varying chemical substances within the plant matrices. Therefore for food analysis, amino acids determination content is the preferred method of assessment, as interfering substances are less likely to affect results (Mæhre *et al.*, 2018). However, the American Meat Association state that gas combustion used by the Fisons, NA 2000 to assess nitrogen content can give some clear advantages over previous analytical methods, such as time, labour and saving on consumption of hazardous waste. Furthermore, Williams *et al.* (1995) found this method gave identical results to the standard Kjeldahl crude protein analysis albeit they both assess total nitrogen rather than protein. Lastly, Williams *et al*. (1995) stated that electrophoresis gave better results due to minimal

interference (Williams, Fox and Marshall, 1995). The Kjeldahl method is still widely used as a standard method with good reproducibility for the estimation of protein in foods. However, in these works a nitrogen analyser was used.

3.1.7 Lipids

Lipids are a class of organic compounds consisting of fatty acids and or their derivatives. They are extracted with relatively non–polar solvents such as ethyl ether, chloroform, or benzene (Morris, 1972). Membrane–associated lipids require polar solvents such as ethanol or methanol, in order to disrupt hydrogen bonds or electrostatic forces found between lipids and proteins (Morris, 1972). Lipid fractions have been evaluated based on methodologies from Folch *et al*. (1957) and Bligh and Dyer., (1959), whereby lipids of biological materials (brain and fish muscle) were rapidly extracted as a total lipid volume. The tissue, when in a mixture of chloroform:methanol and subsequently mixed in water, would yield a monophasic solution (Folch, Lees and Slone Stanley, 1957; Bligh and Dyer, 1959). If, diluted further with chloroform, then the resulting sample would produce a biphasic system (Euvrard *et al.*, 1996). The chloroform phase then contains the lipid fraction. Bligh and Dyer compared the method to previous methodologies (Dyer and Morton, 1956; Saito, 1967; Ros-Freixedes and Estany, 2014) and found their aforementioned method to be least time consuming and simpler (Bligh and Dyer, 1959). Sato and Tsuzuki. (2011) successfully used Bligh and Dyers's method to extract lipids from algae and chloroplasts (Sato and Tsuzuki, 2011). Finally, Fishwick and Wright. (1977), compared different lipid extraction methods and found Bligh and Dyers's to be the most successful when working with plant tissue (Fishwick and Wright, 1977).

3.1.8 Chlorophyll and carotenoids

Chlorophyll and carotenoids pigmentation provides fruit and vegetables with their unique colour (Lancaster *et al.*, 1997). These are present in the chloroplasts, chromoplast and phenolic pigments in the vacuole of a plant cells. This expression of colour found is a result of physical factors, such as the presence of epidermal hairs, cuticular waxes and the shape and orientation of cells in the epidermis and sub–epidermis (Lancaster *et al.*, 1997).

Chlorophyll and carotenoid evaluation can be complex due to the pigment's absorbance overlapping in spectral regions (Lichtenthaler and Buschmann, 2001). However, various methodologies for pigment content determinations may give concentrations differing by as much as 20 % (Linder, 1974). Shifts occur within the spectra based on the polarity of solvents used, for example, for chlorophyll a, the red spectrum can shift from 660 nm to 665 nm (Lichtenthaler and Buschmann, 2001). A common protocol for assessing chlorophyll content is that of Lichtenthaler. (1987), using equations from Lichtenthaler and Buschmann (2001). Whereby, three wavelengths are specifically unique for each chlorophyll and total carotenoids (661.6 nm for Chlorophyll a, 644.8 nm for Chlorophyll b, 470 nm for Total Carotenoids). The pea crop results have been assessed using this method (Torcello-Gómez *et al.*, 2018), for both chlorophylls and total carotenoids. Therefore, the Lichtenthaler and Buschmann. (2001), methodology to assess chlorophyll and total carotenoids were employed in this study. Torcello-Gómez *et al.* (2018) found high levels of chlorophyll a (225 µg/g), within pea plant juice obtained previously at the same institute as the biomass used in this study. Due to high concentrations, being found in the aforementioned

study it may result in a lower content found within the biomass. A hypothesis could therefore be drawn that with, the juice rich fraction having a high quantity of chlorophyll, carotenoids and micro-nutrients amounts present. The resulting biomass/fibre would result in having lower amounts present.

3.1.9 Ash content

Ash content is the measurement of minerals present within foods. Ash is the inorganic residue left after water and organic matter are removed through heating with the presence of oxidising agents. There are three main principle procedures to determine ash content which are based on a wet, dry and low temperature plasma dry basis (McClements, 2003). The most appropriate method used would depend on why one is carrying out the analysis and the food type under investigation. Dry ashing is done at high temperatures using a muffle furnace, with organic substances burning in the presence of oxygen in the air to carbon dioxide, water and nitrogen. During this analysis minerals convert to oxides, sulphates, phosphates, chlorides or silicates. A disadvantage to this method is that some minerals may be partially lost such as iron, lead and mercury due to the greater volatility. Wet ashing breaks down and removes organic matrix which surround minerals so that they are left in an aqueous solution. Dry samples are usually weighed in a container with strong acids and oxidising agents then subsequently heated until the organic matter is digested with only mineral oxides are left in solution. With this method little volatile minerals are lost because lower temperatures are used. However, it is labour intensive and hazardous chemicals are necessary, with low sample throughput. Low temperature plasma ashing involves breaking down oxygen to nascent oxygen with an application of an electromagnetic radio frequency field. The organic matter is rapidly oxidised

and water evaporated due to an increase in temperature. Similar to wet ashing, low temperature plasma ashing reduces the loss of trace elements through volatilisation (McClements, 2003). However, the methodology requires the availability of equipment. Dry ashing is considered to be the standard method procedure for assessing ash content within samples (A.O.A.C., 2000). A.O.A.C have four methods for determining ash content of foods and one method for assessing acid insoluble ash. The four main methods tend to be for specific materials such as flour (method 923.03), animal feed (method 942.05), milk (method 945.46) and mineral ash (method 942.05). The mineral ash method has changed over time. Thiex *et al. (*2012), trialled fifteen varying animal feed samples using the 942.05 method (600 ºC for 2 Hr), to investigate its performance on ash content. In order to test its performance, they varied the method conditions including:

1) 600 ºC for 4 Hr,

2) 600 ºC for 2 Hr, cool, and ignite for 2 Hr,

3) 600 ºC for 2 Hr, cool, wet, dry, and ignite 2 Hr,

4) 550 ºC for 6 Hr; 550ºC for 3 Hr, cool, and ignite 3 Hr,

5) 550 ºC for 3 Hr, cool, wet, dry, ignite for 3 Hr (Thiex, Novotny and Crawford, 2012).

They found results differed significantly from the standard A.O.A.C. 942.05 method and recommended modifications to the original method. These differences may possibly be due to the amount of time for which a sample is heated, as well as their water content. The ash content method of A.O.A.C. (2000) states that a material is heated at 550 ºC overnight, which may either diminish some minerals but may ensure that organic substances are fully

oxidised within this time frame. Therefore this adapted yet older method, is chosen as the basis of analysis in this study.

An increased cultivation of *Pisum sativum* has been ascribed to improve crop rotations, a reduce nitrogen demand of fertilisation and has helped diminish the over production of cereals (Åman and Graham, 1987). Åman and Graham. (1987) found that mature pea seeds constitute around 50 % of the whole crop. With such an upsizing in production of this crop it is ideal, as one to valorise the unused portion, to create an additional product for human consumption.

3.1.10 Aims of this chapter

Therefore, ultimately the aim is to:

- Valorise pea crops utilising the wasted portion after pea harvest,
- Calculate the chemical composition of this mixed biomass,
- Assess the dietary and health benefits of using pea biomass as an ingredient in a food product,
- Later, assess properties of this material and how it can be physically manipulated through processing, compared to other food grade polymers as a comparison.

Results will quantify the composition of what will be a new novel functional food ingredient after modifications described in Chapter 1.

3.2 Materials and methods

3.2.1 Materials preparation:

On harvest day whole pea crop (mature crop once seeds are removed and without roots) was collected from a farm in Driffield, East Yorkshire, Green Pea Company Ltd (The Green Pea Company, 2019). The pea crop aka halum includes the stems, leaves, tendrils and pods.

1) Batches of the biomass were water washed at ambient temperature using a hose pipe and home-made large sieves, which were used to remove stones and other debris that may have been collected during harvest.
2) The whole wet pea crop was put into a large electric salad spinner (Sammic 12 kg ES-200, Nisbets plc, Bristol, UK) for 3 minutes for hydro-extraction to remove excess/entrained water.
3) Damp whole pea crop (course-cut) was pressed using a commercial twin-screw juicer (Angel 7500 twin gear juicer, Juiceland, St Helens, UK) at ambient temperature to separate the juice (green intra-cellular liquor contents) and fibrous/pulp rich (cell-wall residue) fractions, known as Pea Biomass (PB) for the remainder of these works.
4) 200 g batches of PB was placed in sealed containers in a -80 °C freezer (Denley CFC-Free -80 °C freezer, China) immediately after juicing.

Juice fractions were not used in any part of this study.

All PB used for the project was processed within a 14 Hr period from one single harvest collection. When needed for assessment purposes, PB in its wet form was used after leaving to thaw at 25 °C for 3 Hr.

Solka Floc 900 (SF) was used as a comparison as an example of a pure cellulosic system in other results chapters (International Fibre Corporation, New York, USA). Details of the composition can be found in results 3.3. SF was stored at 25 ºC in a dark cupboard.

3.2.2 Drying and storage

The fibre, once defrosted, was then oven dried for 24 Hr at 105 ºC (UN 110, Memmert, Germany) before each compositional assessment. Water content was assessed using Equation 4. The sample was then placed in a desiccator with phosphorus pentoxide (Sigma Aldrich, UK), for 3 Hr, to remove any further water and calculated based on calculations from the A.O.A.C, 2000 method. Water content was used in order to ensure the PB was fully dried prior to any analysis.

Equation 4 $$\boldsymbol{Water}\ (\%) = \frac{(\boldsymbol{Weight\ (g)\ \ before\ drying}) - \boldsymbol{Weight\ (g)\ after\ drying})}{\boldsymbol{Weight\ (g)\ before\ drying}} \boldsymbol{x100}$$

After oven drying, PB was stored in a sealed container in a dark cupboard.

3.2.3 Analytical methods

All reagents used in these works were sourced from Sigma Aldrich with a purity of > 99 % unless stated otherwise.

3.2.3.1 Sugar composition of hemicellulose and cellulose

In order to calculate the cellulose and hemicellulose content of PB the following protocols were followed:

1) 30 mg of PB to 1 ml of 12 M sulfuric acid was added, incubated in a 37 °C water bath (Grant, Shepreath, England) for 1 Hr.
2) 11 ml of RO water was subsequently added to make the PB dispersion 1 M and incubated in a water bath at 99 °C for 2 Hr.
3) Samples were then cooled to stop any further reaction.
4) The dispersion was then vortexed for 1 minute (min).
5) 100 µl of supernatant (ensuring no large particles) from the suspension was pipetted off and added to 10 ml of RO water.
6) Samples were centrifuged at 5000 rpm for 5 min to settle any remaining particles (Rotina, 380R, Hettich, Shelton technical ltd, Milton Keynes, UK).
7) 1 ml of the supernatant after centrifugation was added to Dionex vials for sugar analysis using high-performance anion exchange chromatography with pulsed amperometric detection (Dionex AS ICS-3000, ThermoFisher Scientific, UK), using a CarboPac PA20 column with isocratic elution at a working flow rate of 0.5 ml/min.

Monosaccharide standards glucose, xylose, arabinose and galactose were combined as a stock combination solution made diluted using 10 mM of sodium hydroxide (Pellets purity 98 %, Honeywell Fluka). Finally using these standards a calibration curve was constructed (Ibbett *et al.*, 2011).

For reported pectin amounts (assessed through galacturonic acid content), a total acid hydrolysis protocol was applied to the PB and the work was carried out as part of a collaborative study, of which the paper is currently under review (Ibbett *et al.,* 2019).

3.2.3.2 Lignin content

In order to calculate lignin content of PB the following protocols were followed:

1) 0.1 g of PB were incubated in a 4 ml solution of 25 % v/v acetyl bromide: acetic acid at 50 °C for 2 Hr.
2) The PB dispersion was then cooled for 5 min to prevent any reaction further occurring.
3) Standards contained 0.01 g of lignin (Low sulfonated, pH 10.5, Sigma Aldrich) and were dissolved in a 6 ml solution of 75 % v/v acetone.
4) The standards and samples were then vortexed (0.05, 0.1, 0.2, 0.3, 0.4 and 0.5, see Table 2): acetone solution was transferred to fresh reaction tubes containing a 0.5 ml solution of 25 % acetyl bromide in acetic acid.
5) Then samples and standards were incubated for 30 min at 50 °C and additionally cooled after.
6) In order to prepare the samples for spectrophotometry, a 12 ml solution of acetic acid was added to treated samples (not lignin standards).
7) 0.5 ml was extracted from the PB dispersion and standards into a fresh tube then to make up analysis in 0.2 ml acetone.
8) Furthermore, 0.5 ml 25 % acetyl bromide: acetic acid was used as a blank.
9) Samples were mixed using a vortex so that they were homogenous.
10) Finally, 1 ml of the blank, PB dispersion and standards, was dispensed in a quartz cuvette (no UV interference) and each sample was read using a wavelength of 280 nm on a Cary U-VIS

spectrophotometer (Varian Cary 50 probe UV-vis spectrometer, Agilent technologies, USA) (Sluiter *et al.*, 2008).

Table 2 Calibration of lignin sample

Components	**Sample and blank (ml)**	**Calibration samples (ml)**					
		0.05	**0.1**	**0.2**	**0.3**	**0.4**	**0.5**
Sample	0.5	0.55	0.6	0.7	0.8	0.9	1
Glacial acetic acid	2.5	2.5	2.5	2.5	2.5	2.5	2.5
0.3 M sodium hydroxide	1.5	1.5	1.5	1.5	1.5	1.5	1.5
0.5 M Hydoxylamine hydrochloric acid	0.5	0.5	0.5	0.5	0.5	0.5	0.5
Glacial acetic acid	5	4.95	4.9	4.8	4.7	4.6	4.5

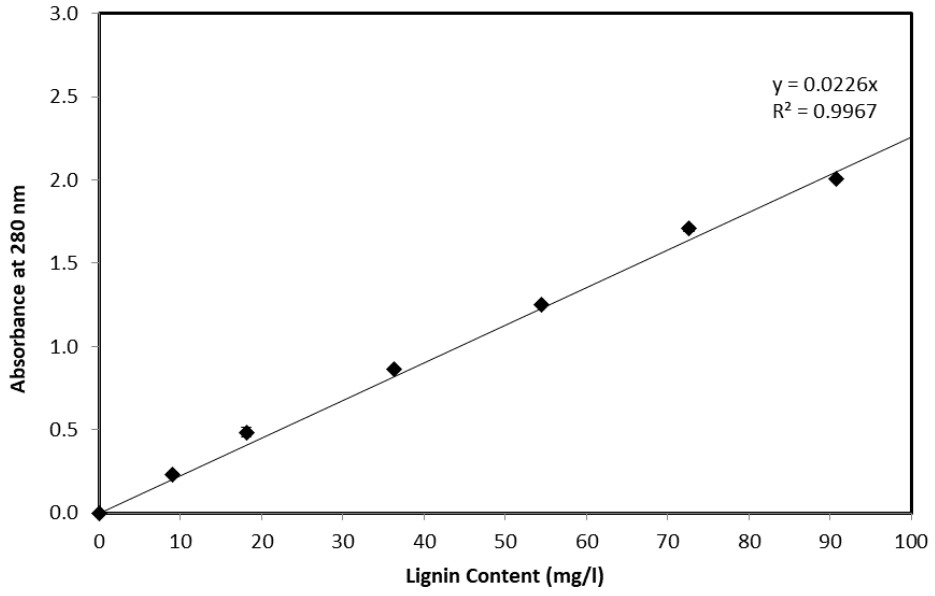


Figure 11 Example of a standard calibration curve for lignin obtained.

3.2.3.3 Starch content

Starch was assessed by using a SA20-Total Starch HK assay kit from (Megazyme, Ireland). In order to calculate starch content of PB the following protocols were followed:

1) 0.1 g of dried PB was added to a 20 ml solution of dimethyl sulfoxide,
2) The PB dispersion was then vortexed for 1 min.
3) A 5 ml solution of 8 M hydrochloric acid was subsequently added,
4) The PB dispersion was then again vortexed for 1 min.
5) The PB dispersions were then incubated for 30 min at 60 ºC,
6) After incubation 50 ml of RO water was added to the PB dispersion and the pH of the dispersion was adjusted to 5 using a 5 M solution of sodium hydroxide.
7) The PB dispersion when at room temperature was made up to 100 ml using RO water.
8) To continue the starch assay the following solutions (Table 3) were made.
9) The starch assay solutions were incubated for 15 min at 60 ºC and cooled after incubation to prevent further reactions.
10) For the glucose assay the following solutions (Table 4) were made and incubated for 15 min at 20 ºC.
11) PB dispersions, glucose assays and starch assay solutions were measured for absorbance at 340 nm using a Genesys 10S Vis spectrophotometer (Themo Fisher Scientific, China).

Table 3 Calibration amounts calculated for Starch assay reagent.

Tube	Starch assay reagent (ml)	PB dispersion (ml)	Water (ml)
Starch assay reagent blank	1	0	1
Sample blank	0	1	1
Glucose assay reagent blank	0	0	2
Sample test	1	1	0

Table 4 Calibration amounts calculated for Glucose assay reagent.

Tube	Glucose assay reagent (ml)	Sample volume (µl) (solutions from starch assay)
Starch assay reagent blank	1	50
Sample blank	1	50
Glucose assay reagent blank	1	50
Sample test	1	50

The starch content was determined using Equation 5:

Equation 5

$A_{\text{total blank}} = (A_{\text{sample blank}} - A_{\text{glucose assay reagent blank}}) + A_{\text{starch assay reagent blank}}$

$$\text{Starch (mg/ml)} = ((\Delta A)\left(\frac{\text{TVSA}}{\text{SVA}}\right)\left(\frac{\text{TVGA}}{\text{SVGA}}\right)(\text{MW starch}))/((\varepsilon)(\text{d})(1000)) \quad \text{(Eq:6)}$$

Abbreviations for starch mg/ml:

$\Delta A = A_{\text{test}} - A_{\text{total Blank}}$

TVSA = Total Assay Volume from Starch Assay in mL = 2ml.

SVSA = Sample Volume from Starch Assay in mL = 1 ml.

TVGA = Total Assay Volume from Glucose Assay in mL = 1.05 ml.

SVGA = Sample Volume from Glucose Assay in mL = 0.05 ml.

Starch MW = 162.1 g/mole or equivalently or 162.1 µg/µmole.

ε = Millimolar Extinction Coefficient for NADH at 340 nm millimolar^{-1} cm^{1} or equivalently (mL/µmole)(1/cm) = 6.22 mM^{-1}cm^{-1} .

d= Light path (cm) = 1 cm.

1,000 = conversion Factor for µg to mg.

3.2.3.4 Protein content

Protein content was measured indirectly on a dry weight basis through N_2 using a Fisons nitrogen analyser Na2000 (Fisons instruments, Italy). This will be an overestimate as non-proteinaceous sources of nitrogen will additionally be recorded. Protein estimate was calculated via Equation 6. Nitrogen conversion factor used based on the findings of Mossé, 1990 for pea seeds.

Equation 6 $$\boldsymbol{Protein\ estimate}\ (\%) = \boldsymbol{Nitrogen\ x\ 5.48}$$

3.2.3.5 Lipid content

In order to calculate lipid content of PB the following protocols were followed:

1) A 1.2 ml solution of 2:1 chloroform: methanol was added to 0.1 g of dried PB.
2) The PB dispersion was then vortexed for 1 min.
3) A 0.3 ml solution of 0.9 % sodium chloride solution was subsequently added to the PB dispersion.
4) The PB dispersion was then again vortexed for 1 min.
5) The PB dispersion was then centrifuged at 3000 rpm for 10 min (Rotina, 380R, Hettich, Shelton technical ltd, Milton Keynes, UK).

6) The lowest phase (supernatant) of the three phases now observable in the PB dispersion was transferred using a glass pipette to a new empty centrifuge tube.
7) A 1.2 ml solution containing chloroform: methanol (2:1) was subsequently added in the same manner and centrifuged then pipetted until no pooled lipid layer remained (repeating steps 1, 2, 5 and 6).
8) The centrifuge tube containing extracted lipids was then syringed with a connected 0.45 µm PTFE filter (Whatman, Sigma Aldrich, Dorset, England), into a pre-weighed bijoux bottle.
9) The then filtered PB dispersion extract was dried under 2 bars of nitrogen for 30 min^{-1} Hr.
10) The dried lipid extract from the PB dispersion, in the pre-weighed Bijoux bottle was then subsequently re-weighed. Total lipid was calculated by the following:

Equation 7 $$\boldsymbol{Total\ lipid}\ (\%) = \frac{\boldsymbol{Weight\ of\ dry\ lipid\ extract\ in\ Bijoux\ bottle}}{\boldsymbol{Weight\ of\ pre-weighed\ Bijoux\ bottle}} \boldsymbol{x\ 100}$$

3.2.3.6 Chlorophyll content

In order to calculate lipid content of PB the following protocols were followed:

1) 1 ml of pure acetone was added to the dried lipid extract from section 3.2.4.1.5.
2) The lipid acetone dispersion was then vortexed for 1 min.
3) The lipid dispersion was diluted with acetone to a factor of 1:1000 using a two-step serial dilution.
4) 1 ml of the diluted lipid dispersion was transferred to a glass cuvette and read using a Genesys 10S Vis spectrophotometer (Themo Fisher Scientific, China).

Three wavelengths were then measured on the spectrophotometer:

1. 661.6 nm (Chlorophyll a)
2. 644.8 nm (Chlorophyll b)
3. 470 nm (Total Carotenoids)

For calculating pigment concentration firstly pigments (µg/ml) of each Equations 8, 9 and 10 for Chlorophyll a (Ca), Chlorophyll b (Cb) and total Carotenoids (Car) must be calculated (Lichtenthaler and Buschmann, 2001):

Equation 8 $$\boldsymbol{Ca = (11.24\ x\ A661.6) - (2.04\ x\ A644.8)}$$

Equation 9 $$\boldsymbol{Cb = (20.13\ x\ A644.8) - (4.19\ x\ A661.6)}$$

Equation 10 $$\boldsymbol{Car = \frac{(1000\ xA470) - (1.90\ x\ Ca) - (63.14\ x\ Cb)}{214}}$$

Then pigment concentration (%) can be calculated using:

Equation 11 $$\boldsymbol{Pigment\ content}\ (\%) = \frac{\boldsymbol{Concentration}\left(\frac{\mu g}{ml}\right)\boldsymbol{x\ dilution}\ \text{factor}\ (1000)}{\boldsymbol{Weight\ of\ sample}}$$

3.2.3.7 Ash content

1 g of dried PB samples from water content assessment were placed in crucibles and ashed, in a Muffle furnace (AAF 1100, Carbolite ltd, UK) at 550 °C for 8 Hr. The ash content was calculated using Equation 12 (A.O.A.C. 2006):

Equation 12 $$\boldsymbol{Ash\ content}\ (\%) = \frac{\boldsymbol{Ash\ weight}}{\boldsymbol{Dried\ sample\ weight}}\ \boldsymbol{x100}$$

3.2.4 Statistics

Information regarding statistics can be found in the techniques chapter.

3.3 Results

3.3.1 Composition of Pea biomass

The composition of PB consisting of pods, stems, tendrils and leaves (after juicing) was investigated through differing analytical measurements and the results are depicted in Figure 12. The results depict that the majority of the system consists of polysaccharides, and summarised in Table 5.

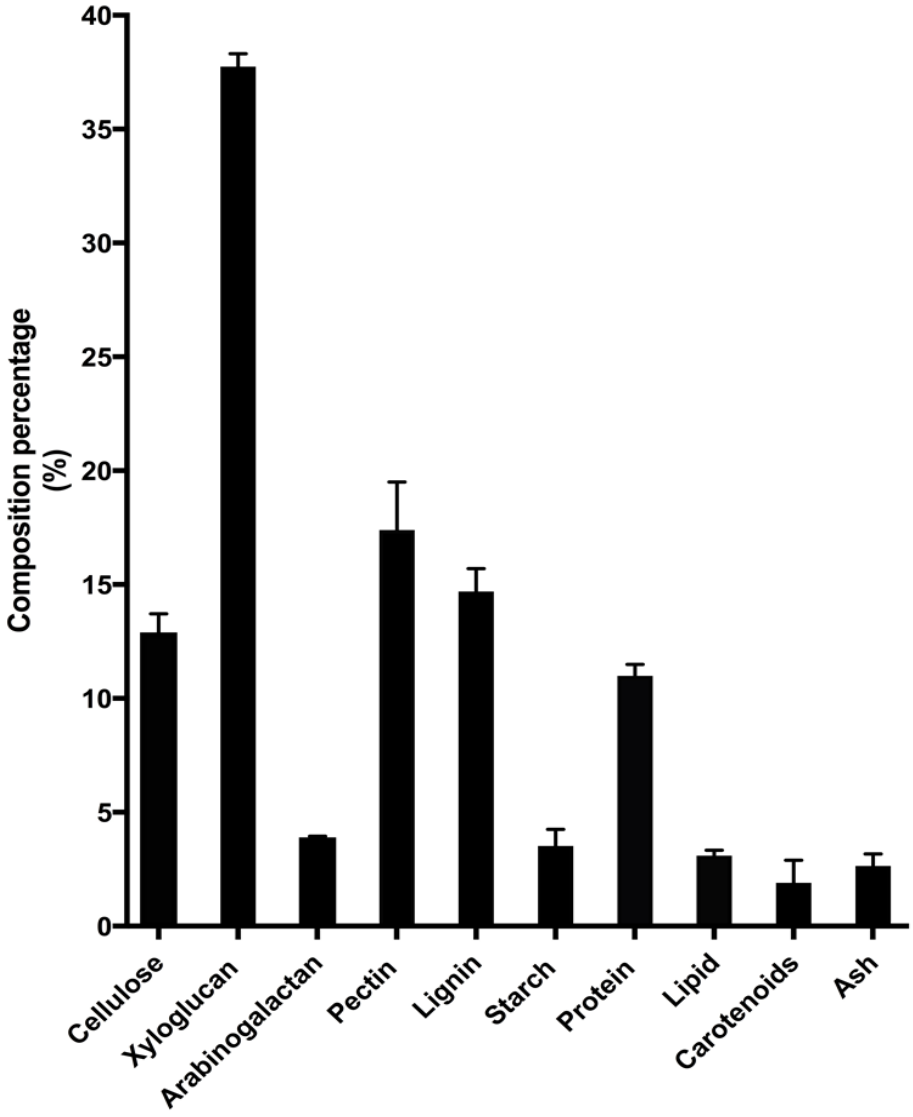


Figure 12 Composition (%) of Pea Biomass (error bars depict Standard Error (SE) off means).

Table 5 Summarised dry matter yields (%) for the present study's PB (cellulose from glucose and hemicellulose calculated from xyloglucan and arabinogalactan), Åman and Graham (1987) and Treviño, Centeno and Caballero, (1986) for whole crop peas, stems, leaves and pod/seeds or flowers. Carotenoids not included as comparison studies did not evaluate it. Values are rounded up or down, without decimals.

		Åman and Graham (1987) (%)				**Treviño, Centeno and Caballero (1986) (%)**			
Nutrient type	**PB**	**Whole plant**	**Stem**	**Leaf**	**Pod/ flower**	**Whole plant**	**Stem**	**Leaf**	**Pod seed**
Cellulose	13	23-31	14-35	9-25	6-24	14-15	23-31	12-22	7- 10
Hemicellulose	42	10	15	9	19	5-12	8-13	5-12	10
Lignin	15	5-8	10.5-16.5	4.5-14.5	2- 9	4-6	6-13	3-7	2
Pectin	17	5-9	7-10	9-14	4-10	-	-	-	-
Protein	11	22-40	3-9	15-22	5-35	16-20	11-22	8- 11	20-26
Starch	4	4-24	1-6.5	1-7	5-9	8-22	4-7	6-8	14-34
Lipids	3	1-4	1-2	1-4	1	-	-	-	-
Ash	2	6-8	4-6	6-8	2-6	8-9	9-11	9-14	4-5

3.3.2 Cellulose

The cellulose fraction was derived from the glucose concentration once glucose associated with xyloglucan was subtracted and comprised around 12.9 % of the total mixed biomass.

In pea crops, Åman and Graham (1987) recorded concentrations for all macronutrients for the whole crop as a mixed biomass, as well as for individual botanical fractions (see Table 5). In the whole crop, the Non-Starch Polysaccharide (NSP) concentration (which include cellulose, hemicellulose and pectin), was around 22.5-39 % ± 1. This depended on the maturity of the crop and the time of year tested. The first harvest is when immature pea seeds are forming, the second harvest when pea seeds are formed, the third harvest when peas are filled and the fourth harvest in which the botanical fractions undergo senescence. In the mixed whole crop biomass, glucose (which was directly linked to cellulose) was found to vary between 8.5-29 %. In individual botanical fractions (stems, leaves, flowers and pods) they found that the NSP concentrations increased during growth

and development. Specifically, the glucose content: stem were 14-35 %, leaf 9-24.5 %, flower and pod 6-23.5 %, respectively. Such variation is thought to be due to differing harvest periods and maturity of the crop. The higher the concentration of cellulose can be linked to the maturity of the plant. However, in comparison glucose in pea seeds (5-9 %) seems to be substantially lower than the other botanical fractions. Additionally, Treviño, Centeno and Caballero (1986), also investigated nutritional composition of pea plants and their botanical fractions, and found that cellulose was around 14-15 % ± 0.68 for the whole crop, as a mixed biomass (see Table 5), which is more associated with findings found in these works. With individual botanical fractions containing 23-31 %, 12-22 % and 7-10 % for stems, leaves and pods/seeds, respectively. The two studies show a lot of variability in glucose concentration due to the stage of maturation. Therefore, the results obtained in this current study are similar to those found by Åman and Graham (1987), in their mature mixed pea crop biomass and slightly less than that of Treviño, Centeno and Caballero (1986). This suggests that Åman and Graham's use of a sodium acetate buffer and enzymatic method from Larson and Bengtsson (1983) provides similar results to those presented here (Larsson and Bengtsson, 1983). Whereas, Treviño, Centeno and Caballero (1986), modified a detergent system of Robertson and Van Soest (1981), providing a lower measured concentrations (15 > 34 %). The differences found here may be due to environmental conditions, which have been shown to affect nutrient composition, such as climate and origin of the crop. This may be due to mechanisms of extraction with the larger differences witnessed between the whole crops mixed as one biomass. Moreover, neither study took into consideration the ratio of glucose to xylose in xyloglucan fractions of hemicellulose and therefore did not subtract this glucose amount from their total cellulose concentration. If, used in sufficient

amounts as an ingredient, this material would provide a nutrition claim to a product by the European Commission and European Union as a source of high fibre, due to the content of dietary fibre within the sample (European Commission, 2018). Furthermore, as cellulose is a major compositional component within this material it has the potential to be modified into a functional food ingredient with differing properties such as, a thickening agent and providing structural reinforcement properties (Saha and Bhattacharya, 2010). However, as cellulose only consists of less than a third of the overall system composition other macronutrients/biopolymers may impinge modification and affect the objective properties.

3.3.3 Hemicellulose

The hemicellulose fraction taken from combining the xyloglucan and arabinogalactan was found to be 41.65 % (±0.61) in the mixed pea biomass. Xyloglucan was calculated based on the ratio of 4:3 glucose to xylose, respectively (Kajiwara and Miyamoto, 2004). Therefore the total glucose amount (34.5 %) observed had 21.6 % of the 34.5 % glucose associated with xylose (16.2 %) and thus xyloglucan amounts were 37.8 % in total. Arabinogalactan (3.9 %) was calculated by adding both arabinose (2 %) and galactose (1.9 %), which assumptions were made that these sugars were only associated with hemicellulose though they could additionally be associated with pectin.

In pea crops Åman and Graham (1987), measured the amount of xylose, rhamnose, arabinose and galactose and found them to constitute up to 10 % of the mixed whole biomass. In other botanical fractions these sugars constituted up to 15 % in the stem, 9 % in the leaf and 18.5 % in the flower

and pod. Treviño, Centeno and Caballero (1986), found the hemicellulose amounts in mixed whole crops to be between (5 and 12 % ± 0.57) and 8-13 %, 4-8 % and 7-10 % in the stems, leaves and pods/stems, respectively. Again variations are dependent on maturity of the crop. Therefore results presented in the current works have accounted for more hemicellulose than aforementioned studies. Similarly, with cellulose, this may be due to mechanisms of extraction (extractions mentioned in section 3.1.1) and origin, climate of growth and crop maturity. Furthermore, neither study took into consideration subtracting glucose from cellulose for xyloglucan observations. Therefore neither study had similar results to the findings presented here. Thus with the addition of cellulose content as a raw material the added hemicellulose (within a PCWM) would provide a food ingredient with added dietary fibre.

3.3.4 Lignin

After acetyl bromide extracts of the mixed pea biomass were used to measure lignin and a value of 14.72 % (±0.91) obtained. Åman and Graham (1987), investigated the Klason lignin concentration of pea plant botanical fractions and of the entire plant as one mixed biomass. They found the lignin content in the whole plant to be between 5–7.5 %. Then 10.5-16.5 %, 4.5-14.5 %, 1.5-9 % in the stem, leaves and flower/pod, respectively. Also the lignin content was highly variable, with the highest concentration found was when the pea plant was in its most mature form. Treviño, Centeno and Caballero (1986), additionally measured lignin in a mixed biomass and botanical fractions of a pea plant. They found the lignin concentration to be 3-7 %, 6-13 %, 2 % and 4-6 % in the leaves, stems, pods/seeds and in the whole plant, respectively; which depended on the crop maturity. In

comparing these two studies with results in this study it suggests that the acetyl bromide extraction method results in a significantly higher (nearly 3 x more) extracted lignin than permanganate lignin (Robertson and Van Soest, 1981) used by Treviño, Centeno and Caballero (1986) and Klason method used by Åman and Graham. As aforementioned the acetyl bromide method can over estimate lignin content due to oxidative degradation of other polysaccharides namely components of hemicellulose. Moreira-Villar *et al.* (2014), found that the Klason method provided similar results to those found in these works, when original lignin concentrations were high. This provides assumptions that either the acetyl bromide method was more appropriate for assessing lignin within pea biomass, due to concentrations of lignin being below a particular threshold, or the concentration amount found in the current study is an overestimation, due to the solubility of other components within the matrix. Over 100 % of the composition biomass is measured and accounted for in this study, which allows some confidence in the data for slight overestimations.

3.3.5 Pectin

Pectin was evaluated through analytical methods as part of a collaborative study, Ibbett *et al*. (2019) found the amount within the sample to be 17.21 ±2.1% taken purely from galactouronic acid content.

Åman and Graham (1987), investigated the amount of galactouronic acid of pea plants as a mixed biomass or as botanical fractions. They found the amounts of pectin to be: total biomass (4.5–8.5 %), leaves (9-14 %), stem (7–10 %), flower and pod (4–10 %) depending on maturity and year. Therefore pectin content evaluations used in the current study are higher

than the amount found in a mature mixed crop by Åman and Graham. The resulting overestimation could be due to other components not being fully solubilised in their assessments of analysis. However, in earlier findings by Åman and Graham, lower concentration for lignin and hemicellulose were found. Pectin is a natural viscosifier (Flutto, 2003) and the concentration of pectin within the materials in this study is over 10 %, which therefore may provide viscosifying and gelling properties when used as an ingredient in a product.

3.3.6 Starch

The starch content measured within the mixed pea biomass was 3.5 % ±0.8. Åman and Graham (1987), investigated the starch content of pea plants in botanical fractions and found the contents to be: stem (<1-6.5 %), leaf (>1-7 %), flower and pod (5-9 %) and mixed biomass (4-23.5 %). The concentrations measured again varied with maturity. However, an opposite trend was witnessed in comparison to lignin, whereby starch concentration decreases with maturity. This may be because sugars are translocated, which is the movement of materials in a water medium by the phloem (tissue) of the plant (Raven, Evert and Eichhorn, 1999), to the pea seeds during maturation. They also found that starch amounts increased slightly in the pea seeds and had the highest concentration of starch in comparison to other botanical fractions. Treviño, Centeno and Caballero (1986), also measured the starch content in fractions and as a whole biomass of pea plants and found stems (3.52-7.13 ± 0.38 %), leaves (5.80-7.60 ± 0.52 %) and as a whole plant (7.51-22.24 ± 0.83 %). They found similar trends to Åman and Graham in that the starch content is highest when the plant is most immature and through maturity it decreases (Treviño, Centeno and

Caballero, 1987). This is not observed when the plant is analysed as a mixed biomass. The mature crop has the highest content of starch, which may be caused by the seeds additionally being within their mixed biomass assessment. The reason for their mature crop results being higher (20 %) than that found present in the mixed biomass of this study, may be due to the lack of seeds as the crop had been harvested. Therefore, relative comparisons of extraction methods cannot be discussed as the samples are too different. Focusing on the material used in this study, per 100 g, only 3.5 g would consist of starch making that proportion providing 13 kcal and therefore could be used as a low calorie ingredient. Therefore if this material was to be used as an ingredient, for the purpose as a bulking agent and in the correct amounts, it has the potential to reduce the calorific loading within a product and allow the production of a low-energy density product (European Commission, 2018).

3.3.7 Protein

Crude protein was measured by nitrogen content; the value for mixed pea biomass was 11 % (±0.56). Åman and Graham (1987), used crude protein (N x 6.25) and protein solubility to measure protein content. As a whole crop, they found the crude protein content (at maturity, third and fourth stage of growth) to be around 22-40 %. Individual botanical fractions showed that during growth, the crude protein content decreased in the pea (from 24-20 %) but this was minimal in comparison to other botanical fractions (Åman and Graham, 1987). By the third and fourth harvest, crude protein content decreased in all botanical fractions. This is from immature to mature crops, in the stem (3-9 %), leaf (15-22 %), flower and pod (5-35 %). This could be linked to the exponential phase of pea plant growth between the harvest

periods, as during growth it is proven that nutrients are translocated from stems, leaves and pods to the pea seed themselves (Kerr, 2016). Thereby the seeds content is only depleted minimally (> 5 %) in comparison to other fractions. Protein solubility showed that the crude protein increased from about 22-40 % during the first two harvest. Once seed formation occurred a decrease in solubility of crude protein was observed. These supported findings of crude protein content. Therefore, this suggests that as the values found in this study are much lower (10-28 %) than those found by Åman and Graham, the protein is most likely translocated to the pea seeds. As pea seeds were not assessed in our biomass but were by Åman and Graham, this may be an explanation for this difference. Additionally differing values of nitrogen conversions were used based on greater specificity to the material being assessed rather than a generalised nitrogen conversion calculation. Furthermore, Lund *et al*. (1981) state that when protein is assessed as one entire biomass, in comparison to individual botanical fractions, and their protein concentration subsequently added together, the amount of protein found will still be a lower amount in comparison. The lower protein content of our material when used within a product, enables a statement of containing high protein content. Although, as the content is just 11 %, it can suggest that it is a source of protein (European Commission, 2018).

3.3.8 Lipids

The lipid content, using the Bligh and Dyer (1959) methodology, found that the mixed pea biomass contained 3.1 % (±0.23).

Åman and Graham (1987) found the dry weight lipid content of leaf was around 6 %, the stem, flower and pod to be around 1-2 % and finally the

mixed biomass was between 1-4 % depending on the harvest time where the highest content was found in immature plants (Åman and Graham, 1987). These findings are more similar to the results found in this study. This slight difference may be due to differing lipid extraction methodologies. Åman and Graham (1987) used a diethyl ether in a Tecator Soxtec HT after an acid hydrolysis method. Fishwick and Wright (1977) compared different lipid extraction methods and found Bligh and Dyer's to be the most successful for studying plant tissues. Additionally, this slight difference may be due to variability of *Pisum sativum*, climate growth and soil conditions. Since, 100 g of this material only contains 3 g of fat, when used as an ingredient in a product formulation, it could potentially be classed as a low-fat product and saturated fat free (European Commission, 2018).

3.3.9 Chlorophyll and carotenoids

The chlorophyll and carotenoid concentration within PB was found to be 1.9 % (±1). Whereby the highest proportion 1.6 % was that of carotenoids rather than a total of 0.3 % for each individual chlorophyll. The weight ratio typically of chlorophylls to total carotenoids are (*a*+*b*)/(x+c) and are used as an indicator of the greenness of a plant. These ratios may vary depending on the sun exposure of the plant. Lower ratio values indicates senescence of the plant, stress or damage to the plant and photosynthetic apparatus (Lichtenthaler and Buschmann, 2001). As the results obtained in the present study suggest a higher ratio of carotenoids than that of chlorophyll, it suggests that the PB was mature upon harvesting, which is suggested through other findings and comparisons to with Åman and Graham (1987) and Treviño, Centeno and Caballero (1986). Consequently, it may suggest that the biomass had already started undergoing senescence or had stress

applied to it, once harvested, thereby the conversion ratio was predominantly through storage, handling and assessing the content amounts within the sample.

3.3.10 Ash

The ash content and therefore mineral amounts found within PB were 2.66 % (±0.5). Åman and Graham (1987) used the standard method of dry ashing to assess ash content of botanical fractions of whole pea crops. They found that from the immature to the mature whole crop, the content varied between (6-8 %). The individual botanical fractions (stem, leaf, flower and pod) produced similar ash contents (6 %) when immature. However, when mature, both the stem and flower/pod fractions were 9 %, whilst leaf contained 12 %. This is quite high for a fresh food which rarely exceeds 5 % but can reach up to as high as 12 %, as witnessed in dried beef (McClements, 2003). Treviño, Centeno and Caballero (1986) also measured the ash content in the whole crop with seeds and found it varied between 8.83-7.90 % ±0.86. Both studies report more than double the ash content found in this study. However, both studies use A.O.A.C. methods (1980), which the earliest (1980) has been adapted since (sample heated to 550 ºC overnight) and used here. Furthermore, these results suggest that earlier reporting of PB have increased micro-nutrient composition compared to that of the present day. However, in the comparison studies whole crop biomass contained pea seeds, which are not accounted for in this study. Therefore, the decreased amount of micro-nutrients reported in these works in comparison to Treviño, Centeno and Caballero (1986) and Åman and Graham (1987) suggests that pea seeds contain high quantities of micro-nutrients, and therefore may provide many health benefits (Dahl, Foster and Tyler, 2012). However, as

the PB used here does not include the pea seeds it cannot be suggested to provide health benefits associated with micro-nutrient content. Furthermore, since this is PB has also had the juice removed, which has been shown to have large amounts of micro-nutrients within it (Torcello-Gómez *et al.*, 2019), explain the lower concentrations found in this study. Both this work and that of Torcello-Gomez were carried out using the same crop, from the same field, it is interesting to note that the juice rich fraction provides a high source of micro-nutrients and could potentially be used as a micro-nutrient supplement for individuals suffering from deficiencies (Torcello-Gómez *et al.*, 2019).

3.3.11 Composition of Solka floc 900

Solka floc is manufactured by the International Fiber Corperation. It is a purified powdered cellulose, sourced from wood and has been stated to be produced from acid hydrolysis (Winkworth-Smith, 2014). The composition of Solka Floc is β–1→4 glucan units and it contains 99 % DF, providing zero calories, with an average fibre length of 110 µm and a water retention capacity of 9.5 g/g. It is a white, ordourless and flavourless material and has been stated to increase volume and reduce shrinkage in baked products, as well as improving the flowability in dry powder systems (International Fiber Corporation, 2018). Winkworth-Smith (2014), reported Solka Floc 900 having a high aspect ratio and furthermore, it has been found to provide binding of liquids, in oil and water food systems (International Fiber Corporation, 2018). Solka Floc is a food grade material currently used in food products, is composed almost entirely of DF and provides strong binding, viscosifying and textural properties.

3.4 Conclusion

To conclude, postharvest botanical fraction residues of PB (halum) were assessed for their nutritional composition, after juice fractions had been removed, as one whole mixed biomass. For, the purpose of valorising this material to ultimately be modified and used as a functional food ingredient, within a product. Furthermore, with the aim that the material would contain fewer calories and provide advantageous health benefits through consumption versus high-energy dense ingredients, currently in market.

Results and discussions found that:

- The mixed biomass: contained high amounts of DF; can be used to as an added source of protein and contains low amounts of fat. As a residue, micro-nutrient amounts found within the biomass were lower than expected and in comparison to others reported (Åman and Graham, 1987; Treviño, Centeno and Caballero, 1987).
- This ingredient would aid in reducing calorific intake and fat intake.
- A high degree of cellulosic composition implies modification as a functional ingredient is achievable. PCWM found within PB may provide structural reinforcement and gelling properties. Ultimately providing differing textural properties within a food matrix. However, cellulose is less than a third of the total mass; the additional material may affect/impinge future modification and/or sought-after properties.

Estimations in this work acknowledge that particular analytical equipment will overestimate composition amounts (i.e. protein, starch and calculations for hemicellulose complexes). Therefore, results obtained estimated 110.28 % ± 7.67 of the total composition of PB and thus must be an overestimation. However, with this overestimation there is still confidence in the amounts explained in this chapter.

Chapter 4 Design of Pea Powder Biomass

4.1 Introduction

4.1.1 Ball milling

Ball milling (BM) was first used in the late 19th century and became successful during the invention of steam and the industrial revolution (Lynch and Rowland, 2005). It became a dominant method of fine grinding materials by the 20th century. BM is a mechanical method that can either be performed with wet or dry materials. Originally used for grinding flint for pottery (Lynch and Rowland, 2005), it is now used extensively for biofuel production (Lin *et al.*, 2010) in order to enhance the enzymatic hydrolysis of cellulosic and other polymer composites to alcohol.

BM is used to decrease particle sizes (Baheti, Abbasi and Militky, 2013) and optimises the interaction between the fibre and matrix within polymer composites (Ruan *et al.*, 2004), in addition to causing a decrease in the degree of polymerisation (Hess, Kiessig and Gundermann, 1941). BM causes a decrease in cellulose crystallinity (Ago, Endo and Hirotsu, 2004; Zhao *et al.*, 2005; Lin *et al.*, 2010; Paes *et al.*, 2010; Winkworth-Smith, 2014; Nemoto *et al.*, 2017), this being the reason for its use in this study. BM alters the physiochemical properties of cellulose as well as the crystalline form (for example swellability/water uptake). The parameters and their decreasing/increasing effects are dependent upon differing parameters of the experimental throughput, these include; speed (rpm), milling time and material composition of balls and cups (Howsmon and Marchessault, 1959). However, currently BM is not used widely in the food manufacturing industry due to insufficient understanding and knowledge of industrial scale up parameters. In BM a semi-crystalline polysaccharide undergoes a phase

transition via amorphisation to a metastable state, whereby the transformed material lacks ordered structure (Avolio *et al*., 2012). This occurs through centripetal forces of the balls and cups causing collision, friction, impingement, shear or other mechanical disruptive actions on a cellulosic material, breaking the crystalline fractions which are built upon hydrogen bonding between and within the crystalline regions (He *et al.*, 2014). The level at which this occurs relates to the BM parameters aforementioned (Howsmon and Marchessault, 1959; Paes *et al.*, 2010).

4.1.2 Properties of Cellulose: Crystallinity, glass transitions and re-crystallisation.

As stated previously in Introduction Chapter 1, plant cell walls mainly comprise four polymers, namely cellulose, hemicellulose, lignin and pectins. Crystallinity is determined by ordering via inter- and intra-molecular hydrogen bond formulation (Wüstenberg, 2014). The amount of these and other compositional information for each polymer is discussed in Introduction Chapter 1. The main polysaccharide of interest for modification in this particular work is cellulose, albeit curiosity and intrigue remain in the BM effects on and within a naturally mixed polysaccharide PCWM hierarchical structure, opposed to other work carried out on pure cellulose (Paes *et al.*, 2010; Winkworth-Smith, 2014; Holland, Tuck and Foster, 2018).

Cellulose has differing allomorphs and orientation planes, which can therefore be altered (Wüstenberg, 2014) (Figure 13), unlike the other remaining polysaccharides. The effects of BM and as a result, any rehydration of said BM material should result in an altered form. Type 1 seed crystals need to be excessively removed in order for this phenomenon to

occur (Winkworth-Smith, 2014). Cellulose is a semi-crystalline material with a crystallinity index that can vary between 40 and 60 %, depending upon the plant based source (Avolio *et al*., 2012). However, when found in other sources, such as bacteria, the crystallinity index can be much higher (Avolio *et al*., 2012). The naturally occurring crystalline phase in higher plants is present in two forms, the Iα (triclinic unit cells) and I_β (monoclinic unit cells) (Avolio *et al*., 2012). The percentage of each vary depending upon the origin of the cellulose and treatment process.

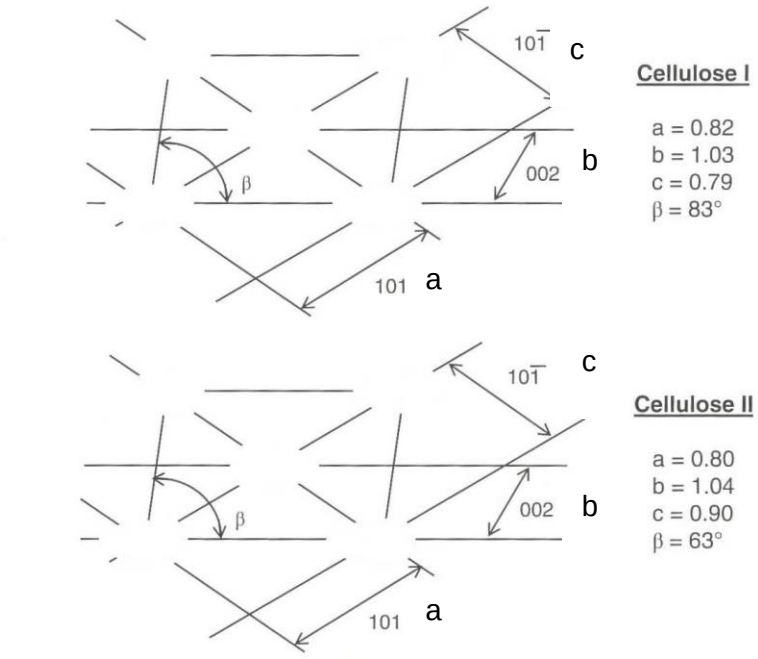


Figure 13 Cellulose allomorphs I and II depicting orientation arrangements on planes of cellulose, taken from (Wüstenberg, 2014).

Their stability varies for example, cellulose I is thermodynamically less stable than its other crystal allomorph structures of Cellulose II, III, and IV (Klemm *et al.*, 1998). Amorphous cellulose compositions can re-crystallise to the metastable type cellulose I with the presence of remaining nuclei within the

samples, most similar to its natural form. The nuclei act as seed crystals (Liang, Gu and Ding, 1993; Paes *et al.*, 2010). However, it has been reported to re-crystallise into the other forms (Hermans and Weidinger, 1946; Howsmon and Marchessault, 1959; Kim *et al.*, 2006). When the amorphous content is greater than 75 % it will re-crystallise to the more thermodynamically stable allomorph type II (Winkworth-Smith, 2014). This consists of anti-parallel packing with a modified hydrogen-bonding system instead of the type I allomorph consisting of parallel packing with no modifications to hydrogen units (Langan, Nishiyama and Chanzy, 2001). Creating amorphous cellulose in PB, in order to re-crystalise structure in food application is an objective of this work. The functional properties of cellulose, such as the susceptibility to enzymatic degradation, melting and dissolution, are all predominantly determined by these aforementioned crystalline fractions (Chen, 2014).

Few studies have been done on the effects of BM on decreasing the crystallinity of cellulose within vegetable matter as one whole mass. Research available refers to using the methods for bioconversions into biofuel (Kumar *et al.*, 2009; Canilha *et al.*, 2012; Peng *et al.*, 2012). However, a conclusive assessment using multiple techniques was used by Avolio *et al*., 2012, to assess the effects of BM on Arbocel cellulose fibres. The conclusion made was that cellulose fibres were predominantly amorphous with a mean crystallinity index from 0.53 to 0.15, the latter being reached after 60 min (speed in the form of rpm were not disclosed) of BM, indicating that BM progressively reduces the amount of crystalline regions and so significantly increases the amount of amorphous regions. Findings show that with increasing amorphisation, as a consequence of additional milling time, the amount of water absorbed upon rehydration increases, as crystalline

domains are anhydrous and thus less accessible to interact with water molecules (Child, 1972). They concluded that BM decreases the thermal stability of cellulose by 12 °C from the un-milled sample, especially at higher milling times.

Thermal degradation can be linked to the glass transition (T_g) of materials. T_g is defined by the temperature assigned to a region above which amorphous materials are fluid or rubbery and below which are simply frozen in a disordered, non-crystalline state (Duncan, 2008). This is a different state to crystalline/solid like-materials as molecular movements may occur over long periods. A material is defined as being glassy when in this state (Duncan, 2008). Partially and semi-crystalline materials can additionally go through a T_g usually followed by melting. The T_g phenomenon occurs due to energy involved in movement (Duncan, 2008). When a temperature of a material is increased enough so that one molecule of structure moves independently of another, softening of a material occurs when enough long chain molecules exhibit small transitions of rotations and T_g can be observed (Duncan, 2008). Ciolacu and Popa (2011), found that the crystallinity index and crystalline form of cellulose affects its thermal stability to degradation (Ciolacu and Popa, 2006).

Paes *et al*. (2010) looked into the effects of the T_g and crystallisation of BM cellulose (Eucalyptus pulp). Results showed that the T_g of the dry cellulose were between 47-107 °C, this was dependent on water content with a second transition at 117 °C being only weakly water dependent (Paes *et al.*, 2010). Some calorimetry methods were unable to detect T_g. Other studies report difficulty in quantifying the T_g of cellulosic materials (Batzer and Kreibich, 1981; Vittadini, Dickinson and Chinachoti, 2001). This is mainly due to the relaxation being close to that of the degradation temperature, in

addition to small changes of heat capacity (Batzer and Kreibich, 1981; Vittadini *et al*., 2001). Though the work of Szcześniak *et al*. (2008), found that DSC cooling runs are more suitable for measuring T_g. Bizot *et al*. (1997) used calorimetry to determine the T_g of dried pea amylose extracted from smooth pea starch and found it to be 127 °C (Bizot *et al.*, 1997). Both studies explained a correlation between the relationships of water content and T_g, as well as, an observation that T_g was higher in materials with semi-crystalline forms compared to those more predominately amorphous. The required thermal energy necessary to break the intermolecular bonds is higher than the temperature required to break the intramolecular bonds. This can result in the degradation of said material (Beyler and Hirschler, 2002). There is substantial evidence to suggest that cellulose may go through a liquid intermediary during pyrolysis (albeit this is not the T_g) with high temperature treatments (Paes *et al.*, 2010; Abbaszadeh, MacNaughtan and Foster, 2014; Winkworth-Smith, 2014), though prior to degradation or not, it is yet to be fully understood and not the main aim of this work to investigate.

Abbaszadeh *et al*. (2014) and Winkworth-Smith (2014) have explored the rehydration effects and subsequent re-crystallisation effects of BM cellulose and cellulosic composites. Both studies show that when cellulose is BM and depolymerised, upon the addition of water, it re-crystallises to the more thermodynamically stable allomorph II. However, depending on the extent of amorphous material (thereby allomorph I seed crystals remain) upon rehydration both allomorph I and II crystals will be formed. As PB is a natural mixed composite material containing varying polysaccharides and lignin, an interest of this work is to build evidence on the work from Abbazadeh *et al.* (2014) and Winkworth-Smith *et al.* (2014) that a mixed system of non-purified cellulose may additionally re-crystallise to a similar degree. Thereby

investigating whether the presence of lignin, pectin and hemicellulose impinges de- and re-crystallisation.

4.1.3 Aims of this chapter

Whilst aforementioned studies have researched the effects of BM on cellulose materials, thus far, no research has been performed into the effects of BM on a mixed PCWM, utilising side-stream valorisation of vegetable matter. Therefore the focus of this work is:

- To characterise effects of BM on crystallinity and amorphisation,
- To investigate subsequent transformations upon rehydration such as re-crystallisation and misicibility within a dispersion,
- To measure rheological properties of a rehydrated BMPB systems,
- To make a functional food ingredient.

Investigating BM on PB, as a mechanical process, to provide functionality qualities to fully or partially replace starch within a model product, which is later tested in Chapter 6.

4.2 Materials and methods

4.2.1 Materials

Pea Biomass (PB) in its raw wet form after juicing is discussed previously in (Chapter 3). It was used after leaving to thaw at 25 °C (approx. 2 Hr) from the -80 °C freezer (Denley CFC-Free -80°C freezer, China).

4.2.2 Drying and storage

The fibre, once defrosted (section 4.1), was then oven dried for 24 Hr at 105 ºC (UN 110, Memmert, Germany). It was then placed in a desiccator over phosphorus pentoxide (Sigma Aldrich, UK), for 3 Hr, to remove any residual water. Measured water content of PB did not deviate significantly for five different trials using the oven drying method. Therefore, remaining experimentation, on PB, with the preparation of oven drying, were no longer subsequently stored in a desiccator thereafter. The water content expressed from the oven results are reported on a wet weight basis and used to prepare samples prior to BM. The results were determined by the following standard equation (A.O.A.C., 2000) after oven drying (Equation 4).

The water content expressed from the TGA results were done on a dry powder weight basis. The results was determined by methods of 4.2.4.4.

After oven drying and/or ball milling samples were stored in a sealed container in a dark cupboard.

4.2.3 Processing methods

4.2.3.1 Ball milling

The PB was milled using a Planetary Micro Pulverisette 7 (Fritsch GmbH, Germany), at 600 rpm with 10 min of milling followed by 10 min of pause in order to allow heat to dissipate. Each zirconium oxide pot contained six zirconium oxide balls (10 mm Ø) and 0.5 g of dried PB.

As the nature of the PB is that of a polysaccharide and therefore fibrous, Fritsch (GmbH, Germany) recommend ceramic (zirconium oxide) composition of balls and cups instead of the alternative metal (aluminium) ones.

4.2.3.2 Rehydration of ball milled pea biomass

Samples 1 and 2 were rehydrated by dispersing the Ball Milled Pea Biomass (BMPB) in an excess of Reversed Osmosis (RO) water (4 and 3 mls per 1 g of BMPB). Method of samples varies as follows:

1. Unstirred (UN): Water was added to BMPB powder and mixed until no dry powder remained then stored at an ambient temperature for 24 Hr (two concentrations) and left to swell.
2. Stir Mixed (SM): Water was added to BMPB powder and stirred using a magnetic flea, on a magnetic stirrer (Fisher Scientific, UK) at an ambient temperature for 4 Hr. It was additionally covered with foil to help reduce water evaporation, at the two concentrations (25 % and 33 %).

Therefore, there are four rehydrated samples in total.

- 33 % UN
- 33 % SM
- 25 % UN
- 25 % SM

4.2.4 Analytical methods

4.2.4.1 Light microscopy

BMPB was spread on a glass slide and images were taken using an optical microscope (EVOS FL, AMG Washington, USA) at magnifications of 20 x and 40 x, prior to rehydration. All measurements were performed at ambient temperature.

4.2.4.2 Polarised light microscopy

Rehydrated BMPB samples 1 (UN) and 2 (SM) at both concentrations, were mounted on a glass slide with a cover slip and images were taken using polarised light imaging (Olympus BX61, USA) 2.5 x magnification. All measurements were performed at ambient temperature.

4.2.4.3 Dry Particle Size Distribution (PSD)

The dry PSD of samples was determined using a Life Sciences (LS) 13 320 Series Particle Size Analyser with a docked Tornado Dry Powder Module System and optical model glass (Beckman Coulter; High Wycombe, UK). Calibration was carried out using LS control G35D, which is a garnet grain specifically used for dry powder systems and equated to 35 μm (Beckman

Coulter; High Wycombe, UK). The BMPB samples were added into a plastic vial no more than 1 cm in depth and then measured using a 5 mW diode laser. The laser instrument operated in the size range of 0.4 μm to 2000 μm with the Fraunhofer approximation. Obscuration was set at 7 % with background and alignment measurements every 30 min, respectively. A minimum of 3 replicates were taken for results reported. A Tornado Cleaner Garnet Abrasive (Beckman Coulter, High Wycombe, UK) was used between each sample as a cleaning agent. Un-milled PB were unobservable due to the size of the fibres.

The wet PSD was determined using a different LS 13 320 Series Particle Size Analyser to the dry powder previously explained, with a docked Liquid Module System and optical model glass (Beckman Coulter; High Wycombe, UK). Calibration was carried out using an LS control again (Beckman Coulter; High Wycombe, UK). 0.5 g of BMPB was added to 24.5 g of water, making a 25 g dispersion. The laser instrument operated in the size range of 0.4 μm to 2000 μm with the Fraunhofer approximation. Subsequent drops were pipetted into the module until the required amount was obtained. Obscuration and alignment measurements were made as for the dry powder. A minimum of three replicates were taken for results reported over three batches of trials due to the shape of the material being ellipsoidal rather than the recommended spherical. Particles, which are non-spherical and possess refractive indices that are close to that of the medium may also deviate further from the Fraunhofer prediction and thereby cause errors in findings (Annapragada and Adjei, 1996). The system was flushed with water each time as a cleaning agent.

4.2.4.4 Thermogravimetric Analysis (TGA)

A 100 µl aluminium pan was loaded with sample and placed inside a TGA/DSC-1 (Mettler Toledo; Leicester) and used to measure weight loss and so consequently water content. All samples were heated from 25 °C to 400 °C at a rate of 10 °C min^{-1} in nitrogen atmosphere. Blank subtraction was based on loss of an empty pan used prior to analysis and was necessary due to the buoyancy effect.

4.2.4.5 Differential Scanning Calorimetry (DSC)

Thermal transitions were monitored using a heat flux Mettler Toledo DSC 823e (Mettler Toledo, Leicester, UK) with auto sampler and intracooler. Samples were made up under ambient conditions after being freshly transferred from the ball mill cups. Stainless steel sample pans of 6.5 and 7.5 mg of BMPB volume were used to ensure that samples could be run to 200 °C with minimal risk of leakage. An empty pan and lid was used as the reference sample. Samples were typically run from a temperature of 0 °C to 200 °C at a rate of 5 °C min^{-1}. Samples were then cooled at a rate of 40 °C min^{-1} to 0 °C and a reheat using the same parameters were carried out. The DSC was calibrated for temperature using the onset temperatures of melting of indium and cyclohexane and for heat flow using the enthalpy of transition of indium. Enthalpy and associated values were calculated using Mettler Toledo Star^{e}software with any reported T_g being calculated from the reheat.

4.2.4.6 Wide Angle X-Ray Diffraction (WAXD)

X-Ray diffraction patterns were carried out using a Bruker D5005 (Bruker AXS, UK) at the angular range of 3-38 2θ, with a step size of 0.05 (2θ). Slit

focus geometry was used with a total acquisition time for each sample of 56 minutes and a recording each 2.5 sec and a spin rotation of 60 rpm. Plastic holders were filled with randomly orientated dry BMPB. The control samples had to be ground with a pestle and mortar. The Copper K alpha-1 (CuKα) radiation (λ=1.5218 nm) was used and the machine at 40 kV and 40 mA. Slight variations in peak positions result from small errors in the height of samples. The crystallinity calculations were performed using an intensity vs 2θ data in the Microsoft Excel software package with the Solver add in (Carrillo *et al*., 2003 and Abbaszadeh *et al*., 2014).

For rehydrated samples the same method was performed after samples were re-dried in an conventional oven at 105 °C for 24 Hr (A.O.A.C., 2000), in order to use them for WAXD they were subsequently crushed slightly with a pestle and mortar prior to filling the sample holder.

4.2.4.7 ^{13}C Cross polarization Magic Angle Spinning Solid State Nuclear Magnetic Resonance (^{13}C CP-MAS NMR)

^{13}C CPMAS NMR spectra were recorded on a Bruker AVANCE III 600 NMR spectrometer with narrow bore magnet and 4-mm triple resonance probe. The parameters and conditions used in CPMAS experiments were: proton 90º pulse length; 3 µs, field strength of the proton and spin locking fields during the contact period; 83 kHz. The samples were packed into 4 mm rotors and spun at 10 kHz. Chemical shifts in parts per million (ppm) scales were referenced to the upfield peak of adamantane (29.5 ppm) run as an external standard. Proton decoupling was provided by a Spinal-64 sequence and for all CPMAS experiments, a contact time of 2 ms was used. Recycle delay was 2 seconds. For variable contact time, measurements the contact

time was varied approximately logarithmically from 10 μs to 10 msec. Samples were measured containing varying water contents of between 5 and 7 %.

For rehydrated samples the same NMR parameters were used with the wet samples once they had been dried in an oven at 105 °C for 24 Hr (A.O.A.C. 2000) and subsequently crushed in a pestle and mortar in order to fill the rotar.

Data processing of spectra was performed using MNOVA (MNOVA, Mestrelab Research S.L., Santiago de Costela, Spain), which included 5 k of data points recorded being zero filled to 16 k. Each sample was apodised using exponential window function with 50 Hz line broadening. Then Fourier-transformed and phased with zero and first order corrections. Lastly baseline fitting routines were applied.

4.2.4.8 Dynamic Vapour Sorption (DVS)

A Dynamic Vapour Sorption analyser (Surface Measurement Systems Ltd, London, UK) equipped with a Cahn D200 microbalance was used to measure the water sorption isotherms of the BMPB. The experiment and repeats were carried out at a temperature of 25 °C and relative humidities (RH) from 0 to 95 % and then back to 0 %. The initial weight of the samples was approximately 10-20 mg. Samples were firstly dried under oven drying methods and contained an initial water content of around 7 % and were subsequently hydrated in RH steps of 10 %. Samples were then considered equilibrated when the change in mass per unit was > 0.0005 mg/min^{-1}.

4.2.4.9 Rheology of rehydrated Ball Milled Pea Biomass

Steady shear and oscillatory measurements were carried out using an MCR 301 Rheometer (Anton Parr, UK), with a serrated parallel plate (40 mm diameter, 1 mm gap) geometry at 25 °C. Shear viscosity was monitored by increasing the shear rate from 0.001 to 100 s^{-1}. Amplitude sweeps were performed between 0.01 and 100 % strain and were carried out to ensure measurements were within the Linear Viscoelastic (LVE) region. Where the dynamic storage modulus (G') and loss modulus (G'') are independent of the stress amplitude, in order to apply the given strain for frequency sweeps. Frequency sweeps had a strain setting of 0.05 % (selected from LVE region) and were performed at 10 rad/s.

Equation 13 and 14 show the calculation of Complex viscosity and Tanδ, respectively.

Equation 13

$$\eta* = \sqrt{\frac{(G')^2+(G'')^2}{\omega}}$$

Equation 14

$$Tan\ \delta = \frac{G''}{G'}$$

4.3 Results

4.3.1 Water content of Pea Biomass and Ball Milled Pea Biomass

In all oven drying analysis of PB, water content did not vary significantly (p-value > 0.30), in accordance with standard regression analysis, and it was found that Juiced PB comprises of 78 % water, with similar results for water content obtained by Huber *et al.* (2016). This would suggest that the solid content is 22 %. Typically after drying using this methodology one would assume that all available water has been removed. Though using TGA Table 6, it was found that the dry PB still contained around 6 % ±1 water content, showing the fibres have a strong water holding capacity.

Table 6 TGA water content on dry PB before and after BM. Performed using a heat ramp from 25-400 °C at a rate of 10 °C min^{-1} in nitrogen atmosphere.

Sample	Water content (%)
Native PB (un-milled)	5.75
10 min BMPB	5.75
30 min BMPB	6.75
50 min BMPB	6.75
70 min BMPB	7.00
90 min BMPB	6.80

Upon BM derived PB Table 6 shows that with an increase in processing time there is an increase in the amount of water content found within samples as measured by TGA. This increase in water content is likely to be due to an increase in the water binding capacity of the polymer composites, due to the increase in amorphous regions. Lastly, this shows that after oven drying for a 24 Hr period, the native PB retains with 5.75 % water or gains this water content in storage between assessments.

4.3.2 The effects of Ball Milling on Pea Biomass morphology

In order to look at the effects of BM on the morphology of PB, light microscopy and particle size analysis were used. Figure 14 (Figures A through to E) shows that for different BM times variations in size rather than shape changes are observed. It can be observed that smaller particulate sizes are produced with an increase in BM times. This is due to mechanisms within the milling process, enabling large fibres to be milled down to fine powders, with a significant decrease in the sample size overall volume (as observed before and after milling). However, Figure 14.E (90 minutes BM) shows an increase in particle size, which may be an agglomeration of particulates due to over processing or be based upon other agglomerations that are heat induced, through mechanical energy used in the BM process. To try and combat this induced phenomena, pauses were imposed in the milling methodology. This agglomeration was not investigated and therefore the true cause of it is unknown. Food powder particle shape can play a key role in the characteristics of bulk density, compressibility and flowability of the system (Barbosa-Cánovas, Harte and Yan, 2012). Many applications favour spherical (uniform) shapes over ellipsoidal (which are predominantly displayed here), as the size distribution of particulates can affect the taste, appearance, stability, processability and functionality when incorporated into a final product (Engelen *et al.*, 2005).

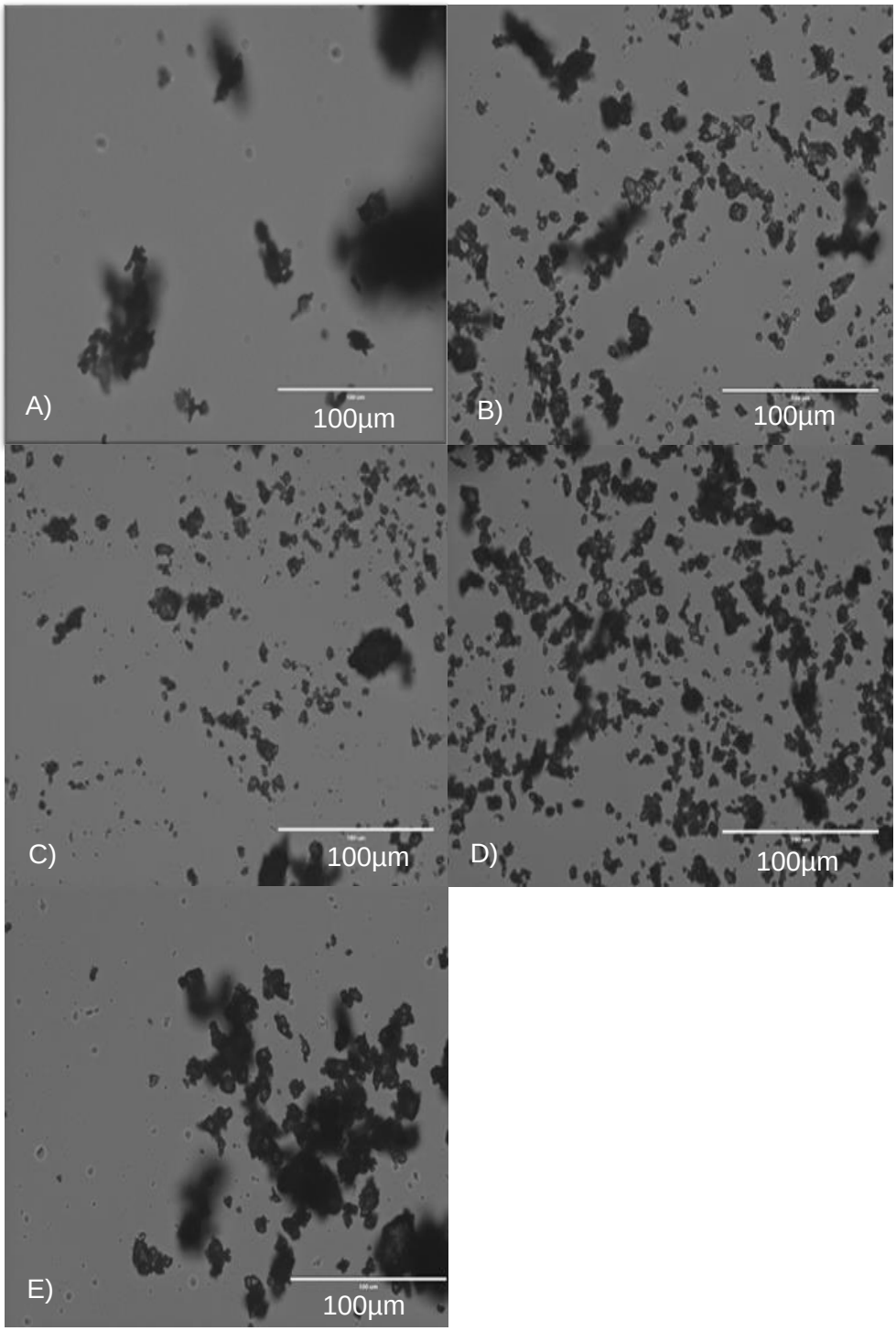


Figure 14 Light microscopy images depicting differences between dried PB samples with varying Ball Milling (BM) times. (A) 10 minutes, (B) 30 minutes, (C) 50 minutes, (D) 70 minutes and (E) 90 minutes of BM. Observed at x 40 magnification.

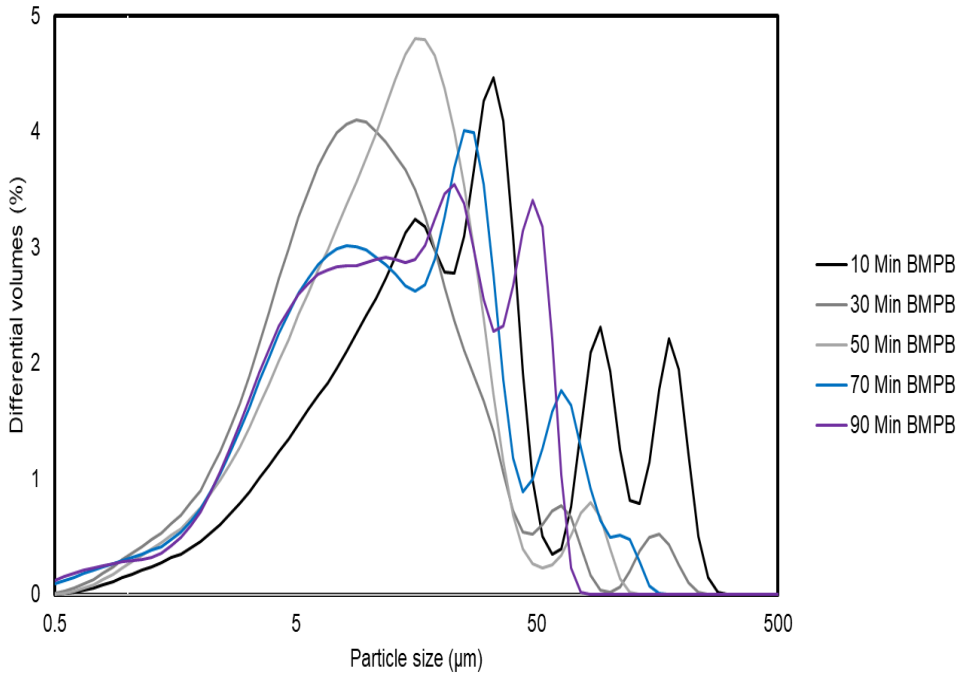


Figure 15 Differential Volume (%) and particle size of various milling times performed on dry PB.

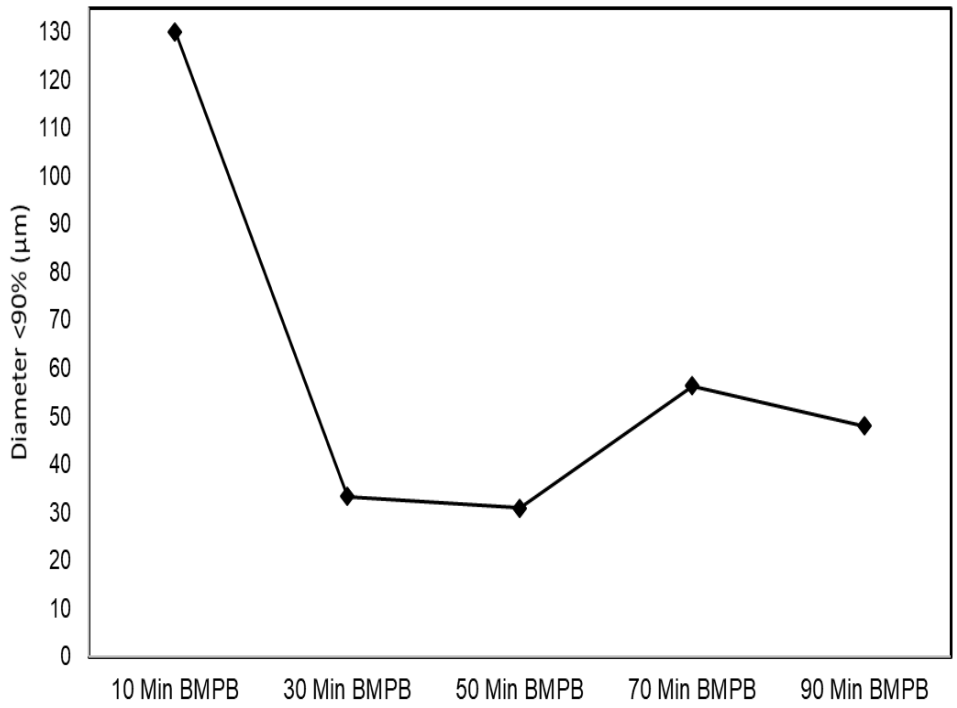


Figure 16 Average particle size diameter at < 90 % of the differential volume for BMPB at various milling times.

Both Figure 15 and 16 suggest that none of the milling times provided monodisperse particles. If, uniformity is required as an end pre-requisite then a different processing method should be explored. Manufacturing standards of raw materials usually require higher standards on their materials to ensure product quality. Particle sizes differed significantly depending on the amount of milling time (p-value > 0.05). Milling for different times showed that there was little difference seen beyond milling for 50 min, with particle size decrease found up to that time. A study done by Fadda *et al.* (2009) hypothesised that particle breakup may occur initially in the first stages of milling, but an equilibrium is reached between re-agglomeration and de-agglomeration, meaning that the particle sizes may not reduce further with increasing time (Fadda *et al.*, 2009). Further to this, in the case of cellulose, Yu and Wu (2010), confirmed this observation with a decrease of particle size within the first hour of BM. However, with extensive BM (1-7 Hr), a slight increase in particle size was observed (Yu and Wu, 2011). They hypothesised this was caused by agglomeration of finer particles, which the BM time would be dependent on the material and its compositional matrix. This provides evidence that long BM is ineffective at reducing particle size of cellulose and other polymer/non-polymer composites. Though Winkworth-Smith (2014) showed an agglomeration of particles which then reduced to finer particles, with less aggregation and was observed with excessive BM (> 610 min). Therefore, a reason as to why after 50 minutes of BMPB an increase in size is observed, is plausibly due to an equilibrium from this particular material is reached. From the standard deviation values found in these works, it would seem that 10 min BMPB produces a similar particle size to potato flour and 50 min BMPB to corn, cassava and wheat flours according to commercial flour sizes found by Hossen *et al. (*2011). However, 10 min BMPB was not fully converted from a fibrous biomass to a powder

and clumps of small fibres were still witnessed, with the least amount of uniformity observed. Lastly, 50 min BMPB produced the most bimodal-like distribution across varying milling times observed.

4.3.3 The effects of Ball Milling on the crystallinity of Pea Biomass

Figure 17 and Table 7 depict the loss in crystallinity of PB in cellulose type I allomorph, through the effects of the mechanical energy throughput in the BM process. A multi-peak deconvolution method was used for calculating crystallinity (Figure 18), using the experimental and theoretical fits against areas which define peaks, for the native allomorph of form I (Lad *et al*. 2013). However, with this method it is advised the data is subjected to a +/- 5 % error.

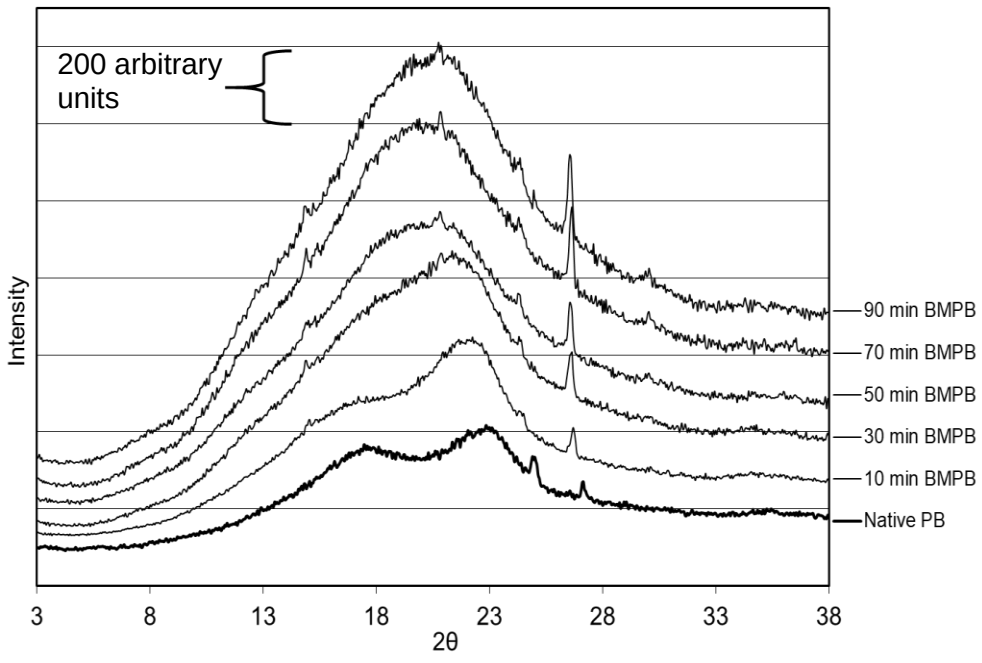


Figure 17 WAXD spectrum of differing BM times on PB and native PB that has not been milled, conducted from 3-38. 2θ with a total scanning time of 60 minutes. Major cellulose peaks found between 15-25. 2θ. With additional peaks 25 and 27. 2θ indicating trace elements such as salt.

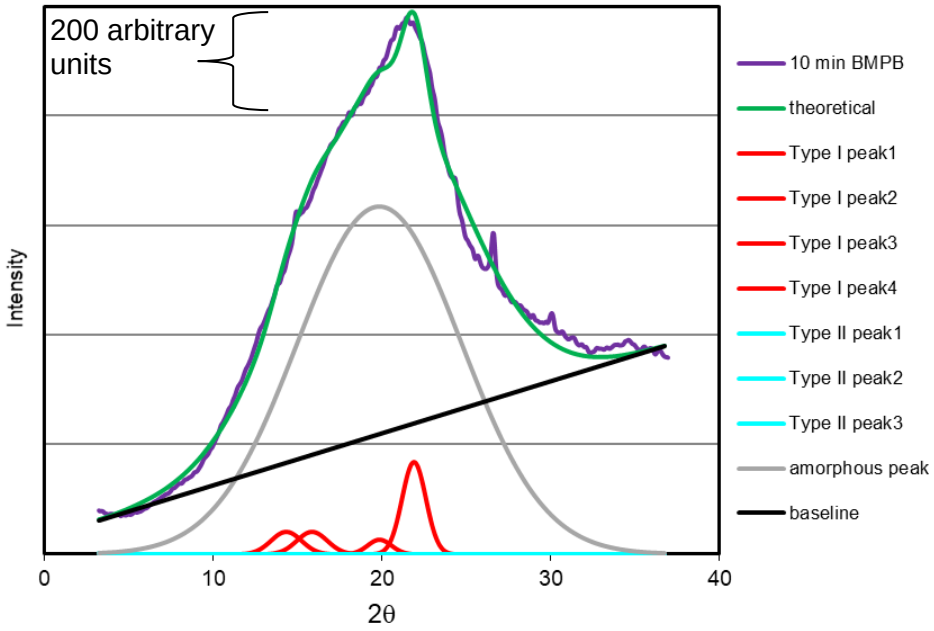


Figure 18 Multi-deconvolution method to determine crystallinity and particular amount in each allomorph I and II. Example of 10 min BMPB that contained no type II allomorph. It should be noted that each sample should be subjected to a ± 5 % error (Paes et al., 2010; Winkworth-Smith, 2014; Holland, Tuck and Foster, 2018).

Crystallinity indications are shown by a loss of peak between 15 and 25 ° (2θ). The peak after 25 ° (2θ) is indicative of trace elements such as salt naturally present within the PCWM (Lad *et al.*, 2013). This trace element peak shows an increased intensity of signal as BM times increase. This may be due to the mechanical forces opening structures or creating a by-product, (which is supposedly salt) as a consequence of breaking down the PCWM and thus increases the intensity of signal. Cellulose crystallinity decreased significantly with increase in BM times. Crystallinity that remained was all in the allomorph I form. Quantification methods suggest that after 30 min BMPB the sample becomes predominantly amorphous. Levels of crystallinity below 2 % were unreliable using the present X-Ray apparatus and fitting routines of the multi-deconvolution method. Therefore, attempts to fit 70 and 90 min BMPB data using the fitting program were un-successful.

Anomalously large values of crystallinity were returned, which were invalid as the peak positions were shifted during the fitting procedure. A possible improvement to this procedure would be to use a reference amorphous background for a truly amorphous sample and could be tested for reductions in molecular weight.

This suggests the minimum BM run time for to create predominately amorphous material is suggested at 50 min, which also corresponds to the time after which no further particle size reductions were seen. Paes *et al*. (2010), Winkworth-Smith. (2014) and Holland, Tuck and Foster. (2018) all observed a decrease in crystallinity with BM using the same fitting programme in order to calculate crystallinity.

***Table 7 Crystallinity index (CI) percentages of various BMPB with crystallinity amounts for each allomorph I and II forms. The subsequent amorphous content assumed as a result from mechanical forces through BM. Calculated using Microsoft Excel with the addition of solver from* (Carrillo *et al.*, 2003 and Abbaszadeh *et al*., 2014).**

Sample	Type I allomorph (%)	Type II allomorph (%)	Crystallinity index (CI) (%)	Amorphous content (%)
Native PB	11±0.35	0	11±0.35	89±0.35
10 min BMPB	6±0.33	0	6±0.33	94±0.33
30 min BMPB	5±0.10	0	5±0.10	95±0.10
50 min BMPB	2±0.34	0	2±0.34	98±0.34
70 min BMPB	0	0	0	100
90 min BMPB	0	0	0	100

In order to confirm the effect of BM on crystallinity ^{13}C CP-MAS NMR was performed. Figure 19 refers to the NMR spectra reported for the varying milling times and shows the same trend of crystallinity as that of the WAXD. Figure 20 helps to indicate differing crystalline regions of allomorphs I and II,

typically displayed on a NMR spectra for cellulose. The most relevant areas being that of cellulose in the C-4 regions (80-93 ppm) and C-6 regions (64-68 ppm) (Park *et al*., 2010). A loss in peak of these regions indicates a reduction in crystallinity, observed with increase in milling time and shown to be less defined/loss from 50 min of BMPB. Moreover, a decrease in hemicellulose peaks also indicates a reduction in crystallinity. This may indicate that opening up the cellulose structure liberates hemicellulose to also be affected by the milling process. The additional peaks present in the PB are from the additional varying PCWM polysaccharides such as hemicellulose, lignin and pectin, which is observed in Figure 21. Other PCWM did also vary significantly; pectin, lignin and cutin lie within some of the cellulose peaks but additionally they can differ and can be found around 20-35 ppm (Jarvis, 1994; Jarvis and Apperley, 1995), which has also shown to decrease in peak heights and shapes. Lignin has one peak in particular that also differs with more BM time significantly, which can be found around 180 ppm. This suggest that BM has altered the structure of the lignin, pectin or possibly cutin within BMPB and decreases the amount present in NMR with more extensive BM. Results for NMR and WAXD can be coupled and conclusively suggest after 50 min of BMPB the sample is predominantly amorphous, which was a particular purpose of this work.

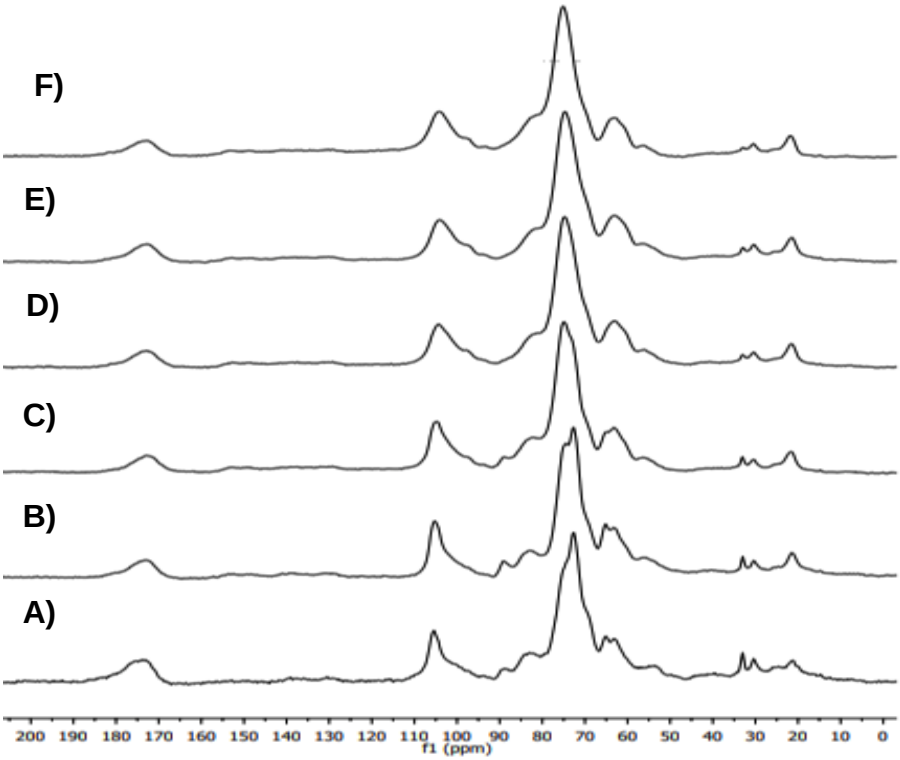


Figure 19 ^{13}C CPMAS NMR of BM PB from A) Un-milled PB, B) 10 minutes BM PB, C) 30 minutes BM PB, D) 50 minutes BM PB, E) 70 minutes BM PB, F) 90 minutes BM PB. Depicting amorphisation through ball milling from a crystalline state in the regions of C2 and C3 in 65 and 85 ppm respectively. Spectrums were formatted using MNOVA software.

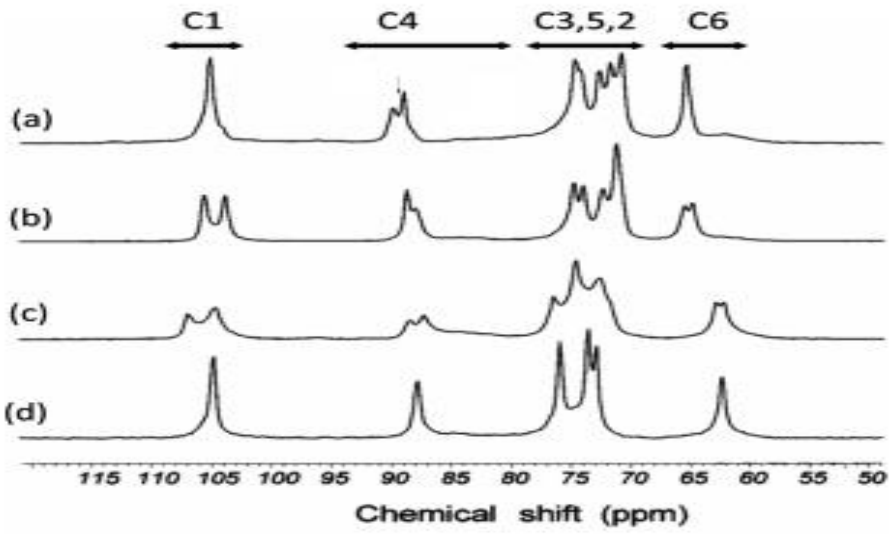


Figure 20 NMR spectrums of differing cellulose polymorphs (a) Iα from Glaucocystis, (b) Iβ from tunicate, (c) II, and d) III. The region of chemical sift for each carbon is labelled. Crystalline fractions are indicated by peaks and their amount by intensity, curved or baseline fractions of the spectra indicate amorphous regions. Figure taken from* (Kim, Lee and Kafle, 2013)*. With modifications removed and was originally Copyright of American Chemical Society (2003).

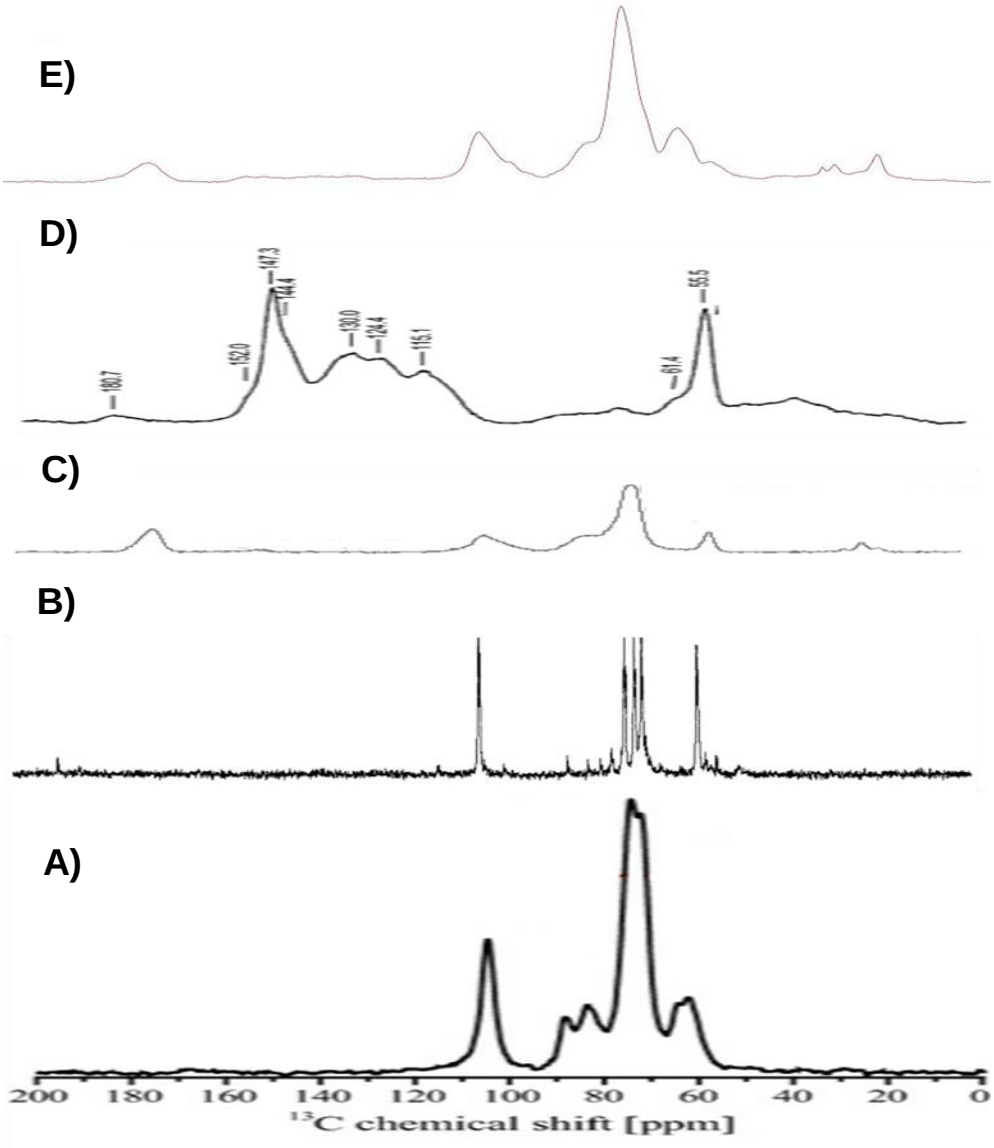


Figure 21 ^{13}C CP- MAS NMR of A) Cellulose from sugarcane biomass (Lima et al., 2013). B) Hemicellulose from bamboo (Wen et al., 2011). C) Pectin from sugar beet pulp (Syntsya, Copikova and Brus. 2000). D) Lignin from cocoa shell (Redgwell et al., 2003) and E) 50min BMPB.

4.3.4 Thermal analysis and DVS of Ball Milled Pea Biomass

TGA provides information of water loss and sample degradation (through pyrolysis), which can be inferred to the time and temperature at which chemical reactions take place in the particular material observed. Therefore, one can deduce differing structures based on their degradation temperatures. Water contents given in Table 6, show that the samples

through various BM times do not differ immensely (p-value < 1.25 %). The difference and higher water contents observed in samples with extended BM times, in comparison to un-milled PB is possibly due to the more open structure and higher surface area of the fully amorphous cellulose (Stubberud *et al.*, 1996; Mihranyan and Strømme, 2004; Winkworth-Smith, 2014). Avolio *et al*. (2012) states that an increase in milling time provides amorphous regions accessible to water due to their increase in sorption sites (hydroxyl groups) available (Mihranyan and Strømme, 2004; Kocherbitov *et al.*, 2008; Avolio *et al.*, 2012). Therefore Figure 22 shows the rate at which mass is lost of the PB with varying milling times. The data indicates that the rate at which mass is lost does not differ significantly across the samples (p-value < 0.05) especially after 200 °C. Furthermore, besides 10 min BMPB, Figure 22 suggests that with additional BM the rate at which mass is lost does increase, which is to be expected as there are more amorphous regions compared to crystalline regions.

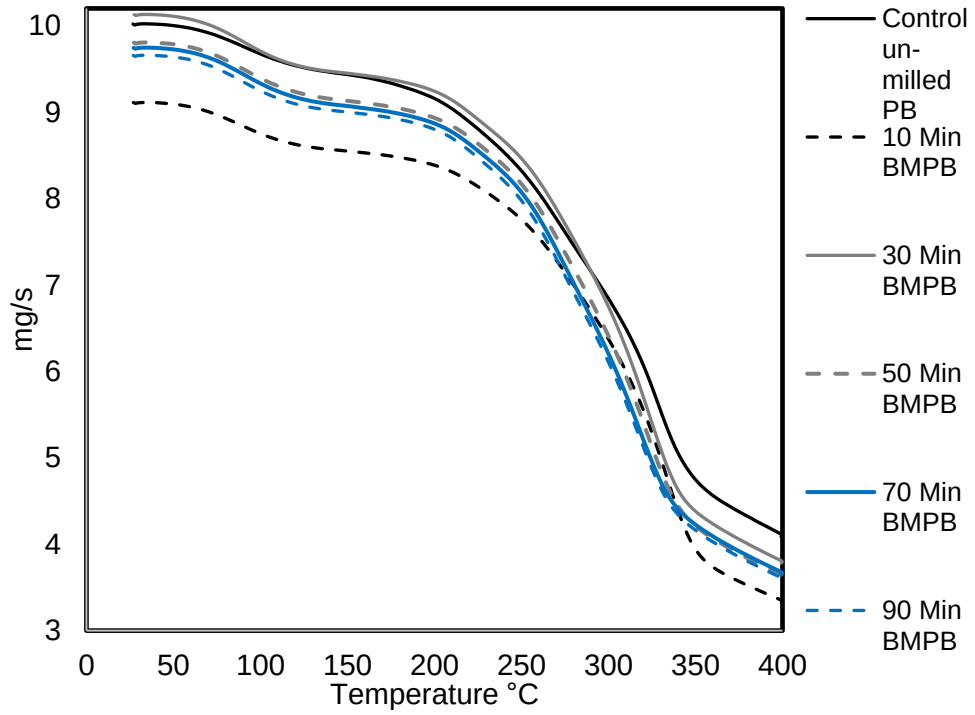


Figure 22 TGA plots of un-milled PB to 90 minutes of ball milling PB.

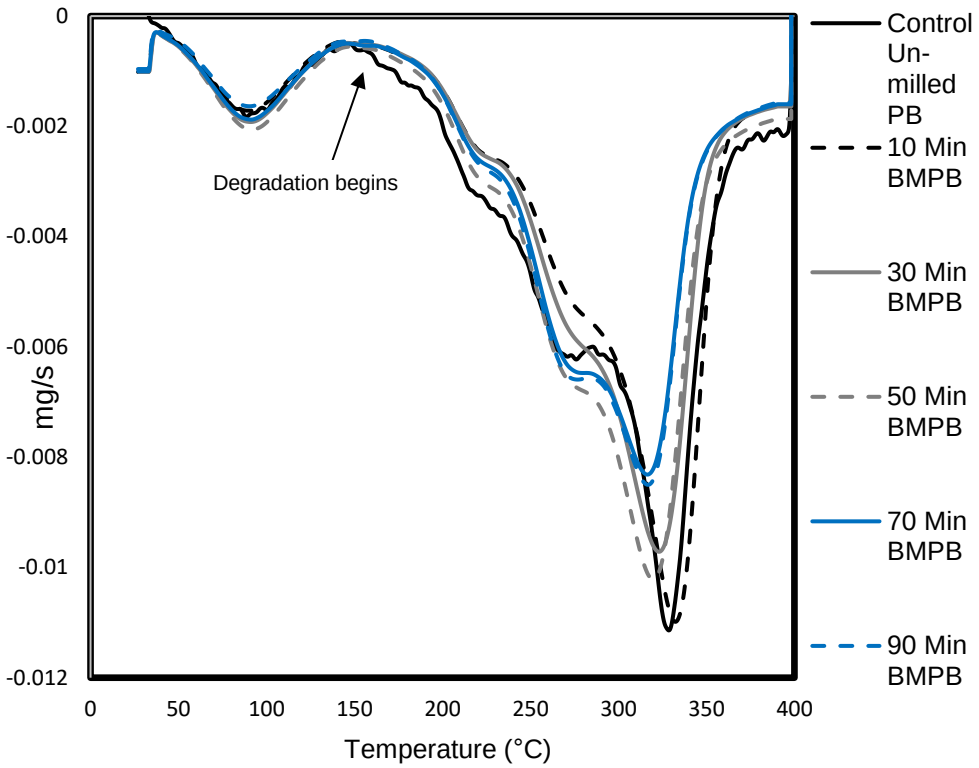


Figure 23 Differential thermal analysis (1st derivative taken from the original TGA plots of Figure 22) for un-milled PB to 90 minutes of ball milling PB.

Whereas, Figure 23 depicts the differential thermal analysis of the TGA plot taken from the 1st derivative. This suggest that the first initial trough, which is relative to water loss is not significantly different across the samples (p-value < 0.05). However, the larger trough that occurs around 300-325 °C depicts the major pyrolytic degradation point of cellulose. The results suggest that BM is subsequently reducing this degradation temperature, namely due to the increase in amorphous regions compared to that of crystalline regions. This correlates with information found by Calahorra *et al.* (1989), showing that thermal stability decreases as molecular weight decreases which is relative to the degree of polymerisation (Calahorra *et al.* 1989). Winkworth–Smith additionally found that BM and loss of crystallinity additionally lowers the degree of polymerisation and degradation

temperature, but for pure cellulose. Lastly, the shoulders prior to the larger degradation pyrolysis trough could be indicative of PCWM (hemicellulose) within the PB degrading prior to cellulose. Barneto *et al*. (2011) studied the differential thermal analysis of flax fibre and found that cellulose main degradation pyrolysis occurred at 300-350 °C, with lower shoulder temperatures thought to be hemicellulose and the broad tail at high temperatures thought to be lignin, which may coincide with results found in this study (Barneto *et al.*, 2011).

DSC enables one to see thermodynamic and kinetic parameters associated with chemical changes associated with a substance as a function of temperature. These transitions are seen within a material, prior to degradation in the form of transitions of state, requiring or releasing energy. Micro-DSC has been ascribed as a more suitable method to assess proposed glass transitions within lignocellulosic materials (Winkworth-Smith, 2014), though they have also been reported through DSC measurements (Bizot *et al.*, 1997; Szcześniak, Rachocki and Tritt-Goc, 2008; Paes *et al.*, 2010). Lignocellulosic biomass studies have found that pyrolysis can be divided into four individual stages: water loss, hemicellulose decomposition, cellulose decomposition and lignin decomposition (Yang *et al.*, 2004 and 2007). Figure 24 depicts an endotherm which is in common with known physical ageing or enthalpic relaxation peak of polymers at 50-80 °C, which disappears upon the sample reheat (Bizot *et al.*, 1997; Paes *et al.*, 2010). Bendler (1985) and Kalichevsky *et al.* (1992), stated that this endothermic event is common amongst polysaccharides (Bendler, 1985; Kalichevsky *et al.*, 1992). Furthermore, Shogren (1992) stated that this endotherm occurs in amorphous and semi-crystalline polymers below their T_g and this reflects a slow decrease in volume of glass towards that of its equilibrium value

(Shogren, 1992; Abbaszadeh, 2014). Even though this is a mixed system differing in lignocellulosic polymers, the resulting degradation temperature onset of the material is similar to that of pure cellulose. At around 145 °C an exotherm is caused by either re-crystallisation of the amorphous BMPB or degradation of the polymer composite. In comparing results by Paes *et al*. (2010) on Eucalyptus pulp cellulose, which suggest that at 10 % water content (most similar to the water content of 50 min BMPB) a similar exotherm is produced at 137 °C. Additionally, Abbaszadeh (2014) investigated DSC of BM polysaccharides and found that cellobiose had a similar exotherm at 125 °C and microcrystalline cellulose at 145 °C (Abbaszadeh, 2014). These minimal differences in temperatures may be explained by the fact that PB contains various polymers compared to that of the work of Paes *et al*. (2010) and Abbasszadeh (2014) and those various polymers may affect the exotherm temperature point. Furthermore, Paes *et al*. (2010), suggested that this re-crystallisation was water content dependent, the higher the water content, the greater the re-crystallisation. Giving some evidence that BM has effectively enabled the PB to re-crystallise upon influx of temperature and relative humidity at low water content. As this system needs to be compared to that of starch for apparent properties, native starch commodities, such as potato, cassava, wheat, waxy maize and field pea starch show that they have a lower degradation and gelatinisation temperature (Jayakody and Hoover, 2008). With most starch commodities being $\frac{1}{3}$ of that from the BMPB (Jayakody and Hoover, 2008). Theoretically this may be due to the higher crystalline content as said starch commodities have not been modified by mechanocatalytic depolymerisation of the ball mill.

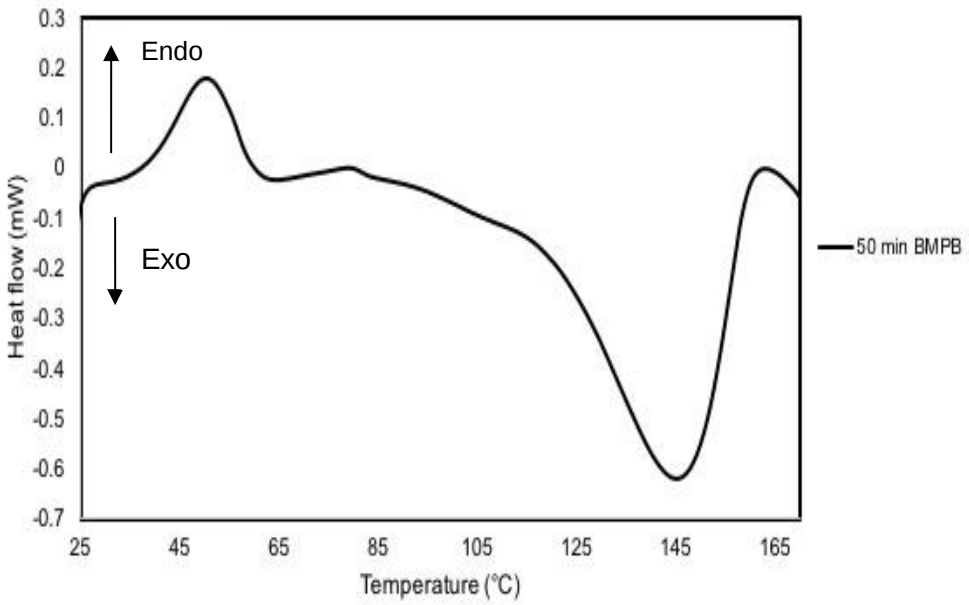


Figure 24 Differential scanning calorimetry of amorphous 50 min BMPB, showing endothermic and exothermic events as a function of heat flow. Heated from 30 °C to 170 °C.

In using DVS to assess solvent uptake and re-crystallisation through differing relative humidity (RH), results showed that the weight of the 50 min BMPB increased rapidly after 40 % RH. The amount of water that was absorbed by 50 min BMPB is relatively high for example at 95 % RH, the water uptake was about 33-34 % of its dry weight. As cellulose has been ascribed earlier to absorb small quantities of water and provide minimal swelling, these findings provide some evidence that the native structure of the cellulose and various other polymers in PB have been adapted/changed by the mechanisms of BM. There was a significant difference between both cycles of sorption and only minimal differences in desorption of the cycles witnessed in Figure 25. The percentage of isotherm hysteresis is minimal but still apparent (Figure 26). These differences in isotherm hysteresis formed due to water being trapped within the sample matrix, which could not be removed completely during the desorption measurement. This hysteresis

loop is prominent at lower RH, which is thought to be due to strongly bound water to the sample i.e. swelling, as for example at higher RH it would be associated with high porosity of the sample. Rattihallik (2010) investigated DVS of citrus fibre and found at 95 % RH the weight of the sample was around 35 % of its dry weight, similar to that of 50 min BMPB. Furthermore a hysteresis loop apparent at lower RH similar to the one observed in Figure 26 was apparent and comparable to 50 min BMPB (Rattihallik, 2010). During cycle 1 the onset RH for re-crystallisation is seen at 75 % (as shown by arrows) and is indicated by a major gain in mass, possibly due to water uptake. When the cycle is repeated (stepped increase and decrease in RH) the results show only minimal differences in onset of re-crystallisation and minimal deductions in the change of mass. Therefore, the 50 min BMPB once hydrated then subsequently dried and rehydrated uptakes water differently. Though the differences can be plausibly deduced from the initial re-crystallisation during the first rehydration steps, whereby water mobilises the amorphous regions initiating re-crystallisation, thus in the second cycle it is subsequently forced out by crystalline regions (Kocherbitov *et al.*, 2008), thus causing differences of water uptake and release. This is shown more readily in the DVS isotherms of cycle 1 and 2 in Figure 26, which show slight differences and therefore indication of an irreversible structural change, due to this uptake of water/RH. Though this structural change is minimal but still apparent. Thereby giving evidence that the PB would re-crystallise with the addition of a higher water content and/or RH, which are necessary requirements, as seen when comparing with DSC results.

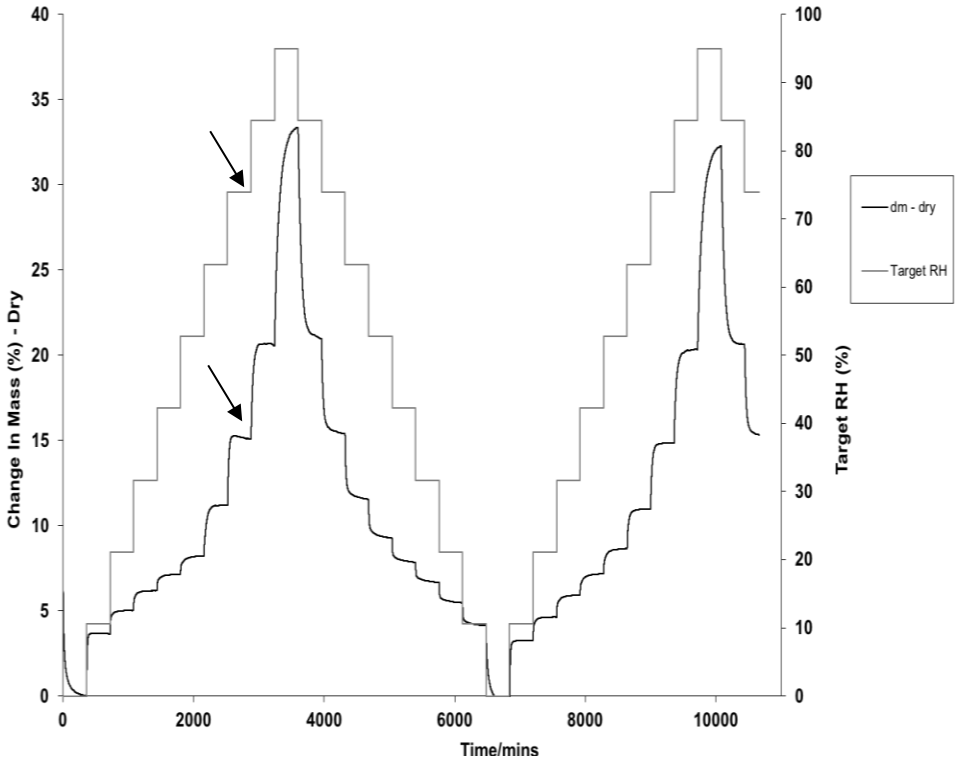


Figure 25 Dynamic vapour sorption of amorphous 50 minute BMPB with an initial step relative humidity function followed by a repeat of the conditions following normalisation of humidity.

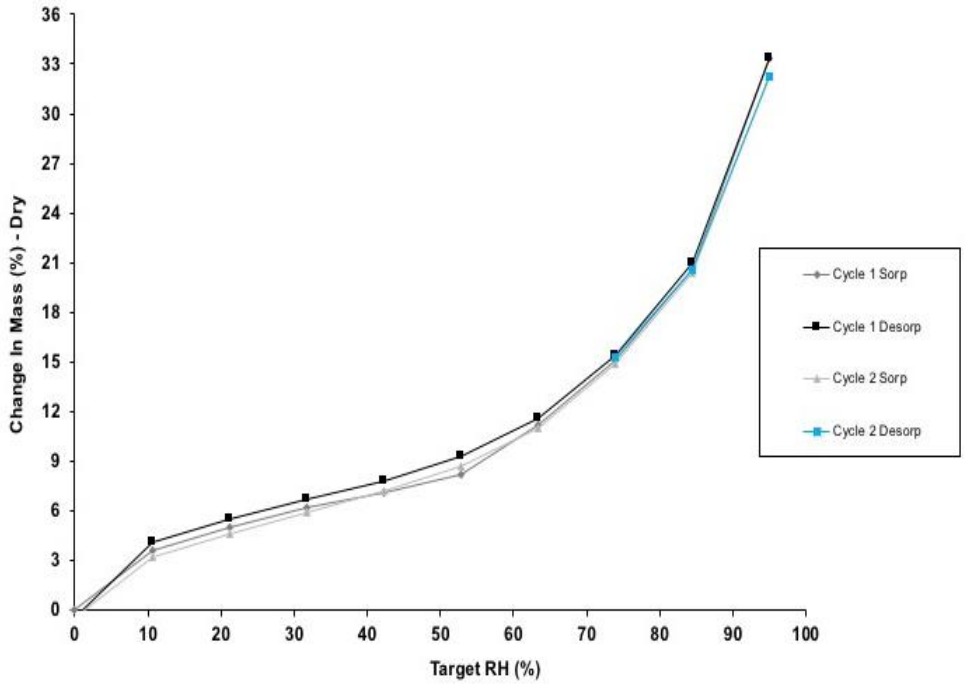


Figure 26 Dynamic Vapour Sorption isotherms of cycle 1 sorp (sorption), cycle 1 desorp (desorption), cycle 2 sorp and cycle 2 desorp of amorphous 50 min BMPB.

4.3.5 The effects of rehydration on an amorphous Ball Milled Pea Biomass

Re-crystallisation can be defined as the formation of a new grain structure in a deformed (amorphous) material by the formation and migration of high angle grain boundaries driven by a stored energy of deformation (Doherty *et al.*, 1997). The process of dispersing a dry powder in a liquid can be devised into four steps (Schubert, 1993): (i) wetting, (ii) submerging, (iii) dispersing and (iv) dissolving (if soluble).

In order to ascertain whether 50 min BMPB became re-crystallised with the addition of an excess of water, different quantities of water were added in order to physically analyse the effects of required water content. It was found that at 10 % and 20 % solid contents, sedimentation effects occurred and an excess of water remained on top, showing incomplete miscibility and homogeneity indicating little dissolution, and the formation of a dispersion. Therefore, if tested rheologically, then it would not provide appropriate anisotropic results. Experiments performed to 25 and 33 % solids (4 and 3 mls added respectively) showed no visible sedimentation and incomplete miscibility. At contents higher than 33 % solids, it was found that not all of the powder would mix entirely as it would agglomerate and turn into a solid.

Additionally the mixing at these concentrations may also affect the water distribution and therefore there would be a comparison between those that are stir mixed (SM) using a magnetic flea for 1-2 Hr depending on the solid contents, at ambient temperature and those left to swell once briefly mixed and therefore unstirred (UN) for a 24 Hr period. These methods were then used for a comparison of efficiency of swelling, crystallinity and in order to determine if re-crystallisation is time dependent within such samples. Moreover, it is known that powder wetting on an industrial scale in snacks

production undertakes minimal direct mixing, and therefore such a comparison is meaningful, albeit at longer timescales than those used during large-scale manufacture.

1.4.1.1.1 Morphology of rehydrated 50 min Ball Milled Pea Biomass

Polarised light microscopy can indicate whether materials have crystals present because they will emit birefringence. Figure 27 A and D shows that the amorphous 50 min BMPB emits no birefringence. However, Figures 27 B and E containing 25 % solid contents and C and F at 33 % solid contents clearly emit birefringence. They depict that some areas (but not the entirety of the samples) have re-crystallised. Samples did not seem to vary visually between rehydration methods. The theory of birefringence is an optical technique of measuring orientation in an optically anisotropic sample having a refractive index that is dependent upon polarisation and propagation direction of light. We can be assured that this emittance of light is that of re-crystallised cellulose and not of another polymer composite within the mixed biopolymer system. This assurance is based on evidence that lignin and pectin, in their native forms, are amorphous, as well as hemicellulose when it is not directly bound to cellulose.

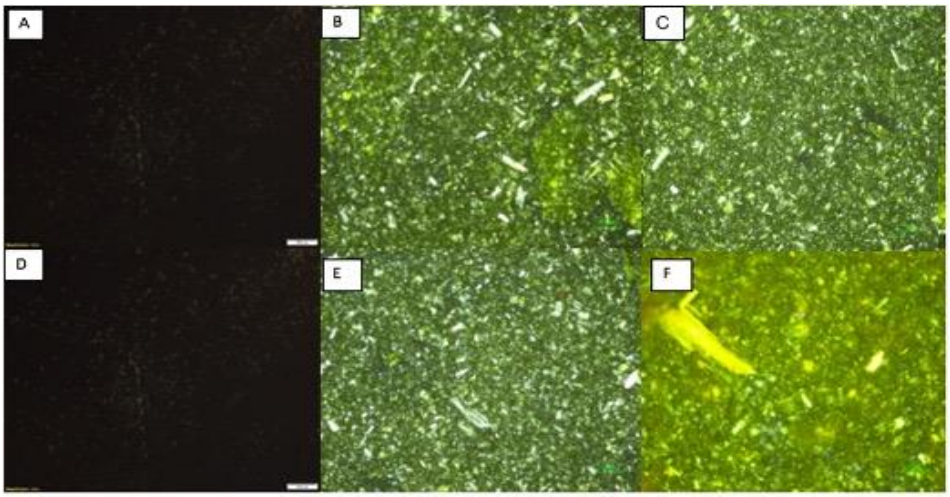


Figure 27 Polarised microscopy of 50 minute BMPB (A and D) rehydrated at two varying concentrations, B and E refer to 25 % solid content, C and F refer to 33 % solid content and both rehydrated samples display birefringence.

It is known that re-crystallising cellulose creates changes to main-chain conformation through absorption of water (Kimura *et al*., 1974). This is mainly due to the influences of swelling; this causes the degree of freedom for molecular motion to increase and a subsequent decrease of the intra- and inter-molecular forces by the cleavage of hydrogen bonding (Kimura *et al*., 1974). It has been estimated by Sobue and Fukuhara (1959) that the explanation for this could possibly be derived from micro-Brownian motion (the random motion of particulates colliding) (Sobue and Fukuhara, 1960; Kimura, Hatakeyama and Nakano, 1974). These theories may explain the results in Table 8, whereby the particle size of the 50 min BMPB has more than doubled in size from 30.94 to 70.60 µm (based on averages of < 90% diameter volume) from its dry form upon rehydration. Typically, the lower swelling power equates to a low gel strength. Though in comparing these to its supposed replacement and or coinciding with, starch commodities specifically potato, which has been ascribed to having a swelling power 10-100 times greater than that of cereal starches (Lisińska and Leszczyński,

1989). One can assume that on average the hydrated potato starch particle sizes would be much larger than that of the rehydrated 50 min BMPB. These findings would be more similar morphologically to that of cereal starches or tapioca (Lisińska and Leszczyński, 1989).

Table 8 Differential particle size distribution of < 90 % volume of rehydrated 50 min BMPB powder (0.5 g of 50 min BMPB in 25 g of RO water).

Sample	Size (μm) < 90 %
Rehydrated 50 min BMPB	70.60

1.4.1.1.2 The effects of rehydration on the crystallinity of amorphous Ball milled Pea Biomass.

In order to quantify the level at which the samples re-crystallised, WAXD and ^{13}C CP-MAS NMR was performed. For continuity, the multi-peak deconvolution method for calculating crystallinity was used. The WAXD spectrum (Figure 28) showed that all rehydrated samples have re-crystallised, which was indicated by an increase in the intensity of the main peak between 15-25° (2θ). A small shoulder is observed in the rehydrated samples that is not observed in the amorphous 50 min BMPB sample. With the addition of water the samples have gained an average of 8-9 % crystalline lattices, shown in Table 9. The crystalline lattices restructured into predominantly the allomorph II form, which is thermodynamically more stable as stated previously. Abbaszadeh (2014) also looked at the re-crystallisation of BM amorphous polymers and found that microcrystalline cellulose and eucalyptus cellulose re-crystallised to around 13 % in the type II allomorph. This indicates that in their work the samples were made more/completely amorphous prior to re-crystallisation and therefore had no seed I crystals remaining, initiating re-crystallisation completely in the type II

allomorph. This is only 1 % higher than the total re-crystallisation found in these works. Furthermore, Abbaszadeh (2014) found when co-milling polymers and subsequently re-crystallising them (for example xyloglucan and microcrystalline cellulose), produced lower levels of re-crystallisation (2-5 %) albeit all in the type II allomorph (Abbaszadeh, 2014). Therefore, as PB is a mixed PCWM, a lower level of re-crystallisation may be apparent due to other polymers within the matrix impinging the phenomena.

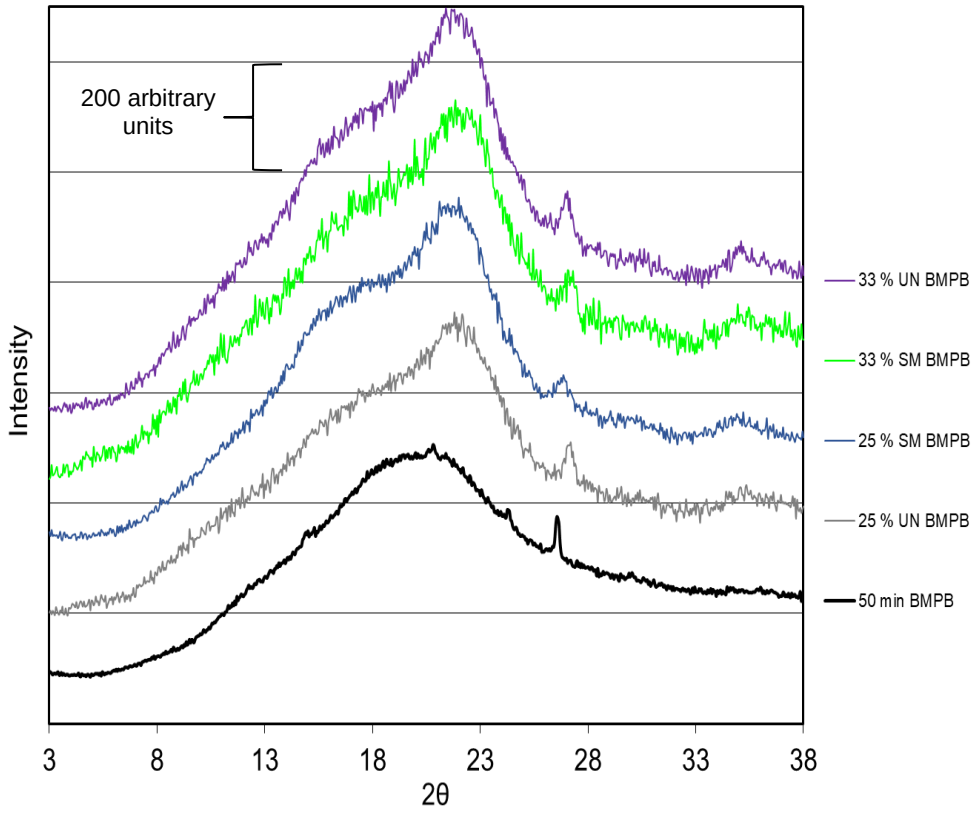


Figure 28 Wide Angle X-Ray Diffraction in angles 3-38 (2θ). Main cellulose crystallinity peak found between 15-25 (2θ). Additional peak around 27 (2θ) is indicative of trace elements in the sample.

***Table 9 Crystallinity percentages in each allomorph type, total crystallinity index and amorphous content for rehydrated 50 minute BMPB at varying concentrations (25 and 33 %) with two varying solubilisation methods. The crystallinity amounts were calculated using the multi–deconvolution method with modifications from* (Carrillo *et al.*, 2003).**

Sample	Type I allomorph (%)	Type II allomorph (%)	Crystallinity index (CI) (%)	Amorphous content (%)
25 % UN BMPB	2 ± 0.04	10 ± 0.44	12 ± 0.39	88 ± 0.39
25 % SM BMPB	5 ± 0.10	7 ± 0.19	12 ± 0.29	88 ± 0.29
33 % UN BMPB	3 ± 0.18	9 ± 0.03	12 ± 0.17	88 ± 0.17
33 % SM BMPB	2 ± 0.37	10 ± 0.09	12 ± 0.29	88 ± 0.29

***Table 10 NMR crystallinity for rehydrated 50 minute BMPB at two concentrations (25 and 33 %) taken from a contact time of 2 m/s calculated using a macro programme on Excel with solver with modifications from* (Paes *et al.*, 2010).**

Sample	Type I allomorph (%)	Type II allomorph (%)	Crystallinity index (CI) (%)	Amorphous content (%)
25 % UN BMPB	0	20	20	80
25 % SM BMPB	0	21	21	79
33 % UN BMPB	0	21	21	79
33 % SM BMPB	0	19	19	81

Further to this ^{13}C CP MAS NMR confirmed the re-crystallisation of the amorphous 50 minute BMPB with an increase in peak signals of the C4 region between 80–93 ppm and C6 regions of 64–68 ppm (Park *et al*., 2010), as shown in Figure 29. Furthermore, assessments using NMR for crystallinity calculations can be found in Table 10, which state that re-crystallisation occurred to a similar degree as results obtained from WAXD, given that using the multi-deconvolution method results are subjected to ± 5 %. Though differences were observed between the amounts of re-crystallisation in each allomorph, WAXD accounted for crystallinity in both allomorphs, whereas NMR only accounted for crystallinity in type II. It is more reasonable to presume that WAXD assessments are correct due to the small amount of type I seed crystals remaining after 50 minutes of BM (prior to rehydration) and therefore this residual form acts like a template for the crystallising material (Paes *et al.*, 2010). Differences of 8 % crystallinity were also observed between analytical equipment (NMR and WAXD), which may be explained by NMR assessments, which depend on the contact time chosen in the experimental protocol (due to amorphous regions decaying), as well as the water content of the sample (Paes *et al.*, 2010). However, both assessments, by themselves, independently provide evidence that the material has re-crystallised predominantly to the allomorph II form. Differences in crystallinity values between analytical assessments, as well as type I allomorph being present in WAXD was also found by Paes *et al.* (2010) in the BM of eucalyptus pulp and subsequent re-crystallisation.

Both assessments show re-crystallisation but to a small degree for a rehydrated amorphous material, this may give some indication that PB as a mixed PCWM with the addition of other polysaccharides and lignin may impinge the re-crystallisation of cellulose to an extent, when compared to a

purified cellulosic system, as found by Abbazadeh (2014) and Winkworth – Smith. (2014). Moreover, no differences are observed between 20-30 ppm and 180 ppm, which therefore shows an irreversible structural change to the chemical groups in either cutin, pectin and/or lignin fractions depicted here, which do not change upon rehydration effects. Thereby structurally making rehydrated 50 min BMPB a less crystalline and more disordered material, which in general would provide interesting rehydration properties, which are probed in the application chapter (Chapter 6).

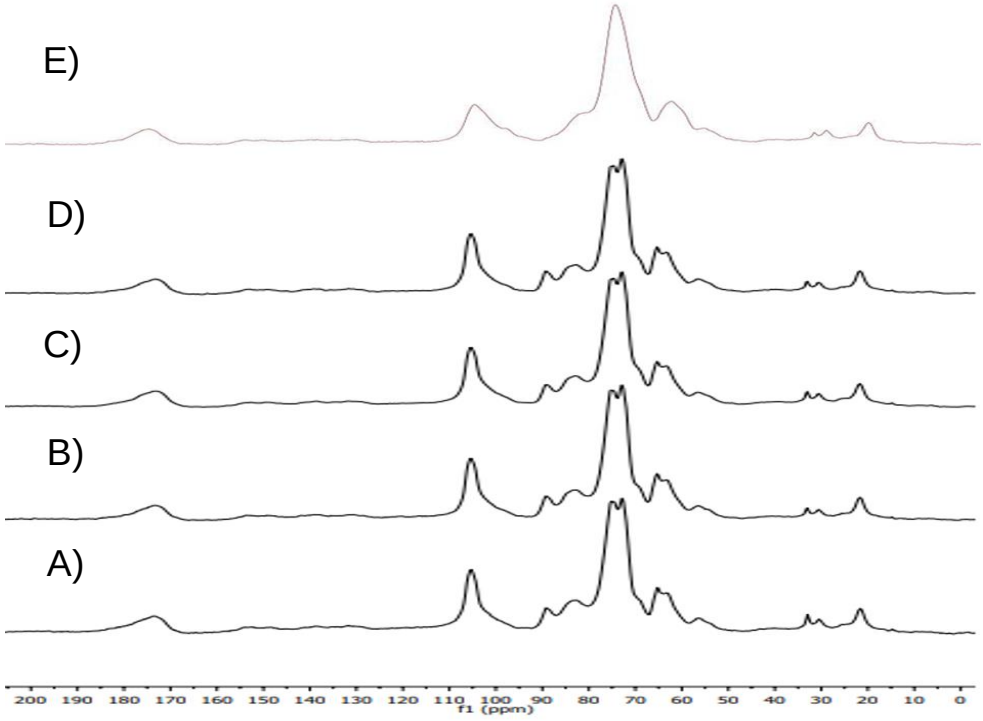


Figure 29 ^{13}C CP-MAS NMR of rehydrated amorphous (50 minute) BMPB, A) 25 % SM BMPB, B) 25 % UN BMPB, C) 33 % SM BMPB, D) 33 % UN BMPB, which are now re-crystalised and E) the original predominantly amorphous 50 min BMPB shown in light grey. The Spectrums were formatted using MNOVA software.

1.4.1.1.3 Rheology of rehydrated Ball Milled Pea Biomass

In order to quantify visco-elastic properties of rehydrated BMPB, rheological measurements were performed. Cellulose is a hygroscopic material meaning that it only swells minimally in water (Wüstenberg, 2015). It has been previously explained that amorphous cellulose has a higher capacity of water uptake (thereby swellability) than that of semi-crystalline and crystalline lattices. In order to assess the linear viscoelastic (LVE) region of the rehydrated BMPB at 25 and 33 % solids, amplitude sweeps were performed. Such rheological analysis will shed light on whether the samples can provide structure upon rehydration, which is similar to or an improvement on currently used ingredients, and the extent of stirring required for maximum hydration, ultimately achieving a homogenous viscoelastic material.

Figure 30 shows that rehydrated BMPB provides a short LVE range up to 3 % strain, then clearly has a cross over point where the material deforms. However, this is not the case for the unstirred sample at the highest solid level (33 %). This may begin to indicate that either homogeneity and/or breakage of interparticle connections when stirred produce weaker physical structures. It is worth noting however that these observations are not witnessed at low solid concentrations. Samples are significantly different to one another (p-value < 0.001) between different solid concentrations and different methods of swellability and therefore hydration.

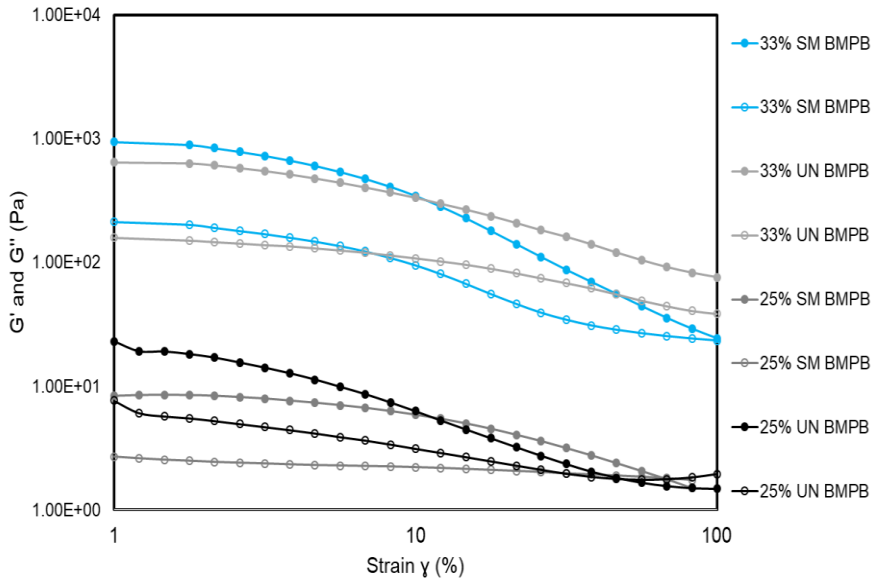


Figure 30 Amplitude sweep performed at 10 rad/s containing 50 minute BMPB at a solid concentration of 25 and 33 % then rehydrated with two varied methods of solubilisation/swellability. G' indicated by a filled marker and G'' indicated by an empty marker to show storage and loss modulus in pascals.

Frequency sweeps give additional information on how a material behaves. Figure 31 shows that rehydrated BMPB with differing methods of hydration behave like a visco-elastic material as shown by G' > G''. Samples are significantly different (p-value < 0.05) between samples with the same solid concentration but different methods of swellability. Furthermore, results showed that the SM samples have a significantly higher (p-value < 0.001) complex viscosity value than that of the UN samples for varying concentrations of solids, as shown in Figure 32. This provides evidence that the samples, which are SM would form a stronger paste/gel-like structure than that of the UN samples. These results are to be expected as the structures within the sample have been allowed to mix and suspend more evenly throughout. Thus indicating an interconnectivity of swollen particles with an input of energy and force. However, the upturn of result with higher frequency indicates the samples are losing structure.

Therefore, they are not be stable at frequencies above 3 rad/s and begin to deform. Moreover, in Figure 32 the tanδ values for the particulate dispersions show that the samples have a tanδ > 1, and therefore act as a viscoelastic gel or solid. The noisy tanδ result of 25 % UN BMPB and slightly lesser noisy tanδ of 25 % SM BMPB indicates a loss of structure, which begins to behave more liquid-like than gel-like and therefore indicates heterogeneous characteristics. This may be due to an excess of water not being sufficiently used by the lower solid contents of BMPB compared to those of 33 % solid contents, indicating less effective particle interactions. Furthermore, the stirring methods may have an effect as SM is significantly less noisy than that of UN, which would indicate that a stronger particulate network has formed, which does not deform as readily.

Thereby concluding that, BMPB dispersions in general behave as viscoelastic gels and so possibly have the ability to function as a replacer for high-energy dispersed ingredients. Concentration variabilities provided a linear trend with similar properties upon strain and frequency. Thereby showing that the competition for water was similar across samples. The increased complex viscosity of 33 % solid content samples indicates that an increase in solid content provides more gel-like solutions. Therefore, at 33 % concentration of solids there is still sufficient water to allow particulate binding and provide an increase in viscosity. This effect is reduced at lower solid contents. Furthermore, that stirring methods impacted the rheological properties of BMPB, stirring the solutions for longer periods allow them to mix and suspend more evenly providing greater visco-elastic properties.

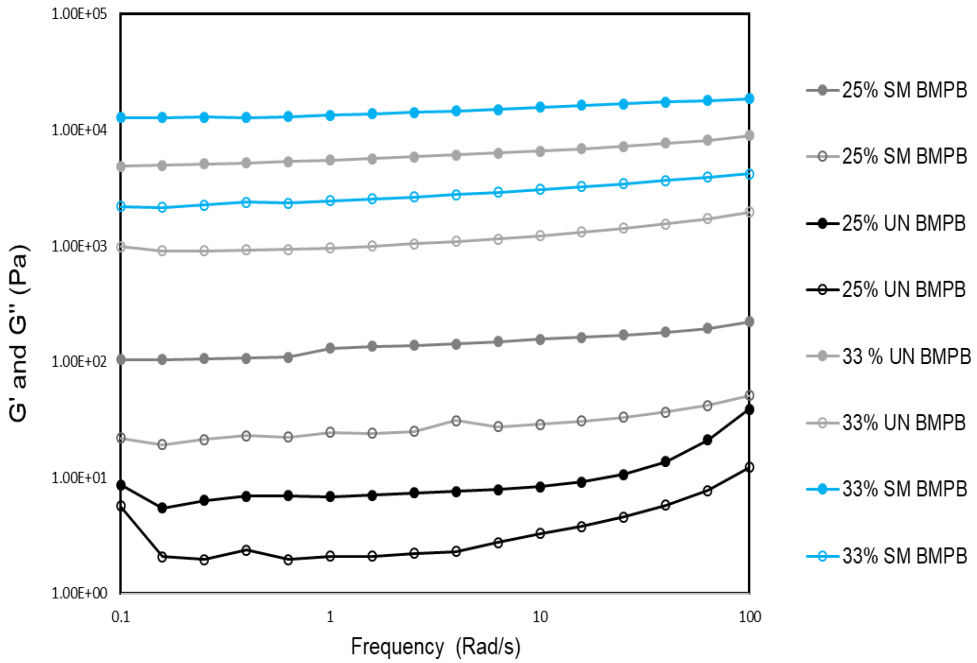


Figure 31 Frequency sweep performed at a strain of 0.5 % containing 25 and 33 % solid contents of 50 minute BMPB, rehydrated with two varied methods of solubilisation. G' for storage modulus is indicated by a filled marker whereas G'' for loss modulus is indicated by an empty marker both of which are in pascals.

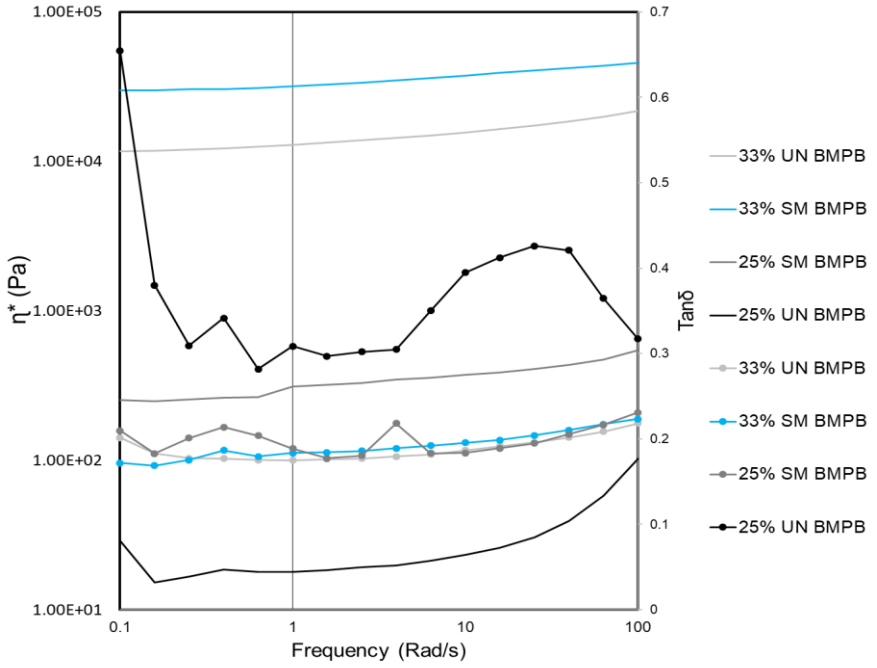


Figure 32 Frequency sweep performed at a strain of 0.5 % containing 33 % and 25 % solid contents of 50 min BMPB, rehydrated with two varied methods of solubilisation. Complex viscosity (pascal) is given as a straight line with no marker and tanδ is additionally provided and given as a marker with a straight line. With the complex viscosity assessed at an angular frequency of 1 rad/s.

4.4 Conclusion

Pisum sativum (PB) can be effectively BM when dried, to give characteristics comparable to that of other natural pure cellulosic materials. It is found that:

- BM PB causes a decrease in crystallinity from the native state (13.43 %) to less than 2 % after 90 minutes of BM and thereby becomes an amorphous mass, as confirmed by WAXD and ^{13}C CP-MAS NMR.
- An overall decrease of particle size with increased milling was observed in the PB (from 44.36 μm to 16.84 μm). Further BM over 50 minutes resulted in an increase in particle size; possibly due to agglomeration of particles caused by heat induced forces of energy from the balls within the ball milling process. This phenomena can be consistent with lowering of DP of the constituent materials within the mixed PB.
- Furthermore, a decrease in secondary order thermodynamics of PB and water content were also observed with an increase in milling time. As well as comparisons made to pure cellulosic materials for lack of glass transitions through DSC methods assessed. Though, comparisons could be made and witnessed for onset degradation temperature.
- Rehydration of amorphous BMPB indicates an increase in particulate size (as shown by light microscopy and particle size analysis) and a re-crystallisation event as observed by polarised light microscopy, WAXD and ^{13}C CP-MAS NMR. The results indicate that the materials re-crystallises with both allomorph I and allomorph II seed crystals, when analysed after 50 minutes of BM.

- Rheological data provided evidence that the material, when rehydrated, behaves like a visco-elastic material. At higher solids level this showed little to no sedimentation and exhibited comparisons to a paste/gel like structure, thereby providing future indications of properties akin to those witnessed for current food materials.

Therefore, BMPB powder is deemed to have the capacity to be a structural material and may provide advantageous microstructure properties when used in a composite. Thereby this material may have the potential to be incorporated into high-energy dense food-based products, as an added ingredient to partially replace starch commodities. The particle swellability and re-crystallisation might be compared to starch gelatinisation events, with hydrated pastes providing properties of gel-like cohesion seen for starch (Evans and Haisman, 1980). Future idealisations of using this functionalised material would provide great benefits to the public when used as a replacement for current high-energy dense ingredients. The material hypothesised here contains a low calorimetric index with additional benefits of being high in fibre and providing added protein.

Chapter 5 The production of Micro-fibrillated cellulose from Pea Biomass

5.1 Introduction

5.1.1 Introduction to fibrillation

It is well established that micro-fibrillated cellulose (MFC) has a unique application in material reinforcement (Lavoine *et al.*, 2012). These micro-fibrillated celluloses are used in various commercial applications such as paper-industry, pharmaceutical, food and medical industries (Turbak, Snyder and Sandberg, 1982; Lavoine *et al.*, 2012, Agarwal *et al*., 2019). Fibrillated materials were first ascribed in the late 1970's-80's by Turbak (1983), where wood pulp showed gel-like behaviour after being passed through a high pressure homogeniser (Turbak, Snyder and Sandberg, 1982). Currently, few companies manufacture MFC on an industrial scale by this method, such as Borregaard AS, UPM and Innventia AS (Borregaard, 2019; Innventia, 2019; UPM, 2019). Furthermore, it has the potential to be utilised in food applications, if prepared in a food grade manner. According to the Food Standards Agency and approved in the EU, fibrillated materials would come under legislation as E460 as cellulose, microcrystalline cellulose and powdered cellulose, which is used as an emulsifier, thickener and/or stabiliser. Currently used as a bulking agent in food (Unites States Department of Agriculture, 2018) and fibrillated materials are most commonly used in vitamin supplements or tablets, as well as cosmetic products (Turbak, Snyder and Sandberg, 1982).

Fibrillation defined as an act or process which increases the amount of individual fibres and/or fibrils adapted from (Merriam-Webster, 2018). Thereby a material has an increase in surface area compared to the original

material (Turbak, Snyder and Sandberg, 1982; Herrick *et al.*, 1983; Hult, Iversen and Sugiyama, 2003).This increase occurs due to treatments and processing of virgin fibrous material, resulting in fibrils separating away from the main mother fibre also known as a macro-fibre in these works (see Figure 33). The resulting fibres are often described as looking “hairy” or like whiskers more commonly referred to as micro-fibres or micro-fibrils (see Figure 34), when mechanical disruption such as sonication or acid hydrolysis is often applied (Garcia de Rodriguez, Thielemans and Dufresne, 2006; Oksman *et al.*, 2006; Petersson, Kvien and Oksman, 2007; Siró and Plackett, 2010) or a colloid mill in the instance of Figure 33.

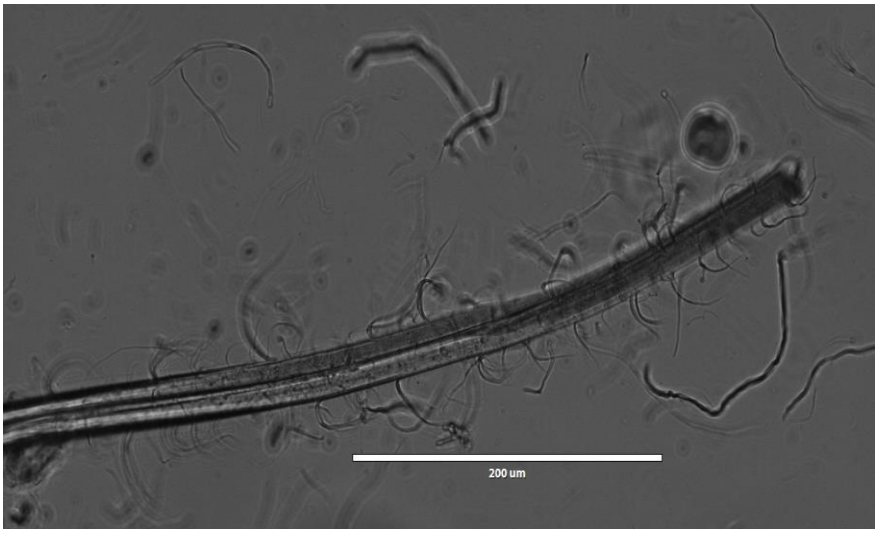


Figure 33 A Lyocell fibre that has been fibrillated using a colloid mill (Fryma Maschinenbau vertical MZ-50/R toothed, Germany) (0.5 % solution processed for 3 min and maximum speed). Smaller fibres coming away from the main mother fibre, showing an increase in surface area.

The degree of fibrillation/amount or dimensions of these micro-fibres depends on the processing/pre-treatments of the mother fibre also known as a macro-fibre. Different dimensions and homogeneity of these micro-fibres behaves differently in a suspension. Additionally the micro-fibres, coming away from the main mother fibre, may become detached and held

within a suspension or sediment over time. Furthermore, with additional treatment and/or processing these micro-fibres can become nano-fibrillated cellulose (Lavoine *et al.*, 2012) (see Figure 34). There are inconsistencies that exist with cellulosic literature regarding nomenclature (Siró and Plackett, 2010). This could be due to the material being inhomogeneous and containing fibres, fibre fragments, fines and fibrils (Chinga-Carrasco, 2011), until specific pre-treatments are used which can, in certain instances, facilitate homogenity. Therefore as a summary of the mixed nomenclature stated it is possible to produce or extract two families of micro- and nano-sized cellulosic elements from native cellulose, namely Cellulose Nano-Crystals/Nano-Fibres/Nano-Cellulose Whiskers (CNC/NFC/ NCWs) (Azizi Samir, Alloin and Dufresne, 2005; Bras *et al.*, 2011; Lavoine *et al.*, 2012; Lu *et al.*, 2013) and Micro-Fibrillated Cellulose (MFC) (Siró and Plackett, 2010; Lavoine *et al.*, 2012). NanoCrystals/Nano-Fibres can appear as rod-like particulates with the later definition usually being formed by bacteria and the crystals are usually produced through hydrolysis of plant and woody based cellulose, via severe chemical or enzymatic applications but both additionally consist of elementary fibers in their native form (Pääkkö *et al.*, 2007; Siró and Plackett, 2010; Alila *et al.*, 2013). Whereas MFC may be considered to be a bundle of less ordered (amorphous) elementary fibres that still contain some crystallinity, whereby the fibers pull away from the mother fibre in less ordered areas (Lavoine *et al.*, 2012).

Though definitions still remain uncertain, with debates over the topic regarding structure (due to variability of cellulose origin) and the level of quantification necessary to ascribe the majority as either being macro-fibres, MFC or CNC/NFC (Chinga-Carrasco, 2011). Therefore, upon processing, as stated by Chinga-Carrasco (2010) it will be expected that there will be

different populations of these separate fractions of fibres. Where, in the present works, MFC and NFC terminologies will only be used to ascribe the two differing population sizes of fibres as presented in Table 11, until later findings confirm the terminology based on the diameter of the fibres. Definitions of diameters for each two families of micro- and nano-sized cellulosic elements are also contended. Differing research states different diameters for each, with an example in Table 11 showing the size range, of each type of fibre. It would seem appropriate to deem the mass produced in this study as a mixed fibrillated system unless one can quantify it differently.

Table 11 Adapted from (Siró and Plackett, 2010; Chinga-Carrasco, 2011) diameter of fibrillated fibres depending on terminology used.

Cellulose Structure	Diameter (μm)
Nano-fiber (NFC)	0.002-0.1
Cellulose whisker (NWC)	0.002-0.2
Micro-fibrillated Cellulose (MFC)	0.01-0.04
Macro-fibrils	>1
Cellulose fibre/Tracheid	10-50

In order to define each of these sizes (MFC and NFC) it is necessary to give evidence to the size and proportions/fractions of fibrillated fibres as well as, morphology to which diameter governs the majority of the system (Chinga-Carrasco, 2011). Chinga-Carrasco (2011) ascribed MFC as a biological structure currently existing in nature whereas NFC introduces secondary engineered structures, which typically become detached from the mother fibre/macro-fibre and held within suspension (see Figure 34).

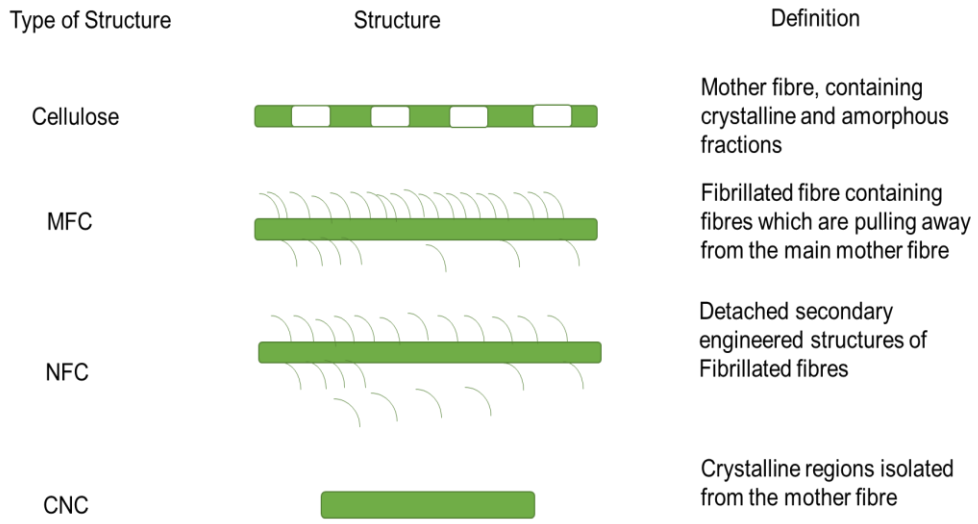


Figure 34 Schematic of types of cellulosic structures achieved through fibrillation and their definitions. Cellulose crystalline fractions are given as an example for green and white for amorphous regions. MFC and NFC would additionally contain amorphous regions (not shown to reduce complexity). Fibres within a dispersion could contain a mixture of these types of structures and fibres depicted here are not to scale but with relevant scales of each provided in Table 11.

5.1.2 Properties of fibrillated materials

Fibrillated materials have been credited with having excellent mechanical and physical properties, such as high elastic modulus, high porosity, high strength and stiffness, usually at relatively low usage levels (Wada *et al.*, 1995; Saheb and Jog, 1999; Guhados, Wan and Hutter, 2005; Siró and Plackett, 2010) and high crystallinity (Czaja, Romanovicz and Brown, 2004). The crystallinity of MFC depends upon the origin of the starting material and may explain the difference in the other physical properties of fibrillated materials (Lavoine *et al.*, 2012). Alemdar and Sain (2008) found that wheat straw and soy hull had crystallinity values of 78 % and 70 %, respectively (Alemdar and Sain, 2008) and Heux *et al*. (1999) finding sugar beet to be about 30-40 % (Heux, Dinand and Vignon, 1999). Higher crystallinities of MFC up to 84-89 % have been reported in wood (Lavoine *et al.*, 2012). Crystallinity has been shown to decrease with passes on specific high

pressure homogenisers due to the mechanical disruption action on hydrogen bonds converting crystalline regions into amorphous regions (Iwamoto, Nakagaito and Yano, 2007, Agarwal *et al*., 2019). Additionally a phenomenon called hornification may occur in fibrillated fibres, whereby strong hydrogen-bonds are formed during drying of MFC fibers within the amorphous regions. This formation of aggregates upon drying of MFC, due to both hydrogen bonding and van der Waal force interactions, is then termed the hornification (Iwamoto, Nakagaito and Yano, 2007). Literature suggests that high crystallinities have been related to greater yields of CNC, as if cellulose is depolymerised excessively during manufacturing the fibre aspect ratio is decreased/altered (George and Sabapathi, 2015). This is due to the low amount of amorphous domains remaining particularly in the case of nano-crystals (George and Sabapathi, 2015). However, it is well established that as the number of passes increases through the homogeniser, the apparent viscosity of the MFC suspension increases (Herrick *et al.*, 1983). This reaches an equilibrium, where a dispersion shows a stable viscosity (Aulin *et al*., 2010). This highly depends on the source and technology used to produce MFC/NFC (Siró and Plackett, 2010). Typically, a 2 % aqueous dispersion of MFC shows shear thinning and pseudoplastic behaviour (Aulin, Gällstedt and Lindström, 2010; Zimmermann, Bordeanu and Strub, 2010, Agarwal *et al*., 2019). Furthermore, Iotti *et al*. (2011) confirmed this with MFC dispersions varying in concentration from 1-4 % and detailed a hysteries loop, showing that high shear rates can promote dilatant behaviours (Iotti *et al.*, 2011). The impact of the degree of fibrillation will affect the volume packing of a dispersion, which may influence the shear viscosity of the dispersion especially with varying concentrations and that will determine the hysteresis behaviour at higher shear rates.

5.1.3 Treatments to enable/facilitate or improve properties of fibrillated masses

Typical methodologies for converting a biomass into homogeneous fibrillated dispersions include heat, chemical, mechanical, enzymatic and bacterial processes or in combination of two or three process (Henriksson *et al.*, 2007; Pääkkö *et al.*, 2007; Siró and Plackett, 2010; Lavoine *et al.*, 2012).

5.1.3.1 Thermal treatments to aid in fibrillation properties

For thermal treatments the use of simultaneous ultrasonic wave, microwave assisted techniques and hydrothermal techniques have been reported in the literature (Lu *et al.*, 2013; Hiltunen, Heiskanen and Backfolk, 2018). Hiltunen, Heiskanen and Backfolk (2018) processed enzymatically derived MFC dispersion from hardwood through hydrothermal treatment at various temperatures to see the effect on the dispersion's gel-like properties and polymer matrixes. They found that various hydrothermal temperatures did not affect the viscosity of the MFC. High temperatures did affect the water retention capacity of the MFC gels by lowering it, which was thought to be due to hydrolysis of hemicellulose and reductions in cellulose chain lengths, which had been subsequently affected by the hydrothermal heat treatment. Therefore, if, this had been a material that additionally contained other polymers such as lignin and pectin, then it would indicate that these would also slightly degrade within the matrices. Gould *et al*. (2013) used hydrothermal techniques to relocate lignin to the surface of PCWM. It is not fully understood whether lignin is advantageous within a matrix of fibrillated mass or an inhibitor of greater fibrillation. Lu *et al.* (2013) used ultrasonic wave and microwave assisted techniques on acid hydrolysis prepared nano-cellulose whiskers in order to accelerate production and yield. They found

that the synergetic effect of ultrasonic waves and microwaves decreased the yield of fibrillated mass produced under high temperatures and long treatment times. This may additionally have been due to the degradation of cellulose and/or other polymers within a matrix. Though, it is apparent that chemical and mechanical treatments have been extensively researched for their abilities to produce greater yields of fibrillated masses in comparison to thermal treatments (Siró and Plackett, 2010; Lavoine *et al.*, 2012). Furthermore, the use of thermal methods has mainly been used for post-treatments to enhance/differentiate fibrillated mass properties. Therefore, research is necessary to see if thermal methods used as pre-treatments can improve the properties of fibrillated plant based materials; also fundamental understanding of the impact of high temperatures on the structural/functional properties of other polymers within the matrixes is required.

5.1.3.2 Chemical and enzymatic treatments to aid or enable fibrillation

Chemical pre-treatments are commonly used to reduce mechanical energy and time of fibrillation (Ankerfors, 2012). Furthermore, for mixed cell wall materials, pre-treatments can be used to purify/fractionate the mixed PCWM to remove or partially remove lignin, pectin and hemicelluloses. Thereby, increasing cellulose purity and possibly improve yields of fibrillation if the other polysaccharides and lignin were impinging or protecting production of fibrillated cellulose. However, these chemical pre-treatments are often not food applicable, mainly consisting of severe acid hydrolysis, TEMPO mediated oxidation and use of alkaline chemicals (Dufresne, Cavaille and Vignon, 1997; Saito *et al.*, 2006, 2009; Habibi and Vignon, 2008; Lasseuguette, Roux and Nishiyama, 2008). The use of such chemical pre-

treatments result in solubilisation of lignin, but in turn can degrade cellulose if hydrolysis is not at the fibre surface, although lignin supposedly inhibits improved fibrillation (Spence *et al.*, 2010; Ferrer *et al.*, 2012; Solala *et al.*, 2012). In some studies low amounts of hemicellulose has been shown to promote the flocculation of micro-fibrils within the fibrillation process, especially for the production of cellulose nano-materials (Iwamoto, Nakagaito and Yano, 2007; Suopajärvi, Liimatainen and Niinimäki, 2010). This may be due to collisions in processing and intertwining of the fibrils themselves, due to natural apparent bond formations of hemicellulose and cellulose. Recently, Agarwal *et al*. (2018 and 2019) has studied the impact of polymer additives on the structure/functionality of MFC from spruce. Additionally, chemical post-treatments can be used to improve MFC or bequeath it with differing properties, depending on potential application (Lavoine *et al.*, 2012) (though post-treatments are not explored in the current study). Source of cellulose, pre-treatment solvents, conditions and process parameters such as reaction time, temperature and solvent concentrations have significant impact on MFC/NFC yield. Lu *et al*. (2013) used sulfuric acid with varying process parameters in order to quantify the effects on NFC yields (Lu *et al.*, 2013). Reaction time caused a decrease in yield over prolonged periods due to a decrease in crystalline cellulose as a result of hydrolysis. This trend is similar when applied to the reaction temperature and concentration. Therefore, it is reasonable to conclude that to produce high grade MFC with a high yield either by chemical and/or mechanical treatments it would depend on the source of cellulose. Appropriate optimisation of the production is required depending on the source of raw material.

Thus, different chemical methods including an ethanol wash (ethyl alcohol) with or without the addition of a sodium hydroxide (alkali) wash were applied to the PB in these works. Ethanol washes were chosen based on their ability to solubilise Brauns and organosolv lignin (Chen, 2014) when it has moved to the surface of the primary cell wall layer, as acid lignin is not soluble in any solvents (Chen, 2014). The lignin will supposedly reorganise and move to the surface of the PCWM based on the hydrothermal technique used prior to any chemical applications (Ibbett *et al.*, 2011; Gould, Garcia-Garcia and Wolf, 2016). Through condensation and degradation lignin is separated into soluble and insoluble fractions, if phenolic hydroxyl and carboxyl are present the lignin will dissolve in alkali solutions (Chen, 2014). Though acetyl bromide and hexalfluoroisopropanol are supposedly the best solvent for most separated lignin (Chen, 2014), in this instance they were not used as a food grade chemical solvent was sought after (Chen, 2014). Thereby, seeing if a food grade version of lignin and possibly other polysaccharides removal has an increase in production yield of fibrillated fibres. Furthermore, the use of alkali washes were chosen based on the work of Cuissinat and Navard (2006) where they found that an 8 % solution at -5 °C, is the best condition leading to a heterogeneous ballooning phenomenon, where swelling of cellulose takes place along selected zones of the fibre (Cuissinat and Navard, 2006). It is acknowledged that the fibres would then have to be subsequently washed in order to meet legislation requirements of health and safety, similar seen with Konjac glucomannan (Armisén and Galatas, 2009). An explanation for this phenomenon is that swelling of cellulose chains, within the secondary wall causes the primary cell wall to extend and burst (Budtova and Navard, 2016). The expanded swollen cellulose then moves through and tears the primary wall. Swelling occurs as hemicellulose is solublised in sodium hydroxide solvents (Budtova and Navard, 2016).

Therefore using this particular method to explore whether hemicellulose removal or ballooning of cellulose improves the yield efficiency of fibrillated materials. Albeit, agricultural crops have been stated to need less energy than wood based materials, as cellulose is in the primary cell wall and therefore easier to separate than secondary cell wall (Dufresne, Cavaille and Vignon, 1997).

Bacterial cellulose is a biopolymer that is formed by nanofibrils, through synthesis of *Acetobacter xylinus* and *Acetobacter hansenii* for example and other bacterial forms (Wang *et al.*, 2018). Enzymatic pre-treatments such as mono-component endoglucanase coupled with mechanical shearing in order to facilitate fibrillation may also occur (Pääkkö *et al.*, 2007). These conversion routes can produce longer and highly entangled nanoscale fibres in comparison to those produced from aggressive acid hydrolysis and additionally shorter fibres as well as. These have advantageous properties of strong reinforcement and in some cases form strong aqueous gels 10^2 Pa at concentrations of 1 % w/w (Pääkkö *et al.*, 2007). Though, enzymatic pre-treatments were not explored in these works but acknowledged as a potential future conversion route.

5.1.3.3 Mechanical treatments to facilitate fibrillation

For mechanical treatments, most commonly used methods include high–pressure homogenisers, microfluidisers, grinders, cryo-crushing, electro-spinning, blenders or ultrasound in order to produce micro and nano-fibres (Herrick *et al.*, 1983; Dufresne, Cavaille and Vignon, 1997; Huang *et al.*, 2003; Li and Xia, 2004; Zhao, Feng and Gao, 2007; Alemdar and Sain, 2008; Siqueira *et al.*, 2016). However, using only heat and mechanical processes

equates to production of MFC and CNC/NCW/NFCs being time consuming with low yields of production for the amount of energy required to create a fibrillated mass (Chinga-Carrasco, 2011). As a result, there is a need to improve the production efficiency. In more recent years, companies such as Borreguard AS (Norway) and Innventia (Sweden) have optimised new innovative production technologies with higher efficiencies and currently patenting differing methodologies to produce fibrillated cellulosic materials through just mechanical disruption, which results in both MFC and NFC with a reduced energy requirement necessary to do so (Holtan *et al.*, 2017).

5.1.4 Aims of this chapter

PB, as a valorisation material, has been used as the raw material for producing fibrillated material, which has created mixed fibrillated fibres of MFC and NFC with various aforementioned treatments. For use of comparison, Solka Flock 900 (SF), a purified cellulose was used, to identify what the yield, crystallinity and rheology would be with just mechanical means as those materials have not had any chemical pre-treatments.

The main objectives are:

- To investigate the production of a fibrillated mass from PB and understand the effect of pre-treatments on the proportion of MFC that additionally may have differing populations of fractions containing differing fibrillated masses as ascribed earlier.
- Hydrothermal and chemical pre-treatments designed to test the effect of inherited hemicellulose and lignin from the source, with a view to increase the efficiency of production of valourised PB.

- Compare two mechanical treatment processes of fibrillation on their production efficiencies and properties of fibrillated masses, with and without pre-treatment.

5.2 Materials and methods

5.2.1 Materials

PB in its raw wet form after juicing (see Chapter 3 section 3.2.1) was used after leaving to thaw at 25 °C from the -80 °C freezer for a few hours (Denley CFC-Free -80 ºC freezer, China).

Solka floc 900 (SF) was additionally used as a comparison of a pure cellulosic system (International fibre corporation, New York, United States of America) and was stored at 25 °C ± 1.

5.2.2 Processing methods

An outline of the way in which the PB has been processed to test whether fibre fibrillation is possible can be seen in Figure 35 and described in detail in the following sections.

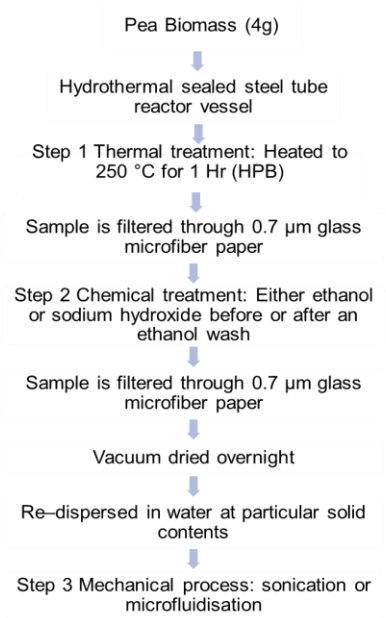


Figure 35 Processing schematic of pea biomass, in order to achieve fibrillation, going through steps 1-3. Details of each step and the resulting sample types are to follow.

5.2.2.1 Heating Method

4 g of raw PB was inserted into a (Internal 22 mm and external 26 mm) hydrothermal vessel and RO water was added to the biomass at a 1:10 wet weight ratio. The vessel was then heated to 250 °C for 1 Hr in a Muffle furnace (AAF 1100, Carbolite ltd, UK) (step 1), (adapted from (Ibbett *et al.*, 2011). This process created hydrothermally treated Pea Biomass (HPB).

5.2.2.2 Chemical washes

HPB was then subjected to either an ethanol wash for 30 min or 1 Hr, step 2, with or without a sodium hydroxide (alkali) wash (Pellets purity 98 %, Honeywell Fluka) before or after the ethanol (ethyl alcohol) wash (Figure 36).

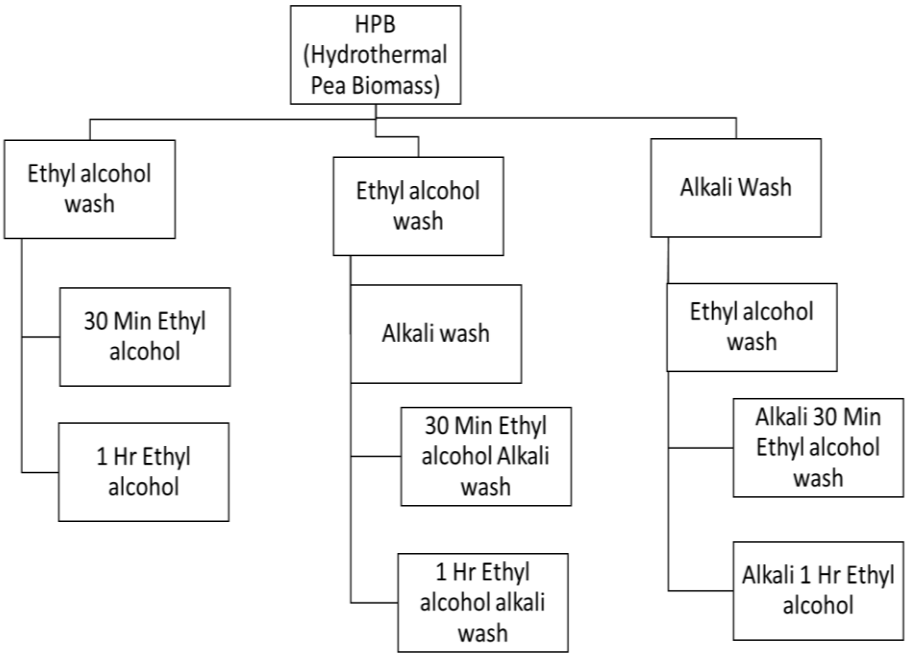


Figure 36 A flow hierarchy diagram showing, the initial HPB is treated by three differing chemical methods, with each chemical method having two various ethanol wash times, either 30 minutes of 1 hour. Details of washes to follow.

Ethyl alcohol wash entailed using 99.9 % ethanol (Sigma Aldrich, UK) in a Soxhlet extractor with an attached water flow system, within a fume cabinet. After ethyl alcohol washed HPB was then filtered using Whatman GF/A Glass microfiber (Whatman, Sigma Aldrich, Dorset, England), within an opened high vacuum environment (units unable to be measured due to the open environment and therefore fluctuations). The material was then left in a fume cupboard overnight to allow the required remaining ethanol to evaporate.

Alkali washes involved using an 8 % aqueous sodium hydroxide solution (Honeywell Fluka, Romania). 0.1 % concentration of HPB mass to alkali, with or without a prior ethyl alcohol wash, was mixed with the sodium hydroxide solvent. The alkali wash then occurred in a -5 °C oil bath using dimethyl polysiloxane for 30 min (Grant TC120, Shepreth, England). After the alkali wash the material was subsequently filtered as for the ethyl alcohol wash (Cuissinat and Navard, 2006) and then left in a fume cupboard to let remaining sodium hydroxide evaporate.

5.2.2.3 Mechanical disruption

HPB that had been chemically treated (ChemPB) was then subjected to a further step (3) of mechanical disruption by using either sonication or a microfluidiser to facilitate fibrillation. This was either sonicated for 3 or 6 Hr, or subjected to 2, 4 or 6 passes (P) through the microfluidiser (Figure 37).

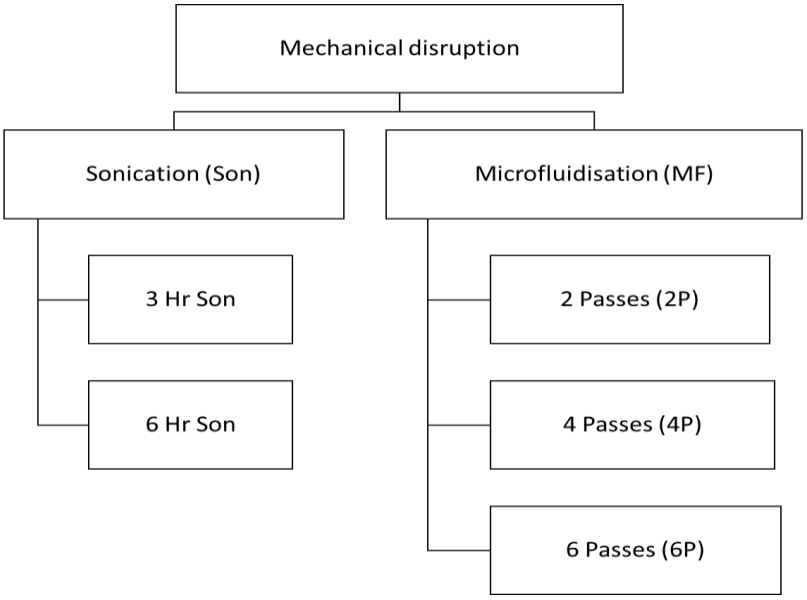


Figure 37 Flow diagram depicting differing mechanical disruption methods to use on the differing Chemical PB. Abbreviations as follows, 3 hours of Sonication (3 hr Son), 6 hours of Sonication (6 hr Son), 2 Passes on the Microfluidiser (2P), 4 Passes on the Microfluidiser (4P), 6 Passes on the Microfluidiser (6P). Details of sonication and microfluidiser settings to follow.

Sonication (Son) was performed at setting of 9 (240 w per hour) using a (VWR ultrasonic cleaner, Malaysia). This setting was chosen based on the principle that it is the maximum the equipment can perform at and therefore maximises the mechanical disruption to the material (PB). Ice-cubes (Scotsman ice machine, Suffolk, England) were frequently added to the sonication bath to prevent samples overheating, where bath temperatures fluctuated between 5 and 20 °C but mostly were kept at around 10-12 °C. Samples were kept in glass beakers for the duration of the sonication.

A microfluidiser (MF) (LM20-30 S/N 0076, Microfluidics, Massachusetts, US) was used at 30,000 psi with a Z chamber and an ice bath system was put in place to cool elements in an attempt to prevent overheating during the multiple passes, as otherwise samples could reach up to 50 °C without this element. Water was used as a cleaning agent between the samples. Prior

to the microfluidiser a thermomix was used for 3 min at setting 9 (Vorwerk, Australia), a pre-process which prevented blockages in the microfluidiser.

5.2.3 Storage of MFC/NFC samples

Samples which were used for direct characterisation were stored as a dispersion at 1 and 0.5 % w/w at 4 °C. Alternatively samples were dried overnight at 120 °C and the dried MFC were stored at 25 °C in a vacuumed desiccator.

5.2.4 Analytical methods

Figure 38 describes the differing characteristics and properties investigated with the fibrillated masses at differing stages of the investigation processing parameters.

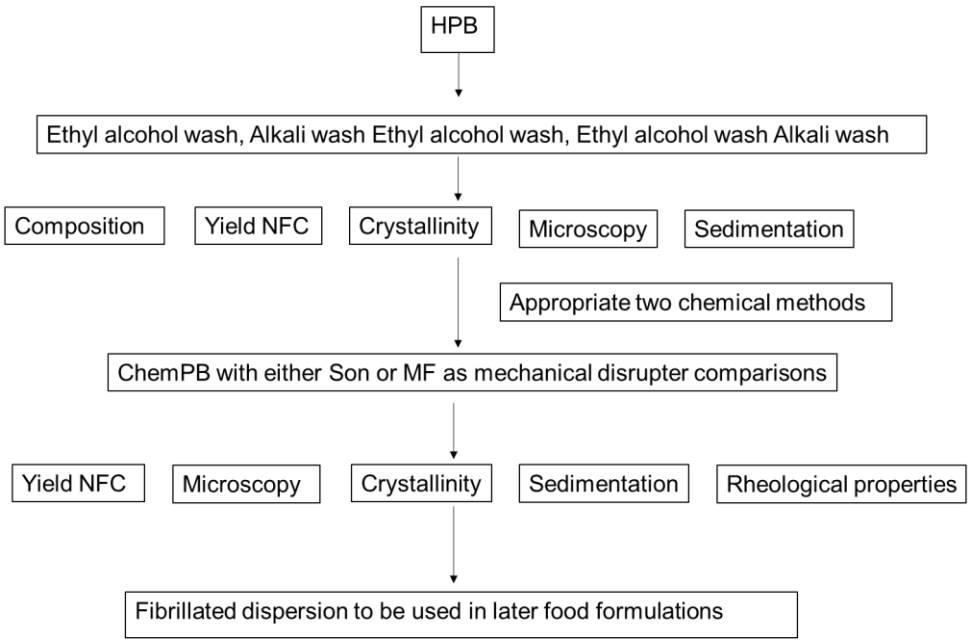


Figure 38 Schematic of each process step and property information gained through analytical equipment in order to find a fibrillated dispersion suitable for later use in a food formulation.

5.2.4.1 Composition characterisation after different chemical treatments

For calculating cellulose and hemicellulose content, 30 mg of dried treated biomass (HPB, ethyl alcohol wash, alkali wash) was added to 1 ml of 12 M sulfuric acid and incubated in a 37 °C water bath (Grant, Shepreath, UK) for 1 Hr. Then 11 ml of RO water was subsequently added to make the biomass dispersion of 1 M sulphuric acid and incubated in a water bath at 99 °C for 2 Hr. The dispersion is then cooled under running cold water to stop the reaction and 100 µl of supernatant was pipetted off and added to 10 ml of RO water. Then centrifuged at 5000 rpm for 5 min to break apart any remaining large particles. After centrifugation, 1 ml of the supernatant was added to Dionex vials for sugar analysis using High-Performance Liquid Chromatography (HPLC) (Dionex AS ICS-3000, ThermoFisher Scientific, UK). Monosaccharide standards are analysed, glucose, xylose, arabinose and galactose. A combination solution of the sugars is made and diluted using 10 mM of sodium hydroxide then a calibration curve was constructed.

In order to calculate lignin content, 0.1 g of treated sample were bathed in 4 ml of 25 % v/v acetyl bromide:glacial acetic acid and incubated at 50 °C for 2 Hr. The mixture is then cooled for 5 min under cold running water to stop the reaction from continuing. For standard of 0.01 g of lignin (Low sulfonated, pH 10.5, Sigma, UK) was used and dissolved in 6 ml of 75 % v/v dioxane, and then vortexed of lignin:dioxane solution was transferred to fresh reaction tubes containing 0.5 ml of 25 % acetyl bromide in glacial acetic acid. Samples were then incubated for 30 min at 50 °C and then additionally cooled under running cold water afterwards. 0.2 ml dioxane with 0.5 ml 25% acetyl bromide in glacial acetic acid was used as a blank. In order to prepare the samples for spectrophotometry 12 ml of glacial acetic acid was added to

treated samples (not lignin standards) and 0.5 ml was extracted into a fresh tube. Then the tubes were mixed using a vortex so that they were homogenous and dispensed in to a quartz cuvette (no UV interference) and each sample were analysed using 280 nm on a U-VIS spectrophotometer (Varian Cary 50 probe UV-vis spectrometer, Agilent technologies, USA, as published by Gould, Garcia-Garcia and Wolf (2016).

5.2.4.2 Yield of NFC after mechanical disruption

A 0.1 % w/w suspension of MFC (once heating, chemical and mechanical treatments had ensued) was centrifuged (Rotina, 380R, Hettich, Shelton technical ltd, Milton Keynes, UK) at 5000 rpm for 10 min (min) (based on similar parameters used by Alila *et al.* (2013), separating the MFC/NFC material (in the supernatant fraction) from the macro-fibres and MFC partially fibrillated fibres, which form the pellet. The pellet was subsequently dried in a vacuum oven (Gallenkamp, Weiss Technik, Germany) within the centrifuge tube at 50 °C for 24 Hr, then assessed an hour later to ensure no weight alterations occurred. The yield was calculated from (Alila *et al.*, 2013) and is seen in Equation 15.

Equation 15

$$NFC\ Yield\ (\%) = \left(1 - \frac{Weight\ of\ dried\ sediment\ (pellet)}{Weight\ of\ diluted\ sample\ x\ solid\ content\%}\right) x\ 100$$

5.2.4.3 Optical properties of NFC

MFC dispersion used for yield (%) in section 5.2.4.2 had the supernatant extracted and was introduced into quartz cuvettes, in order to see if any other MFC or NFC fibres remain. The transmittance was measured between 400 and 800 nm using a Genesys 10S Vis spectrophotometer (Themo Fisher Scientific, China). Water was used as a blank (Alila *et al.*, 2013).

5.2.4.4 Electron Microscopy

Scanning Electron Microscopy (SEM) images were acquired with a (JSM7000F + XPG2, JEOL/XENOS, Japan) equipped with an electron beam lithography. An alleration voltage of (10 Kv, 20 Kv) and working a distance of (1 cm x 1 cm) were used in the analysis. The samples were dried in an oven at 105 °C for 24 Hr before being mounted on a sample holder and coated with a gold layer of about 5 nm.

Transmission Electron Microscopy (TEM) were acquired with a (Tecnai G2 12 Biotwin, FEI, ThermoFisher Scientific, USA) equipped with a Gatan digital camera used at either 100 Kv or 200 Kv.100 µl for each sample were pipette on to 500 Holey Carbon copper grid mesh and then excess removed, by dabbing with paper.

5.2.4.5 Wide angle X-Ray Diffraction (WAXD)

For sonicated samples X-ray diffraction patterns were carried out using a Bruker D5005 (Bruker AXS, UK). At the angular range of 3-38 2θ, with a step size of 0.05° (2θ). Slit focus geometry was used with a total acquisition time for each sample of 56 min with recording times every 2.5 sec and a spin rotation of 60 rpm. A 1 % w/w MFC dispersion was dried and then filled into

a plastic holder. The Copper K alpha-1 (CuKα) radiation (λ=1.5218 nm) from the anode was generated at 40 kV and 40 mA. Slight variations in positions were a result of small errors in the height of samples. Crystallinity of MFC films were calculated by using the multi-peak deconvolution method (details of this method can be found in results Chapter 2. Intensity vs 2θ data is then processed using a Microsoft Excel spreadsheet with the Solver add in.

For microfluidised samples and compared sonicated samples X-ray diffraction patterns were carried out using a MiniFlex600 benchtop XRD (Rigaku, Sevenoaks,UK) at the angular range of 3-38 2θ with a step size of 0.02°. Slit focus geometry was used with a total acquisition time for each sample of 4 min and 31 sec with recording times every 0.6 sec and a spin rotation of 10 rpm. Zero background holders were filled with a dried 1 % MFC film. The CuKα radiation (λ=1.5218 nm) from the anode was generated at 40 kV and 40 mA. For a comparison crystallinity calculation manipulations were performed using the aforementioned multi-peak deconvolution method. Different x-ray diffraction equipment was used due to Bruker equipment failing during experimentation and having to outsource measurements.

5.2.4.6 Turbiscan on phase separation/sedimentation of fibrillated dispersions

Turbsican measurements were performed on a Turbsican (Formulaction, France) using backscattering and transmittance to determine a Turbsican Stability Index value (TSI) calculated using built-in software. 0.5 % w/w dispersion of MFC were measured over 10 min, 1 Hr. Further information regarding the calculation and details of TSI can be found in Chapter 2:

Techniques. MFC samples were stored at 25 °C in a dark cupboard in between measurements.

5.2.4.7 Rheology of fibrillated dispersions

1 % w/w MFC dispersions were used for amplitude sweeps and frequency sweeps. Amplitude sweeps and frequency sweep settings are found in section 4.2.4.9 (Rheology of rehydrated Ball Milled Pea Biomass).

5.3 Results

Initially a comparison of PB without processing was made, in order to see if the fibre could be fibrillated. This indicated that pre-processing was a necessary requirement (as seen from the non-fibrillated fibre in Figure 39) in order to reduce unsustainable energy requirements, which is the focus on the rest of the chapter.

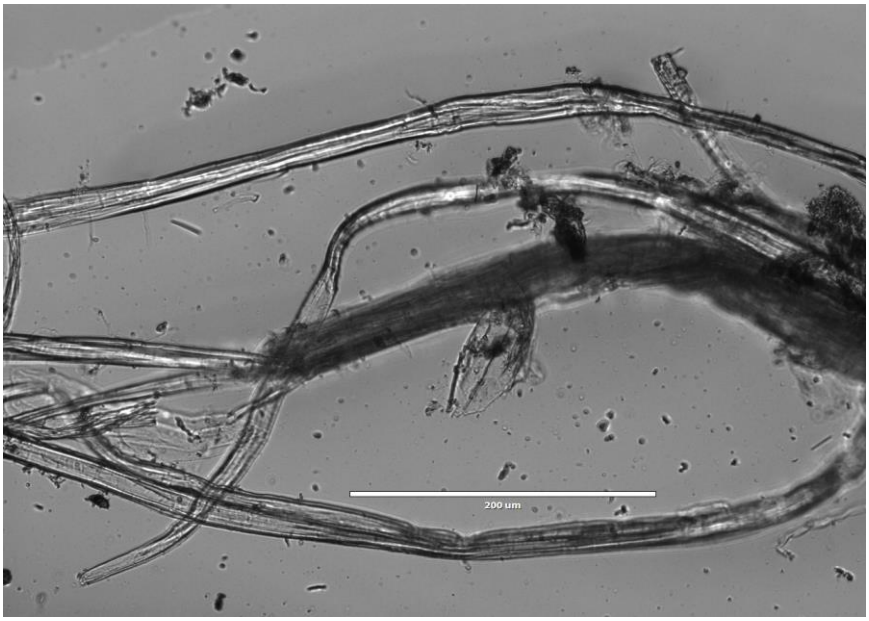


Figure 39 PB fibre after 5 Hr of sonication with no chemical pre-treatment, taken at x 20 magnification scale 200 μm.

5.3.1 Chemical composition of polysaccharides after thermal and chemical treatments

The varying chemical treatments and initial HPB treatment had differing effects on the amount of individual polysaccharide content of the fibre samples, as shown in Table 12. An increased amount of pure cellulosic fibres were observed after thermal and chemical treatment as compared to initial chemical composition analysis given in Chapter 3, Figure 12 and Table 5. This may be due to the effects of the heating and chemical treatments (HPB, ethyl alcohol wash and alkali wash), for example the alkali wash may

reduce proportionally more glucose from hemicellulose fractions than that of cellulose, resulting in a concentrated cellulose (glucose) fraction (shown in Table 13). Furthermore, the trend for the treated samples shows that the sodium hydroxide successfully decreases the amount of hemicellulose (through swelling/ballooning phenomena) within the sample (from 18.51 to > 0.37) as hypothesised, though decreases the amount of cellulose (from 34.55 to > 10.81 %) as a result of using the wash. Therefore, hemicellulose is proportionally reduced to cellulose as seen in Table 13. These effects of cellulose reduction are reduced when the alkali wash is followed by an ethyl alcohol wash (from 22.27 to > 10.81 %), this is possibly due to the reaction being stopped by the ethyl alcohol wash, where as it could continue in the air vacuum drying process after the alkali wash. The ethyl alcohol wash only minimally reduced the amount of lignin, this is shown by a decrease (from 10.5 - 8.8 %) in observations from the HPB to 30 min ethyl alcohol and 1 Hr ethyl alcohol but this was not significant (p-value > 0.98). The use of alkali before and after ethyl alcohol further decreased the amount of lignin content and significantly more than that of just ethyl alcohol wash (from 8.8 - 2.6) (p-value < 0.0246). However, lignin is not reduced proportionally to cellulose across samples (Table 13). Thereby showing evidence that alkali is more efficient at removing lignin than ethyl alcohol washes and HPB as shown by proportional differences from 0.30-0.24 % besides alkali 1 Hr ethyl alcohol. Others have reported that various concentrations of alkali washes reduce the amount of lignin within lignocellulosic materials (Lima *et al.*, 2013; Modenbach and Nokes, 2014). This is thought to be due to saponification and cleavage of lignin linkages by removing cross-links and bonds between hemicellulose and lignin.

Furthermore, these results may suggest that alkali washes before, but mainly after, ethyl alcohol washes may not provide as high of yields of fibrillated masses than using just ethyl alcohol washes, due to the lack of cellulose present in comparison. Although with a greater reduction of lignin and hemicellulose, in comparison to the ethyl alcohol washes, it may provide higher yields. Though, as aforementioned some research has found that other PCWM polymers are necessary/exhibit improved fibrillation (Iwamoto, Abe and Yano, 2008; Spence *et al.*, 2010; Suopajärvi, Liimatainen and Niinimäki, 2010; Ferrer *et al.*, 2012; Solala *et al.*, 2012) so this may not be the case. Lastly, statistically the samples are significantly different to one another (p-value > 0.0001) as a total. Independently, alkali samples prior to ethyl alcohol washes do not vary in cellulose content (p-value < 0.245), nor do the various ethyl alcohol wash times with one another and with the HPB treatment (p-value > 0.999). Showing that the ethyl alcohol washes do not deplete cellulose content after using a thermal treatment such as HPB. The amount of hemicellulose does significantly vary for the samples bar HPB treatments vs alkali treatments (p-value 0.023-0.0018). As seen in Table 12 up to 80 % of the material biomass is unaccounted for. It is believed that this is a result of the washing/bathing process, alkali crystals are found on the surface of the fibres and may have impinged extraction, as well as added inorganic matter to the total mass.

Table 12 Varying cellulose and hemicellulose (glucose, xylose, arabinose and galactose) polysaccharides and lignin concentrations with various chemical treatments or just HPB treatment, as well as raw PB found previously in table 5. Pectin was not assessed for this particular assessment. The remainder is suggested to be unaccounted for or plausibly pectin.

Sample	**Cellulose (%)**	**Hemicellulose (%)**	**Lignin (%)**	**Unaccounted (%)**
Raw PB	13	42	15	0
HPB	34.55	18.51	10.5	36.44
30 Min ethyl alcohol	34.67	13.61	9.56	42.16
Alkali 30 Min ethyl alcohol	26.27	3.68	6.93	63.12
30 Min ethyl alcohol alkali	10.81	1.54	2.57	85.08
1 Hr ethyl alcohol	37.43	9.06	8.81	49.7
Alkali 1 Hr ethyl alcohol	21.6	3.03	6.23	69.14
1 Hr ethyl alcohol alkali	13.99	0.37	4.22	81.42

Table 13 A proportional comparison of changes in composition from results obtained in chapter 3 (composition of raw PB) and chemically pre-treated PB

Sample	***Hemicellulose: Cellulose (%)***	***Cellulose: Hemicellulose (%)***	***Lignin: Cellulose (%)***	***Cellulose: Lignin (%)***
Raw PB	*3.23*	*0.31*	*1.15*	*0.87*
HPB	*0.54*	*1.87*	*0.30*	*3.29*
30 Min ethyl alcohol	*0.39*	*2.55*	*0.28*	*3.63*
Alkali 30 Min ethyl alcohol	*0.14*	*7.14*	*0.26*	*2.73*
30 Min ethyl alcohol alkali	*0.14*	*7.02*	*0.24*	*4.21*
1 Hr ethyl alcohol	*0.24*	*4.13*	*0.24*	*4.25*
Alkali 1 Hr ethyl alcohol	*0.14*	*7.13*	*0.29*	*3.47*
1 Hr ethyl alcohol alkali	*0.03*	*37.81*	*0.30*	*3.32*

5.3.2 Impact of chemical treatment and mechanical disruption method of sonication

5.3.2.1 Yield and optical properties of NFC comparing chemical methods and sonication methods

Figure 40 shows the yield of the NFC after different chemical pre-treatment of HPB and Son as mechanical treatment. No significant difference (p-value < 0.72) was observed between different processing (Figure 38 on analytical methods, steps to achieve fibrillated masses) on yield of NFC. However, 1 Hr ethyl alcohol 3 Hr Son does produce slightly higher yields as compared to other pre-processing, but the yield difference is minimal 0.35 %. Importantly no significant difference (p-value > 0.05) was observed when comparing yields of the PB system and purified cellulose (SF). The similarities in yields may suggest that the chemical pre-treatments along with the initial HPB treatment have been successful in fibrillating the PB biomass. Thereby, removing the protection of lignin, allowing the PB to fibrillate to the similar degree/greater degree than that of pure cellulose. Furthermore, this means the alkali washes may not be a necessary addition for the increase in yield of fibrillation, thereby reducing environmental impact.

The greater yield of the 1 Hr ethyl alcohol 3 Hr Son sample, by 0.3-0.4 % increase, may not be an anomaly due to the differences being so minute and not significant. Lastly, the trend seems to be that the lower processing i.e 3 Hr rather than 6 Hr Son shows in general (besides SF and alkali 30 mins ethyl alcohol) to produce non-significantly higher yields, which may be due to over-processing. As there are minimal differences between yields, it would be expected and hypothesised that there will also be minimal differences observed in the supernatant fraction of the analysis. Furthermore, as such high yields are accounted for in the pellet, it would indicate that very little

amounts of NFC are expected to be found in the supernatant fraction of the analysis. Lastly, results indicate that removal of hemicelluloses as observed in section 5.3.1, does not significantly affect the production of fibrillated masses in comparison to PB that has a higher proportion of hemicellulose still in its composition. Therefore liberating the monosaccharide hemicellulose may not be a necessary requirement in order to improve or reduce production yields of fibrillated masses from PB.

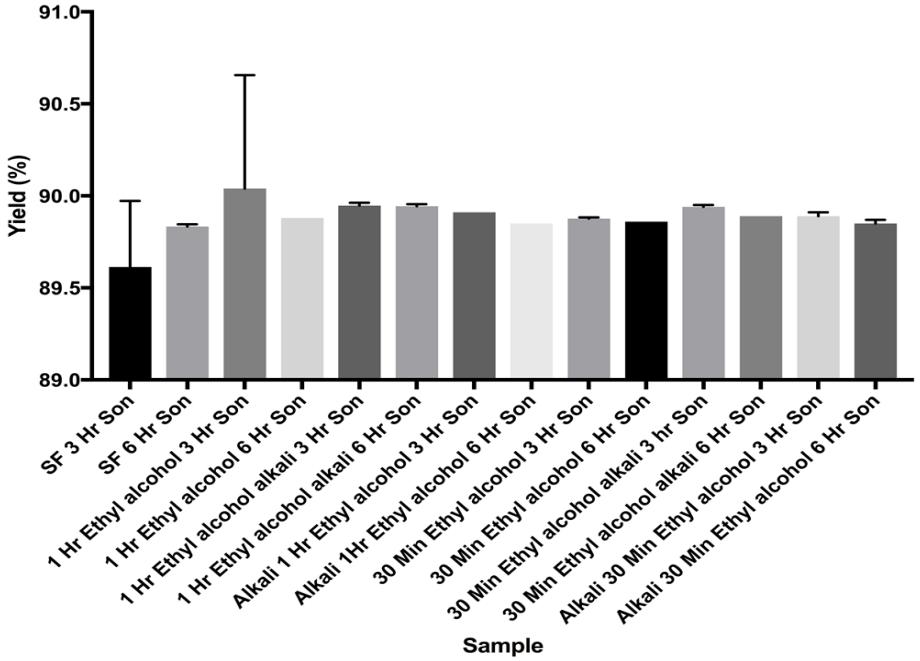


Figure 40 Yield (%) of the pellet weight created through centrifugation, variously treated sonicated NFC dispersion. Error bars provided by means of standard deviation, if not visible than the error is too small. All points are not significantly different at p<0.05.

The optical properties used to witness nano-particulates in the supernatant phase of the centrifuged treated fibrillated samples, are shown in Figure 41. This information indicates particle size, and therefore the smaller the size, the confidence that the material is NFC and transmits light more, whereas the larger the size the material is more likely to be MFC and therefore transmits less. A significant difference (p-value > 0.0001) was observed

when comparing different processing of PB on the amount of NFC in the supernatant. It is evident from Figure 40, the addition of alkali washes as a pre-treatment before ethyl alcohol wash, results in lower yields of nano-particles. The PB simply washed with ethyl alcohol and Son for the shortest time frame provide the highest yields and even higher than the purified cellulose (p-value > 0.0001). This can be explained by the results found in section 5.3.1, which suggest lower concentrations of cellulose from using alkali has shown to impinge the amount of yield achieved through fibrillation. This highlights that the suggested alkali crystals, left in the system, after pre-treatment as mentioned in (Table 13) is impinging/protecting cellulose from the fibrillation process, possibly preventing fibrils coming away from the main mother fibre due to hardening on the surface (discussed later in more detail with microscopy). Though no clear confirmation exists to which polysaccharide and its proportions directly govern the ease of fibrillation (Alila *et al.*, 2013). In these results it would suggest that higher concentrations cellulose and hemicellulose i.e. glucose amounts promotes greater yields of NFC. Alila *et al.* (2013) found that with varying agricultural crops those with the highest proportions of xylose i.e. hemicellulose, provide higher yields and those with the least amount of cellulose produce the lowest yields, which is counterintuitive to these findings. However, lignin was not mentioned in the aforementioned study and therefore its presence may adapt the effects of fibrillation. Furthermore, Iwamoto *et al.* (2008) also found that a high content of hemicellulose facilitated the nano-fibrillation of wood pulp. Moreover, hemicelluloses linked to cellulose microfibrils are assumed to span the gap between them. This presence of hemicellulose may reduce the interaction through hydrogen bonding amongst cellulose microfibrils and thereby facilitate separation and individualisation of cellulose microfibrils during Sonication. Therefore a plausible reason for higher yields may be due

to 1 Hr and 30 Min Ethyl alochol having the highest proportions of hemicellulose and lignin than other chemically treated samples as shown in section 5.3.1. Lastly, 1 Hr ethyl alcohol 3 Hr Son provides the highest total yield in all diameters of fibrillated masses from both the pellet and the supernatant phase as a total volume calculated.

In summary, it was evident from both the pellet yield and optical properties data that depending on the pre-treatment process the ChemPB produces a blend of different microstructures, which in combination of prolonged sonication treatment results in proportions containing large quantities of NFC. However, for such multicomponent dispersions there will be additional factors such as other varying polysaccharides (hemicellulose and pectin), lignins (which may enable greater fibrillation) and other varying materials (lipids, micro-nutrients) found in the composition chapter, which may have a significant impact on the yield and functional properties of MFC and or combinations of NFC dispersions. Finally, based on the yield results ethyl alcohol washes seems to be the better pre-treatment method to produce cellulosic materials, which can be processed into fibrillated material. However, further functional properties of these PB fibrillated dispersions cannot be discounted and will be explained in the next few sections.

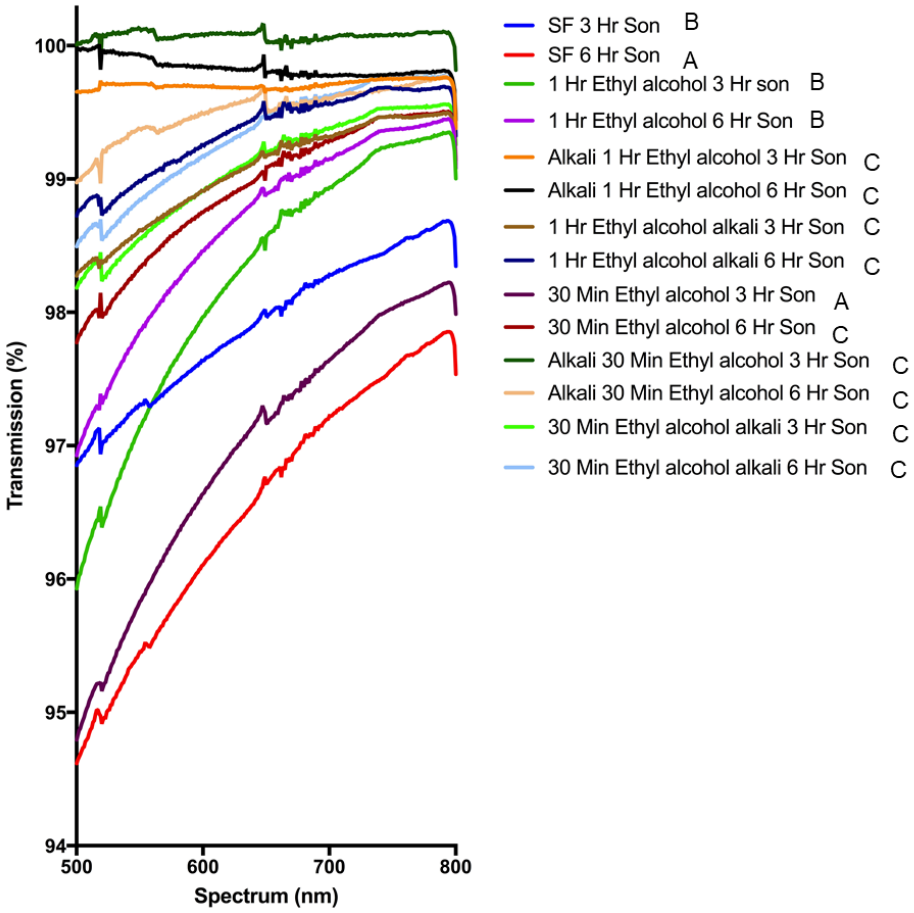


Figure 41 Yield of supernatant transmission, in varying chemically pre-treated sonicated fibrillated dispersions (0.1 %). Colour coded error bars provided through standard deviation are within thickness of lines and curves with the same letter are not significant at p<0.05.

5.3.2.2 Microstructure characterization (SEM) of fibrillated material prepared after chemical and sonication process

As stated previously, visual aspects of fibrillated materials are necessary for adequate perceptions on morphology, which have in particular aided nomenclature to differentiate different fibre structures. Figures 42 and 43 show microstructure (using SEM) of different cellulosic samples with differing chemical pre-treatment methods and Son time. Both SEM grouped images of 1 Hr ethyl alcohol and 30 Min Ethyl alochol variables show a branch-like structure with a mixture of fibres differing in diameter, similarly

witnessed by Chinga-Carrasco (2012). Alkali samples on rows 2 and 3 (in Figure 43) show some crystals on some fibres at x 230 magnification (as shown by the arrow), these are further exemplified in the Figure 44, which may be due to the sodium hydroxide not being washed away when the fibres are neutralised, thereby upon oven drying the crystals have formed. This consequently caused the fibres to agglomerate and harden forming bundles in comparison to those that have simply been ethyl alcohol washed. Furthermore, this may impinge the PB from forming more NFC and MFC through Sonication. Samples images on the first row of both Figures 42 and 43, which that have only been ethyl alcohol washed show larger entities with greater aspect ratios and therefore are more likely to be MFC than NFC and observably show a tighter network of web-like structures, especially in the case of 30 Min ethyl alcohol. This may be due to the higher amounts of cellulose, hemicellulose and lignin content in comparison to alkali treated samples. Possibly indicating that the presence of these facilitates a higher fibrillation of cellulosic fibres, in comparison to samples, which has lower amounts of other cell wall components, which have been removed during pre-treatments. Plate-like structures appear across the samples (as shown by the arrow in E1), which under further inspection showed that they consist of smaller micro-fibres. It should be noted that in the preparation of the samples for SEM, they were dried, which can make the fibril structures collapse from their fibrillated state, which are difficult to re-disperse in water, this irreversible change in microstructure is known as hornification in paper and pulp industry. This may be an explanation for the plate-like structures in the SEM images, likely to be collapsed MFC and NFC. It is extremely difficult to suggest whilst comparing the samples purely through microscopy, which samples differ in macro-fibres, (MFC and NFC), which is to be expected after the yield results in section 5.3.1 and 5.3.2 showed no significant difference.

Though it is apparent in the results that the fibrillated dried dispersions seem to be Macro and MFC, therefore would be classed as MFC, until other results suggest otherwise. It is also apparent that the samples that have been ethyl alcohol washed are more homogenous in comparison to those alkali washed, which are bundled and have hardened (Figure 44). Thereby possibly indicating that they would be difficult to re-disperse or mix when applied to a system in a dried form without sufficient washing of the sodium hydroxide first. Though it has been found that the addition of other polymers enable greater re-dispersion and protect against hornification (Agarwal, MacNaughtan and Foster, 2018).

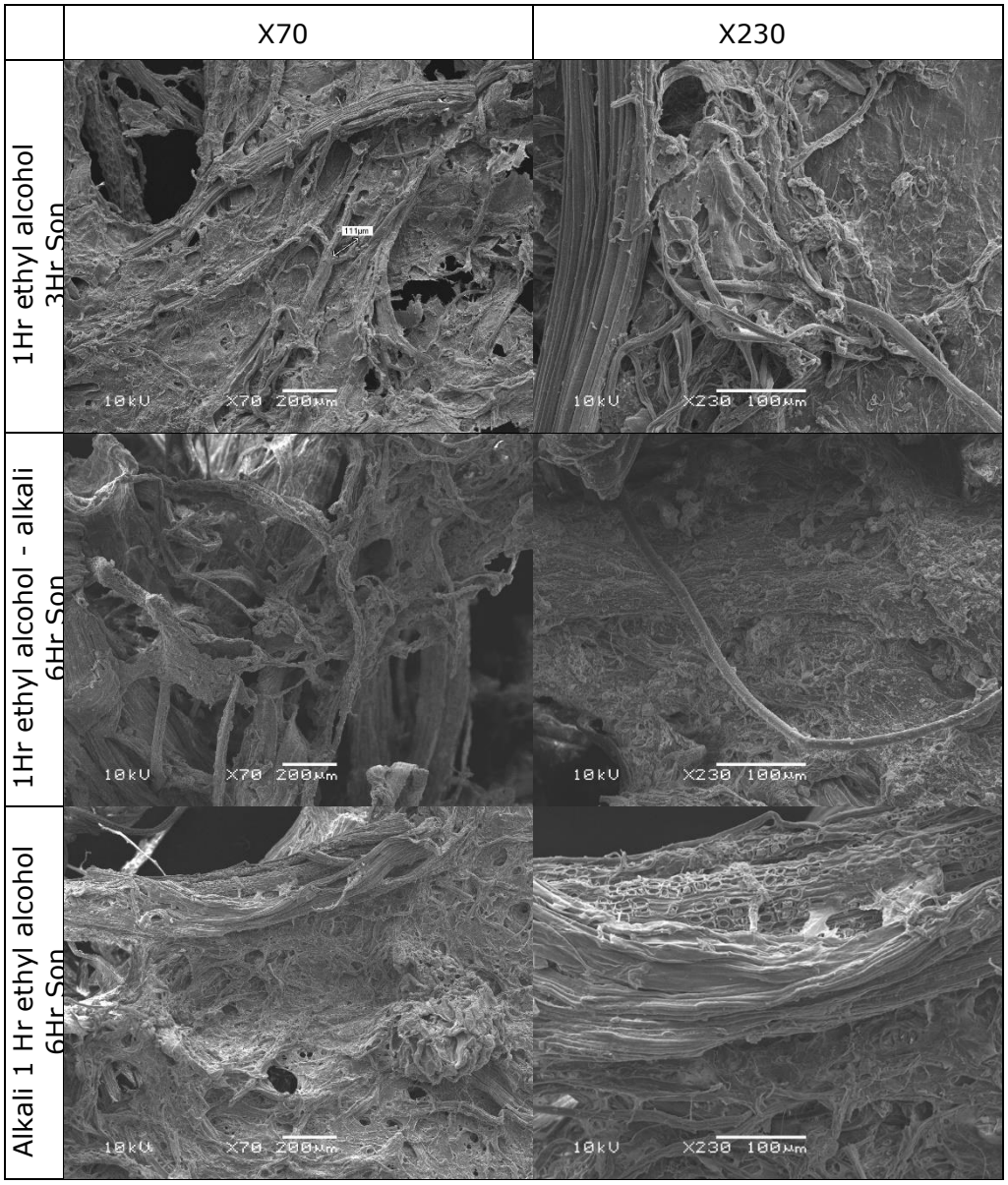


Figure 42 SEM fibrillated 1 % dried forms. First row: 1 Hr ethyl alcohol 3 Hr Son, second row: 1 Hr ethyl alcohol alkali 6 Hr Son, third row: alkali 1 Hr ethyl alcohol 3 Hr Son. First column x 70 and second column x 230. Showing a range of diameters of mixed fibrillated masses within a dried dispersions.

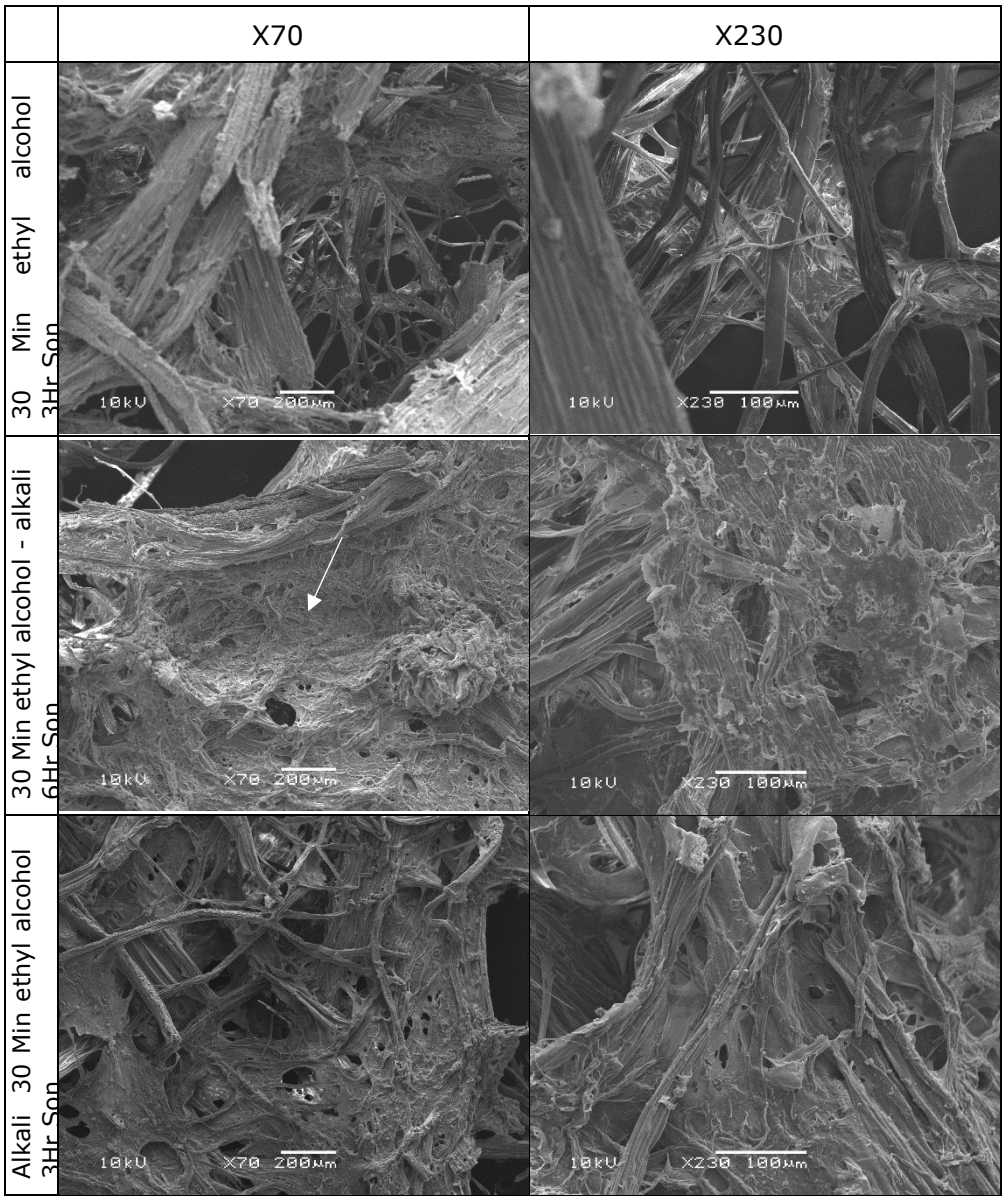


Figure 43 SEM fibrillated 1 % dried forms. First row: 30 Min ethyl alcohol 3 Hr Son, second row: 30 min ethyl alcohol, alkali 6 Hr Son, third row: alkali 30 Min ethyl alcohol 3 Hr Son. First column x 70 and Second column x 230. Showing a range of diameters of mixed fibrillated masses within dried dispersions.

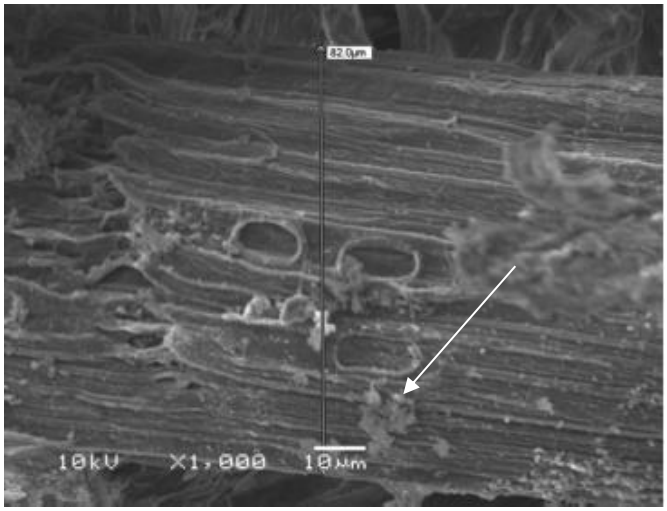


Figure 44 SEM fibrillated 1 % 30 Min ethyl alcohol alkali 6 Hr Son depicting crystals as shown by the arrow) possibly left by the alkali wash. Further indication of hypothesis made in section 5.3.1, of inorganic matter being present in the compositional analysis. Example of diameter is given, magnification x 1000.

5.3.2.3 Crystallinity of MFC comparing chemical and Sonication methods.

The crystallinity of the dried Sonicated fibrillated material are given in Table 14. The differently treated samples show that those which are more fibrillated in terms of production yields, have the highest crystallinities. Samples have been shown to re-crystalise into both allomorph I and II forms, which is plausibly a function of the chemical pre-treatments. Samples however are still predominantly allomorph I, which will be a function of allomorph I seed crystals remaining after treatments, but the samples are still able to re-crystallise (to various degree's) in the more thermodynamically stable allomorph form II. Furthermore, the samples that have the highest amount of cellulose also have the highest crystallinity, which is to be expected. As other polysaccharides within the PCWM are mainly amorphous. Though this does not suggest that a higher crystallinity is indicative of greater production yields. This assumption can be observed with SF as the

model is completely cellulosic and has the highest crystallinity significantly (p-value >0.0001), yet does not produce greater production yields than the ethyl alcohol washed treated PB. Therefore, one would still assume that it could be the amount of hemicellulose and or lignin within the system that enabled greater yields. Higher crystallinities have been related to higher production yields (George and Sabapathi, 2015), which is witnessed in this study, whereby crystallinity increases with the amount of fibrillation via sonication. This is contradictory to findings made previously by Alila *et al.* (2013) and thereby vindicates a comparison of mechanical fibrillation methodologies. This can be observed in comparing results in Table 12 and Figure 40 (depicting yield and polysaccharide concentrations) showing those with larger quantities of cellulose produced greater yields. Foster *et al*. (1996) used ^{13}C CP-MAS NMR to assess the crystallinity of raw pea stem. They found it to contained up to 35 % crystalline fractions, which is significantly different to findings of the mixed biomass found in these works (Foster *et al.*, 1998). Winkworth–Smith, (2012) found that ball milled cellulose (with a low degree of polymerisation), once re-dispersed (solids) in an excess of water, will re-crystalise to a higher degree and this processes occurred faster than if it had a higher degree of polymerisation to begin with. It is hypothesised that the chemical process PB is taken through in these works, is effective at rendering it more amorphous than previously. Therefore, this has enabled the PB to re-crystalise due to possibly having a lower degree of polymerisation as a consequence of the chemical pre-treatment and then mechanically dispersed in excess water. Additionally, in the works of Abbazaddeh, MacNaughtan and Foster (2014), locust bean gum was found to act as a protective mechanism to cellulose de-crystallisation, which then also accelerated re-crystallisation. Therefore, it is hypothesised that when hemicellulose and pectin is still present within the

PB system (in enough quantities), an increases in crystallinity is observed, for example ethyl alcohol in comparison to alkali. Furthermore, in terms of crystallinity, no significant difference (p-value < 0.087) was observed while comparing ethyl alcohol washed samples with the addition of alkali for 30 min ethyl alcohol samples (p-value > 0.05). Whereas the rest of the samples show significant difference (p value > 0.0001) in total crystallinity. Lastly, crystallinity found in fibrillated PB is greater, on average, than that of 30-40 % found in fibrillated sugar beet (Heux, Dinand and Vignon, 1999). Though lower than that of typical wood sources of 84–89 % (Lavoine *et al.*, 2012), which was to be expected.

Table 14 Crystallinity in the first column type I allomorph, in the second column type II allomorph calculated using the multi-peak deconvolution method, of oven-dried solutions of 1 % sonicated PB with varying chemical treatments.

Sample	Type I (%)	Type II (%)	Total Crystallinity (%)
Native PB	11	0	11
1 Hr ethyl alcohol 3 Hr Son	45	15	60
1 Hr ethyl alcohol 6 Hr Son	40	16	56
Alkali 1 Hr ethyl alcohol 3 Hr Son	26	16	42
Alkali 1 Hr ethyl alcohol 6 Hr Son	25	16	41
1 Hr ethyl alcohol alkali 3 Hr Son	41	11	52
1 Hr ethyl alcohol alkali 6 Hr Son	37	15	52
30 Min ethyl alcohol 3 Hr Son	49	17	66
30 Min ethyl alcohol 6 Hr Son	61	19	80
Alkali 30 Min ethyl alcohol 3 Hr Son	19	17	36
Alkali 30 Min ethyl alcohol 6 Hr Son	32	12	44
30 Min ethyl alcohol alkali 3 Hr Son	33	15	48
30 Min ethyl alcohol alkali 6 Hr Son	30	16	46
SF 3 Hr Son	20	45	65
SF 6 Hr Son	55	21	76

5.3.2.4 Impact of chemical pre-treatments and Sonication on phase separation/sedimentation of fibrillated dispersions

The turbsican stability index (TSI) is a value that measures destabilisation kinetics in a given sample. The sample with the greatest intensity differentiation over time is thereby the one that has changed most and is thus least stable. Therefore, Figures 46 and 47 show the TSI for Sonicated samples of a 0.1 % dispersion that have been allowed to settle for 10 min and 1 Hr, respectively. After 10 min some of the samples are significantly different to one another (p-value > 0.001) shown by the letters on the graph. However, after 1 Hr some of the samples namely those with ethyl alcohol and alkali wash Sonicated for 3 and 6 Hr seem to be significantly different (p-value > 0.001). The sample, which sedimented most was SF 6 Hr Son, which is shown by the rapid rate increase in TSI. Whereas, the two most stable samples were alkali 30 Min ethyl alcohol 6 Hr Son and 30 Min ethyl alcohol alkali 6 Hr Son, shown by the slowest TSI rate increase. A sample, which showed quite a constant TSI, was 30 Min ethyl alcohol alkali 3 Hr Son, which can be observed by the plateau witnessed by the sample. Both samples treated with alkali before and after seem to sediment the least of all samples and are therefore more stable. This indicates that higher proportions of NFC (as shown through optical properties and SEM of alkali treated samples) produces greater stability. Another hypothesis is that this may be due to the clumped/aggregated fibers (caused by the remainder sodium hydroxide crystals) explained in sections 5.3.2.3, creating a higher aspect ratio of fibers at the bottom of the turbiscan vials and thereby staying in the same position and not altering the TSI. Heights of samples in vials can be observed in Figure 45. Possibly indicating that differing preparation methods or separation of the aggregated fibres should be explored, in order to make results more reliable. Ethyl alcohol treated samples and SF (which

contain more MFC) are less stable, which is to be expected as they are larger fibres and the rate at which they destabilise is far greater than NFC (alkali treated samples). It is apparent that samples with just ethyl alcohol wash show that further processing, beyond 3 Hr, would make the sample less stable. However, with samples that have been additionally bathed in sodium hydroxide it seems necessary for them to be processed for long times in order to make the sample more stable, this additionally may be due to the aggregation of the fibers. Furthermore, the data states that samples washed with ethyl alcohol before alkali creates the highest stability, which as aforementioned is indicative of higher proportions of NFC. Therefore this would indicate from previous findings that the removal of some lignin content first followed by removal of hemicellulose content seems to change the way the material processes and produces an increase of NFC. Whereas, alkali washes prior to ethyl alcohol washes samples is indicative of being less stable with MFC fibres, which indicates that the removal of hemicellulose prior to washing lignin created production of larger proportions of MFC than NFC. However, work at the University of Nottingham has indicated that co-processing cellulose with additional polymeric additives proves to be advantageous over purely cellulosic MFC, with improved reinforcement properties (Agarwal, MacNaughtan and Foster, 2018; Agarwal *et al*., 2019). In having blends of MFC, the addition of the polymeric additive have synergistic mechanisms which aid the fibres to form inter-/intra-molecular bonds upon a drying process. These have shown to aid stabilisation of microfibrils within an MFC dispersion. Therefore, these blends of MFC from cellulose and other polymeric additives have found to be easily re-dispersible and have a higher mobility of water in a network structure (Agarwal, 2016). Therefore, it is still not known with this PB system whether

naturally occurring polymers and lignin have an advantageous effect on the stability of MFC dispersions.

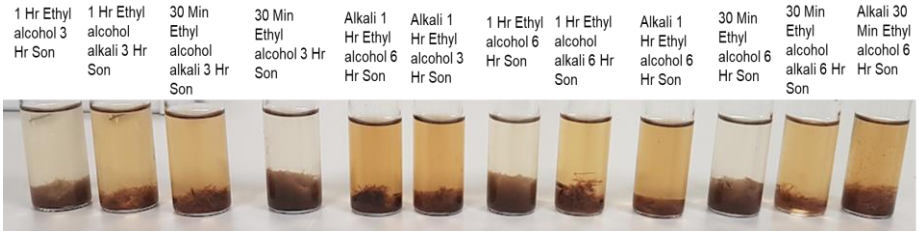


Figure 45 Various chemical pre-treatment methods with varying sonication times of PB fibrillated samples within turbiscan vials, indicating colour difference between samples, colour indicative of either resulting chemical residue or nano-particulates in the upper phase. Displaying differing volumes of fibrillated biomass.

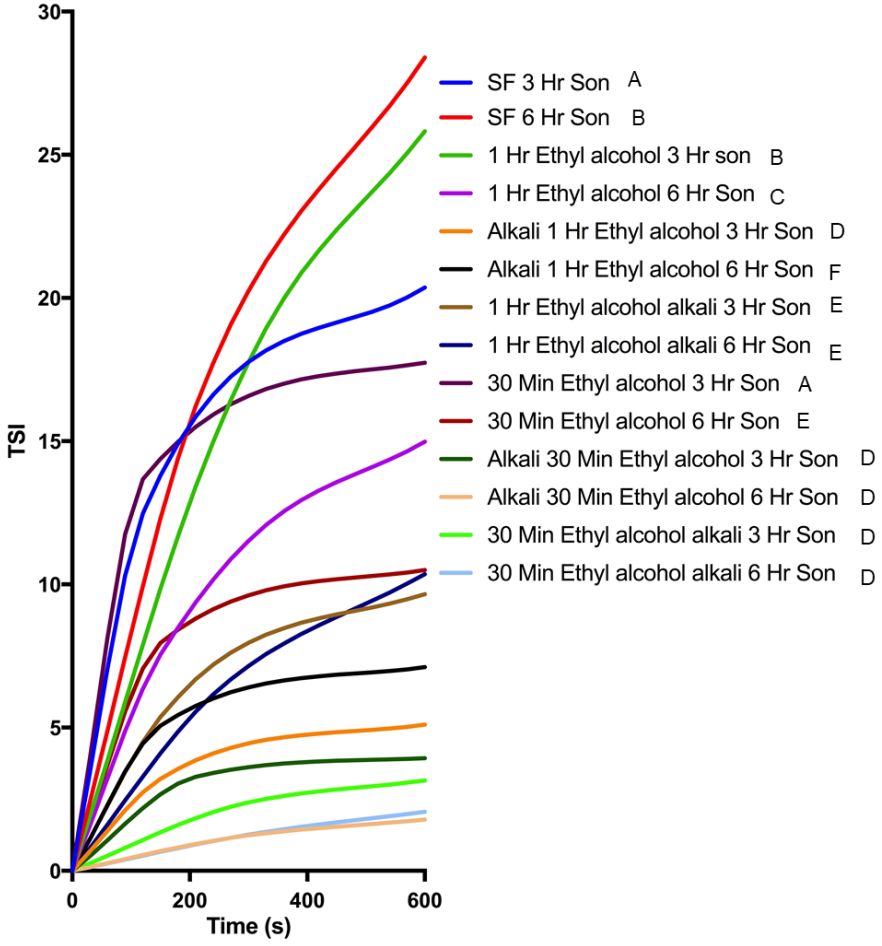


Figure 46 TSI within the first 10 minutes of all fibrillated samples through Sonication at 0.5 % with various chemical pre-treatments. Error bars calculated through standard deviation for each sample are indicated by thickness of the symbol and line. Curves with the same letter are not significant at p<0.05.

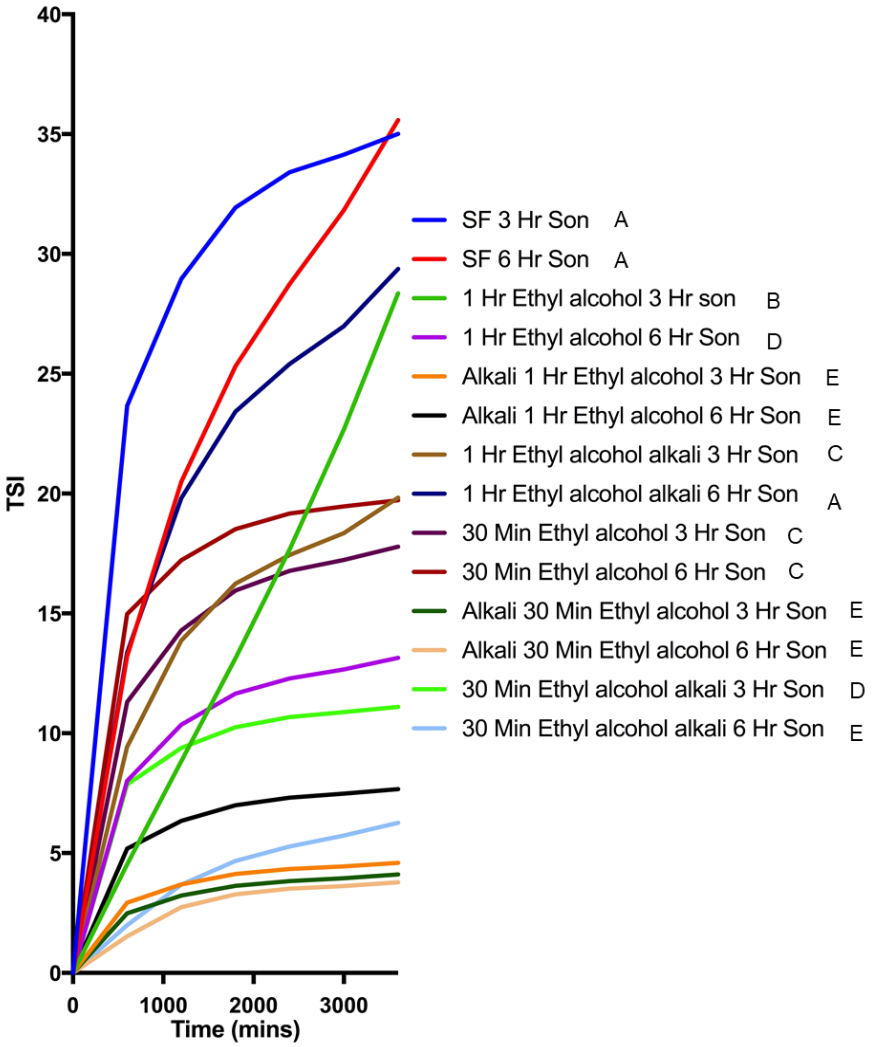


Figure 47 TSI for Sonicated samples at 0.5 % with various chemical pre-treatments over 1 hour scanning time. Error bars calculated through standard deviation for each sample are indicated by thickness of the symbol and line. Curves with the same letter are not significant at p<0.05.

5.3.2.5 Impact of chemical treatment - Conclusions of Sonicated samples

Results provided evidence to support particular hypotheses, for example literature estimated that alkali washes would reduce the amount hemicellulose content within the PB samples and this was proven in the compositional analysis. However, it was additionally hypothesised that ethyl alcohol washes would proportionally reduce the amount of lignin within the

PB and results showed only minimal reductions that were not proportional to cellulose reduction. For the next subsequent analysis of comparing mechanical disruption methods, a particular chemical pre-treatment method was necessary to be chosen to be used as a comparison. Findings suggested that yields were not significantly different. Turbiscan and optical properties showed that ethyl alcohol washes provide fibrillated samples with a higher proportion of MFC then NFC in comparison to alkali wash samples. As NFC is not yet food grade and ultimately the focus of the fibrillated material is to be used as a bulking agent, in a composite material as a replacement for starch. Larger fibre sizes (MFC > NFC) may provide better textural properties and additionally be food grade. Furthermore, the fewer treatments required to produce the fibrillated material is advantageous from a sustainability, environmental, and production cost point of view. Therefore based on these findings ethyl alcohol washes have been chosen as the chemical pre-treatment to further compare the mechanical disruption methods of sonication and microfluidisation.

5.3.3 Impact of differing mechanical disruption methods (Sonication and Microfluidisation) on chemically pre-treated PB (ethyl alcohol washed)

5.3.3.1 Yield and optical properties of fibrillated dispersions comparing mechanical disruption methods of Sonicated and Microfluidised samples

In this section, two different methods of fibrillation through mechanical disruption are compared in terms of production yield for both SF (Control cellulose) and ethyl alcohol washed fibrillated PB. Figure 48 shows the

comparison of yields of fibrillated fibres, where Son samples are seen to be significantly different (p-value > 0.001) to MF samples. It is clearly apparent that microfluidisation is more effective at producing greater yields of NFC than that of Son. No significant difference (p-value > 0.087) was observed between the number of passes through MF independent of the starting material, indicating that the time which PB is treated with ethyl alcohol wash is not playing a role. Interestingly the 4 pass samples have the highest yields, which may suggest that the materials may be susceptible to over-processing. The MF samples produce the highest NFC yields, possibly due to the increased amount of mechanical energy used by the equipment in comparison to Son. Furthermore, the different nature of the applied energy used by the MF indicates it has an improved ability to tear/pull apart microfibrils from the main mother fibre, through processing at high pressures in a water medium. Whereas the agitation through frequencies used by Son may not have as much energy to enable as higher proportions of microfibrils to separate and then detach themselves from the mother fibre. Thereby fewer MFC are detached, fewer NFC (secondary engineered structures) will be created even upon further processing.

The amount of NFC after centrifugation of a 0.1 % dispersion of MF and Son PB dispersions was monitored by using optical properties of the dispersions. Higher amounts NFC was evident for both SF and ethyl alcohol washed PB fibrillated by using the MF as compared to the Son (Figure 49). Additionally, each MF treated sample has a higher amount of NFC than that of SF but this was not the case with Son samples. A possible reason for the increased amount of NFC witnessed through the MF, may be due to the increased mechanical energy used by the equipment, as mentioned in the previous section. Additionally, the equipment's ability to convert high fluid pressure to

intense shear forces is exemplified in comparison to the Son. In a review by Lavoine *et al.* (2012), high pressure homogenisers were reported to produce greater yields of fibrillation through mechanical methods compared. 1 Hr ethyl alcohol and 30 Min ethyl alcohol MF treated samples are all significantly different to one another; it shows that an increased ethyl alcohol wash may only benefit yields on the MF. This is counter to the argument and results found in yield of NFC from the pellet, which had no significant difference between MF samples apart from SF 6P. As well as, being counter to the argument found when comparing chemical pre-treatments for Son samples. This may again be indicative of samples needing to be centrifuged for longer times as stated previously in optical properties comparing chemical pre-treatments. Conversely, this may indicate that longer ethyl alcohol washes are necessary to soften the fibers to enhance the fibrillation mechanisms provided by the MF, which then increases NFC yields. Furthermore, the difference may also be indicative of slightly larger entities being found within the dispersion, thereby impinging transmission through the samples, which therefore would be indicative of some NFC to MFC diameter ranges. However, unlike the Son samples (apart from SF) the MF samples show that the number of passes may not be significantly different whether it is 2P to 6P. This data however would not suggest that 1 Hr ethyl alcohol 4P is significantly different to the others but has the highest yield of NFC.

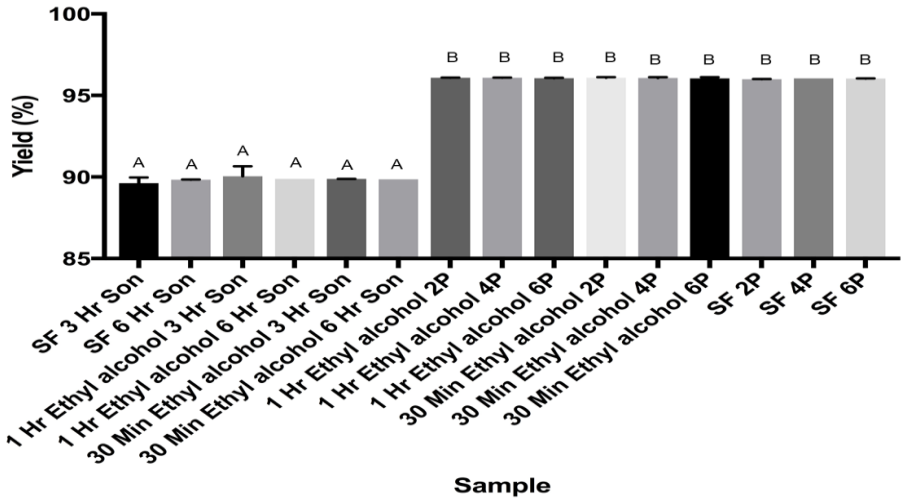


Figure 48 Yield of NFC through centrifugation of a 0.1 % fibrillated dispersion of MF and Son samples (comparisons between mechanical methods) both with hydrothermal and various ethyl alcohol wash treatments. Points with the same letter are not significantly different at p<0.05. Error bars are provided by standard deviation, if not shown the error was too small.

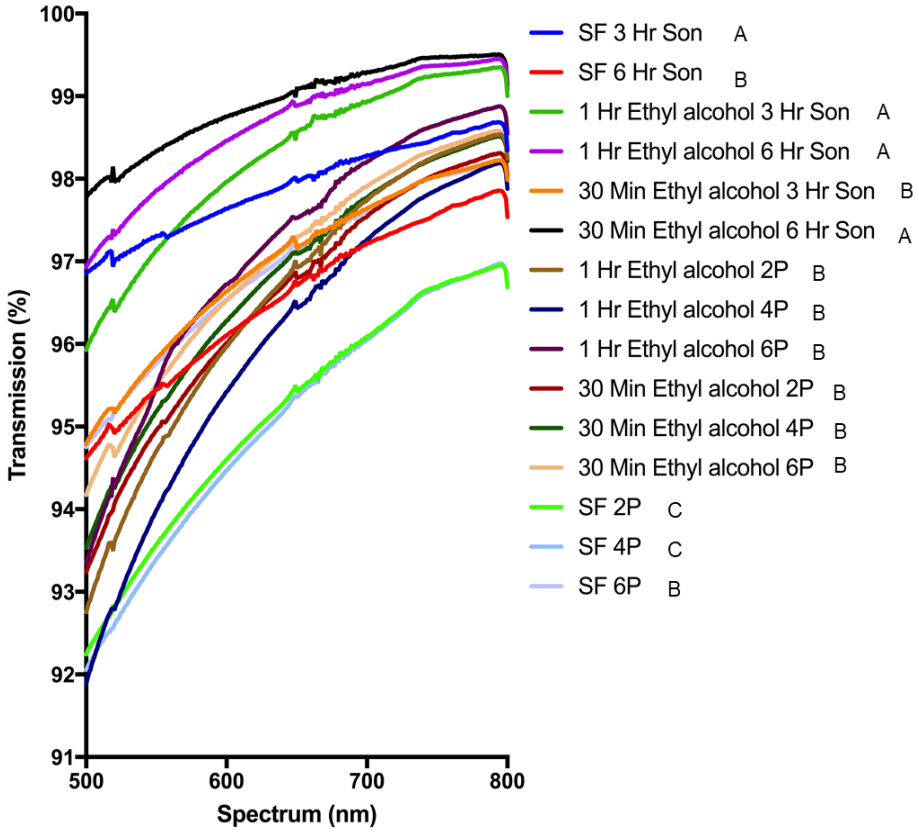


Figure 49 Transmission (%) of NFC remaining after centrifugation of a 0.1 % fibrillated dispersion of hydrothermal, ethyl alcohol washed comparing between mechanical methods. Each individual treatment is colour coded with error bars provided through standard deviation by showing differing thickness of lines. Curves with the same letter are not significant at p<0.05.

5.3.3.2 Impact of different mechanical disruption treatments on the microstructure characterisation (SEM and TEM)

The impact of mechanical treatments on the resulting microstructure of PB (treated 1 Hr ethyl alcohol and 30 min ethyl alcohol) were studied using SEM (Figure 50 and 51). Higher amount of small fibres (MFC) are evident with MF treatment compared to Son treated (Figure 40 and 48). Therefore, MF fibrillated dispersions can be deemed to have a higher proportion of NFC and with fewer, if any, macro-fibres remaining. This is clearly observed as the smallest possible magnification in order to see detail, which was at x 300 for MF samples, in comparison to x 70 with Son samples. Son samples containing clearly visible macro-fibres. The MF samples appear similar to the plate-like structures seen in section 5.2.3, which may again be explained by the drying and collapsing of MFC and NFC fibres. This provides further evidence that the microfluidised mechanical application produces a higher degree of smaller diameters fibres, than that of Son. Furthermore, the MF samples are more homogeneous than those of the Son samples, possibly indicating that the MF samples would be more readily applied to a particular food system, than that of Son samples. The reason for this is mainly due to uniformity of material and therefore greater confidence in functionality, evenly dispersed across the material when applied to a food formulation. Similarly, with the Son samples in section 5.3.2.3, it is extremely difficult to denote overall structural differences between the samples differing in number of passes and amount of time ethyl alcohol washed. Though it is apparent that these samples require higher magnification in order to see branched, web-like structures and that they seem to have debris within the samples possibly created through the high pressures experienced with an increasing number of passes. Chinga-Carrasco (2011) stated that debris, fibre fragments and fines can cause inhomogenity within fibrillated samples,

though the ethyl alcohol wash may have enabled facilitation of homogeneity due to samples, which will be quantified in section 5.3.3.3. The exact nature and content of the debris would need further investigation but it was not observed with Son samples and an example of the debris is provided with an arrow in Figure 50 (third row). Lastly, in these images no crystal-like structures are observed providing supporting evidence that those seen in Figures 43 and 44 were a result of the presence of sodium hydroxide crystals after the chemical pre-treatment. The MF material then seems to be more applicable as a food ingredient than Son samples in terms of providing texture and sensory attributes, as the system would have less clumping/aggregation and be more uniformly dispersed. Furthermore, the higher degree of smaller fibres may be less detectable in sensory applications than those that are on a macro-scale exhibited with applications of sonication. Though evidence suggests that as low as 25 µm size particles can be detected by the palate (Pratt, 1970). Small particles may cause undesirable textural defects (Engelen *et al.*, 2005) but then large particles can cause gritty sensations (Wills *et al.*, 1988), which is undesirable for snack manufacturing. Furthermore, if particles are hard or irregular they have been shown to be detected through sensory testing at as low as 10 µm in diameter (Utz, 1986). Therefore, future assessments would be necessary to determine if the fibrillated fibre sizes affected sensory perceptions.

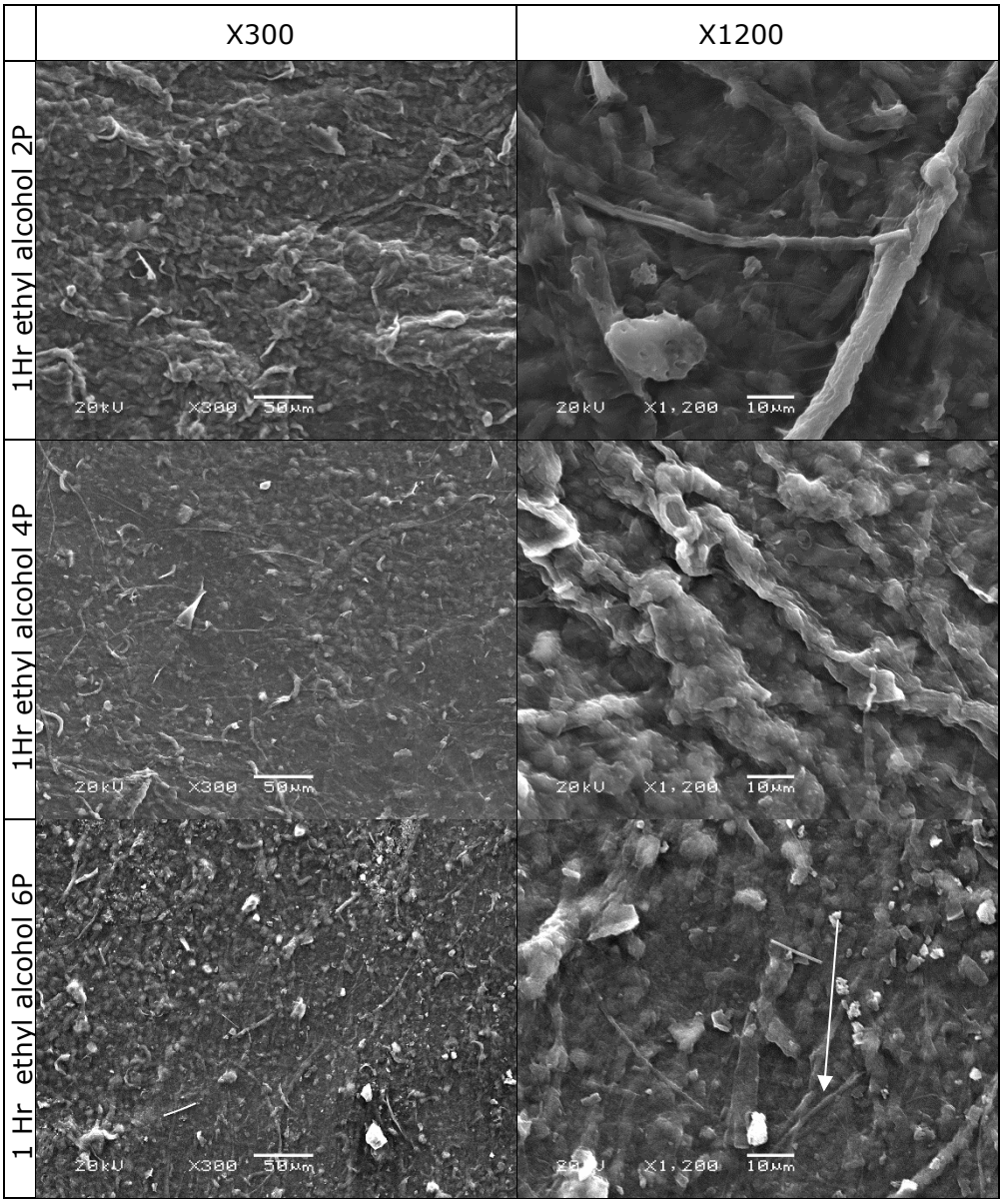


Figure 50 SEM of microfluidised fibrillated 1 % dried forms. First row: 1 Hr ethyl alcohol 2P, second row: 1 Hr ethyl alcohol 4P, third row: 1 Hr ethyl alcohol 6P. First column x 300 scale bar 50 µm, Second column x 1,200 scale bar 10 µm. Debris as shown by arrow. Showing a mixed diameter of fibrillated masses within the dried dispersions.

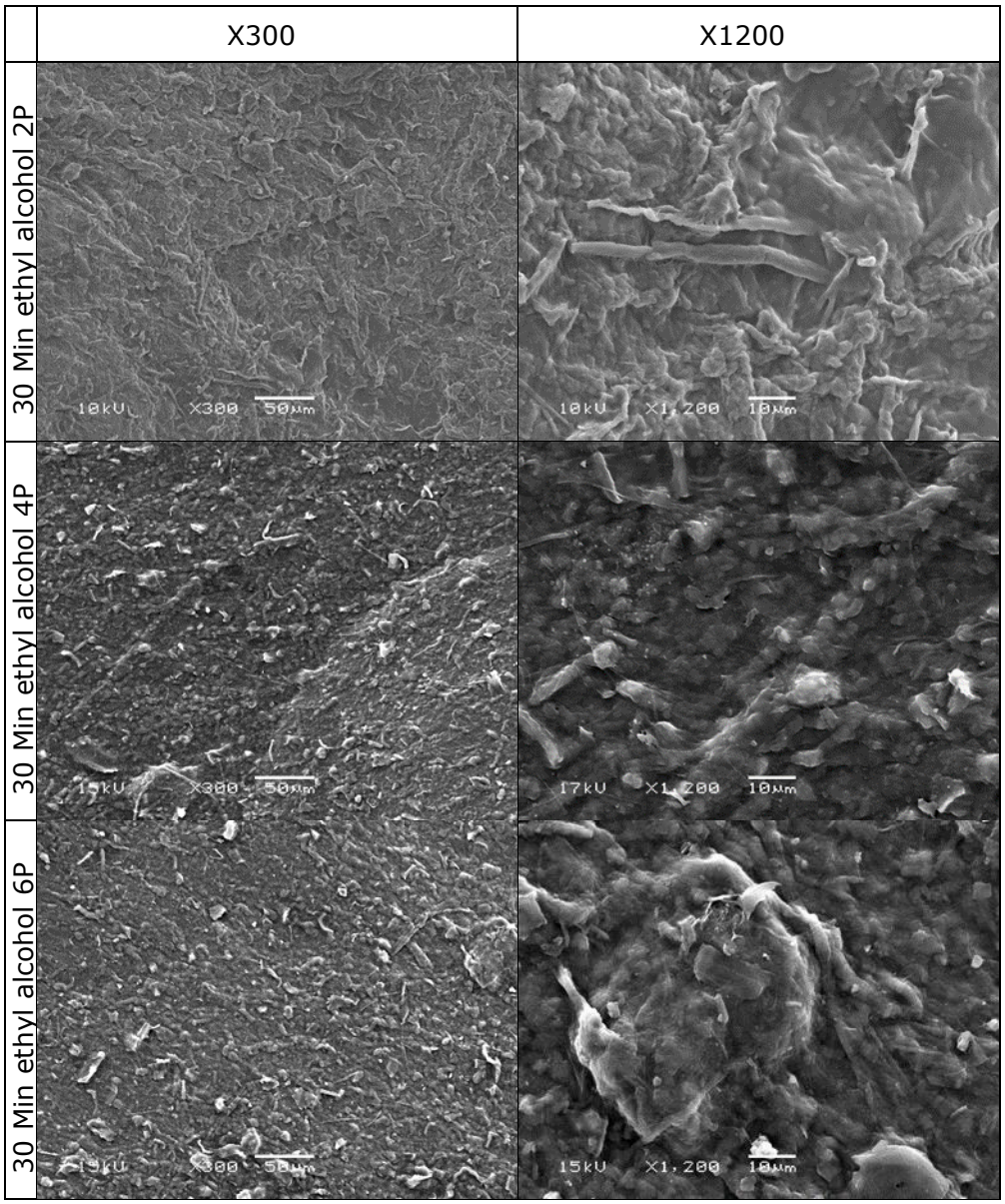


Figure 51 SEM of MF fibrillated 1 % dried forms. First row: 30 Min ethyl alcohol 2P, second row: 30 Min ethyl alcohol 4P, third row: 30 Min ethyl alcohol 6P. First column x 300 scale bar 50 µm, Second column x 1,200 scale bar 10 µm. Showing a mixed diameter of fibrillated masses within the dried dispersions.

The plate-like structures found when viewing the samples using SEM was previously hypothesised to consist of MFC and NFC and conclusions were that higher magnifications are necessary to distinguish the range of structures present. Therefore, TEM (Figure 52) was used to investigate the effects of the different mechanical methods. The TEM confirms the presence of fibres in the diameter range of MFC and NFC. The Son samples consisted of larger macro-fibres and appear more aggregated. Whereas, the MF samples (third and fourth row) are more network-like and homogenous across the Holey carbon copper grid mesh and contain little to no visible macro-fibres. This network structure is similar to that previously witnessed by Chinga-Carrasco (2011). Furthermore, whilst using this technique there were no clear differences when comparing the chemical method times (30 min and 1 Hr ethyl alcohol) for each of the mechanical methods.

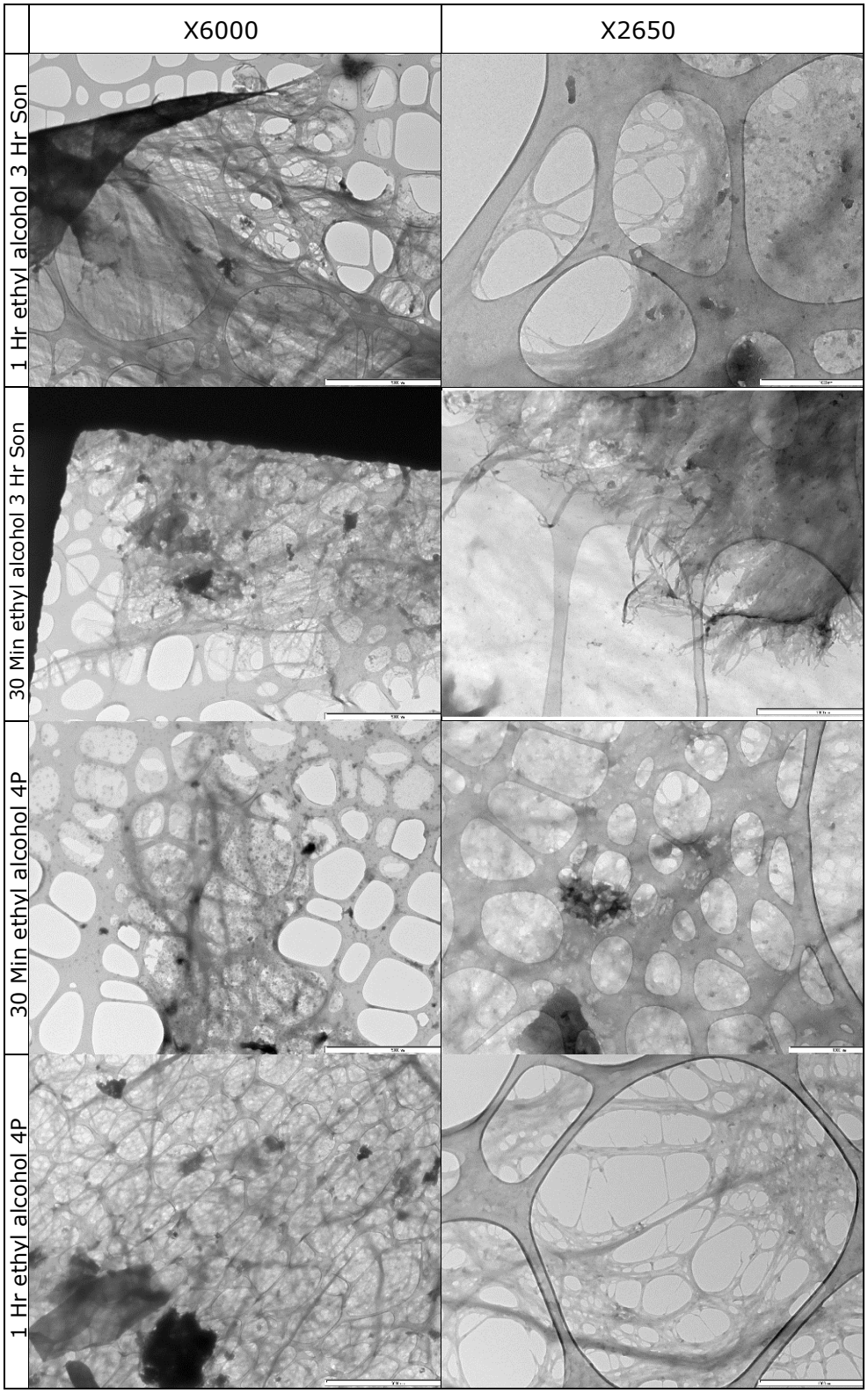


Figure 52 TEM of 1 % fibrillated masses with the first row: 1 Hr ethyl alcohol 3 Hr Son, second row: 30 Min ethyl alcohol 3 hr Son, third row: 30 Min ethyl alcohol 4P and fourth row: 1 Hr ethyl alcohol 4P all on Holey carbon copper grid mesh. Column 1: x 6,000 scale bar 5000 nm and Column 2: x 26,500 scale bar 1000 nm. Showing a mixed diameter of fibrillated masses within the dried dispersions.

5.3.3.3 Stability of fibrillated dispersions produced using different mechanical disruption methods

In comparing the stability of fibrillated dispersions through changing mechanical disruption methods again TSI was assessed after 10 min and 1 Hr, and are shown in Figures 53 and 54, respectively. Figure 53 shows that MF fibrillated samples are significantly different TSI < 1, compared to TSI > 8 for Son samples. Moreover, no significant difference is observed between MF samples for PB or SF (p-value > 0.790-0.999). In comparison to a significant difference observed between Son samples for PB and SF (p-value > 0.0001–0.007). Thereby, MF samples are significantly more stable in the first 10 min and this is probably due to homogeneity and a greater majority of particulates being of a similar size, opposed to the variation of fibre size for the Son samples. Furthermore, this shows that although there is more debris (as found previously in section 5.3.3) in the MF samples, they are more homogeneous and therefore the ethyl alcohol wash may have enabled this, or a different factor may be a cause, which needs exploring further.

After 1 Hr a clear difference is also observed between MF and Son for both PB and SF, with MF producing significantly more stable dispersions than those from Son, again as witnessed by the 10 min scan. Now differences can be more clearly observed between the MF samples created with the increasing number of passes, and chemical pre-treatment. The 30 Min ethyl alcohol samples and SF samples are in general, slightly more stable than those after 1 Hr ethyl alcohol wash and are significantly different to them (p-value > 0.0016-0.0001) but not significantly different to one another (p-value 0.995-0.999). Therefore, the number of passes had no significant difference between SF samples. However, for 1 Hr ethyl alcohol PB samples there was

a significant difference, in that 2P and 4P were less stable than 6P. Though the same observation was not witnessed for 30 Min ethyl alcohol MF samples, showing that chemical variables may affect stability over longer durations of time. This may infer that more passess and therefore longer processing by the MF is necessary to achieve greater homogeneity and thereby stability. Agarwal, (2016) tested gravitational sedimentation on fibrillated dispersion and found with an increase in passes on a homogeniser a decrease in sedimentation and therefore increase in stability was observed. However an equilibrium was reached, whereby liberation of NFC, into the supernatant phase, with further passes decreased the transmittance of the samples. Therefore, the homogeniser speculates an improved microstructure whereby a higher degree of packing can be apparent due to a mixture of differing diameters of fibres. Therefore if the equilibrium is not reached, in general MF samples are more stable and homogenous, therefore application of them would be more suitable than that of Son samples to a modelled system. This stability could infer that they are either MFC and have been enabled to entangle (via the whisker/hairy appearance properties) to one another, providing efficient packing or that they are NFC and therefore take less time to sediment with a higher proportion of NFC creating efficient packing also. Though, longer stability trials should be performed in order to see if chemical variables effect stability further. Thus indicating which methodology is best for stability and most applicable to a model system.

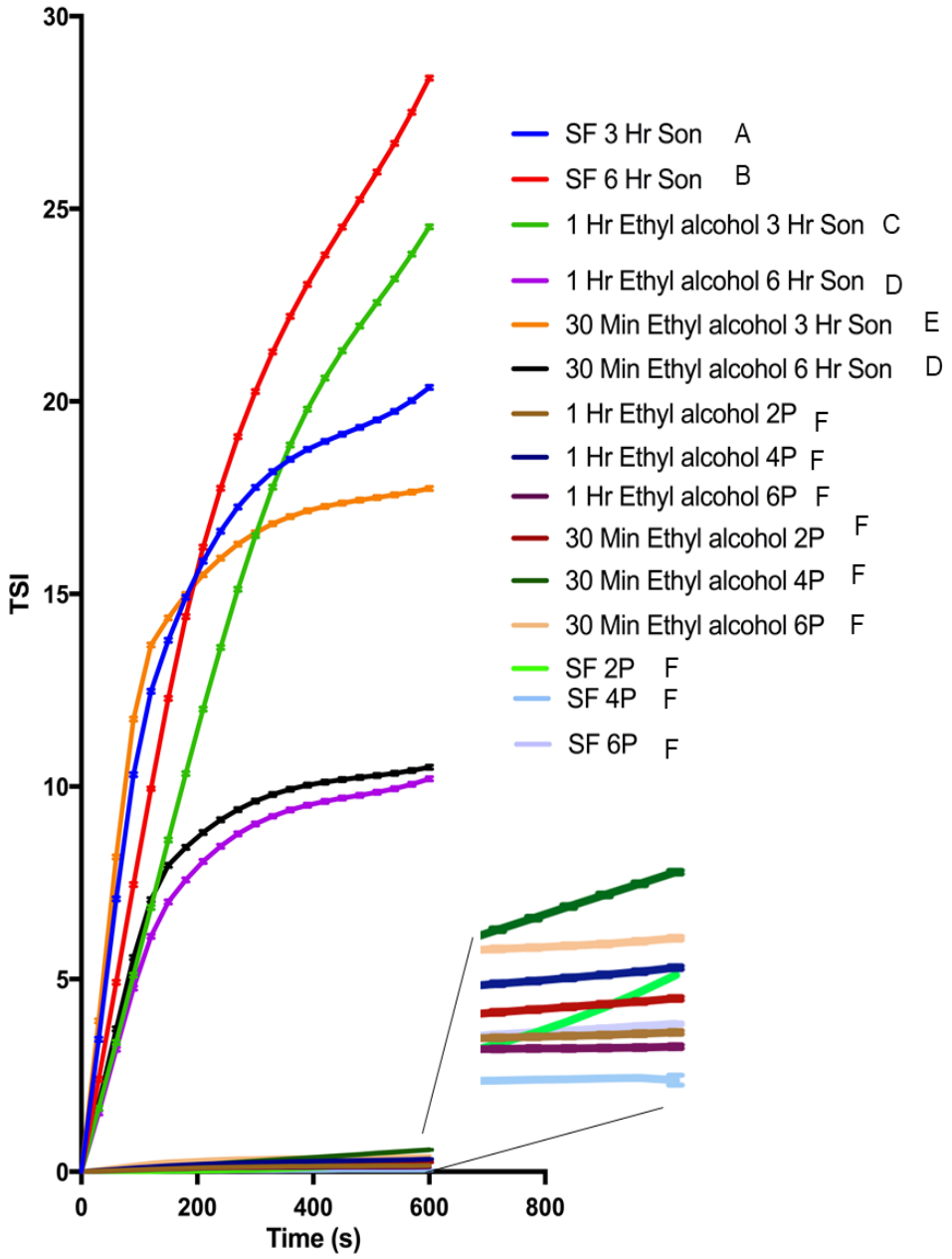


Figure 53 TSI comparing mechanical means of Son versus MF fibrillated dispersions at 0.5 % for the first 10 minutes. Each sample is colour coded. Error bars provided by standard deviation are witnessed by the thickness of the lines. An amplified depiction of results, which are not significantly different is provided due to ease of visibility. Curves with the same letter are not significant at p<0.05.

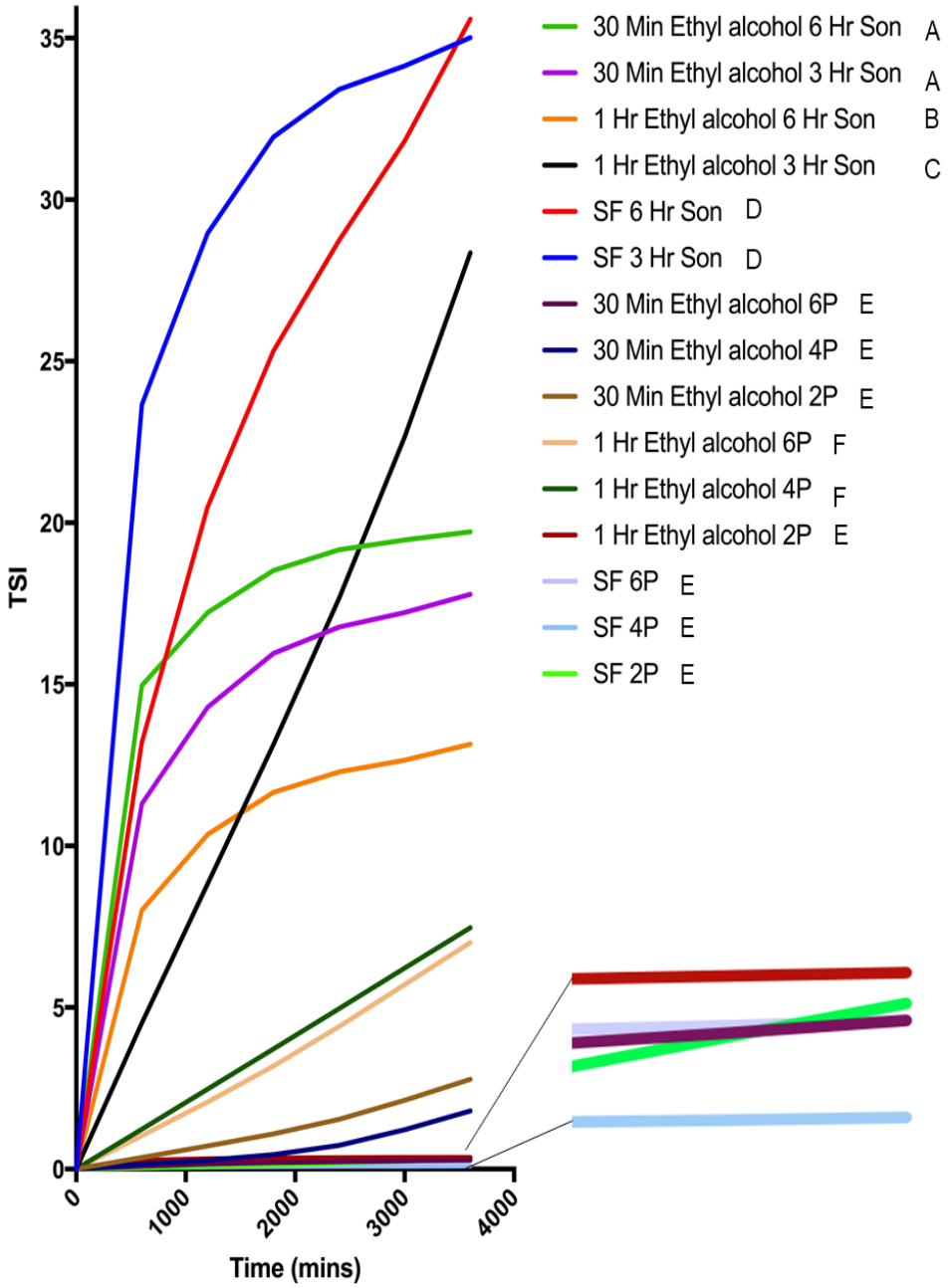


Figure 54 TSI comparing mechanical means of Son versus MF fibrillated dispersions at 0.5 % for the first hour. Each sample is colour and symbol coded. Error bars provided by standard deviation are observable by the thickness of the lines. An amplified version of results with the lowest TSI are given for ease of visibility. Curves with the same letter are not significant at $p<0.05$.

5.3.4 Crystallinity of MFC comparing Sonication and Microfluidisation mechanical disruption methods.

WAXD was used to explore the varying mechanical disruption methods on the crystallinity of HPB and Chem PB. It was found that with Son samples, which had been chemically treated for prolonged time frames had an increased crystallinity of type I allomorph (1 Hr ethyl alcohol > 30 Min ethyl alcohol) provided in Table 15. This may indicate that the ethyl alcohol wash is aiding crystallisation through mechanisms of ethyl alcohol precipitation and/or relocation of lignin, which may enable cellulose fractions to re-crystallise without other polymers in the PCWM impinging this phenomena. Furthermore, the increased amount of crystallinity found through further time frames of mechanical disruption of Son (3 Hr < 6 Hr) indicates that longer processing time and therefore longer time frames of rehydration (after the fibre has had ethyl alcohol vacuumed off), enables greater facilitation of re-crystallisation through having high levels of supersaturation. There is evidence to suggest that Son induces nucleation and increases reproducibility, though these mechanisms of crystallisation remain to be fully established (Luque de Castro and Priego-Capote, 2007). The MF samples results indicate that for 2P and 4P which have been have been chemically treated for shorter time frames and have a higher crystallinity (30 Min ethyl alcohol > 1 Hr ethyl alcohol), which is opposite to what was seen for Son samples. However, this is not the case for 6P, whereby 1 Hr ethyl alcohol has a higher crystallinity. Moreover, the more passes and therefore further processing yields a decrease in crystallinity, which is observed from the initial 2P samples for both time frames of chemical treatments (30 Min ethyl alcohol and 1 Hr ethyl alcohol). However, an increase in crystallinity is observed from 4P to 6P, which again may be a function of increased time frames and or processing. Therefore, again indicating that longer

rehydration times and supersaturation enables further re-crystallisation, though this is not observed with 30 Min ethyl alcohol 6P, which may indicate that 6P over-processes and the pressure of the equipment has broken down more crystalline regions. Though this is not observed with 1 Hr ethyl alcohol 6P. Therefore, with these results it is not apparent whether rehydration kinetics and time frames of MF samples hampers or aids crystallisation of cellulose and further investigation is necessary. However, what is apparent is that no mechanical method nor chemical method modified cellulose from its natural structure to include type II allomorphs, which are thermodynamically more stable. This is different to what was witnessed in section 5.3.2.4 (in comparing crystallinity between chemical treatments), whereby type II allomorphs were witnessed and for samples, which had been ethyl alcohol washed and Son. Lastly, MF samples have a significantly higher crystallinity index than that of Son samples (p-value < 0.05) and therefore provide a fibrillated mass that is structurally stronger. This may be due to a higher proportion of NFC found within the fibrillated mass for the MF in comparison to the Son.

Table 15 WAXD crystallinity index amounts for both allomorph I and II and total crystallinity of varying mechanical disruption methods used in order to fibrillate PB.

Sample	Type I (%)	Type II (%)	Total Crystallinity (%)
1 Hr ethyl alcohol 3 Hr Son	14	0	14
1 Hr ethyl alcohol 6 Hr Son	29	0	29
30 Min ethyl alcohol 3 Hr Son	15	0	15
30 Min ethyl alcohol 6 Hr Son	17	0	17
1 Hr ethyl alcohol 2P	29	0	29
1 Hr ethyl alcohol 4P	19	0	19
1 Hr ethyl alcohol 6P	26	0	26
30 Min ethyl alcohol 2P	37	0	37
30 Min ethyl alcohol 4P	38	0	38
30 Min ethyl alcohol 6P	19	0	19

5.3.5 Impact of different mechanical disruption methods on the rheological properties of MFC/NFC dispersions

In order to see if different mechanical disruption methods impact the flow properties of dispersions rheological assessments were performed. A comparison between the MF (2P, 4P, or 6P) and Son treatments (3 Hr or 6 Hr) on visco-elastic properties of a 1 % aqueous dispersion of treated PB (after HPB treatment with either a 1 Hr ethyl alcohol or 30 min ethyl alcohol wash) are shown in Figures 55-63. The linear visco-elastic (LVE) region was determined by amplitude sweeps for PB and SF presented in Figure 55-57, respectively. It was evident that all Son PB dispersions have a shorter LVE region (strain < 1) as compared to MF suspensions (strain < 10). However, this behavior was minimal with SF dispersions. All of the samples have a G' > G'' indicating that they all behave as visco-elastic solid-like materials. Therefore, it is worth highlighting that the LVE region is dependent on the starting material. In terms of amplitude sweeps, a significant difference was observed when comparing PB treated with the MF and Son (p-value < 0.05). Statistics also suggested that SF samples in general are significantly different (p-value < 0.05) when processed through the two mechanical means. It was also evident that varying passes of the MF and varying processing time for each chemical variable are not significantly different in terms of LVE region. Lastly, there is no significant difference between SF and PB in terms of LVE region for the same mechanical disruption methods (p-value < 0.05).

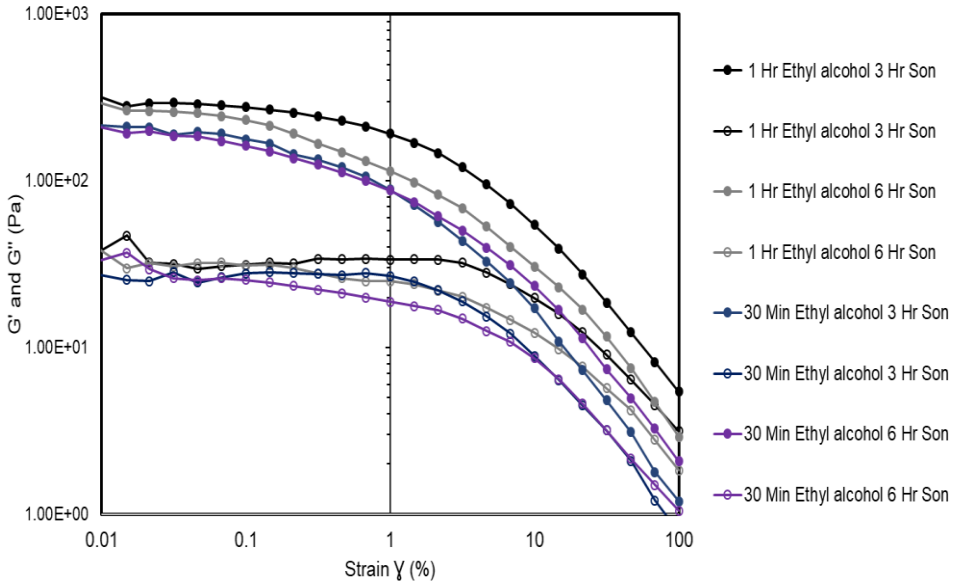


Figure 55 Amplitude sweep of 1 % PB fibrillated dispersions of Sonicated samples with two varying times of being ethyl alcohol washed. Samples are colour coded and G' have filled markers and straight lines whilst G'' have empty markers and straight lines given as unit in pascals.

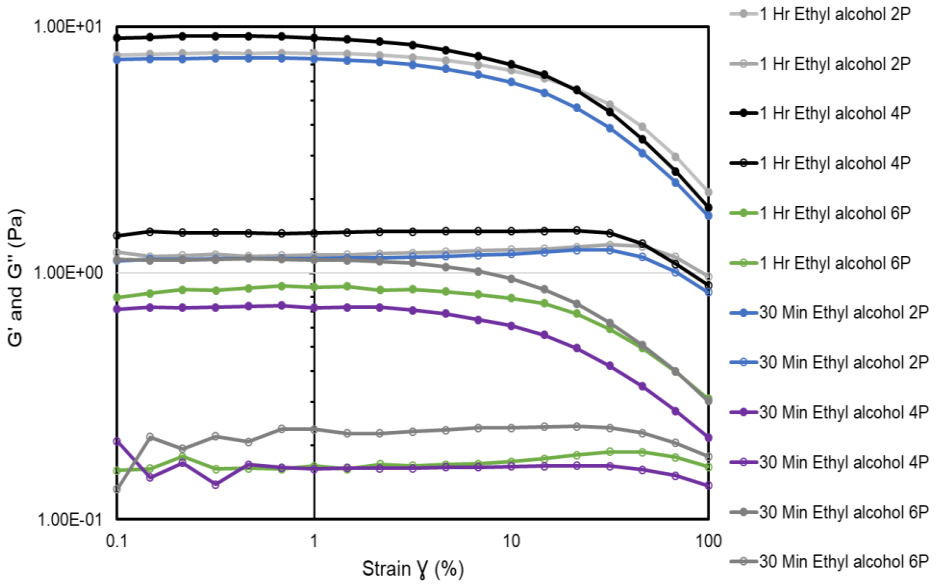


Figure 56 Amplitude sweep of 1 % PB fibrillated dispersions with various ethyl alcohol wash times and various amount of passes on the microfluidiser. Samples are colour coded and G' have filled markers and straight lines whilst G'' have empty markers, units in pascals.

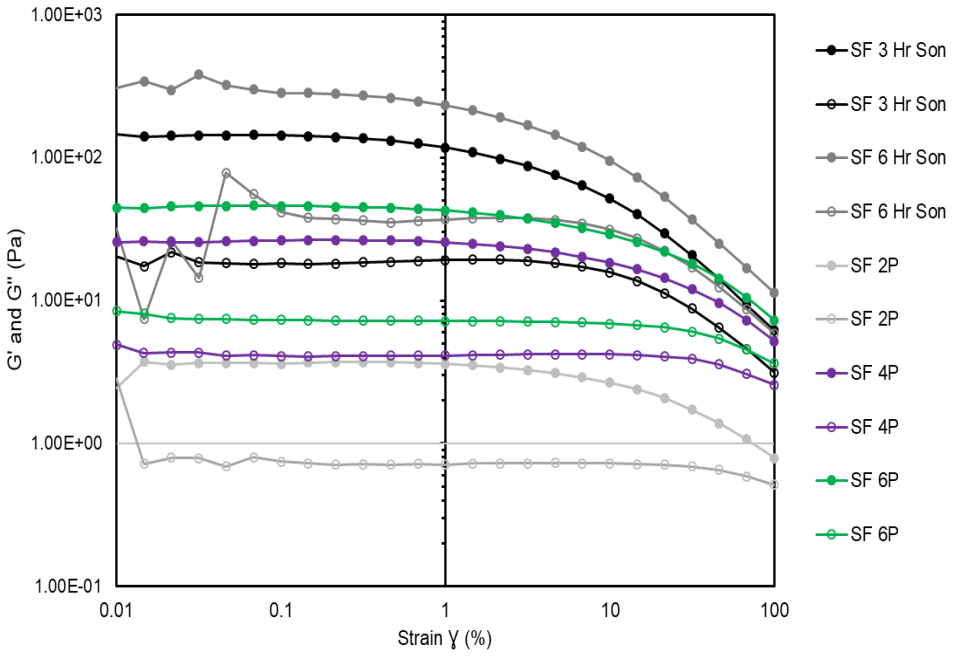


Figure 57 Amplitude sweep of 1 % Solka Floc fibrillated solutions with the two varying mechanical treatments of Sonication and Microfluidisation. Samples are colour coded and G' have filled markers and lines whilst G'' have empty markers and lines, unit provided in pascals. Samples are averages of three.

Storage and loss moduli as a function of frequency at 0.05 % strain (from LVE region) of PB and SF dispersions are presented in Figure 58-60, respectively. All dispersions showed a G' > G'' with increasing frequency, indicating visco-elastic gel-like properties. Figures 61-63 shows the tanδ and η* taken from frequency sweeps at 10 rad/s vary significantly between mechanical disruption methods (p-value < 0.0001). However, the tanδ for each were more similar (p-value > 0.0367) and as they are below 1, they describe the materials as being more elastic rather than viscous. A plausible reason for the η* being significantly higher in Son samples than that of MF, may be due to the diameter of the fibres being greater on a macro- and micro-scale rather than micro- and nano-scale, as seen by previous results. This may conclude that they are therefore more adapted for entanglement. This is indicated by MF and SF samples expressing an upward turn in their

G’ and G’’ upon higher frequencies. Moreover, SF and MF samples express slightly noisy tanδ indicating loss of structure due to deformation. This would therefore indicate that the diameter of MF samples being smaller than that of Son, produces a reduced ability to form entanglement of fibrillated fibres and therefore reduced strength of a network. On mechanical measurements between processing parameters (number of passes) for MF samples, there is also indication of differing strengths and stabilities of networks formed. Both 4P samples show less of the upwards turn of G’ and G’’ at higher frequencies, indicating they are a more coherent network and therefore greatest stabilities of MF samples. However, at 6P the largest upward turn and therefore least amount of stability is observed for samples, indicating over-processing of the fibres. Whereby smaller fibre dimensions are present and therefore less entanglement, with greater amounts of debris (from previous results obtained) is causing greater deformation. Whereas Son samples show little differences in trends of stability and strengths of networks formed, but the only difference being that with increase hours of processing a higher η* is witnessed.

Additionally results shows that for chemical variables, 30 Min ethyl alcohol produces a higher η* than that of 1 Hr ethyl alcohol for MF samples, with 4P producing the highest η*. Though this is not observed with SF as the η* increases further and is the largest value of all MF samples. This possibly implies that the SF has not reached its maximal viscosity and could possibly be passed further. Furthermore, Aulin *et al.* (2010) saw that with an increase in the number of passes through a homogeniser the η* and homogeneity of the samples increased. Lastly PB Son dispersions show an increase in η* with the amount of hours Son, though SF does not. Furthermore, it showed that 1 Hr ethyl alcohol produces a higher η* than

those 30 Min ethyl alcohol, which is the opposite trend witnessed with MF samples. Moreover, PB treated fibres have a significantly higher η* than that of SF, again possibly due to size and diameters of fibres previously aforementioned, resulting in heterogeneity and therefore better packing mechanisms, which lead to an increase in viscosity. As the starting fibre diameter is much smaller for SF compared to PB (as seen in Chapter 3). Lastly, it shows that, when SF is passed for more than 2P it has a higher η* than SF Son.

Therefore, as a summary it would seem apparent that Son samples are more stable than MF samples, due to less frequency dependence and up-turn of G''. Therefore, Son dispersions formed are stronger gels. This would also support findings from the LVE region results, showing similar differences in stability between MF and Son samples. Statistically, η* for each mechanical disruption method were not significantly different from one another (p-value < 0.05). However, comparing between groups and for all SF samples η* were significantly different (p-value > 0.05).

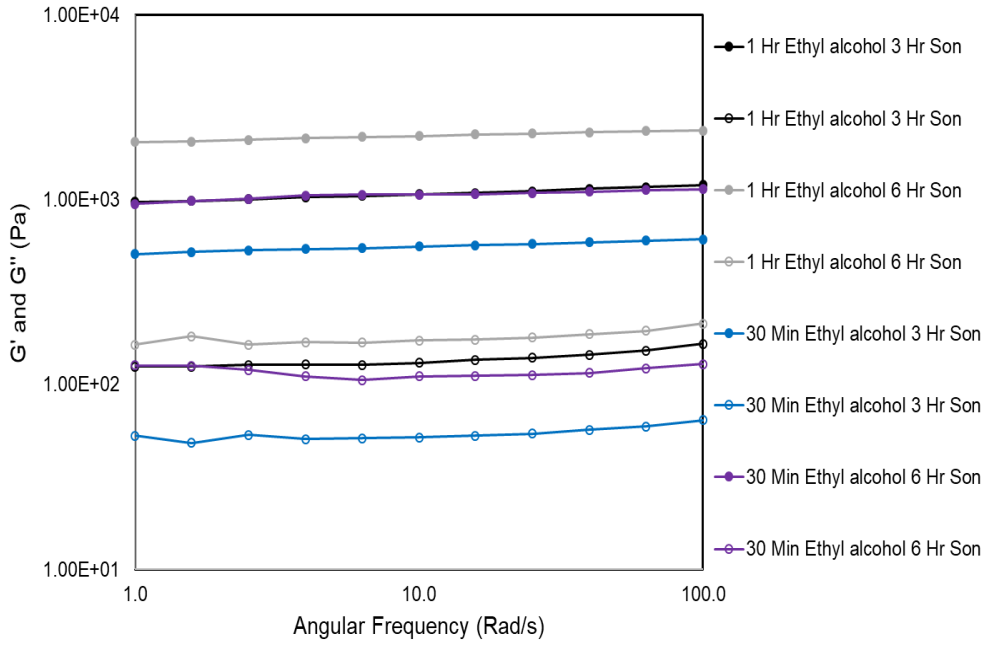


Figure 58 Frequency sweep of a 1 % PB fibrillated dispersions with the mechanical treatment of sonication. Samples are colour coded and G' have filled markers whilst G'' have empty markers markers and lines with units in pascals. Samples are an average of three.

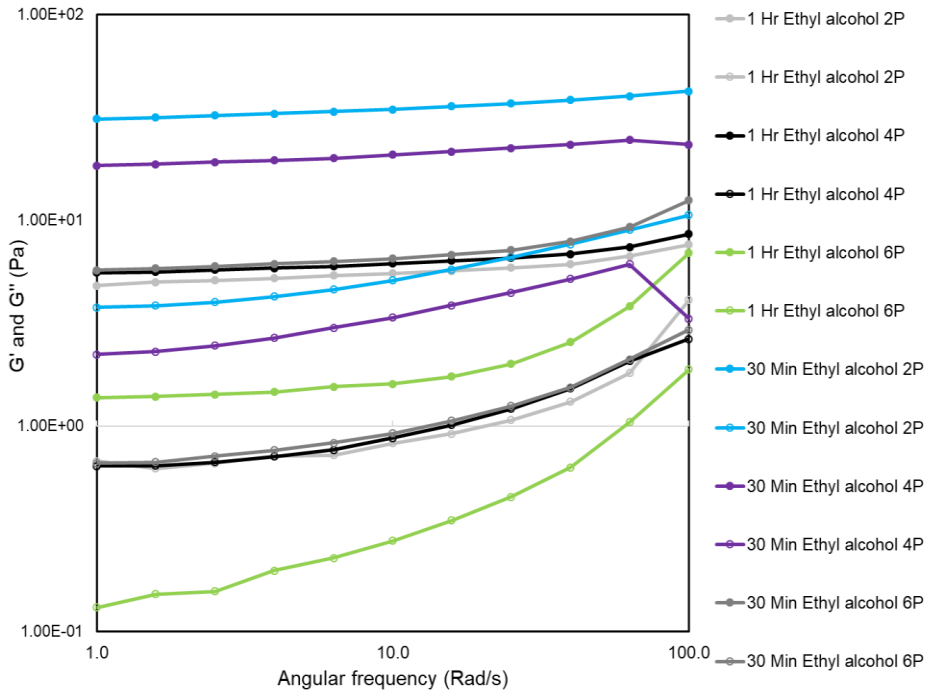


Figure 59 Frequency sweep of a 1 % PB fibrillated dispersions with the mechanical treatment of the Microfluidiser. Samples are colour coded and G' have filled markers whilst G'' have empty markers and straight lines with units provided as pascals.

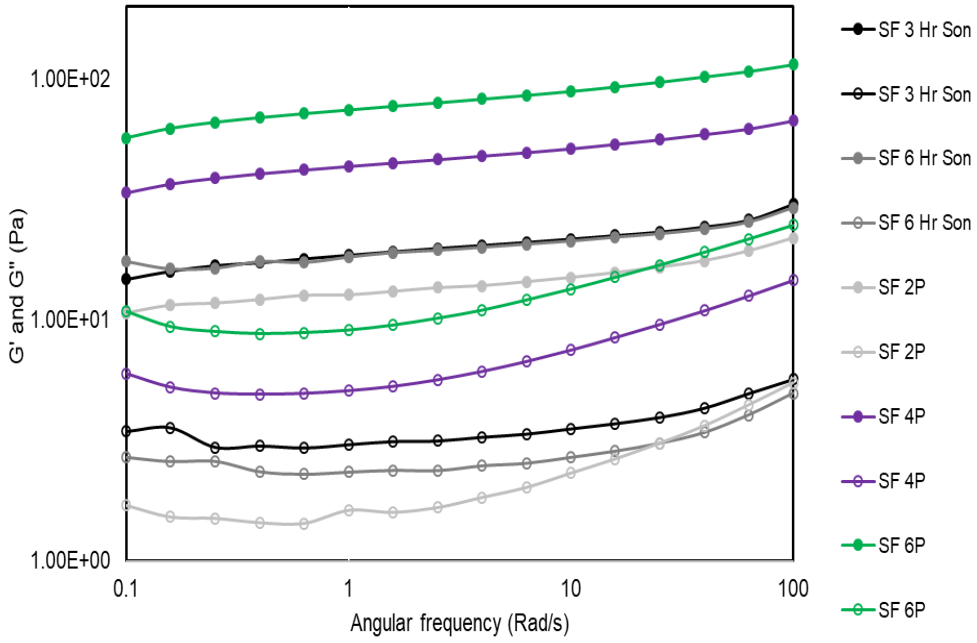


Figure 60 Frequency sweep of 1 % SF fibrillated dispersions with sonication and microfluidsation as the mechanical treatments. Samples are colour coded and G' have filled markers with lines whilst G'' have empty markers and lines and unites provided as pascal. Samples are an average of three.

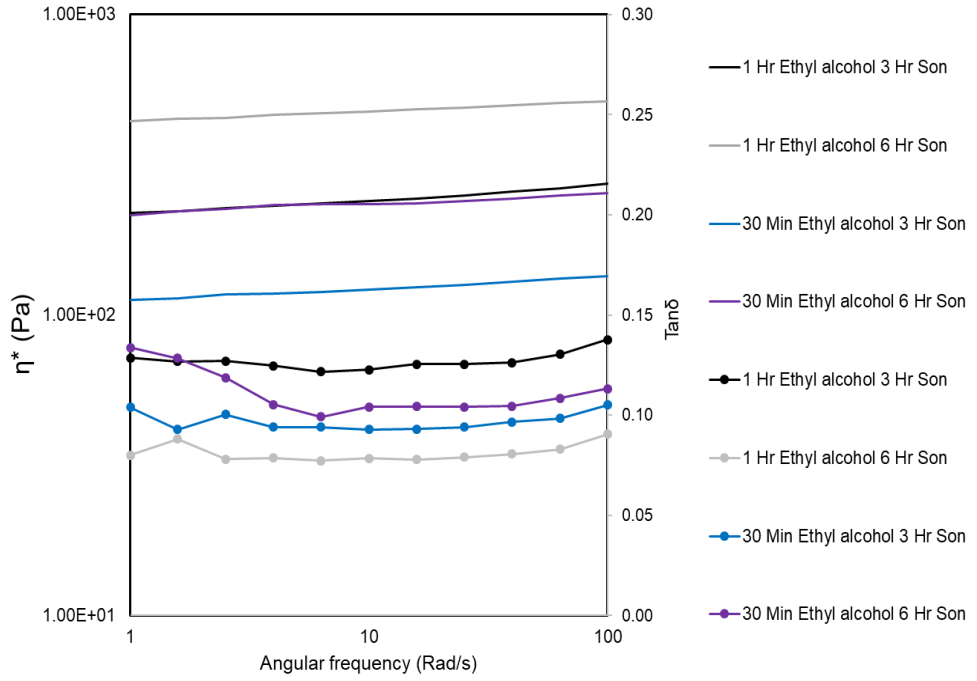


Figure 61 Complex viscosity given as a straight line and Tanδ given as a line with markers for 1 % fibrillated dispersions of Sonicated samples with various ethanol wash times. Values were calculated from frequency sweeps at 10 rad/s and units of viscosity are provided in pascals.

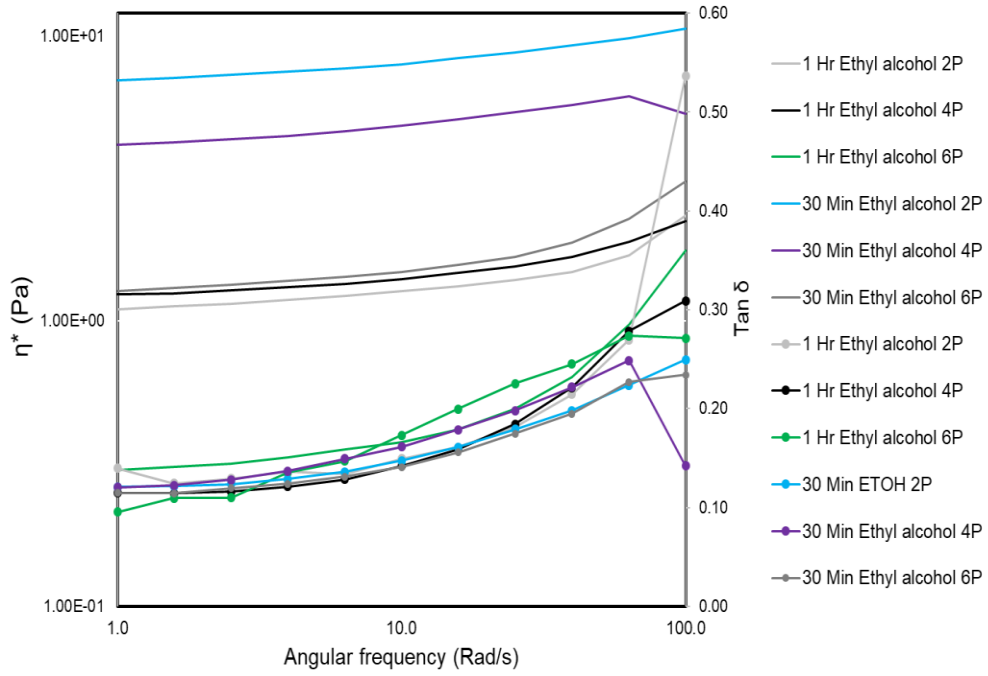


Figure 62 Complex viscosity given as straight lines units in pascals. Tanδ given as straight lines with markers for 1 % fibrillated dispersions of Microfluidised samples with various ethanol wash times. Values were calculated from frequency sweeps at 10 rad/s.

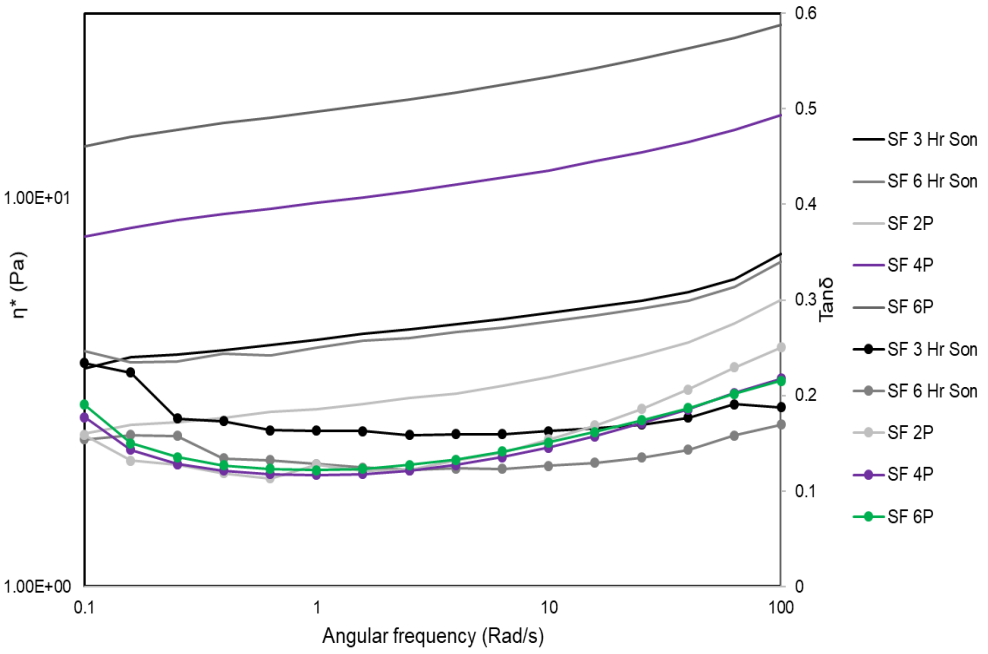


Figure 63 Complex viscosity given as straight lines units provided in pascals. Tanδ given as straight lines with markers for 1 % fibrillated solutions of Sonicated and Microfluidised mechanical treatments on Solka Floc. Values were calculated from frequency sweep at 10 rad/s.

5.4 Conclusion

This work aimed to create fibrillated material from PB, investigating the impact of chemical pre-treatment and two methods of mechanical fibrillation to determine whether MFC/NFC could be formed to create ingredients, which may have effective bulking properties.

The results indicate:

- PB was successfully transformed into a fibrillated mass containing a mixture of macro-fibres, MFC/NFC in varying quantity dependent on treatments used.
- Chemical variables for Son samples did not vary in NFC yields but mechanically MF produced significantly greater yields.
- Microscopy shows that alkali washing created fibrillated fibres that were agglomerated and hardened. For further assessments neutralisation after bathing is recommended. The MF samples were more homogeneous and TEM showed the NFC morphology. Plate-like structures are witnessed in parts of the Son samples. Overall samples fibrillated through MF rather than Son clearly contain more NFC.
- The ethyl alcohol and alkali washes successfully removed fractions of hemicellulose from the PB but proportionally lignin was barely removed. No significant differences were seen in NFC yield amounts, between chemical variables, nor between the purified cellulose. Implying that hemicellulose, lignin and a higher degree of cellulose (which would be present if not degraded by chemicals) may improve NFC yields. Therefore, trials should be done on fibrillating PB through mechanical means with just the application of hydrothermal process, in order to soften the fibril structure. Furthermore,

investigations should be made on the sugar and lignin concentration of samples after said mechanical applications, with and without the addition of chemicals.

- Crystallinity measurements provided convoluted results whereby the chemical treatment on the crystallinity differed for differing mechanical processes, which may due to differing analytical equipment used. Though further processing yielded higher crystallinity and the MF yielded a higher crystallinity than sonication. Results indicated that fibrillated samples have the ability to re-crystallise due to excess saturation during the mechanical processing. It is unclear what the varying chemical time frames (30 min ethyl alcohol and 1 Hr ethyl alcohol) have on the properties of crystallinity of fibrillated masses.
- MF samples were more stable and homogenous than that of Son ethyl alcohol samples, which indicates they have larger proportions of fibrillated fibres with differing sizes and therefore diameters for efficient packing properties.
- Rheology showed visco-elastic gel-like properties of dispersions of both Sonicated and MF samples. Son samples had a significantly higher η*, possibly due to a greater mixture of fibre diameter sizes and those fibres being larger than MF samples, leading to greater heterogeneity and therefore packing ability. Chemical pre-treatments affected each mechanical disruption method differently. In order to see shear-thinning properties aforementioned in literature an increased frequency sweep should be performed.

The results presented clearly show that fibrillated material can be produced from PB, and as such will be tested as an ingredient in Chapter 6.

Chapter 6 Application of Pea Biomass powder and fibrillated mass to model system.

6.1 Introduction

6.1.1 Starch

Starch is a homoglycan composed of a single sugar type unit regardless of its source (Whistler, BeMiller and Paschall, 1984). Designated starch fractions consist of highly branched molecules containing short chains of α-(1-4)- linked D-glucopyranosyl monomers with α-(1-6) linked branches called amylopectin (known as the crystalline region) (Taggart and Mitchell, 2009). Additionally linear molecules of amylose α-(1-4) linked D-glucopyranosyl monomers (known as the amorphous region) (Taggart and Mitchell, 2009), which consist of fewer branches (Whistler, BeMiller and Paschall, 1984).

Starch production is a result of energy storage in higher plant species. It is stored in a semi–crystalline granular structure, whose size and shape differ depending on the source. Amylose and amylopectin content differs in various botanical sources and depends on stage of life, for example amylose content increases with maturity. Additionally, chain lengths differ depending on stage of life, amylopectin chain lengths decrease with increasing granular size. Both starch and cellulose consist of polysaccharide chains of glucose joined by glycosidic bonds. The major difference between the two is cellulose is composed of β glucose and forms long straight chains, whereas starch chains are helical (Whistler, BeMiller and Paschall, 1984), and tend to be found in granules, which consist of α- bonds. Starches, similarly to cellulose, are naturally found in differing crystalline forms, though starch consists of three designated forms compared to cellulose having five

(Wüstenberg, 2014). Potato starch (PS) consists of amylopectin with longer branch chains and phosphorus bound which displays the B-Type WAXD pattern. Whereas, rice starch (RS) consists of shorter chains and displays the A-pattern. Tapioca starch (TS) and pea starch consists of branch chain lengths in-between both A and B patterns and therefore displays the C-pattern (Whistler, BeMiller and Paschall, 1984; Jane, 1996). All of the aforementioned starches are explored in these works within a dough snack formulation recipe. Starches are used based upon their properties of viscosity, sensory and textural attributes. Starches usually increase the viscosity of a sample based on their ability to gelatinise. Starch gelatinisation is defined as an dis-order transition. This occurs in an excess of water (above a gelatinisation temperature), whereby the starch granules swell as hydrogen bonds in crystalline regions are disrupted and water is absorbed (BeMiller, 2011). The crystalline regions ultimately pull apart due to swelling, eventually with an increase in temperature, hydration and melting occurs of these regions (BeMiller, 2011). Thus, an irreversible loss in organised structure occurs. Starch granules in an excess of water upon continuous heating results in volume fractions of swollen granules and leaching soluble components (amylose) into an aqueous phase, creating a new complex dispersion of swollen or deformable granules in a viscous aqueous continuum (also known as starch pastes) (Taggart and Mitchell, 2009; Sullo and Foster, 2010; BeMiller, 2011). However, in limited water (low water) starch is hard to be gelatinised even at temperatures above 100 °C (Fukuoka, Ohta and Watanabe, 2002). This is due to starch granules not interacting with the limited water available and results in only partial gelatinisation (granules that do interact) and therefore a reduced viscosity compared to fully gelatinised pastes/gels occurs. Starch pasting temperatures differ with starch origins (BeMiller, 2011). Whereby the irreversible changes to the

starch granule are determined by its accessibility to hydration. This accessibility is determined by the ratio of amylose to amylopectin, lipid fractions and the presence of phosphate group (Taggart and Mitchell, 2009). Moreover, the temperature at which gelatinisation occurs is dependent upon the temperature required to disrupt the amylopectin chains and therefore the lengths of these chains. Lastly, the resulting properties of starch pastes are determined by the amylose to amylopectin ratio, fine structures, molecular weight distributions of amylose and amylopectin, water availability, time, temperature and shear of the cooking and or heating process (BeMiller, 2011).

6.1.2 Potato Starch (PS) and Potato Flakes (PF)

Potatoes consist of around 65-80 % starch on a dry weight basis depending on variety, area of growth, maturity of harvest and storage history (Whistler, BeMiller and Paschall, 1984). In 2005, half (10 million tonnes) of the potatoes produced (20 million tonnes) globally were processed (FAO, 2008). This processing includes the manufacturing of Potato Starch (PS). Final starch products have a water content of around 17-18 % (Whistler, BeMiller and Paschall, 1984). Of commercial starches besides wheat in some instances, PS withholds the highest consistency on pasting due to its granule size (Singh *et al.*, 2003; Taggart and Mitchell, 2009) and these pastes are sensitive to small concentrations of added electrolytes (Whistler, BeMiller and Paschall, 1984; BeMiller, 2011). Other more favorable functions of PS include; a decrease in viscosity upon further heating and agitation, flexible film formation, binding power, and low gelatinisation temperature (Whistler, BeMiller and Paschall, 1984). Starches can be modified to enable them to be pre-gelatinised. Potato Flakes (PF) are used

in instant foods (Reyniers *et al.*, 2018) and snacks. PF are pre-gelatinised thereby making them cold water dispersible (Whistler, BeMiller and Paschall, 1984). Therefore, being able to be applied to a material without the need to cook it. As PF are already pre-gelatinised they produce a lower viscosity than if they were in their native state (Reyniers *et al.*, 2018). PF are peeled, pre-cooked, whole potatoes that have been dehydrated and therefore they contain PCWM as well as lipids (around 0.6 %) (Emsland Group, 2018), whereas pre-gelatinised starch (PS) is extracted from potatoes and contains no PCWM, protein and extremely low lipid content.

The PS used in this study has an amylose content of 38.8 % and amylopectin content of 45.2 %, the remaining constituents are proteins, lipids and micro-nutrients such as phosphates. Thereby, hypothesising and providing more evidence for expecting PS to have the highest viscosity than other starch commodities used in the formulations of the model system. Furthermore, PF has an amylose content of 29.3 % and amylopectin content of 42.7 %, though this varies between processing and potato variety within the manufacturer (Emsland Group, 2018). The lower amylose and amylopectin ratio provides evidence of the PCWM that coincides with starch in PF compared to PS, the remaining constituents will be protein, lipids, and micro-nutrients. Although this has the smallest content of amylopectin, which produces shear thinning and more viscous paste-like properties, it is expected that the viscosity of this starch will be the lowest compared to all starches examined. This is thought to be due to the lower amylopectin content and that the material is pre-gelatinised during its production. Therefore some of the amylopectin double helical structures have been lost (Taggart and Mitchell, 2009).

6.1.3 Rice Starch (RS)

Within rice grains the endosperm consists of thin-walled cells completely filled with starch granules. Waxy rice endosperms are opaque, whereas non-waxy rice have translucent endosperms (Whistler, BeMiller and Paschall, 1984). In processing rice to obtain RS, sodium hydroxide (concentration of 0.3-0.5 %) is used to purify and soak broken rice (Whistler, BeMiller and Paschall, 1984).

RS has one of the smallest granule sizes of cereal starch commodities (3-20 μm) (Singh *et al.*, 2003). RS varies in its final gelatinisation properties depending on the variety used. The molecular and chemical properties of RS are similar to those of other cereal starches (Whistler, BeMiller and Paschall, 1984). RS has a lower viscosity upon gelatinisation than that of PS (Singh *et al.*, 2003) due to RS having a smaller granular size and length of amylose chains being shorter. Park *et al*. (2007) found that by comparing waxy and non-waxy RS a higher amylose content led to an increased gelatinisation onset and peak temperature with pasting onset. Whereas, amylopectin with shorter side chains provided a more viscous solution within pasting properties (Park *et al.*, 2007).

The RS used in these works is soaked to soften, dried and milled, but not prior cooked. The amylose content is 25.4 % and amylopectin 53.6 % with the resulting composition comprising of protein, lipid and micro-nutrients. RS has the least amylose content and second highest amylopectin content of the varying starches (PS and TS) used in these works. Additionally, due to granule size for rice (3-8 μm) being so much smaller than that of potato (5-100 μm) and tapioca (4-35 μm) its viscosity is expected to be the lowest of all starches bar pre–gelatinised PF.

6.1.4 Tapioca Starch (TS)

Tapioca Starch (TS) is obtained from cassava roots. “Bitter” cassava roots are often used instead of the “sweeter” sources due to their higher starch content (Whistler, BeMiller and Paschall, 1984). Manufacturing of TS from cassava includes washing then peeling of the outer skin. To rupture all cell walls, mild fermentation followed by grinding to a pulp occurs (Whistler, BeMiller and Paschall, 1984). Finally the TS is recovered by screening, washing or centrifugation with a final water of 32-45 % (Whistler, BeMiller and Paschall, 1984).TS is flash dried to obtain a water content of 12-14 %. The viscosity of TS depends on many cultivating factors such as time of harvest and soil fertility. The TS used in these works has an amylose content of 30.5 % and amylopectin content of 54.6 % again other constituents are protein, lipids and micro-nutrients. Therefore, this starch material is expected to have a lower viscosity than that of PS (depending on the granular size of PS being greater than that of TS) but higher than that of RS as the granular size and stability upon shear is greater. Molecular weight and degree of polymerisation also play a key role in gelatinisation.

In comparing these three varieties of starches, one of which is in both native and pre-gelatinised forms, the present work wishes to provide findings on the competition for water between said starches and between said starches within a composite material. Thereby, assessing resulting effects on the gelatinisation and swelling properties of both cooked pastes and within application of a composite snack product.

6.1.5 Manufacturing of Snacks

6.1.5.1 Snack Pellet manufacturing

Snack pellet manufacture is viewed as an alternative method to direct frying of potato slices (Harper, 1988). Often described as a crisp intermediate made from extruded dehydrated tuber and cereal materials (Bouvier and Campanella, 2014). Extruders used are either single or twin screw. Single screw is ideal for basic simple compounds, whereas twin screws are most suitable for specialty compounds, which require high levels of mixing (Harper, 1988). Food extrusion is a commercial technology which first appeared in the mid-1930's (Harper, 1988).

Starch food materials in a raw granular state are known as Native Starch (NS). Some NS are transformed into a continuous mass having visco-elastic properties known as a dough-like substance and have been transformed into what is known as Gelatinised Starch (GS). The combination of mixing and temperature, with pressure and water, causes a process known as cooking, which disrupts and melts starch granules, denatures and orientates protein molecules (Harper, 1988), in order to transform NS to GS. Water is essential for enabling phase transition of NS granules through gelatinisation to GS. Free water and thermal energy transforms amorphous regions of starch to absorb water causing swelling and leaching of amylose, with simultaneous unwinding of the double helical structure of amylopectin (Jenkins and Donald, 1998). This results in separation of crystalline regions into an amorphous state. Water is essential for creating the right proportions of continuous and disperse phase microstructures. This is done by enabling the dehydrated GS at low water content to form a gel network (the continuous phase), which disperses partially GS (dispersed phase) throughout it (van der Sman and Broeze, 2013).

The combination of the different ingredients produces the finished product, which undergo transformations at low water contents that range from 15-35 % (wet basis) (Harper, 1988). Upon exiting the extruder the dough is cut using a die head and cutter with variable speed and die head shapes available. This high temperature, pressurised, dough within the die can puff, producing a ridged open cellular structure, due to the die still maintaining an elevated pressure (Harper, 1988). Expansion of the superheated water within the extruded product on heat release (whilst transported along a belt) occurs upon exiting the die (Harper, 1988). The transport belt aids in air drying of the product. The extruded product is then placed in a continuous dryer until 10-12 % water is achieved. At lower water content the material is deemed to have a longer shelf life. In addition, an equilibrium is reached for water content across the sample. The product is now classed as a pellet, whereby starch is in a glassy state which contains NS and pre-gelatinised starch. The pellet is then stored at ambient temperature until used for frying to enable expansion.

6.1.5.2 Heat-press manufacturing

Heat press processing involves a mould with a stationary platen, onto which a mobile platen compresses down and forms a material composite through temperature, pressure and time (see Figure 64 and 65). This is also a mechanism for snack manufacturing, with similar capabilities of enforcing gelatinisation and gel network formation, of various water levels. With the addition of water within a product system and as a result the thermal energy required by the equipment expansion is also enabled. The heat press used in this study was custom built for the University of Nottingham and made

following an earlier project with similar objectives (production of a pellet without an extruder).

Heat pressing as an alternative to extruding has become a large area of interest to the manufacturing industry. With the correct adaptations (i.e. obtainable through a low water dough system) the process has the capabilities of being more environmentally sustainable and provides a reduction to cost than that of extrusion. This cost saving is mainly due to the after-drying process required after extruding which is estimated to contribute to $\frac{2}{3}$ of the energy requirement within the manufacturing line.

Heat pressing to produce dough sheets has been performed by Tate and Lyle, though high water doughs of 25-60 % and an initial baking step prior to snacking were required (Avashia and Riddell, 2015). The traditional use of heat pressing cellulose fibres was to produce textile fibres and paper. In 2014, Fritto-Lay incorporated heat-pressing into manufacturing Walkers ‘ Pops’ which expanded pellets through pressing rather than through frying, with the purpose of reducing acrylamide formation (Williams and Davies, 2013). As a technique this was first used by the pharmaceutical industry, which consisted of the compression of powder materials between two platens (Vermeire *et al.*, 2005). The works of Williams and Davies and the work presented here incorporates heat in the process, which can facilitate expansion upon the release of pressure.

6.1.5.3 Intermediate product expansion to final product

After extrusion or heat-pressing the second phase of snack manufacture from a pellet to an expanded product is through indirect pellet expansion, through mechanisms of oil frying. Whilst frying, it is hypothesized that the

hilum (the center of the dispersed starch granules) act as nuclei, in which vapour expansion begins (Schwartzberg *et al.*, 1995). Furthermore, vapour bubbles (which are present in the gelatinised starch matrix) form pores in the expanded product via rapid evaporation of superheated water (Moraru and Kokini, 2003). It is essential that the intermediate (pellet) product contains air pockets suitable for expansion as they act as nucleation sites during frying (Cisneros and Kokini, 2002). The material properties of the matrix are also important to retain the voids once produced.

6.1.5.4 Developing a recipe

A cost efficient, stable, valorised material is required to provide resilience and positive nutritional value, by replacing high-energy dense costly ingredients. Additionally the end product must have the ability to contain a lower calorific value than the current product manufactured in developing countries with advantageous health benefits due to an increase in consumer health awareness. Further details and reasons as to why this is required are explained in the general introduction (Chapter 1). The product formulation (also known as dough formulation in this study), is based upon a method produced typically from extruding rather than heat pressing. The project sponsors found that the aforementioned starches (high-energy dense ingredients) were used based upon a combination of cost efficiency and their properties confirmed in sensory studies. Though typically used in extruded snack products cereal grains tend to be low in protein and have poor biological value (Ozer *et al.*, 2004). It has been said that nutritious snack foods can be produced by incorporation of legumes, vegetables, and fruits in the formulation (Ozer *et al.*, 2004).Therefore if the fundamental properties of cereal grains and tubers can be matched (such as microstructure,

viscosity and texture) in performance, then replacing such commodities with a valorised material would be more cost efficient. It should be mentioned that the views in this thesis are based upon those of the researcher and do not necessarily reflect the position or policy of the project sponsors and would require sensory validation (not part of this study).

6.1.6 Aims of this chapter

This study aims to assess the functionality of Ball Milled Pea Biomass (BMPB) upon incorporation and partial or full replacement of starch based commodities, used within the model system. Additionally, the addition of Fibrillated Pea Biomass dispersion (FIB PB) in differing concentrations is also tested. As aforementioned both starches and water play key roles in the manufacture of both pellets and expanded products. Therefore, the aim is to compare a control (model system) with results that incorporate or completely replace starchy materials in the dispersed phase and continuous phase, of both pellet and expanded products respectively. Thereby, ultimately assessing the effects of replacing a high-energy dense commodity with a nutritionally advantageous one, whose properties have been earlier discussed in Chapters 4 and 5. Such comparisons from the Control (model system recipe) to the newly formulated dough recipes will include:

- Microstructure;
- Texture;
- Viscosity properties, and;
- Nutrient profile.

6.2 Materials and methods

6.2.1 Processing parameters chosen to convert Pea Biomass to a functional food ingredient

6.2.1.1 Ball milling parameters

The PB, once defrosted, was then oven dried for 24 Hr at 105 ºC (UN 110, Memmert, Germany). The PB was then milled using a Planetary Micro Pulverisette 7 (Fritsch GmbH, Germany), at 600 rpm with 10 min of milling followed by 10 min of pause, in order to allow heat to dissipate, for a total milling time of 50 min and called BMPB. Each zirconium oxide pot contained six zirconium oxide balls (10 mm Ø) and 0.5 g of dried PB. Parameters were chosen as a result of findings in Chapter 4.

6.2.1.2 Fibrillation parameters

The PB once defrosted was subjected to heating methods from section 5.2.2.1 of Chapter 5. The then hydrothermally treated Pea Biomass (HPB) was subjected to a 1 Hr ethanol wash (1 Hr ethyl alcohol) followed by 4 passes (4P) on the Microfluidiser LM20-30 S/N 0076 (Microfluidics, Massachusetts United States of America) at 30,000 psi with an attached Z chamber and to create FIB PB. Prior to the Microfluidiser, in order to prepare the material and prevent blockages, a thermomix was used for 3 min at setting 9 (Vorwerk, Australia). Parameters were chosen as a result of findings in Chapter 5.

6.2.2 Manufacture of pellet and expanded snack

2.5 g of Dough Formulations (DF) (Table 17) were used to create pellets of an average thickness of 1 mm ± 0.1 in the heat press. Starch commodities from the Control formulation (Table 16) were replaced proportionally or completely with:

1. BMPB

In addition to starch commodities being replaced or partially replaced with BMPB, RO water was replaced with solutions of:

2. FIB PB and therefore the sample name is known as BMPB FIB PB (BMPB plus FIB PB).

The dough formulations were then placed in an aluminium cup (Length 40 mm x Width 40 mm x Height 25 mm) (Figure 66) and heat-pressed using a custom made heat-press at the University of Nottingham (see Figure 64 and 65), at 120 °C for 30 sec, at 4 bars. As found in previous study, Davies (MPhil) project of the University of Nottingham (2018). ~~(Thesis not accessible).~~

The subsequent pellet was stored for 5 days at ambient temperature in a sealed environment to ensure water distribution equilibrated evenly across the sample; a typical industrial step within pellet manufacturing (Riaz, 2000). Lastly, the pellet was fried (Wilko 0.9 L deep fat fryer, Worksop, UK) using sunflower oil at 185-190 °C for 15 sec (parameters specified by the sponsor of the project) in order to obtain an expanded final snack product.

Table 16 Dough formulation recipe for the intended use of producing a pellet/intermediate product.

Ingredient list	100 g batch	(%) of total Starch blend	Total Starch
Potato Starch (PS)	39.20	56	69.96
Potato Flakes (PF)	19.53	28	
Rice Starch (RS)	6.28	9	
Tapioca Starch (TS)	4.95	7	
Salt	0.70		
Proprietary mixing aid	0.28		
Sugar	1.05		
Proprietary mixing aid	3.48		
Vegetable oil	0.28		
RO Water	24.24		
Total (g)	99.99		

Table 17 Dough formulation adapted to partially or fully replace all Starch commodities in ratio fractions with BMPB.

Ingredients	90:10% Starch :BMPB	70:30% Starch :BMPB	50:50% Starch :BMPB	30:70% Starch :BMPB	10:90% Starch :BMPB	100% BMPB
PS	35.28	27.44	19.6	11.76	3.92	0
BMPB	3.92	11.76	19.6	27.44	35.28	39.2
PF	17.58	13.67	9.77	5.86	1.95	0
BMPB	1.95	5.86	9.77	13.67	17.58	19.53
RS	5.65	4.40	3.14	1.88	0.63	0
BMPB	0.63	1.88	3.14	4.40	5.65	6.28
TS	4.46	3.47	2.48	1.49	0.50	0
BMPB	0.50	1.49	2.48	3.47	4.46	4.95
Total Starch (g)	62.96	48.97	34.98	20.99	7	0
Total BMPB (g)	7	20.99	34.98	48.97	62.96	69.96

Table 18 RO water replacement in dough formulation with FIB PB dispersion. Increase in percentage represents the amount of fibrillated masses added to coincide with the same percentage fraction replaced by the BMPB on Starch commodities.

Sample	Concentration of FIB PB in the 24.4 g of water added to the dough formulation (%)	Fib PB in total water based formula (%)
90:10 Starch:BMPB FIB PB	0.29	7
70:30 Starch:BMPB FIB PB	0.87	21
50:50 Starch:BMPB FIB PB	1.44	35
30:70 Starch:BMPB FIB PB	2.02	48
10:90 Starch:BMPB FIB PB	2.60	63
100 % BMPB FIB PB	2.89	70

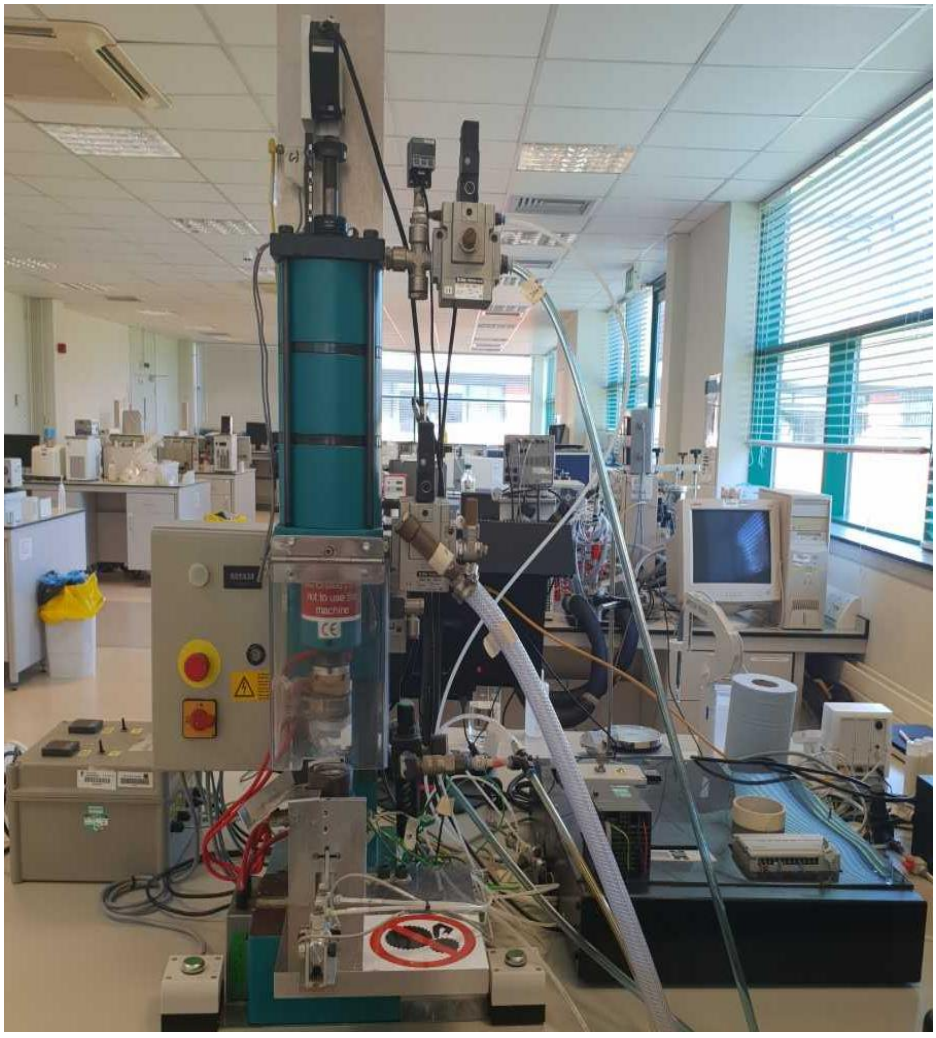


Figure 64 Custom designed heat-press equipment for The University of Nottingham used in this study.



Figure 65 Custom designed heat-press platens. A sample within an aluminium cup is placed in between the two platens and covered with a sheet of cloth to prevent the material sticking to the platen that makes contact with the samples surface. The aluminium cup prevents the bottom from sticking to the platen. Both top and bottom platens were the same temperature.



Figure 66 Example of Control dough formulation within an aluminium cup prior to heat-pressing.

6.2.3 Analytical methods

6.2.3.1 Expansion Ratio (ER)

The ER of the pellet (intermediate product) to final product (expanded) was calculated on a volume basis the following equation with a minimum of three measurements for each dimension and averaged. ER can be calculated by the following Equation 16:

Where W = Width (mm), T = Thickness (mm) and L = Length (mm)

Equation 16 $$ER = \frac{(W \times L \times T)of\ intermediate\ product}{(W \times L \times T)of\ expanded\ product}$$

6.2.3.2 Rapid Visco-Analyser (RVA)

3 g of dough formulations were mixed with 17 g of RO water. To test the impact of replacing starch with BMPB, 30 % of starch was removed (2.1 g starch : 0.9 g BMPB). The RVA profile consisted of:

1) A starting temperature of 25 °C and mixing speed of 960 rpm for 10 sec,
2) The remaining profile comprised of a mixing speed of 160 rpm, with a heat ramp increasing from 25 °C to 90 °C within 5 min and held for 3 min at 90 °C,
3) Finally, this was followed by a decrease in temperature over 5 min to 25 °C and then held at 25 °C for 5 min, equating to a total run time of 20 min. Recordings were measured every 4 sec.

6.2.3.3 Rheology–Amplitude and Frequency sweeps

Dough formulations of both BMPB and BMPB FIB PB, once mixed and cooked using the RVA were then tested using the same rheology settings and parameters as shown in Chapter 4 in section 4.2.4.9 with the exception of a gap setting of 0.5 mm and a smooth parallel plate was used instead of serrated.

6.2.3.4 Confocal Laser Scanning Microscopy (CLSM)

Samples of mixed doughs containing starches and BMPB, in different ratios produced on the RVA were used for CLSM. This was of a total solid content of 15 % (10.5 % starch and 4.5 % BMPB). In order to perform CLSM two stages were performed:

1. Component staining: Samples, approximately 1 g, were simultaneously stained to visualise the distribution of the starch and fibre components in the dough formulations. Rhodamine B (Sigma Aldrich, 0.1 g/L), was used to label starch, and Calcofluor White (1:1 with 10 % potassium hydroxide, Merck) was used to bind to the cellulose within the PB matrix.
2. Microstructural Imaging: Images of the component structure of the dough mixes were acquired using CLSM. Samples were mounted on a glass slide, and examined using a Zeiss LSM880 Laser Scanning Microscope (Zeiss, Germany). An overlay of the two channels (Rhodamine B and Calcofluor white), to the same area, gave the final image of the network seen in the samples, showing in yellow the starch, and in blue the fibrous/cellulosic components. The dark holes represent air incorporated into the dough during the mixing phase. A band pass filter between 420-510 nm was selected for the detection of Calcofluor White; when excited at 405 nm, and 545-590 nm for the detection of Rhodamine B; when excited at 561 nm. Images were acquired using a x 20 objective, with a diode laser, and a diode pumped solid-state laser respectively.

6.2.3.5 Micro Computed Tomography (Micro-CT)

Particular dough formulations of expanded products were chosen for Micro-CT analysis. The Micro-CT used was a GE Nanotom 180 KV NF. The energy current of the X-rays were performed at 60 kv and 160 µA. Projection images were around 1440 per full rotation. The total exposure time was 250 milliseconds with an image produced every 6 milliseconds, which was a result of an average of six images (averaging all six/compiling them), in order

to reduce noise. Image acquisition and reconstruction software used was Pheonix Datos x 2 acquisition and reconstruction. Three stages occur in the full analysis:

1) Scan;
2) Reconstruct and;
3) Image processing.

Image analysis is used in order to account for voxels/voids/pores (pores) and percentages thereof using VGSTUDIO MAX software, whereby a mask is created for the samples, which is then inverted from the material sample revealing pores. Furthermore, it is used to take images at differing angles and cut through of the samples. Resolution of images were taken at 4 µm.

6.2.3.6 Texture analysis (TA)

To measure the break strength of the pellets (intermediate product) and expanded (final product) a three point bend rig fitted to the Stable Micro System Texture Analyser (Surrey, UK) was used. Each sample was placed between two supports of the rig with a probe attached to a maximum load cell of 5 kg in order to break each product. The instrument software recorded time, distance and force of deformation of each sample. The parameters used were as follows:

1) Test mode was set to compression with a pre-test speed of 1 mm/sec, a test speed of 3 mm/sec and a post-test speed of 10 mm/sec,
2) The distance covered was 10 mm in order to completely break each expanded product,

3) The target mode was set to distance requiring a trigger force of only 5 g, and trigger type was set to auto force,
4) The span (40 mm) between the two supports was trialled on each product and measured to be exactly the same between treatments and replicates, this was decided upon based on similar diameters used by Mena Garza, (2015) (Mena Garza, 2015).

6.2.3.7 Dynamic Mechanical Analysis (DMA)

Intermediate products and expanded products were analysed using an 8000 single cantilever mode SYS Dynamic Mechanical Analyser (PerkinElmer, Beaconsfield, UK). To prevent water loss during measurements, samples were initially cryo-milled (IKA A11 Basic, Germany) with liquid nitrogen and sieved to <1 mm in particle size, then deposited into stainless steel material pockets (height 8 mm x length 33 mm x thickness 1 mm-1.3 mm) (Mettler Toledo, Leicester). Each pocket, once filled with sample, had dimensions (height, length and thickness) measured to use as a comparison and model between samples. Empty pockets were run as a control. Samples were heated from -20 °C to 200 °C at a heating rate of 5 °C/min and carried out using a strain % rate of 0.02. Lower temperatures were achieved by feeding liquid nitrogen through an attached canister. Three frequencies of 0.3, 1, and 10 (Hz) were used to characterise the frequency dependency of the products with a 0.005 mm displacement. Force was calibrated daily by applying a force of 0.04 Newtons.

In order to calculate S’ and S’’, referring to stiffness (storage and loss modulus) of the samples both the E’ and E’’ (Storage and loss modulus respectively) were subtracted by 90 % of the total value at the highest temperature. This was done in order to minimize effects of the material

pockets impacting on results. Furthermore, it was also performed in order to get an indirect viscosity (Equation 18) for the samples as a geometry constant was not applicable and therefore complex viscosity could not be calculated. Lastly stiffness moduli were used to calculate Tanδ values using Equation 17 rather than storage (E') and loss moduli (E'') naturally calculated by the software.

Equation 17 $$\boldsymbol{Tan\delta = \frac{S''}{S'}}$$

Equation 18 $$\boldsymbol{Indirect\ Viscosity = \frac{S''}{Hz}}$$

6.3 Results

6.3.1 Rheological measurements of raw materials and composite mix

In order to test rheological properties of the raw materials and to assess their role as viscosifiers within the model system product, RVA was performed. Figure 67 depicts the RVA profile of all raw starch-based materials within the model system recipe. This shows that upon gelatinisation PS has the highest viscosity followed by RS, TS and finally PF. At the end of the cooking process the mixture could be assumed to contain leached amylose, amylopectin and starch granule ghost (Debet and Gidley, 2007). The noise signal at the end of the PS trace was found to be indicative of the starch not fully gelatinising (confirmed by microscopy). This showed that at 15 % solids the PS required a higher proportion of water in comparison to other starches for the material to be fully gelatinised upon the heating and cooling ramp. This may be because of differing amylose and amylopectin amounts in each of the starch commodities, but also due to the granular size/particle size, molecular weight and chain lengths, determining the amount that they can swell. PS having the largest granular size, chain length and molecular weight may be a causal function of its greater viscosity than the other starches. PF are pre-gelatinised through production of the raw material as they are heated to over 100 °C, hence they produce a significantly lower intrinsic viscosity. Through this analysis it would seem evident that the higher proportion of PS replaced or partially replaced in the system by BMPB that the viscosity of the overall product will drastically decrease. However, the conditions of the RVA are not representative of heat-pressing and extrusion as these would be performed at significantly lower water contents. Though the observations witnessed here are likely to follow similar patterns and the difference between samples may not be as significant at lower water contents, with a

different processing system. Sáchez *et al.* (2010) tested the pasting and gel stability of normal and waxy starches from maize, rice, potato and cassava as well as, modified waxy maize starch. They found that the waxy cassava starch had a higher viscosity than the normal (1119 vs 937 cP) and higher than RS, but less than PS (Sachez *et al.*, 2010). Furthermore, Deffenbaugh and Walker (1989) tested PS and TS on an RVA and found that PS had a significantly higher relative viscosity in comparison to TS (Deffenbaugh and Walker, 1989). Values cannot be compared due to differing concentrations between studies, however both studies confirm the trend observed in Figure 67. Figure 68 shows the effect of replacing 30 % of each of the starches with BMPB. It is clear that there is a complex pattern emerging, as a 'dilution' of the swelling power of the starches at lower concentrations (now 10.5 %) would be expected to show a decrease in the viscosity at the point of gelatinisation. This is seen for PS, as expected due to the swelling potential discussed earlier. However, the viscosity only reduces by 400 cp. A similar decrease is seen for RS, but the viscosity of TS increased.

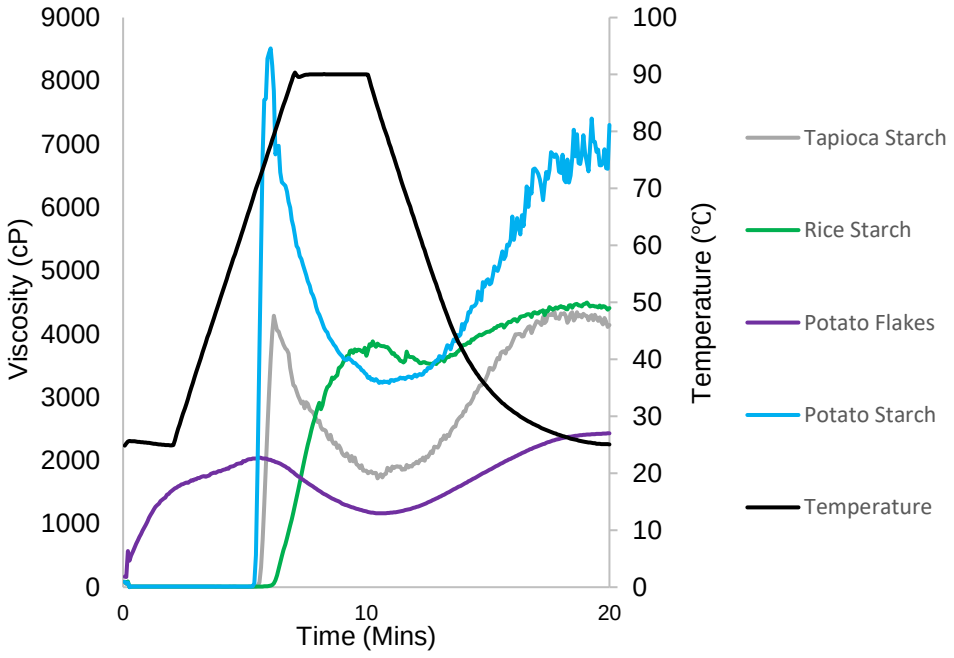


Figure 67 RVA profile of differing starch commodities at 15 % solids.

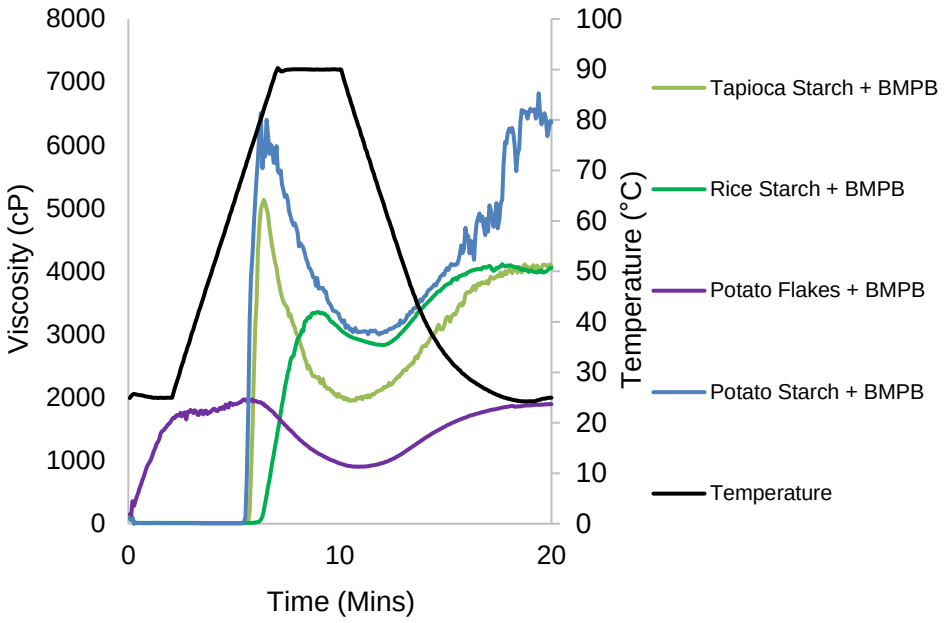


Figure 68 RVA profile of differing starch commodities with each starch having the same proportion of BMPB added at 15 % solids (10.5 % starch: 4.5 % BMPB).

Sullo and Foster investigated the RVA viscosity profiles of starch and cellulose blends and found that when waxy maize starch (8 %) had the addition of methylcellulose or hydroxypropylmethylcellulose at 1 %, an increase in apparent viscosity was observed, which was thought to be a synergistic effect from mutual exclusion of water between starch and hydrocolloids present (Sullo and Foster, 2010). However, they did not substitute any of the starch commodity for the cellulosic based ones. This suggests that the swelling/viscosifying potential of BMPB and or water absorbing capacity can enhance the properties of the starch. Díaz-Calderón *et al*. (2018) found that the addition of bacterial cellulose fibres at concentrations as low as 0.5 % significantly increased the pasting profiles and therefore viscosity of wheat and maize starches. With the largest

increase observed in the peak viscosity of the RVA profiles for the varying starches (Díaz-Calderón *et al.*, 2018).

In assessing rheological measurements of the dough formulations it is necessary to understand the microstructures of the matrix. Moreover, to understand whether synergistic effects leading to an increase in viscosity are plausible with the addition of cellulosic materials (in the powder form). Figure 69 shows CLSM of the differing dough formulations used in Figure 68 (BMPB with each individual starch commodity, mixed and heated, then cooled with an RVA). The starch with the most interaction seems to be that of PF and RS. Whereas for TS and PS they appear to occupy different (phase separated) domains than BMPB. This would be consistent with the previous argument postulated by Diaz- Calderon *et al.* (2018). RS/BMPB mixtures appear to be more compatible and the BMPB appears to be completely dispersed throughout the PS system. Interestingly Diaz-Calderon *et al*. (2018) also discussed the possible interaction between cellulose and starch, and while stereo-chemically the details of how this occurs is limited, it cannot be ruled out. There may be other charge related interactions, which may also occur, but this is clearly an area for future exploration. Research has found that starch and cellulose manufactured together are made up of non-covalent and non-specific interactions (Quiroga Ledezma, 2018). However, these interactions depicted in Figure 69 may give some indication for the increase viscosity difference witnessed between RVA profiles in Figures 68 of starch viscosities.

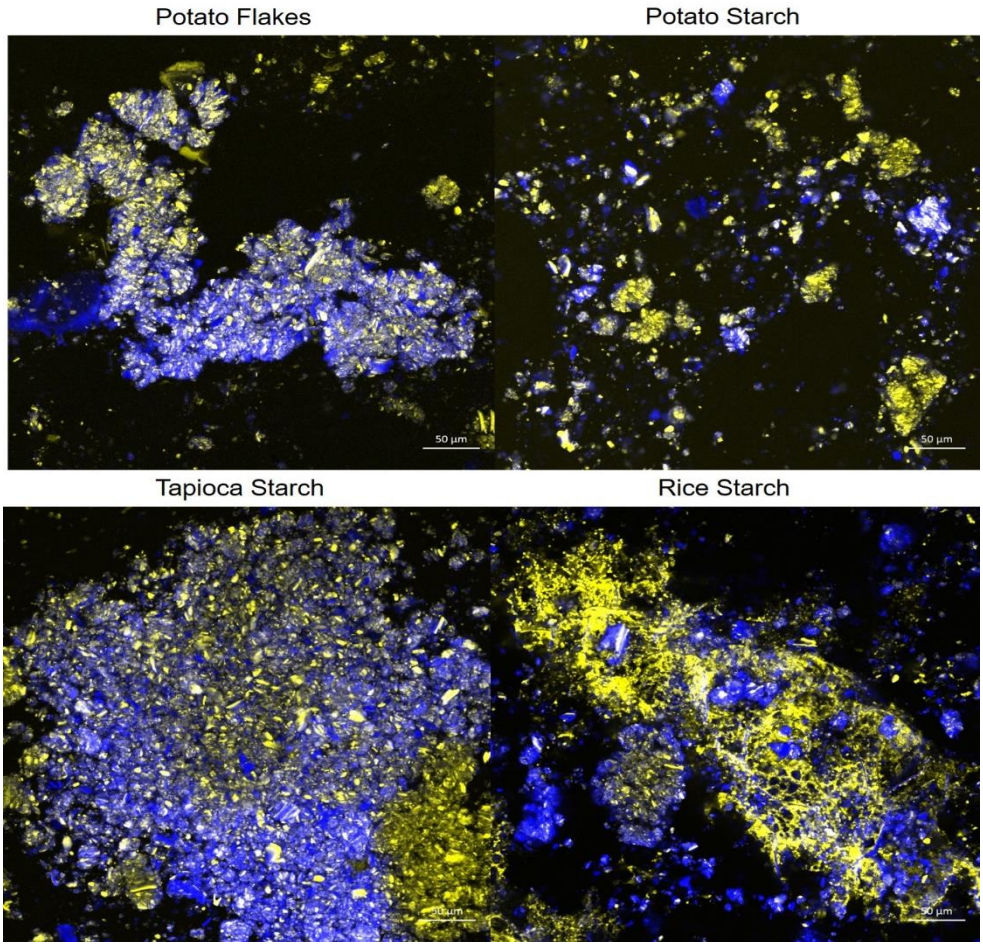


Figure 69 Confocal laser scanning microscopy of differing starch commodities (stained yellow) mixed with the addition of BMPB (stained blue) cooked from the rapid visco-analyser (profile Figure 68), Scale bar 50 µm.

In Figure 70 and 71 it is apparent that the final viscosities at the end of the RVA profile show that up to 30 % of starch replaced by modified PB provides similar viscosities to the control. The explanation provided by Sullo and Foster (2010) of synergistic effects and thermodynamic incompatibility may play a key role. Alloncle and Doublier *et al*. (1991) has ascribed a composite system similar to these as starch granules become embedded in a hydrocolloid solution (Alloncle and Doublier, 1991). Thereby, the viscosity of the resulting composite will be determined by any changes in the two phases as well as the potential for the phases to interact with one another, as

indicated by Díaz-Calderón *et al*. (2018) with bacterial cellulose fibres. A further hypothesis from these results is that the BMPB with RS and TS is forming a new gel network within the continuous phase and this thereby enhances the overall viscosity of the resulting matrix, in comparison to the reference without BMPB, as the presence of a gel network may promote interactions of the granules (Sullo and Foster, 2010).

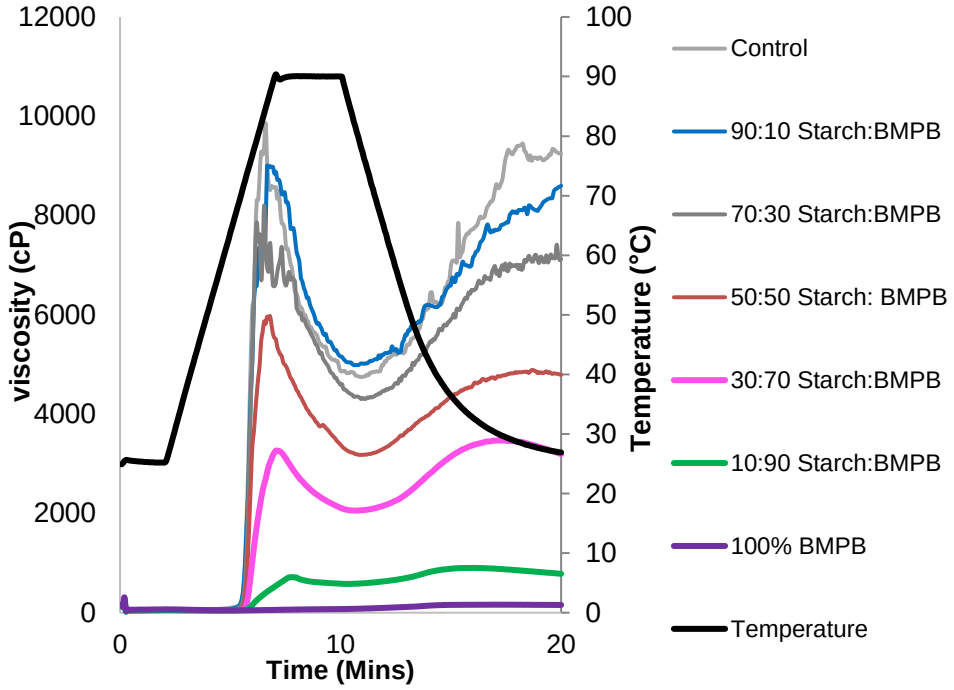


Figure 70 RVA profile of dough formulations for all Starch:BMPB ratio (15 % total solid).

In the dough formulation the starches are blended, as shown in Table 17. Therefore RVA analyse were carried out on the blend and when this blend was replaced by BMPB (Figure 70) and BMPB FIB (Figure 71) in different ratios. These mixed blends at 15 % solid contents will have differing proportions of each starch commodity replaced, for example $\frac{4}{7}$ of PS and $\frac{2}{7}$ for PF. As a blend composite they have a larger peak and set back viscosity in comparison to the same solid contents of a pure starch system. So at up to 30 % starch reduction a comparison can be made to the

Control for both peak and set back RVA profile. Therefore, the previous hypothesis of a new gel network formation, increasing the viscosity of the product even in small quantities, may have occurred, but is not apparent in the final viscosity. Plausibly indicating some synergistic effects between starch and the PB.

However, 90:10 Starch:BMPB FIB PB has a slightly higher final viscosity than that of the Control and is most closely matched. This indicates that including fibrillated matter into the composite mix increases the intrinsic viscosity significantly, as also seen by Díaz-Calderón *et al.* (2018), but only when starch commodities are still found in a higher proportion of the composite. Up to 30 % starch replacement by both formulation types show that the peak and set back viscosities are not significantly different to that of the Controls. When comparing Starch:BMPB with Starch:BMPB FIB PB once > 50 % of starch commodities have been replaced, observable differences are witnessed between the formulations. Lastly both 90:10 formulations and 70:30 Starch:BMPB have the most similar viscosity to the Control. Thereby indicating higher than 30 % starch commodity replacement will provide a composite system with a significantly lower viscosity and therefore structurally will be a weaker/softer system. This indicates that it may potentially affect the texture resulting in hardness of the final product. Peressini *et al*.(2015) found that fibre enrichment (2-7 % inulin) lowered dough consistency due to a reduction in water absorption (Peressini *et al.*, 2015). This may mean starch molecules are more adapted to absorbing water than that of a mainly cellulosic system/fibrous system, and the competition for water equates to a lower viscosity, upon fibre addition. Gomez *et al. (2003)* found that pea dietary fibre had pronounced effects on dough rheological behaviour yielding higher water absorption and smaller

extensibility than formulations without added fibre (Gómez *et al.*, 2003). Fibrillated dispersions have been ascribed rheologically to be pseudoplastic and shear thinning (Herrick *et al.*, 1983; Pääkkö *et al.*, 2007). With Herrick *et al.* (1983) stating that, regardless of the concentration (1.25 to 5.9 %), the MFC dispersions displayed a gel-like behaviour (Herrick *et al.*, 1983). This may be a reason for the increase in viscosity witnessed by Starch:BMPB FIB PB formulations over BMPB alone at even low concentrations of FIB PB. Zimmerman *et al.* (2010) found that MFC acts independently as the MFC is diluted and depending on the source, the viscosity of a 0.5-2 % dispersion can vary between 100 and 390 ml/g (Zimmermann, Bordeanu and Strub, 2010).

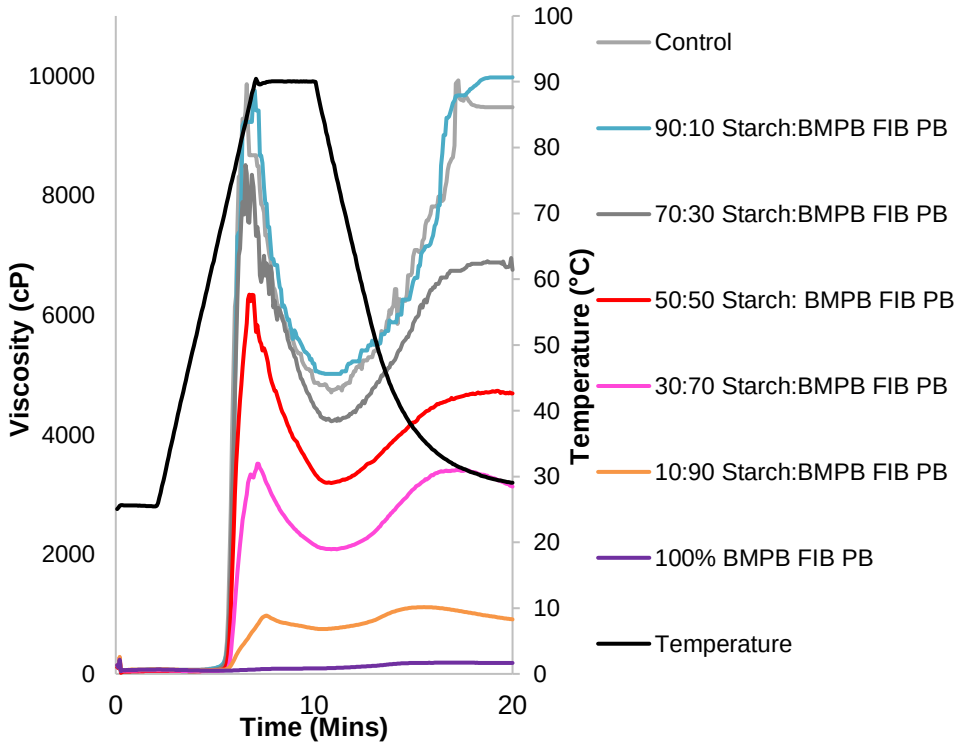


Figure 71 RVA profile of dough formulations of all Starch:BMPB FIB PB ratio's testing for the viscosity of the samples between differing ratios with the addition of heating and cooling. Solid contents vary due to the amount of fibrillated mass added per ratio (15-18 %) respectively for the control to 100 % BMPB FIB PB.

Heated and cooled RVA dough formulations were then tested by amplitude sweeps for BMPB and BMPB FIB PB in Figures 72 and 73, respectively, in order to see the LVE region of each formulation and how they differ from the Control, thereby attaining knowledge of dough deformation.

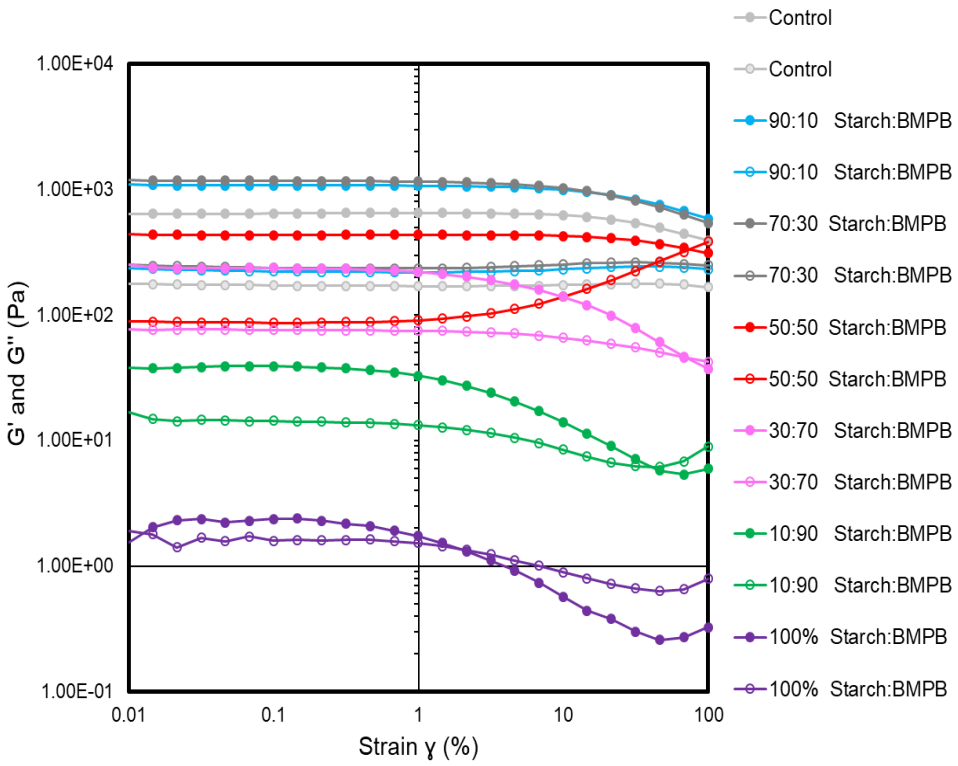


Figure 72 Amplitude sweep of all dough formulations from the RVA for Starch:BMPB ratios. G' indicated by a filled marker whereas G'' is indicated by an empty marker for viscosity with units provided as pascal.

As all samples have a G' > G'' it suggests that they behave as visco-elastic materials and follow Hooke's law rather than Newton's, as the elastic behaviour dominates the viscous one. When considering the LVE region, the Control sample shows the greatest resistance to deformation. At the other extreme the 100 % BMPB sample shows the lowest G' values and deforms before 1 % strain. Only 10:90 Starch:BMPB and 100 % samples shows such low strain to deformation, with a G':G" cross over at 50 % strain. This sample shows an increase in G values but considerably lower than

those of the Control. However, down to 30:70 Starch:BMPB the G' values and longer LVE region are found, as compared to the starch Control. In fact 90:10 and 70:30 samples see an enhancement in measured elastic moduli. This begins to be concurrent with the findings of the dynamic measurement within the RVA itself. Now comparing BMPB with BMPB FIB PB samples, again it can be seen that the 100 % BMPB FIB PB has > 2 magnitude increase in G', indicating that fibrillation is a very good way of increasing the network structure, even in this complex matrix. This is seen for all BMPB FIB PB mixing ratios, and only at >30:70 mixing ratio do the G' values fall below those of the Control.

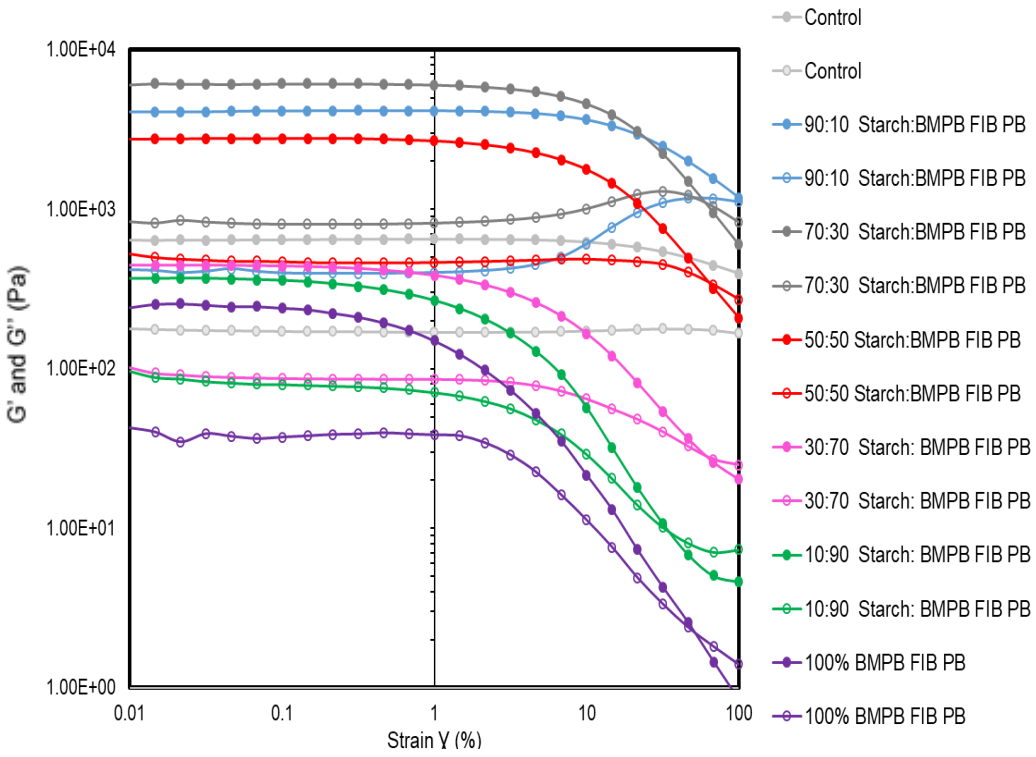


Figure 73 Amplitude sweep of all dough formulations cooked from the RVA for Starch:BMPB FIB PB ratio's. G' indicated by a filled marker whereas G'' is indicated by an empty marker for viscosity with units provided in pascal and samples are an average of three.

Frequency sweeps were carried out, which also allows the measurement of the tanδ and complex viscosity (η*) of each formulation as a function of

frequency. Tan δ provides evidence of how structured a material is and the slope of complex viscosity with frequency as to how gel like it is, with a slope of -1 being expected for a solid gel, whose G' and G'' and frequency independent. Figure 74 and 75 depict the frequency sweeps performed on Starch:BMPB and Starch:BMPB FIB PB, respectively. The Control shows some frequency dependence indicating that the dough produced under shear in the RVA is not completely gel-like, as might be expected, but the frequency dependency for >30 % starch replacement mirror that of the Control (Figure 74 BMPB). Figure 75, for the BMPB FIB PB show slightly less frequency dependence for mixing ratios down to 50:50, which is also mirrored in the lower tanδ values for these mixtures (Figures 76 and 77). Therefore showing that BMPB FIB PB increases or mirrors the Control and thus gives greater replacement of starch than BMPB alone. This is due to the η* values found in Figure 76 and 77 being significantly higher than that of the Control for both formulations above 30 % replacement, and for 50 % replacement for BMPB FIB PB formulations. These results indicate that the fibrillated mass plays a key role as a viscosifier in these complex formulations, due to high proportions of starch enabled to be replaced, which corresponds to findings from the RVA and further provides evidence of synergistic mechanisms increasing the overall viscosity of a system. Pääkkö *et al.* (2007) believed that fibrillated masses increased the storage modulus (G') and therefore elastic properties of samples due to the entanglement of long fibrillated fibres forming a network structure. An alternative hypothesis from this study, is that of synergistic behaviours when mixed with starch may be evident, as recently proposed by Calderon-Diaz *et al*. (2018). Here we have a mixture of PB, where interaction between BMPB and BMPB FIB PB may occur, on top of the two mixed phase behaviours and/or interaction with starch. Therefore the formation of structure of the three main raw materials

(Starch, BMPB and FIB PB) together produce a composite that structurally increases the elastic moduli and the viscosity of a product than just starch alone. However, Peressini *et al*. (2015) found that the incorporation of inulin (up to 7 %) decreased G' of doughs with increasing fibre content (Peressini *et al.*, 2015). Similarly, this is observed for BMPB and BMPB FIB PB formulations after 30 and 70 % starch is replaced respectively. Peressini *et al*. (2015) explains that this is thought to be due to incompatibilities with inulin and starch. Therefore in this study the fundamental mechanical adaptation of the raw PB may have functionally changed the material to better suit a starch matrix, enabling greater viscosity in higher contents of fibre than that of Peressini *et al.* (2015). As stated η* describes the resistance to flow, Starch:BMPB formulations show a comprehensive trend that the more starch replaced by BMPB the less resistance the formulation has and more likely that it is to flow. This coincides with findings from the RVA and the trend observed by Peressini *et al.* (2015) (the material is structurally weaker when a higher proportion of starch is removed). However, η* values of Starch:BMPB formulations indicated that the higher proportion of starch replaced, the weaker the structure becomes and more likely to flow (once more than 30 % is replaced). Though, with the addition of fibrillated mass, formulations are much more resistant than the Control to deformation until 100 % of all starch commodities are replaced. Beyond a 30:70 ratio no trend is witnessed. Interpretation of these data, why a large but brief increase is observed, will require further questioning and investigation.

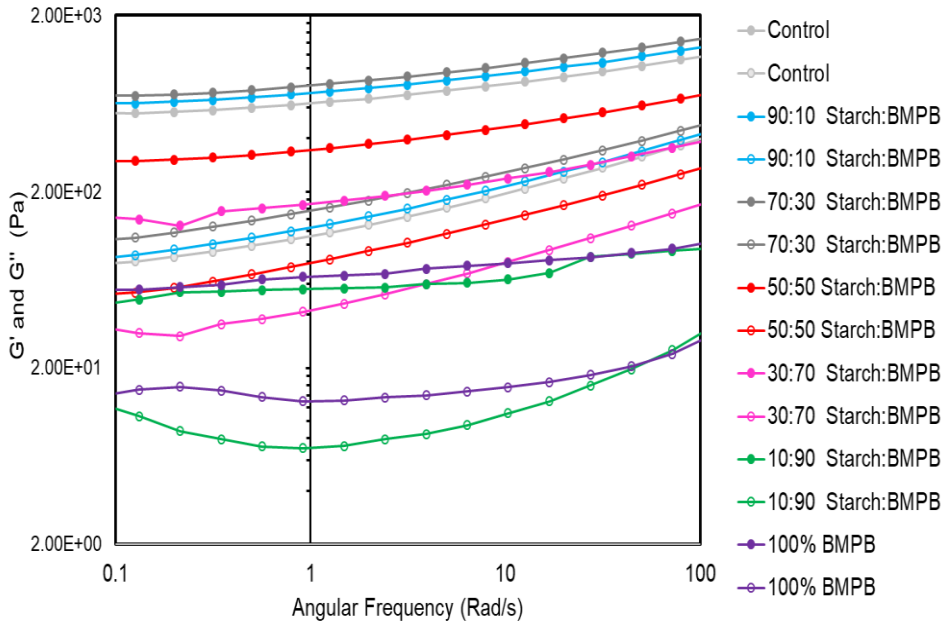


Figure 74 Frequency sweep of all dough formulations cooked from the RVA for Starch: BMPB ratio's. G' indicated by a filled marker whereas G'' is indicated by an empty marker for viscosity, which unit is provided in pascal.

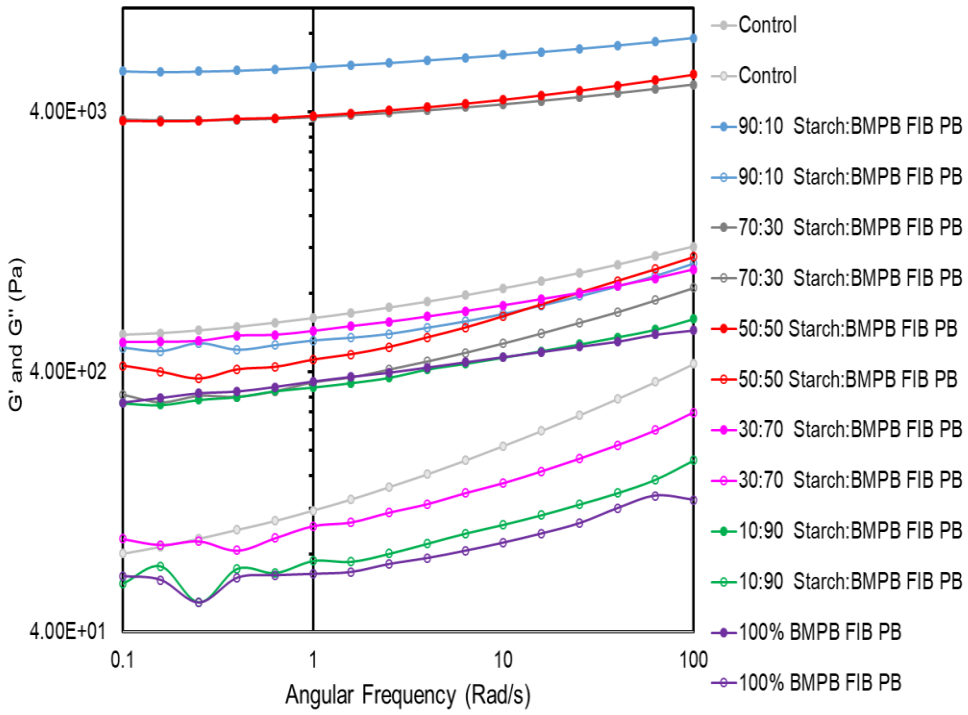


Figure 75 Frequency sweep of all dough formulations cooked from the RVA for Starch: BMPB FIB PB ratio's. G' indicated by a filled marker whereas G'' is indicated by an empty marker for viscosity with unit provided in pascals.

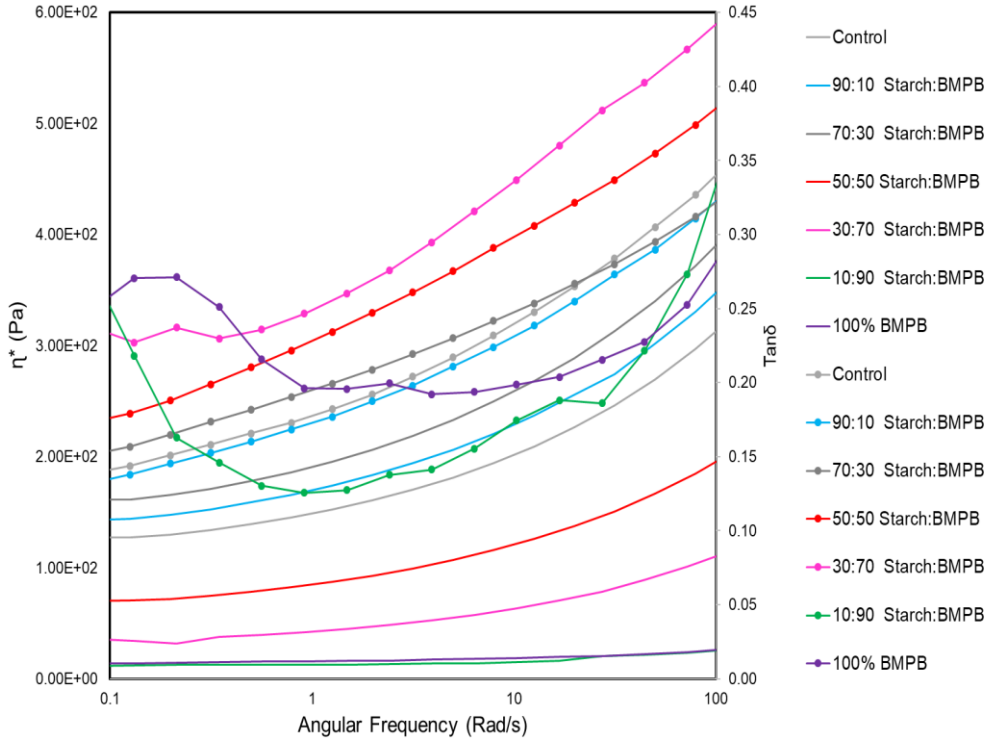


Figure 76 Complex viscosity (lines no markers) provided in unit of pascals and tanδ (markers and lines) for Starch:BMPB ratios taken at a frequency of 10 Rad/s.

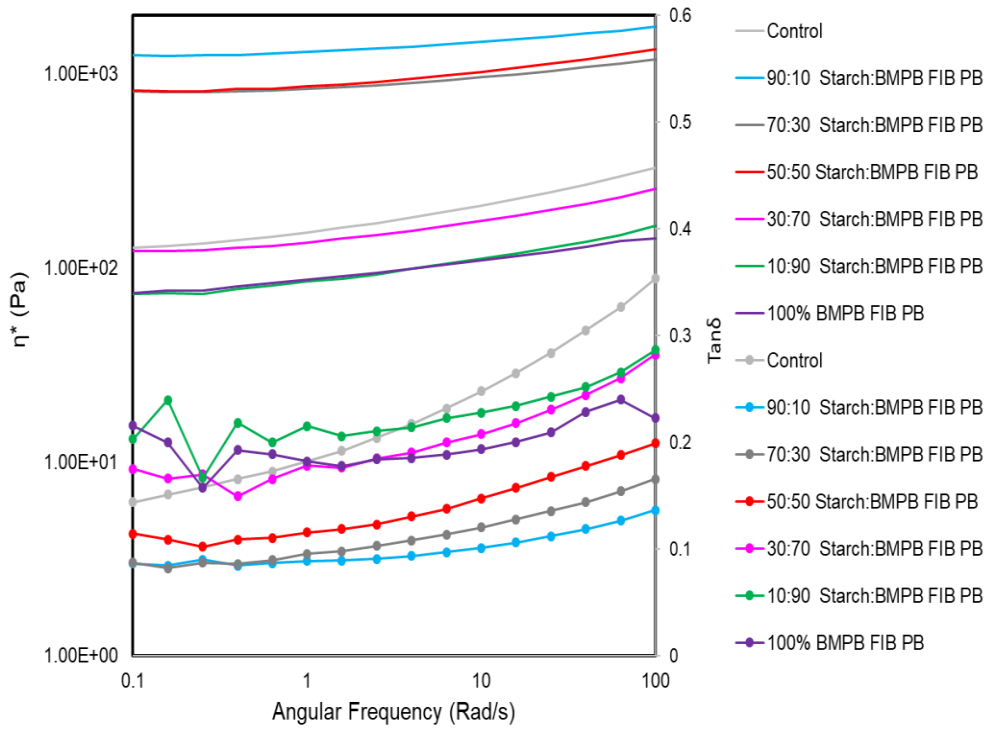


Figure 77 Complex viscosity (lines no markers) provided in unit as pascals and tanδ (markers and lines) for Starch:BMPB FIB PB ratios taken at a frequency of 10 Rad/s.

For the Tanδ values (Figures 76 and 77) all formulations exhibit a G' > G'' and therefore have a tanδ of > 1 and thus are in a gel-like state. The lower the value the more gel-like the mixture is. Therefore, Starch:BMPB FIB PB are less gel-like than Starch:BMPB, at comparative mixing ratios. In terms of product manufacturing these differences in elastic moduli, η* and frequency dependence may provide options in industrial process for stable and functional microstructures to be produced. Additionally, this appears to be possible for up to 50 % of starch replacement, providing properties similar to the 100 % starch Control.

6.3.2 Intermediate and expanded snack product properties

In assessing the appearance of both pellets and expanded product dough formulations (Figure 78) it is apparent that the BMPB adds a brown colour to the products. The higher degree of BMPB in the formulations leads to the highest colouration to a nearly distinctive black colouration in the 100 % BMPB formulation. Furthermore, observations show an increase in BMPB decreases the translucent appearance of pellets. This translucent appearance is used as an indicator of cooked areas showing some gelatinisation has occurred. An apparent translucency results in a commercially friable pellet (in the case of this Control). Surface browning can be a result of acrylamide formation, which from a commercial perspective is advised against (FDA, 2008). It is not known or tested in these works whether the higher proportion of BMPB in the formulation is a result of acrylamide formation. Though as 90:10 Starch:BMPB has a glassy and translucent appearance it would seem more probable that the BMPB and BMPB FIBPB additions are causing the colouration of browning, rather than that of acrylamide formation. Furthermore, previous studies have shown that

an addition of differing types of inulin report higher browning of crusts in bread making (Peressini and Sensidoni, 2009; Morris and Morris, 2012). This phenomenon of dark colouration has been ascribed to a higher content of reducing sugars involved in the Maillard reaction (de Gennaro *et al.*, 2000). Therefore, the increased dark colouration is caused via the addition of higher concentrations of BMPB and BMPB FIB PB, affecting and increasing the effects of the Maillard reaction supporting the previous hypothesis of browning through additions of cellulosic materials aforementioned.

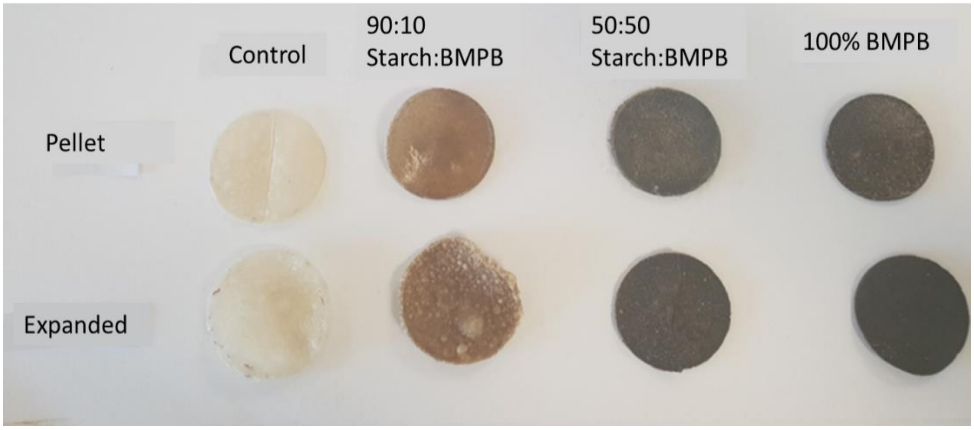


Figure 78 Examples of four dough formulations as pellets (top row) and expanded product (bottom row) versions. Showing differences of colours with larger proportions of BMPB and air pockets once the pellets have been fried.

When comparing Starch:BMPB formulations to Starch:BMPB FIB PB there is no real difference in colour (example shown in Figure 79). There was slight variability in the size of the expanded products but in order to see if these were significant Expansion Ratio (ER) assessments were performed.

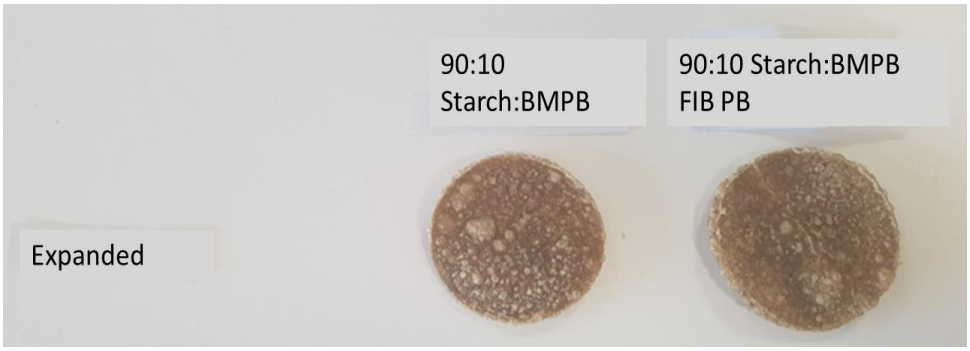


Figure 79 Example of a comparison using 90:10 ratio formulation between Starch:BMPB and Starch:BMPB FIB PB. Colour extremely similar but size and air pockets slightly differ.

Expansion is important for cereal-based extruded snacks in terms of functional properties in the final product (Ozer *et al.*, 2004). Therefore, each formulation of BMPB and BMPB FIB PB had ER assessments performed, data shown in Figure 80 and 81, respectively. Data revealed that only 70:30 Starch:BMPB has a greater ER than that of the Control. All other formulations were lower, however up to 30 % starch replacement was not significantly different than the Control in terms of expansion. An observable trend is witnessed whereby a higher degree of starch replacement leads to less expansion of a product, except for the anomaly of 70:30 Starch:BMPB. This anomaly may be a result of mechanisms improving expansion of the coinciding materials, albeit a similar result would be expected for 70:30 Starch:BMPB FIB PB, which is not observed. However, 70:30 Starch:BMPB FIB PB was not significantly different than that of the Control. Therefore, the reason for this anomaly is unknown and unpredicted. Differences in expansion may be associated with the amount and distribution of water within a system prior to expansion. Therefore, water may not be evenly distributed throughout the formulations due to the addition of BMPB as possibly the crystallisation of said material from an amorphous state,

pushing water out of crystalline fractions, or up taking more water than that of starch commodities. Moreover, competition for water between starch, BMPB and BMPB FIB PB may occur affecting starch expansion. Though it should be noted that these formulations are processed at higher water contents than they would be if manufactured. Studies have found that the addition of sugar beet, hazelnut and apple fibre reduced bread volume (Chen, Rubenthaler and Schanus, 1988; Anil, 2007; Filipovic, Djuric and Gyura, 2007). Peressini *et al.* (2015) found that an incorporation of inulin 2-5 % (high DP) in a dough formulation for extruded snacks had no significant effect on the expansion of the final product. Interestingly inulin with a low DP increased the expansion of the final product, from 2-7 %. As these results are based on higher concentrations of supplemented starch it is hard compare to findings, though it would seem that the formulations in this study are acting like high DP Inulin and decrease with higher concentration. Moreover, others have found with lower (0.4 %) and much higher (28 %) incorporations of fibre in snacks leads to thinning of bubble walls, decrease in bubble diameter, decrease in expansion and increase in hardness (Karkle, Alavi and Dogan, 2012; van der Sman *et al.*, 2018). These findings hypothesised that the fibre acts as a soft filler lacking homogeneity, which breaks cell walls and also allowing steam to escape (preventing bubble growth and expansion) (Karkle, Alavi and Dogan, 2012; van der Sman *et al.*, 2018). Therefore the effect of fibre on the expansion properties would not only depend on the content of the fibre but also the molecular weight and structure of the hydrocolloids (Peressini *et al.*, 2015). Furthermore, as these results are based upon heat-pressing rather than extrusion, different findings may be due to differing methods of processing. Lastly, processing methods play a huge role in expansion such as speed of the screw (Ozer *et al.*, 2004) and fibrillated masses (as explained in chapter 5) collapse under heat and

subsequent drying. Therefore, the addition of fibrillated masses may have reduced expansion mechanisms of other materials upon frying.

Lastly when comparing this data with rheological findings it may be evident that higher viscosities have equated to slightly less expansion than the Control, albeit not significantly different. This may be due to the formulations being more gel-like. Of interest would be to investigate lower additions of BMPB and BMPB FIBPB with greater starch replacements. This may provide viscosities closer to that of the Control especially for BMPB FIB PB formulations. Whereby up to 50 % of total starch replacements equates to a similar expansion that mirrors the Control, but is not exactly the same. However, this provides evidence that the incorporation of BMPB and FIB PB into the composite matrix can be greater than or equivalent to starch commodities alone. Moreover, the incorporation of BMPB and FIB PB, leads to a greater blend complexity and shows less deviation between replicates than that of the Control, apart from the exception of 70:30 BMPB FIB PB. Thus providing some evidence that the incorporation of these cellulosic materials provides greater stability and quality control upon processing. Thereby being advantageous when considering manufacturing.

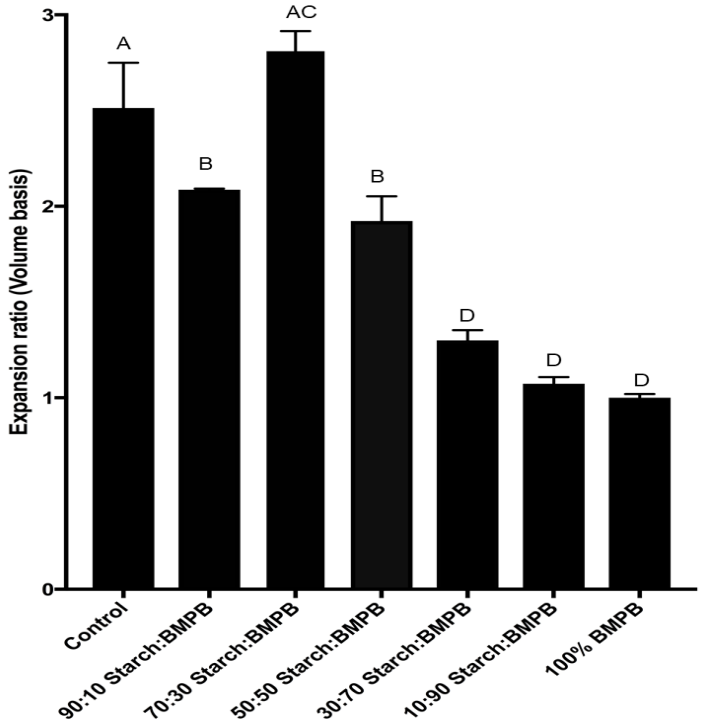


Figure 80 Expansion Ratio on a volume basis of all Starch:BMPB dough formulation ratios from a pellet into an expanded product. Points with the same letter are not significantly different at p<0.05. Error bars are provided by standard error.

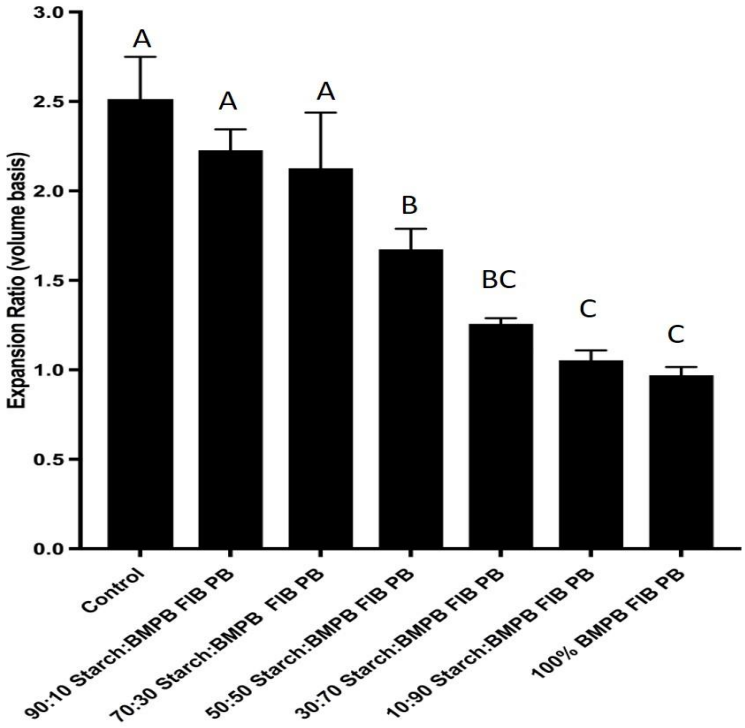


Figure 81 Expansion Ratio on a volume basis of all Starch:BMPB FIB PB dough formulation ratios from a pellet into an expanded product. Points with the same letter are not significantly different at p<0.05. Error bars are provided by standard error.

Micro-computed tomography (Micro-CT) was then used to visually assess the microstructure of the expanded product formulations (Figure 82). Micro-CT assessments show that in general after 50 % replacement with BMPB and/or BMPB FIB PB the pore size and porosity decreased. This was confirmed by void analysis software (Figure 83 and Table 19). Visually the sample with the most similar appearance to the Control was that of 90:10 Starch:BMPB and both 70:30 formulations. An observable difference is that as more starch is replaced fewer pores/voids appear on the surface of the expanded products. This may be due to fewer nucleation sites, which create expansion of snacks, or the mobility of the matrix to retain the air cells as they develop. This would therefore coincide with findings from ER assessments where 30 % starch replacements provided similar expansion. Gimeno, Moraru and Kokini. (2004) found that when 1 % carboxymethyl cellulose or xanthan gum were added to pellets, they produced an increase in expansion. They hypothesised that the viscous hydrocolloids interpenetrated the starch matrix and created a fine network of “holes” across the matrix, which served as additional nucleation sites for expansion (Gimeno, Moraru and Kokini, 2004). These polymers were used at far lower concentrations than that of the BMPB used in formulations here, but interpretations may not be too dissimilar to the compatible nature of the BMPB:PS microstructures shown in Figure 69. This would also coincide with aforementioned findings of using lower amounts of BMPB and BMPB FIB PB to the amount of starch replaced in the current formulations, in order to reduce the viscosity of the dough. Furthermore, Linder and Kleinebudde. (1994) substituted microcrystalline cellulose with cellulose powder and found the resulting pellets had greater porosity and therefore nucleation sites (Lindner and Kleinebudde., 1994). Showing that not only the amount but the properties of the replacement are extremely important in determining

expansion and porosity during heating. This would suggest that PB is acting as a filler and not a nucleation site, or voids may be of a smaller size. Nor *et al*. (2013) created expanded ready to eat snacks containing 5-20 % pumpkin flour and found that increases in the level of the pumpkin flour added resulted in a smaller pore area and size. Whereas findings found here show that up to 30 % starch replacement equate to larger percentages of voids within the matrix for both formulations. Moreover void sizes are not significantly different from the Control for up to 30 % starch replacement for BMPB FIB PB formulations. Though interestingly up to 30 % replacement for BMPB formulations produces significantly greater voids than that of Control. This may hypothesed that the addition of fibrillated mass provides stronger network formation and properties which relate to a void size and thus comparable to starch properties within a complex composite. Whereas BMPB alone produces a weaker network creating voids which may have expanded to a degree that they then collide with one another collapsing into an overall greater void size. This stronger network from the BMPB FIB PB is evident across results and findings from a rheological and expansion aspect. It may be deduced that the entanglement of fibrillated fibres aforementioned may play a key role in greater quantities of starch commodity replacement, with a reduced overall solid mass of a composite product. Lastly, however, water is not thoroughly mixed using the same mechanisms of the manufacturers. As a result, pockets of water which drive voids (through rapid evaporation of a large amount of water in one section of the pellet) may have incurred and additionally resulted in large voids.

Table 19 Void analysis values using Micro-CT software. Voids as a total percentage of the total volume (Void %), average void size (Voids mm^3) of each dough formulation ratio observed.

Sample	Void (%)	Voids (mm^3)
Control	33.75	5.36
90:10 Starch:BMPB	40.02	19.98
90:10 Starch:BMPB FIB PB	38.26	5.21
70:30 Starch:BMPB	37.96	17.53
70:30 Starch:BMPB FIB PB	34.38	6.25
30:70 Starch:BMPB	17.40	2.17
30:70 Starch:BMPB FIB PB	12.94	2.99

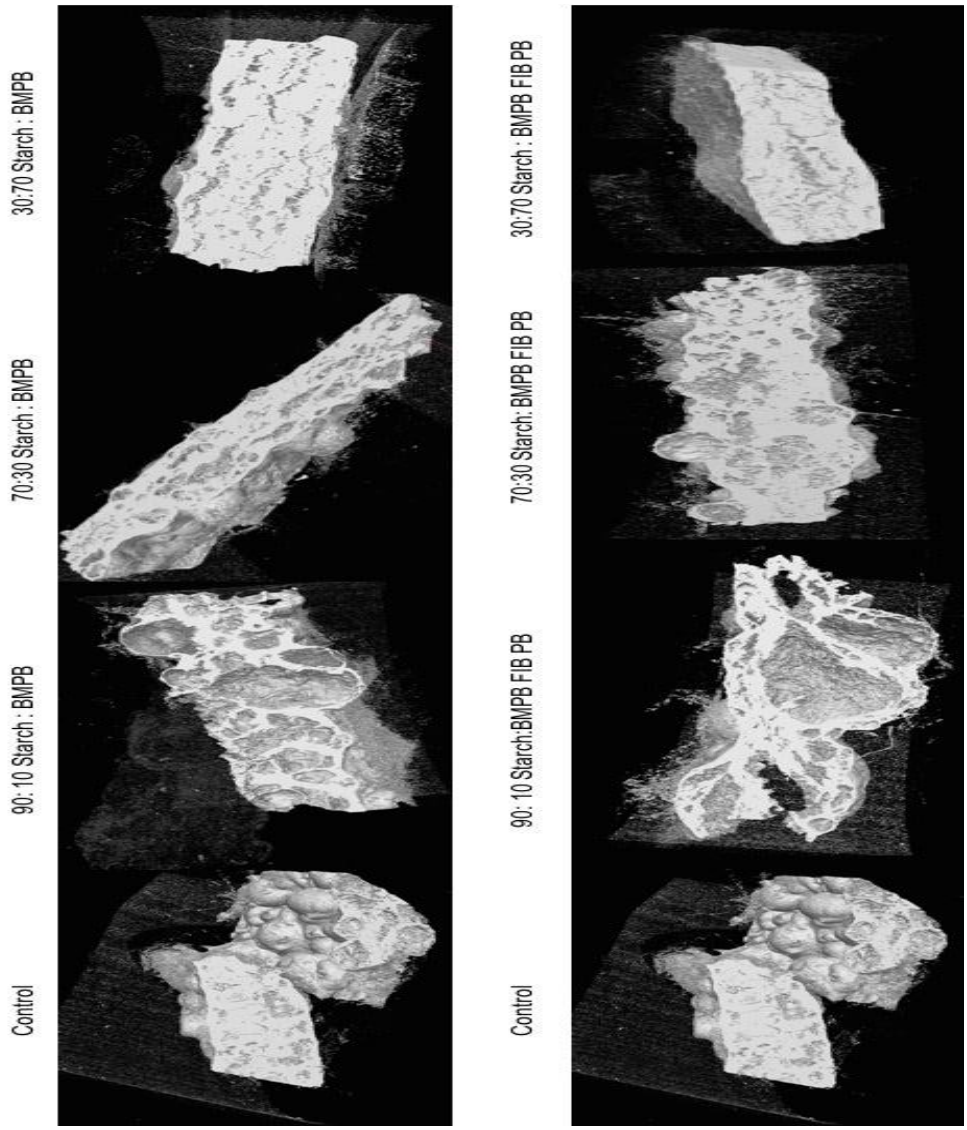


Figure 82 Micro-CT cut through scenes of selected dough formulation ratio's. Control with Starch:BMPB on the first row and Starch:BMPB FIB PB on the second row. Highest Starch proportions to lowest go from left to right. > 50 % starch replacements show still puffed and expanded whereas greater replacements than this provides little to no puffing and expansion.

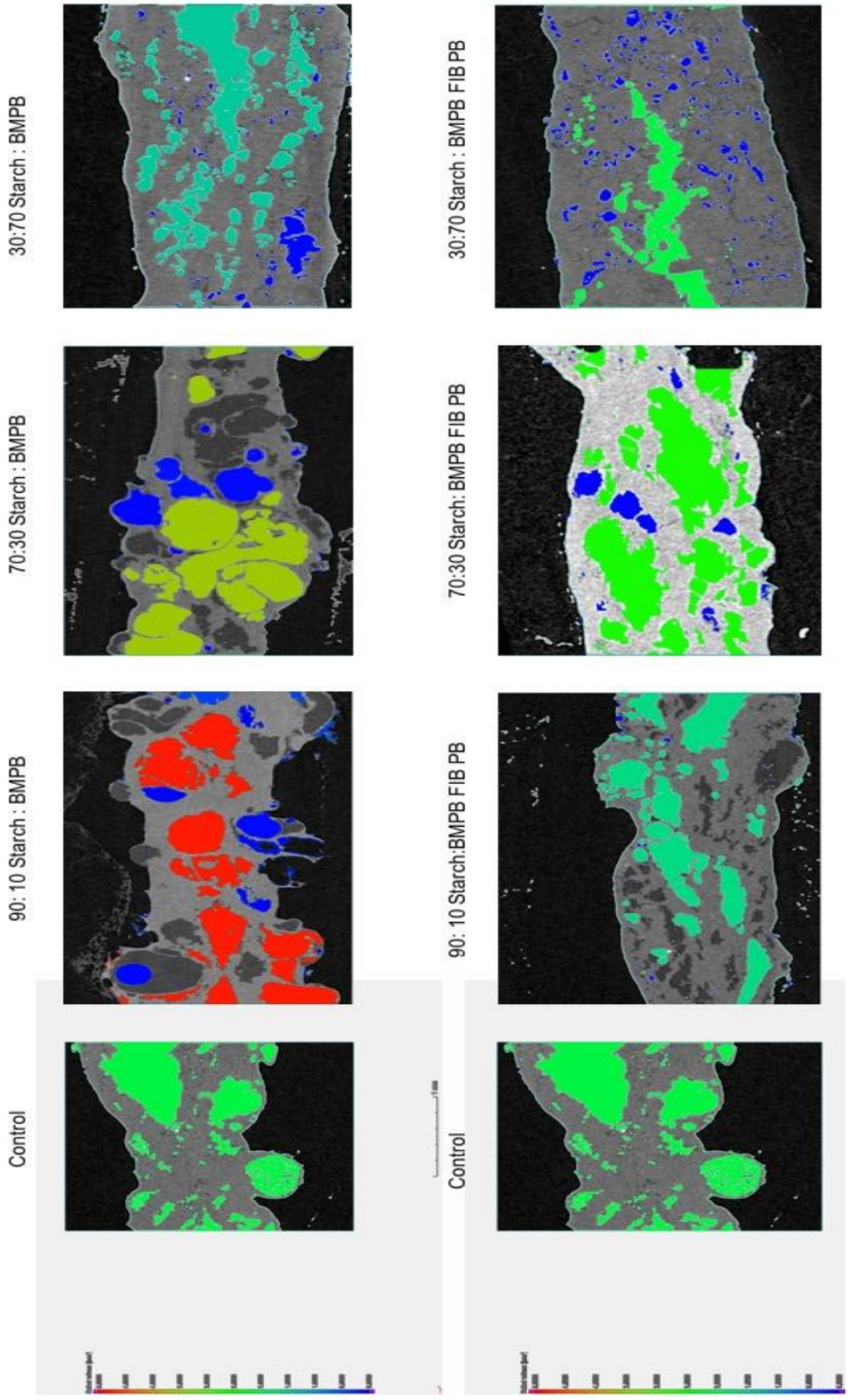


Figure 83 Micro-CT void analysis (voids filled, photos taken at a random cut through of scenes) of selected dough formulation ratio's. Control with Starch:BMPB on the first row and Starch:BMPB FIB PB on the second row. Highest Starch proportions to lowest go from left to right. > 50 % starch replacements show still puffed and expanded whereas greater replacement than this provides little to no puffing and expansion.

Food texture can be measured, whereby solids have an elastic limit and in applying stresses in excess of this limit equates to a rupture or break of the system (Rosenthal, 2015). Therefore, elasticity relating to the degree of deformation can be examined through instrumental analysis such as empirical tests in texture analysis, used in these works. These empirical tests apply forces, which overcome the materials elastic limit, and result in permanent changes to the structure. In assessing the samples of pellets and expanded products, Figures 84 to 87, respectively, for each formulation group, it seems apparent that the expanded products have shoulders with multiple peaks in comparison to the pellets for both formulations. This indicates differing brittleness of expanded products versus the pellets, which may be expected due to the cooking process, leading to expansion and therefore air cells, which could lead to multiple layer fracture. Moreover, it indicates differing breaking forces are required throughout the compression of the samples layers. These differing forces are due to matrix properties plausibly being heterogeneous, as well as particulate size being polydispersed. In comparing between formulations it would seem evident that the pellets containing both BMPB and FIB PB are less brittle than that of BMPB formulations requiring less force to deform and rupture the system. Though when assessing expanded products this trend seems to be reversed in that BMPB with FIB PB are more brittle than BMPB alone formulations, requiring greater force for deformation. A reason for this may be deduced by their higher viscosities and therefore a stronger gel network is expected to form upon heating into a solid. These findings would coincide with rheological measurements depicting a higher η* for BMPB FIB PB formulations. Thus showing that the addition of fibrillated mass creates stronger network formation and strength, now witnessed at both high water (in rheology) and low water contents in the current analysis. Furthermore, a

trend is observable where low amounts of starch commodities are replaced by BMPB or BMPB FIB PB, which equates to the expanded formulations being more elastic rather than solid-like. The TA profiles show an increase in strain to fracture (distance travelled) and therefore the materials are more flexible rather than brittle. Thereby requiring large forces to deform as the material (due to its elasticity) absorbs some of this energy through compression mechanisms and provides multiple fracture points. This is also shown as samples are more brittle for formulations which starch is almost or entirely replaced. It is evident that similar break force is required when as much as 90 % of starch commodities are replaced. This force required to break being similar across formulations may be due to efficient particle packing and orientation due to the mixture of particulate size and shape. Although there seems to be evidence suggesting less fractures occur with these formulations and therefore the resulting expanded product is expected to be less brittle than that of the Control. Furthermore, from the higher water content rheological measurements for 70:30 Starch:BMPB and > 50 % Starch:BMPB FIB PB it might be expected that they are harder/more brittle than the Control, which is confirmed in Figure 85 and 87. Gimeno, Moraru and Kokini. (2004) found that the addition of 1 % carboxylmethyl cellulose and xanthan gum improved the textural uniformity of expanded samples (Gimeno, Moraru and Kokini, 2004). This was thought to be attributed by the gum's contribution in terms of rheology and water sorption capacity (Gimeno, Moraru and Kokini, 2004). This may explain fewer fractures as the samples are deformed because of more uniformity across the samples. Moreover, as aforementioned fibre incorporation in low and high concentrations has been known to increase the hardness of snacks, due to fibre acting as a supposedly soft filling agent which reduces expansion (van der Sman *et al.*, 2018). Uniformity is observed through Micro-CT, and the lack of nucleation

sites in formulations compared to the Control (especially those that are large), may be an indication that the structure would be harder initially. However, as the pores decrease in size the structure additionally becomes less brittle as indicated by formulations containing more than 70 % starch removal. Nor *et al.* (2013) found that when pumpkin flour concentrations were increased in pellet formulations at high screw speeds, this increased the hard texture of the expanded product (N*or et al.*, 2013). This coincides with these findings with up to 30 % starch removal for BMPB and 90 % for BMPB FIB PB, respectively. This may indicate that BMPB on its own shortens the deformation to break and thus the addition of fibrillated mass thereby counteracts this phenomena, causing a harder more connected matrix. Thus indicating that the properties of the FIB PB significantly affect the texture of expanded products, ensuing harder structures that mirror starch based materials for their elasticity. Fibrillated materials have also shown their effectiveness of property reinforcement before (Lavoine *et al.*, 2012).

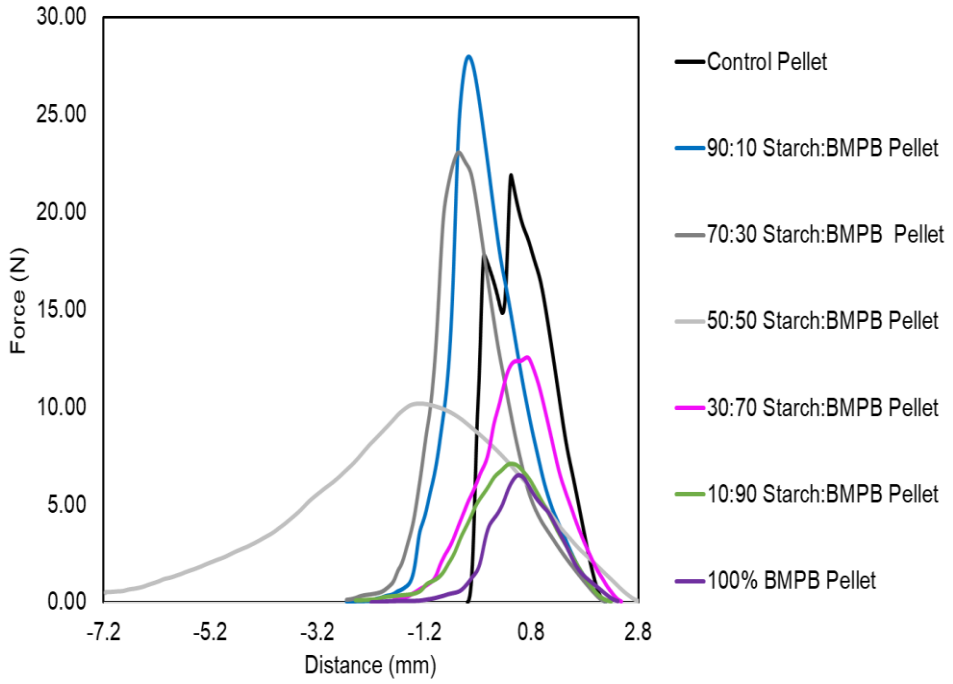


Figure 84 TA calculating the average stress break of multiple pellets for each Starch:BMPB dough formulation ratio.

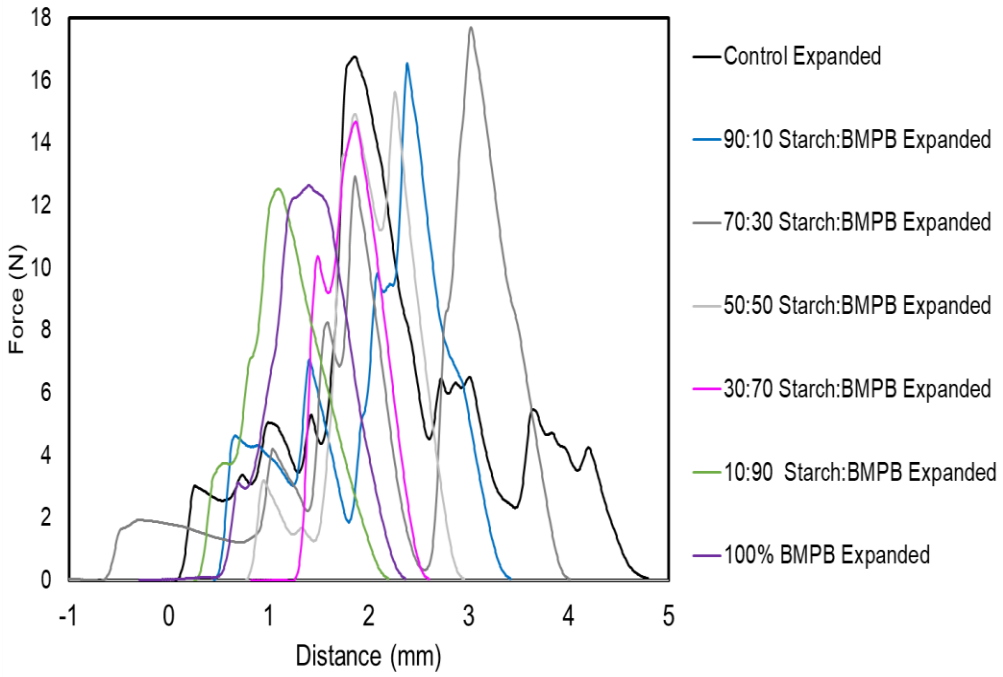


Figure 85 TA calculating the average stress break of expanded products for each Starch:BMPB dough formulation ratio.

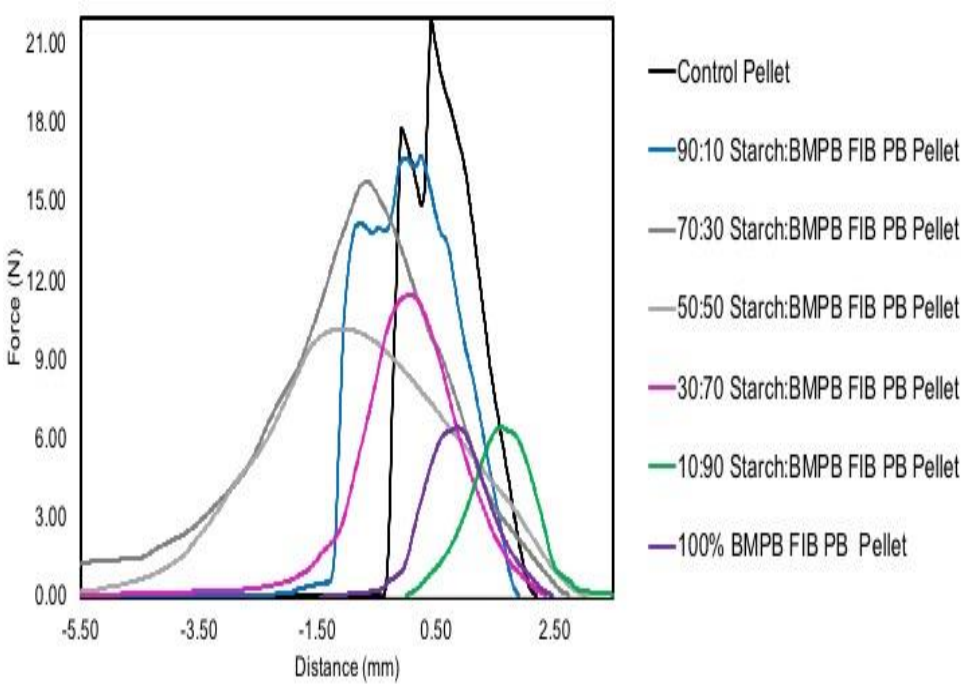


Figure 86 TA calculating the average stress break of pellets for each Starch:BMPB FIB PB dough formulation ratio.

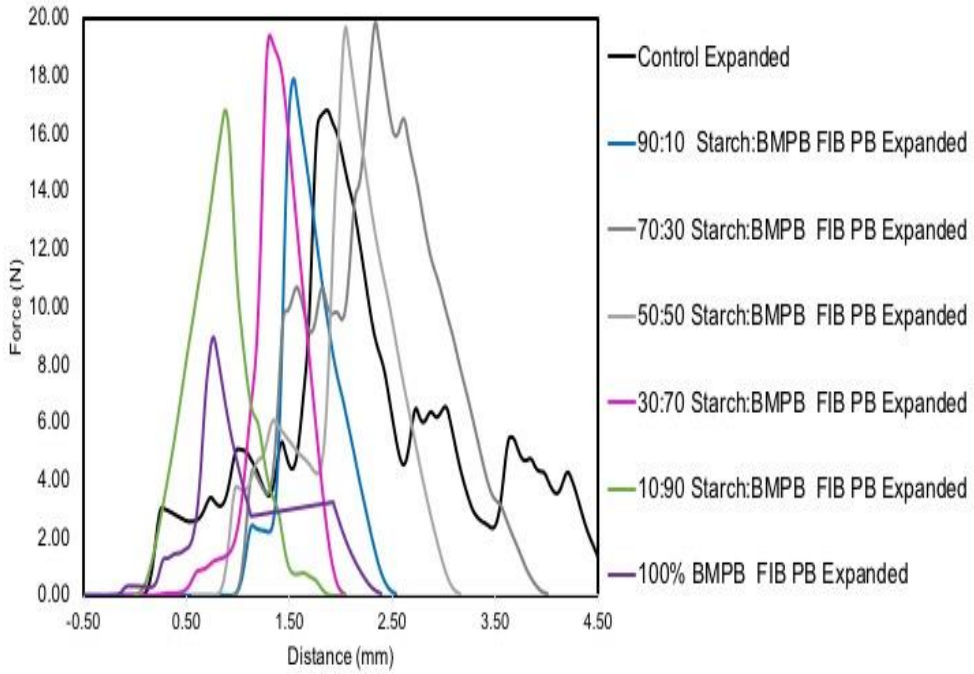


Figure 87 TA calculating the average stress break of expanded products for each Starch:BMPB FIB PB dough formulation ratio.

6.3.3 Rheological properties of Pellets and Expanded Snack Product

In order to assess the rheological characteristics of the pellet and subsequent expanded product (Figures 88-92 respectively), DMA was performed. This method utilises a powder pocket system as the samples cannot be measured directly due to irregular sample sizes, and therefore powders of the samples are generated and analysed (Royall *et al.*, 2005; Raschip *et al.*, 2008). Therefore, it must be noted that the absolute value of E' and E'' obtained using this technique has no true fundamental meaning (Paes, 2008). Thus, results are only indirect measurements of viscosity values rather than absolute/complex, due to the use of material pockets and therefore not having a geometry constant (Duncan, 2008). The use of the 'pocket' allows for an indirect measurement of the enclosed sample, referred to as a stiffness value (S' and S''), which is the unit-less measurement and requires 90 % of the material pocket subtracted from the total properties measured (Duncan, 2008). Therefore, negative values when calculating Tanδ values may occur due to this subtraction. These pockets have been used to determine the T_g of cellulosic materials previously and found to be more successful at doing so than DSC (Paes, 2008). Figure 88 demonstrates the Control at differing frequencies, showing no significant difference in S' between measurements at different frequencies (p value < 0.806), but there was a significant difference between frequencies when presenting Tanδ values. Moreover, melting points and water loss peaks do not seem to be frequency dependent as no significant difference in frequency is observed.

However, only 1 Hz is shown in these works for dough formulations comparisons.

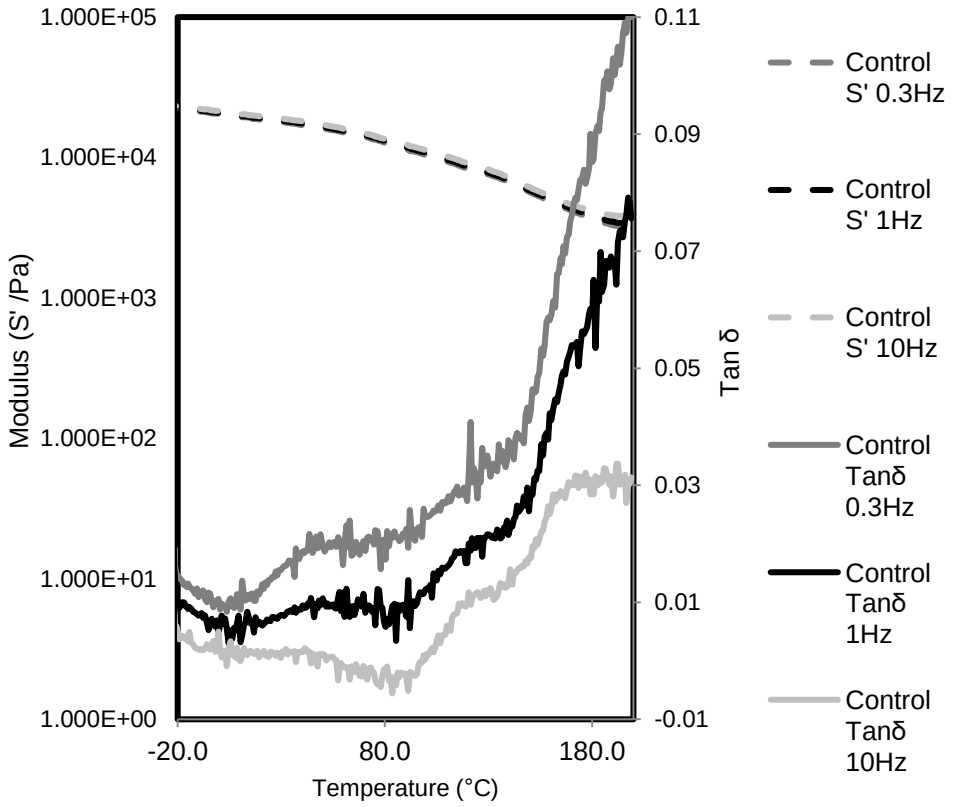


Figure 88 DMA figure demonstrating the control at differing frequency's (0.3, 1, 10 Hz) for Storage Stiffness modulus (S') and Tanδ.

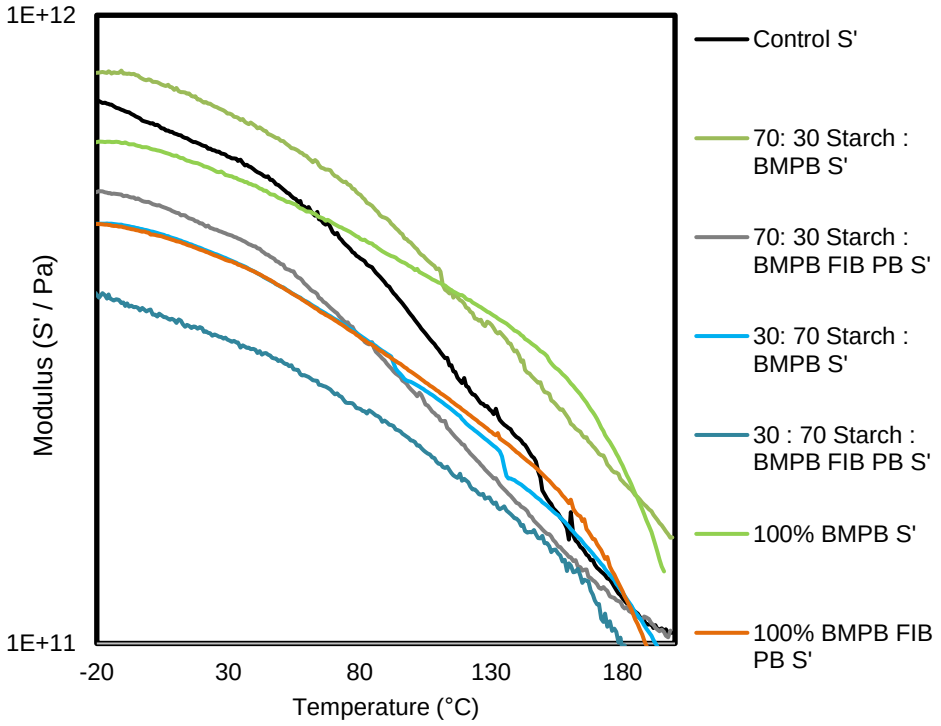


Figure 89 DMA S' of selected Starch:BMPB and Starch:BMPB FIB PB formulations performed at 1 Hz of pellets.

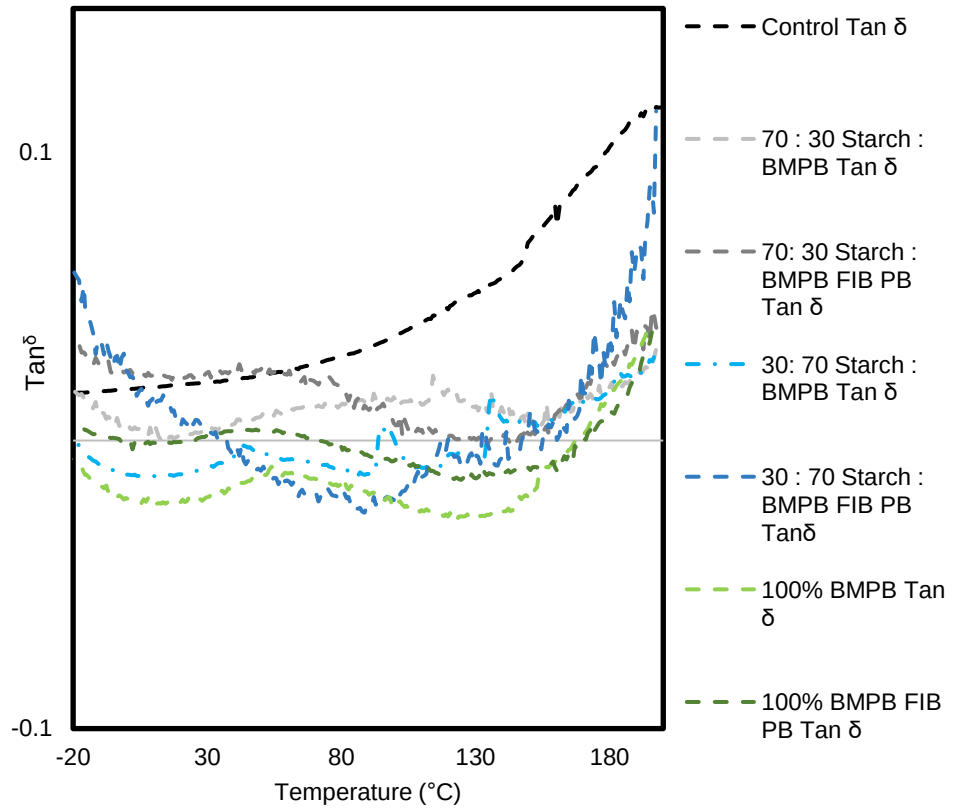


Figure 90 Tanδ of selected Starch:BMPB and Starch:BMPB FIB PB formulations performed at 1 Hz of pellets.

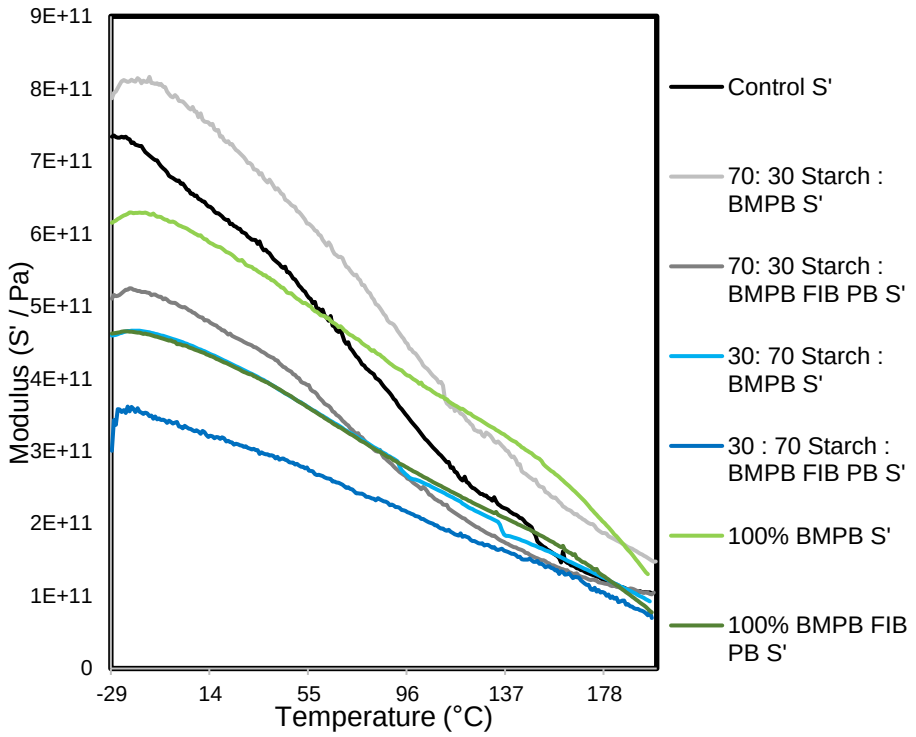


Figure 91 DMA S' of selected Starch:BMPB and Starch:BMPB FIB PB formulations performed at 1 Hz of expanded products.

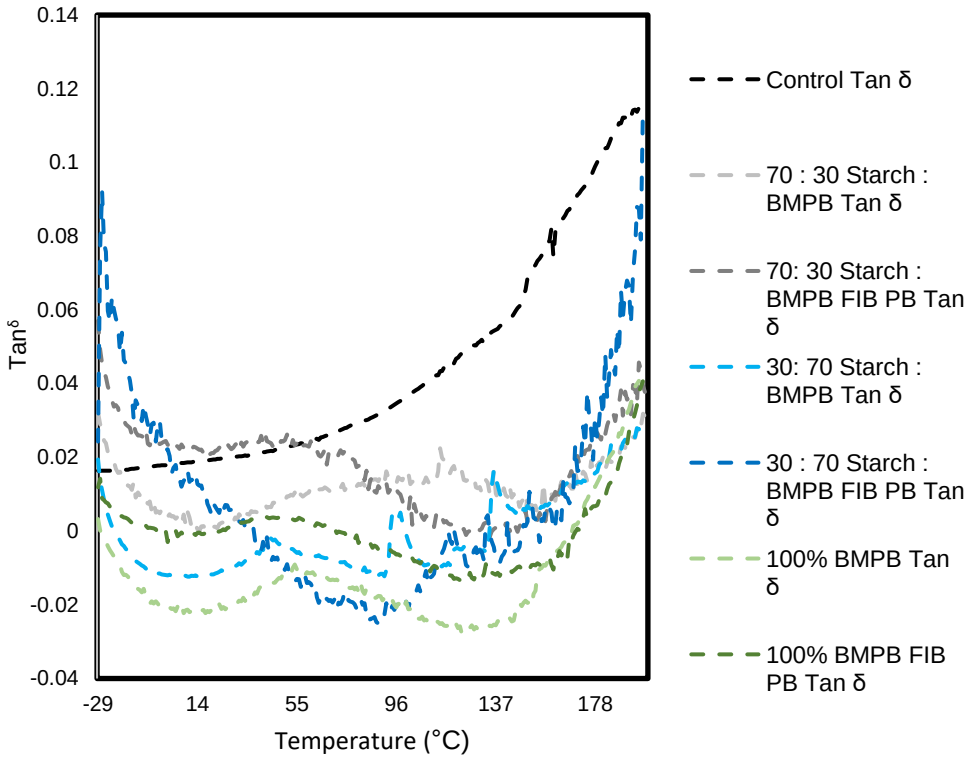


Figure 92 DMA Tanδ of selected Starch:BMPB and Starch:BMPB FIB PB formulations performed at 1 Hz of expanded products.

Figures 89-92 depict DMA spectra of S' and Tanδ for selected formulations, for pellets and expanded products, respectively. Research suggests that samples with a lower damping factor i.e. Tanδ, absorbs less energy, which is stored (Duncan, 2008), which would indicate retaining structure and shape. Moreover, it was found that pockets retained water in the treated samples. Otherwise a loss of water would occur, which would results in a reduction in the Tanδ values (becoming more solid-like) at higher temperatures, when the water in the sample has started to vaporise. Therefore, the Control has the most amount of energy stored in comparison to all formulations. The S' melting profiles of 70:30 Starch:BMPB for both pellets and expanded products (Figures 89 and 91) match that of the Control. This suggests that the melting profiles and therefore thermal properties (when in a solid-like state) behave similarly and would thus process similarly. Additionally, the

final Tanδ values (at > 195 °C) are not significantly different from > 30:70 formulations, in both pellet and expanded products, nor is the Tanδ significantly different at lower temperatures (at > 130 °C) for pellets specifically. This coincides with previous findings, showing that up to 50 % starch replacement provides similar viscosity properties to that of the Control and matches viscosity profiles. Moreover, relating to Micro-CT and ER results, a higher Tanδ upon heating should indicate more expansion, since the bulk material of the pellet should be more elastic for expansion. Whereas DMA findings show that, the formulations of pellets end Tanδ were not significantly different, indicating they would expand to the same degree as the Control. Though in ER results this was not the case, nor were void sizes (indicating expansion) in Micro C-T, whereby only > 30-50% starch replacements provided similar results to the Control. Possibly indicating that another means of expansion and production of the pellets for example from an extruder, may provide more similar rates of expansion to that of the Control, equating to greater replacements of starch commodities overall. However the Control Tanδ is observably more stable (less fluctuations indicating viscosity is less affected by the frequency) than that of other formulations, indicating that different phases of varying systems may be coinciding within the expanded product matrix. These varying systems would be that of gelatinised starch, rehydrated BMPB and reduced water system for the FIB PB, amongst other ingredients (salt, mixing agent, water, oil). DMA results would indicate slight phase separations even at extremely low water contents of the product (mainly at lower (25-130 °C temperatures than that of the Control), which are indicated by variability in DMA profiles, at a steady frequency. The steady Tanδ of the Control sample indicates a material where the ingredients are creating a synergistic matrix (Manard and Menard, 2002) between solids and low water. Therefore initial findings,

which suggested a synergistic relationship between Starch and modified PB at higher water contents (CLSM, Rheological and RVA assessments), may not occur at low water contents, within a semi-dried system. This would need further investigation as to why this may occur, though it is hypothesised that upon drying bond formations may be weaker or non-existent in comparison to a higher water system, whereby water is readily available. Moreover, fibrillated masses when dried may go through the process of hornification and fibrillated structures may collapse providing a weaker less expanded structure (Agarwal, MacNaughtan and Foster, 2018).

For all samples (Figure 89 and 91) the main initial decrease across samples seems to occur at 20 °C. This relaxation in S' and Tanδ values is small and upon increase in temperature there is a shift from low to higher viscosities, indicating the material is behaving more amorphous and therefore kinetically trapped prior to the assessment. This may be due to physical aging of the polymer referred to as glassy state relaxation, which may occur to polymers stored below their T_g, which in turn reveal an endothermic peak during calorimetry measurements (Chung and Lim, 2006; Enrione *et al.*, 2012). These can be mistaken as melting or T_g of materials (Liu *et al.*, 2009). However, between 20-150 °C a transitioning morphological process seems to be occurring, at which the mid-point may be a small T_g phenomenon or conventional water loss in the system. Before or after this point the material would be assumed to be more rubber-like and less glass-like. Additional small peaks in the Tanδ values are indicative of movement within the pockets themselves. The Control shows the greatest shift transition. Shifts are indicative of differing effects frequencies have on the thermal analysis and structure of the sample i.e. water loss, T_g and crystallinities of the samples and thus stability. For example, higher peaks with Tanδ is indicative

of the system being more amorphous and greater molecular movement. The lower the T_g usually indicates higher cross-linking due to lack of energy sufficient to move molecules. This would mean the Control after quenching and cooling may turn into a glassy state, which is amorphous and would be more kinetically trapped than PB addition formulations. This provides evidence of previous hypothesis suggesting after drying the addition of PB changes the system to be less kinetically trapped with differing phases occurring. However, efforts to confirm a T_g were not absolute. Either, differences in moduli between sample replicates are very minimal but still significant, a reason for this could be due to particle size of the sample, a smaller particulate size may have enabled greater differences witnessed or this may be due to method preparation procedures that do not ensure monodisperse particles after milling and sieving.

Indirect measurements of viscosities for each formulation, for both pellets and expanded products are calculated and shown in Table 20. The indirect viscosities show a similar trend observed by rheological measurements, for dough formulations, in that with additional starch replacement provides a decrease in viscosity. However, no formulation had a greater indirect viscosity, than that of the Control, which differs from the results for doughs from rheometry analysis, but coincides with findings from the RVA. All viscosities are significantly higher than viscosities calculated, as shown in Section 6.3.1, which is to be expected, as the materials are now more solid-like rather than elastic-like.

In general Starch:BMPB formulations (for both pellets and expanded products) have a higher indirect viscosity than Starch:BMPB FIB PB, except for 70:30 Starch:BMPB FIB PB pellet. The reasoning behind this may be since fibrillated masses increase the viscosity of the sample (Section 6.4.1).

As these are solid-like materials it is impossible to gain negative viscosity values. Therefore, the negative values for expanded products are assumed errors from subtraction of the properties of the material pockets. Bashaiwoldu, Podczeck and Newton (2004) applied DMA to pharmaceutical pellets and found that an incorporation of microcrystalline cellulose decreased the visco-elasticity from the original sample (Bashaiwoldu, Podczeck and Newton, 2004). Gimeno, Moraru and Kokini (2004b) assessed the addition of 1 % xanthan gum on the elasticity of corn pellets. They found the Young's modulus decreased from 1.2E+09 to 6.0E+08 with the addition of xanthan gum respectively in pellets (Gimeno, Moraru and Kokini, 2004). They suggested that these were due to greater water absorption abilities with the additions of gum, more so with caboxymethylcellulose than that of xanthan gum. Therefore, Gimeno, Moraru and Kokini (2004b) suggested other mechanisms may be at play, such as competition for water from the gums and corn starch.

Table 20 Indirect viscosity (η') calculated at 100 °C at 1 Hz from the stiffness modulus of both pellet and expanded products for each dough formulation. Complex viscosity could not be calculated due lack of information regarding the material constant value, as material pockets were used. Negative indirect viscosity values are due to subtraction of the material pocket.

Sample formulation	Pellet Indirect viscosity (η')	Expanded indirect viscosity (η')
Control	9.27E+09	3.31E+11
70:30 Starch:BMPB	2.653E+09	6.10E+09
70:30 Starch:BMPB FIB PB	4.61E+10	2.13E+09
30:70 Starch:BMPB	3.57E+10	8.56E+08
30:70 Starch:BMPB FIB PB	5.275E+09	-4.34E+09
100% BMPB	1.017E+09	-8.37E+09
100% BMPB FIB PB	8.58E+08	-1.72E+09

6.3.4 Calorific content

Cellulose has no calorific value in the body of humans, though both indigestible biomass and digestible starch have the same heat combustions (USDA, 1973). Therefore, it is apparent that the calorific content of BMPB and FIB PB cannot be determined by simple combustion analysis in a calorimeter. Nor would it be accurate to calculate the total product as it would state that the material is completely digestible. Indigestible biomass can be determined by digesting a sample in dilute acid then in dilute base (USDA, 1973). The resulting residue is dried and weighed, then ignited to a constant weight. The difference between these two weights is the weight of indigestible biomass (USDA, 1973). Once percentages of water, fat, protein, lignin and ash have been subtracted from 100 % of the result, the remaining amount is carbohydrate and therefore can be calculated calorifically (USDA, 1973). The average calorific combustion of 1g of most carbohydrates is about 4 kcal (USDA, 1973). Standard green peas contain 81 kcal per 100 g. Therefore, 0.81 kcal per gram. However, BMPB and FIB PB are made up of stems, leaves and pods. Therefore, we expect the ingredients to be even lower than this hypothetical amount, due to the increased content of fibre and lack of pea starch, in comparison to pea seeds themselves (as explained in Chapter 3). The calorific content discussed here is purely hypothetical. Table 21 describes the hypothetical amount of kcal per 20 g of formulated pellets used in this study (prior to expansion through oil frying). It is apparent and as expected, that with an increase in BMPB and FIB PB addition and therefore subsequently high-energy dense starch commodities replaced, a decrease in total kcal per 20 g is proposed. This shows for example that with 10 % starch commodities replacement, the pre-fried product has had it’s calorific content lowered by 7.55 % relative to the Control. At 30 % and 50 % starch replacement the calorific index of the model product

is reduced by 23 % and 38 %, respectively. Lastly, when 100% of all starch commodities have been replaced the total calorific content is lowered by 74.64 %. Hypothetically, showing evidence that the addition of PB as a replacement of starch commodities (in this model system) has effectively decreased the calorific content of the pellet product and therefore most likely the expanded final product as well as. Therefore having advantageous health benefits combating issues as previously mentioned in Chapter 1.

Nano-fibrillated cellulose (NFC) has been ascribed as a DF exhibiting many health benefits, including its ability to evade hydrolysis during digestion, increase faecal bulk and reduce cholesterol (Yan *et al.*, 2018). Moreover, the majority of the system is indigestible and has the advantage of containing fewer calories than high-energy dense starches, replaced in this study. Furthermore, its oil holding capacity is an important property. DF is highly hydrophilic therefore; it will interact with water and hinder interactions with oil. In processing cellulose to create NFC an increase of active hydroxyl groups become present on the surface (Yan *et al.*, 2018). However, hydrophobic groups can potentially be applied to the surface of fibrillated masses, initiating better oil holding capacities (Yan *et al.*, 2018). Yan *et al* (2018) also found that when NFC had the addition of hydrophobic groups on the surface an increase in the absorption capacity of oil (almost 500 mg fat/g faeces of rats) was observed (Yan *et al.*, 2018). This would ensure better oil and fat absorption in the fibrillated matrix and or product, which may go immediately through the digestive tract and therefore not digested by the consumer. Lastly, DF can effectively absorb intestinal waste and is regarded as an intestinal scavenger (Yan *et al.*, 2018). Therefore DF may bind to carcinogenic compounds and prevent their absorption across the gut thus additions of both BMPB and FIB PB will aid in this, providing reduced risks

of carcinogens (Langley-Evans, 2009). Moreover micro-nutrient additions should also have anti-carcinogenic functions as they have the capacity to neutralise free radicals which modify base sequences of DNA (Langley-Evans, 2009). Thereby with more modifications this material has the potential to have additional health benefits than in its native form. Therefore, such additional health benefits than those of replacing high-energy dense starch-based commodities provide the material of this study with even more attraction attributes, worthy of further study.

Table 21 Total calories for a 20 g pack of an intermediate (pellet) product, prior to frying and expansion, hypothetically formulated using nutritional profile of each ingredient found either from the manufacturer or on particular databases of nutrient profiles used by the manufacturer.

Ingredient	Control	90:10 Starch : BMPB	70:30 Starch : BMPB	50:50 Starch : BMPB	30:70 Starch : BMPB	10: 90 Starch : BMPB	100% BMPB
PF	15.62	14.06	10.94	7.81	4.69	1.56	0
PS	23.52	21.12	16.46	11.76	7.06	2.35	0
TS	4.75	4.28	3.33	2.38	1.43	0.48	0
RS	4.6	4.14	3.22	2.3	1.38	0.6	0
Salt	0	0	0	0	0	0	0
Mixing aid	0	0	0	0	0	0	0
Sugar	0.75	0.75	0.75	0.75	0.75	0.75	0.75
Mixing aid	N/A	N/A	N/A	N/A	N/A	N/A	N/A
Vegetable oil	0.4	0.4	0.4	0.4	0.4	0.4	0.4
Water	0	0	0	0	0	0	0
BMPB	0	1.22	3.66	6.09	8.49	10.94	12.18
FIB PB	0	0.06	0.15	0.26	0.35	0.5	0.56
Total calories (kcal) per (20 g)	49.64	46.03	38.91	31.75	24.55	17.58	13.44

6.4 Conclusion

Modified PB through mechanisms of ball milling and fibrillation were applied as materials to partially or fully replace all starch based commodities within a model commercial system recipe. As a result of this, the subsequent replacement had adverse or beneficial effects on the system when compared to the Control, in terms of; rheological properties, appearance, texture, microstructure and nutritional values. Specifically in more detail:

- Rheological properties: All formulations (bar 90:10 Starch:BMPB FIB PB) showed to have a lower viscosity than that of the Control. Additions of PB increased the stability of the systems (up to 50 % for BMPB FIB PB and 30 % for BMPB formulations) when stress was applied. Up to 30 % additions of BMPB and 50% for BMPB FIB PB complex viscosities of dough formulations were increased. Though when in product form no formulations (bar 70:30 Starch:BMPB FIB PB and 30:70 Starch:BMPB pellets) provided similar stiffness than that of the Control. Thereby showing that when cooked and fried the effects of viscosity may have been advertently changed from the dough formulations, resulting in differing rheological properties of the end products. Namely due to additions of PB adversely decreasing the stiffness of products. These effects are likely due to lower crystallinities and binding abilities of differing ingredients (various starch, polysaccharides, proteins and lipids). Thus varying in texture attributes, within the new formulations and thereby additions of PB provide a less hardened structure relating to stiffness overall. Moreover, DMA results suggested additions of modified PB create a multi-phase matrix within a semi-dried product.

- Appearance: With an increase in the addition of BMPB and FIB PB products had an increase in brown colouration and reduced expansion. The amount of nucleation sites may have decreased with greater additions of PB as seen by expansion ratio and micro- CT results, leading to fewer and decreased pore sizes. This may have been a result of different textures from the ingredients affecting bubble growth. With an observable difference in bubble forms on the surface of the expanded products. The nucleation sites may have decreased due to the greater additions of PB ingredients. Though Gimeno, Moraru and Kokini. (2003) found CMC additions increased nucleation sites plausible due to steric hindurance between starch causing backbones not to join, more air cells, larger holes to form and therefore greater nucleation sites (Chang, 1992; Moraru and Kokini, 2003). This would coincide with findings suggesting semi-dry pellet and expanded systems consist of separated multi-phase systems.
- Texture: For the pellet systems only 90:10 Starch:BMPB required a larger force to break the product. However, for expanded products up to 30% starch replacement by BMPB provided similar characteristics in terms of force required to break and fracture profiles. Whereas, up to 90 % starch replacement by BMPB FIB PB formulations required a similar breaking force to that of the Control. The samples with starch replacement showed less jagged deformation profiles, indicating a more uniform structure. This will impact on eating quality, whereby sensory studies are suggested for any continuation of this work.

- Nutritional content: Hypothetically through modelling and assumptions, both PB formulations indicate a decrease in the calorie content between 8-75 % of the original value of the product.

To conclude it was hypothesised that modified pea biomass could provide starch-like properties, replacing the blend of starch commodities. Findings suggested that this is possible in the form of BMPB and more so if this material (PB) is fibrillated. The 90:10 Starch:BMPB and 90:10 Starch:BMPB FIB PB seem to have the most similar results to that of the Control and therefore would be the most suitable replacement for the current system. Though findings suggest that up to 30% starch replacement is feasible to match a majority of properties. A slight reduction in pasting properties upon replacement of starch with modified PB occurred. However, the new formulated system showed some compatibility through CLSM with plausible synergistic effects. Moreover, up to 30 % starch replacement provided similar or better expansion and microstructure than that of the Control. As well as, DMA findings suggesting BMPB profiles mirror the Control. Lastly, both modifications of PB provide a disadvantage of introducing an added colour to the product. The newly formulated product would reduce the calorie content by up to 8-15 % and provide additional health benefits provided by the addition of DF. Future work is necessary and explained in detail in General Conclusions/Future Work Chapter 7.

Chapter 7 Conclusions and Future work

It has become apparent that in order to incorporate valorised plant based materials, back into the food chain, within composite products, they must firstly be modified. This enables such valorised plant cell wall materials to have advantageous properties and functions over their native structures, which may also have disadvantageous sensory qualities. Therefore, this study has established the composition of pea biomass (leaves, pods, stems and vines) such that it is converted into a functional food ingredient. This composition mainly is comprised of polysaccharides including cellulose, hemicellulose (xyloglucan and arabinogalactan), pectin and lignin. Small quantities of fat and protein were additionally found.

Pea biomass was effectively ball milled into a fine powder, which had minimal crystallinity. Thermodynamic assessments identified no glass transition. Upon rehydration, re-crystallisation to type II allomorph occurred, which with the addition of water, provided visco-elastic properties with concentrations of low water and high solid content (25 % and 33 %), which were similar to the processing requirements. Therefore showing advantageous newly formed microstructures.

To further investigate ways of utilising plant cell wall materials to create structures and functional properties, pea biomass was successfully transformed into a mixed fibrillated mass, comprising both MFC and NFC. The relevant amount of each fraction of fibrillated mass amount depended upon the chemical and mechanical treatments performed. These provided interesting novel microstructures as a mixed biomass. The fibrillated mass provided stable visco-elastic dispersions at low concentrations (1 %). Heat

and chemically pre-treated pea biomass showed to have differing compositions of polysaccharides, where sodium hydroxide washes successfully reduced the amount of hemicellulose within PB. Upon ethanol washing lignin was not proportionally removed, though has been reorganised and hypothesised to have moved to the surface (Ibbett *et al.*, 2011; Gould, Garcia-Garcia and Wolf, 2016). Furthermore, results showed that the PB systems with larger proportions of hemicellulose and lignin provided a greater expanded network, due to larger surface areas and synergistic effects of protection and bond formation of the other varying polysaccharides and lignin. It is thought that this may have resulted in a potentially prodigious bulking agent with properties that include an increase in viscosity, network structure and increase in stability.

Newly formulated microstructures of PB were applied to a composite model material (currently manufactured) and partially or fully replaced starch commodities. It was hypothesised that these newly formulated structures of pea biomass provided starch-like properties, showing successful and advantageous modification to pea biomass properties over its native state. These findings showed that up to 30 % of starch commodities could be replaced with these newly formulated low calorific ingredients and were comparable to the Control in terms of texture, viscosity, expansion and microstructure. Additions of fibrillated material appear to have better attributes for increasing textural hardness, microstructure uniformity and viscosity of the products in general. The mechanisms of how these work are not fully understood and may be a function of entanglement of fibres. However, confocal microscopy and rheological measurements indicate a synergistic effect possibly in the form of weak bond formations between

starch and cellulosic materials found in PB when in a high water content system.

The newly formulated composite, containing 30 % of novel functional microstructure ingredients has the advantage of being 7-12 % less calorific and added dietary fibre, as well as a source of protein. Thereby upon consumption, it would give advantageous health benefits over the Control. Furthermore, as this is currently a wasted material, valorisation into the food chain enables sustainable food manufacturing and production with added value to the producer.

Future work should look into the effects of other routes of modification, namely enzymatic treatments on the properties of pea biomass, for the use of transforming the native mass into a fibrillated functional food ingredient within composites. Moreover, future work should also look into the effects of heat and mechanical disruption without any chemical pre-treatment on the fibrillation of Pea Biomass. This would be in order to see if pea biomass without these specific pre-treatments is able to be fibrillated. Therefore reducing the environmental impact within production and mimicking the work on Solka Floc. Furthermore, results using chemical pre-treatments, especially sodium hydroxide washes should include a neutralisation step after the subsequent wash. Thereby seeing if the functional properties namely expansion of surface area and therefore reinforcement is not inhibited once drying and crystallising of sodium hydroxide wash has incurred. Lastly, reinforcement properties should be tested.

In terms of further application, research should continue into the effects of replacing each individual starch commodity, within a composite with ball

milled pea biomass and fibrillated pea biomass. Thereby finding evidence on the flexibility of use of modified pea biomass adhering to property functions. Overall seeing the greatest impact of replacement from a socio-economic, environmental, nutritional and ethical point of view. Furthermore, formulations of doughs without the addition of ball milled pea biomass and thus only fibrillated mass ingredients, as starch substitutions, should be investigated. Thereby ultimately witnessing the effects of fibrillated mass on its own. Additionally, sensory attributes and consumer trials on the replacement of starch commodities with newly formulated pea biomass ingredients within the composite. Such as the subsequent colouration with the addition of pea biomass and taste differences through subsequent replacement.

Lastly, extensive investigations are required to determine whether starch and cellulosic materials are able to form weak bond formations with synergistic effects, as stereochemically this seems unfeasible, though hypothesis and results seem to indicate this. These investigations should be performed in various water content systems.

This work has attempted to show that by using conversion routes of chemical, heat and mechanical treatments or a combination thereof, can enable plant cell wall materials (with the example of pea biomass) to be transformed into functional food ingredients within a composite material, in various forms. Therefore, this valorised material and plausibly other plant based waste streams have potential for incorporation into the food chain. Thereby adhering to the current and future global crisis relating to food manufacturing and production necessities in order to face an increase in global population and climate changes.

Chapter 8 References

A.O.A.C. (2000) *Official methods of analysis of AOAC*, *International 17th edition; Gaithersburg, MD, USA Association of Analytical Communities*. doi: 10.1007/978-3-642-31241-0.

A.O.A.C. (2006) *Official methods of analysis Proximate Analysis and Calculations Ash Determination (Ash) - item 51*. 17th edn.

Abbaszadeh, A. (2014) *Polysaccharide interactions providing structue control at high and low moisture content*. University of Nottingham.

Abbaszadeh, A., MacNaughtan, W. and Foster, T. J. (2014) 'The effect of ball milling and rehydration on powdered mixtures of hydrocolloids', *Carbohydrate Polymers*. Elsevier, 102, pp. 978–985. doi: 10.1016/j.carbpol.2013.10.020.

Abdullah, F. I., Chua, L. S. and Rahmat, Z. (2017) 'Comparison of protein extraction methods for the leaves of Ficus deltoidea', *Journal of Fundamental and Applied Sciences*, 9(2), pp. 908. doi: 10.4314/jfas.v9i2.19.

Agarwal, D. (2016) *Impact of polymeric additives on the functionality of microfibrillar cellulose*. University of Nottingham thesis.

Agarwal, D., MacNaughtan, W. and Foster, T. J. (2018) 'Interactions between microfibrillar cellulose and carboxymethyl cellulose in an aqueous suspension', *Carbohydrate Polymers*, 185, pp. 112–119. doi: 10.1016/j.carbpol.2017.12.086.

Agarwal, D., MacNaughtan, W., Ibbett, R. and Foster, T. J.(2019) ' Effect of moisture content on thermal and dynamic mechanical properties of microfibrillar cellulose with polymeric additives', *Carbohydrate Polymers*, 211, pp. 91-99.

Ago, M., Endo, T. and Hirotsu, T. (2004) 'Crystalline transformation of native cellulose from cellulose I to cellulose II polymorph by a ball-milling method with a specific amount of water', *Cellulose*. Kluwer Academic Publishers, 11(2), pp. 163–167. doi: 10.1023/b:cell.0000025423.32330.fa.

Alemdar, A. and Sain, M. (2008) 'Isolation and characterization of nanofibers from agricultural residues – Wheat straw and soy hulls', *Bioresource Technology*. Elsevier, 99(6), pp. 1664–1671. doi: 10.1016/j.biortech.2007.04.029.

Alexandratos, N. and Bruinsma, J. (2012) *World agriculture towards 2030/2050: the 2012 revision Global Perspective Studies Team FAO Agricultural Development Economics Division*, *Agricultural Development Economics (ESA) The Food and Agriculture Organization of the United Nations Viale delle Terme di Caracalla 00153 Rome, Italy*. doi: 10.1016/S0264-8377(03)00047-4.

Alila, S., Besbes, I., Vilar, M. R., Mutje, P. and Boufi, S. (2013) 'Non-woody plants as raw materials for production of microfibrillated cellulose (MFC): A comparative study', *Industrial Crops and Products*. Elsevier, 41, pp. 250–259. doi: 10.1016/Journal of Industrial Crops and Products.2012.04.028.

Alloncle, M. and Doublier, J.-L. (1991) 'Viscoelastic properties of maize

starch/hydrocolloid pastes and gels', *Food Hydrocolloids*. Elsevier, 5(5), pp. 455–467. doi: 10.1016/S0268-005X(09)80104-5.

Åman, P. and Graham, H. (1987) *Whole-crop Peas. I. Changes in Botanical and Chemical Composition and Rumen In Vitro Degradability During Maturation*, *Animal Feed Science and Technology*. Available at: https://ac.els-cdn.com/0377840187900496/1-s2.0-0377840187900496-main.pdf?_tid=6436a316-c87c-4d7d-ac6a-5a6b04605a1e&acdnat=1540809756_fe024374b4ef4b4ede6e07b8a2106f33 (Accessed: 29 October 2018).

Anil, M. (2007) 'Using of hazelnut testa as a source of dietary fiber in breadmaking', *Journal of Food Engineering*. Elsevier, 80(1), pp. 61–67. doi: 10.1016/j.jfoodeng.2006.05.003.

Ankerfors, M. (2012) *Microfibrillated cellulose: Energy-efficient preparation techniques and key properties*. Available at: https://www.diva-portal.org/smash/get/diva2:557668/fulltext01.pdf (Accessed: 22 November 2018).

Annapragada, A. and Adjei, A. (1996) 'An analysis of the fraunhofer diffraction method for particle size distribution analysis and its application to aerosolized sprays', *International Journal of Pharmaceutics*. Elsevier, 127(2), pp. 219–227. doi: 10.1016/0378-5173(95)04217-2.

Annunziata, A. and Vecchio, R. (2011) 'Factors affecting Italian consumer attitudes toward functional foods', *AgBioForum*, 14(1), pp. 20–32. Available at: https://mospace.umsystem.edu/xmlui/bitstream/handle/10355/10725/FactorsAffectingItalianConsumer.pdf?sequence=1&isAllowed=y (Accessed: 11 November 2018).

Annunziata, A. and Vecchio, R. (2013) 'Consumer perception of functional foods: A conjoint analysis with probiotics', *Food Quality and Preference*. Elsevier, 28(1), pp. 348–355. doi: 10.1016/j.foodqual.2012.10.009.

Anon. (1987) 'Measurement of the starch content of commercial starches.', *Starch*, 39(1), pp. 414–416.

Ansell, M. P. and Mwaikambo, L. Y. (2009) 'The structure of cotton and other plant fibres', *Handbook of Textile Fibre Structure*. Woodhead Publishing, pp. 62–94. doi: 10.1533/9781845697310.1.62.

Appelhans, B., Waring, M., Scneider, K., Pagoto, S., DeBiasse, M., Whited, M. and Lynch, E. (2012) 'Delay discounting and intake of ready-to-eat and away-from-home foods in overweight and obese women', *Appetite*. Academic Press, 59(2), pp. 576–584. doi: 10.1016/j.appet.2012.07.009.

Armisén, R. and Galatas, F. (2009) 'Agar', in Imeson, A. (ed.) *Handbook of Hydrocolloids: Second Edition*. Wiley-Blackwell, pp. 82–107. doi: 10.1533/9781845695873.82.

Aulin, C., Gällstedt, M. and Lindström, T. (2010) 'Oxygen and oil barrier properties of microfibrillated cellulose films and coatings', *Cellulose*. Springer Netherlands, 17(3), pp. 559–574. doi: 10.1007/s10570-009-9393-y.

Avashia, S. H. and Riddell, M. K. (2015) 'Methods for Making Flour-Based Food Products and Food Products Made Thereby'. Available at: https://patentscope.wipo.int/search/en/detail.jsf?docId=WO2015157702 (Accessed: 14 October 2018).

Avolio, R., Bonadies, I., Capitani, D., Errico, M., Gentile, G. and Avella, M. (2012) 'A multitechnique approach to assess the effect of ball milling on cellulose', *Carbohydrate Polymers*. Elsevier, 87(1), pp. 265–273. doi: 10.1016/j.carbpol.2011.07.047.

Azizi Samir, M. A. S., Alloin, F. and Dufresne, A. (2005) 'Review of recent research into cellulosic whiskers, their properties and their application in nanocomposite field', *Biomacromolecules*. American Chemical Society , 6(2), pp. 612–626. doi: 10.1021/bm0493685.

Baheti, V., Abbasi, R. and Militky, J. (2013) 'Optimisation of Ball Milling Parameters for Refinement of Waste Jute Fibres to Nano/Micro Scale in Dry Conditions', *Journal of Textile Engineering*, 59(5), pp. 87–92. doi: 10.4188/jte.59.87.

Barbosa-Cánovas, G. V, Harte, F. and Yan, H. H. (2012) *Particle size distribution in food powders*, *Food Engineering*. Available at: http://www.eolss.net/sample-chapters/c10/E5-10-01-06.pdf (Accessed: 22 November 2018).

Barneto, A. G., Vila, C., Ariza, J. and Vidal, T. (2011) 'Thermogravimetric measurement of amorphous cellulose content in flax fibre and flax pulp', *Cellulose*. Springer Netherlands, 18(1), pp. 17–31. doi: 10.1007/s10570-010-9472-0.

Bashaiwoldu, A. B., Podczeck, F. and Newton, J. M. (2004) 'Application of dynamic mechanical analysis (DMA) to determine the mechanical properties of pellets', *International Journal of Pharmaceutics*. Elsevier, 269(2), pp. 329–342. doi: 10.1016/j.ijpharm.2003.09.028.

Batzer, H. and Kreibich, U. (1981) 'Influence of water on thermal transitions in natural polymers and synthetic polyamides', *Polymer Bulletin*. Springer-Verlag, 5(11–12), pp. 585–590. doi: 10.1007/BF00255296.

Belitz, H.-D. (Hans-D., Grosch, W. (Werner) and Schieberle, P. (2004) *Food Chemistry*. Springer.

BeMiller, J. N. (2011) 'Pasting, paste, and gel properties of starch–hydrocolloid combinations', *Carbohydrate Polymers*. Elsevier, 86(2), pp. 386–423. doi: 10.1016/j.carbpol.2011.05.064.

Bendler, J. (1985) *Encyclopedia of polymer science and engineering / 3, Cellular materials to composites.* 3rd edn. Edited by H. . Mark et al. New York: Wiley. Available at: https://books.google.co.uk/books?id=NaLgAAAAMAAJ&dq=encyclopedia+of+polymer+science+and+engineering+vol+3+1985&hl=en&sa=X&ved=0ahUKEwi5lIHemqnfAhWISxUIHXzwBNIQ6AEIKjAA (Accessed: 18 December 2018).

Beyler, C. L. and Hirschler, M. M. (2002) 'Thermal Decomposition of Polymers', in *SFPE handbook of the fire protection Engineering 2*, pp. 111–131. Available at:

http://gbhint.tripod.com/papers_5_13_02/368_Beyler_Hirschler_SFPE_Handbook_3.pdf (Accessed: 22 November 2018).

Bizot, H., Le Bail, P., Leroux, B., Davy, J., Roger, P. and Buleon, A. (1997) 'Calorimetric evaluation of the glass transition in hydrated, linear and branched polyanhydroglucose compounds', *Carbohydrate Polymers*. Elsevier, 32(1), pp. 33–50. doi: 10.1016/S0144-8617(96)00146-4.

Bligh, E. G. and Dyer, W. J. (1959) 'A rapid method of total lipid extraction and purification', *Canadian Journal of Biochemistry and Physiology*, 37(8), pp. 911–917. doi: 10.1139/o59-099.

Bogue, J. and Ryan, M. (2000) *Discussion Paper Series Market-oriented New Product Development: Functional Foods and the Irish Consumer*. Available at: https://www.ucc.ie/en/media/academic/foodbusinessanddevelopment/paper27.pdf (Accessed: 11 November 2018).

Boluk, Y., Lahiji, R., Zhao, L. and McDermott, M. (2011) 'Suspension viscosities and shape parameter of cellulose nanocrystals (CNC)', *Colloids and Surfaces A: Physicochemical and Engineering Aspects*. Elsevier, 377(1–3), pp. 297–303. doi: 10.1016/j.colsurfa.2011.01.003.

Borregaard (2019) *About Borregaard*. Available at: https://www.borregaard.com/ (Accessed: 15 February 2019).

Bouvier, J.-M. and Campanella, O. H. (2014) *Extrusion Processing Technology : Food and Non-Food Biomaterials.* Wiley.

Boye, J. I. and Arcand, Y. (2013) 'Current Trends in Green Technologies in Food Production and Processing', *Food Engineering Review*, 5, pp. 1–17. doi: 10.1007/s12393-012-9062-z.

Bras, J. Viet, D., Bruzzese, C. and Dufresne, A. (2011) 'Correlation between stiffness of sheets prepared from cellulose whiskers and nanoparticles dimensions', *Carbohydrate Polymers*. Elsevier, 84(1), pp. 211–215. doi: 10.1016/j.acrbpol.2010.11.022.

Brennan, M., Derbyshire, E., Tiwari, B. and Brennan, C.S. (2013) 'Ready-to-eat snack products: the role of extrusion technology in developing consumer acceptable and nutritious snacks', *International Journal of Food Science & Technology*. Wiley/Blackwell (10.1111), 48(5), pp. 893–902. doi: 10.1111/ijfs.12055.

Briars, R. (2018) 'Post - harvest treatment of post - harvest pea vine field residue for nutrient stabilisation.', in *Manufacturing Food futures*. Nottingham.

Brinkmann, K., Blaschke, L. and Polle, A. (2002) *Comparison of Different Methods for Lignin Determination As a Basis for Calibration of Near-Infrared Reflectance Spectroscopy and Implications of Lignoproteins*, *Journal of Chemical Ecology*, 28(12), pp.2483-2501.

Brunner, G. (2014) 'Processing of Biomass with Hydrothermal and Supercritical Water', *Supercritical Fluid Science and Technology*. Elsevier, 5, pp. 395–509. doi: 10.1016/B978-0-444-59413-6.00008-X.

Budtova, T. and Navard, P. (2016) 'Cellulose in NaOH–water based solvents: a review', *Cellulose*. Springer Netherlands, 23(1), pp. 5–55. doi: 10.1007/s10570-015-0779-8.

Bunzel, M., Schüßler, A. and Tchetseubu Saha, G. (2011) 'Chemical Characterization of Klason Lignin Preparations from Plant-Based Foods', *Journal of Agricultural and Food Chemistry*, 59(23), pp. 12506–12513. doi: 10.1021/jf2031378.

Caballero, B., Trugo, L. C. and Finglas, P. M. (2003) *Encyclopedia of food sciences and nutrition*. Academic Press. Available at: https://www.sciencedirect.com/referencework/9780122270550/encyclopedia-of-food-sciences-and-nutrition (Accessed: 6 November 2018).

CAGR U.S. 2017 | Statistic (2017) *Compound annual growth rate (CAGR) of salty snacks in the United States in 2017, by product claim*. Available at: https://www.statista.com/statistics/787707/salty-snack-cagr/ (Accessed: 30 October 2018).

Calahorra, M. E. Cortázar, M., Eguiazábai, J. and Guzmán, G. M. (1989) 'Thermogravimetric analysis of cellulose: Effect of the molecular weight on thermal decomposition', *Journal of Applied Polymer Science*. Wiley-Blackwell, 37(12), pp. 3305–3314. doi: 10.1002/app.1989.070371203.

Canilha, L. Kumar Chandel, A., dos Santos Milessi, T., dos Santos Milessi, T. S., Fernandes Antunes, F. A., da Costa Freitas, W. L. and das Graças Almeida Felipe, M. (2012) 'Bioconversion of Sugarcane Biomass into Ethanol: An Overview about Composition, Pretreatment Methods, Detoxification of Hydrolysates, Enzymatic Saccharification, and Ethanol Fermentation', *Journal of Biomedicine and Biotechnology*, 2012, pp. 1–15. doi: 10.1155/2012/989572.

Carrillo, F., Colom, X., Valldeperas, J., Evans, D., Huson, M. and Church, J. (2003) 'Structural Characterization and Properties of Lyocell Fibers After Fibrillation and Enzymatic Defibrillation Finishing Treatments', *Textile Research Journal* , 73(11), pp. 1024–1030. Available at: https://journals.sagepub.com/doi/pdf/10.1177/004051750307301114 (Accessed: 21 February 2019).

Carvalho, F. P. (2006) 'Agriculture, pesticides, food security and food safety', *Environmental Science & Policy*. Elsevier, 9(7–8), pp. 685–692. doi: 10.1016/J.ENVSCI.2006.08.002.

Chang, C. (1992) *Study of the mechanism of starchy polymer extrudate expansion.*, DPhil thesis for New Brunswick, N.J., Rutgers The State Univ. of New Jersey. 291 pp.

ChemViews. (2012) '100th Anniversary of the Discovery of X-ray Diffraction', *Wiley-VCH Verlag GmbH & Co. KGaA, Weinheim*, 8 June. Available at: www.chemistryviews.org/details/ezine/2064331/100th_Anniversary_of_the_Discovery_of_X-ray_Diffraction.html.

Chen, H. (2014) *Biotechnology of lignocellulose : theory and practice*. Available at: http://rave.ohiolink.edu/ebooks/ebc/9789400768987%0Ahttp://dx.doi.org/10.1007/978-94-007-6898-7%0Ahttp://proxy.ohiolink.edu:9099/login?url=http://dx.doi.org/10.1007/978

-94-007-6898-7 (Accessed: 22 November 2018).

Chen, H., Rubenthaler, G. L. and Schanus, E. G. (1988) 'Effect of Apple Fiber and Cellulose on the Physical Properties of Wheat Flour', *Journal of Food Science*. Wiley/Blackwell (10.1111), 53(1), pp. 304–305. doi: 10.1111/j.1365-2621.1988.tb10242.x.

Child, T. F. (1972) 'Pulsed n.m.r. study of molecular motion and environment of sorbed water on cellulose', *Polymer*. Elsevier, 13(6), pp. 259–264. doi: 10.1016/0032-3861(72)90004-3.

Chinga-Carrasco, G. (2011) 'Cellulose fibres, nanofibrils and microfibrils: The morphological sequence of MFC components from a plant physiology and fibre technology point of view.', *Nanoscale research letters*. Springer, 6(1), pp. 417-424. doi: 10.1186/1556-276X-6-417.

Choudhury, M. L. (2006) *Postharvest Management of Fruit and Vegetables in the Asia-Pacific Region*. Available at: www.apo-tokyo.org (Accessed: 12 November 2018).

Chung, H.-J. and Lim, S.-T. (2006) 'Physical Aging of Amorphous Starches (A Review)', *Starch - Stärke*. John Wiley & Sons, Ltd, 58(12), pp. 599–610. doi: 10.1002/star.200600547.

Ciolacu, D. and Popa, V. I. (2006) 'on the Thermal Degradation of Cellulose Allomorphs', *Cellulose Chemistry and Technology*, 40(6), pp. 445–449. Available at: https://s3.amazonaws.com/academia.edu.documents/37212625/Ciolacu_Popa_ccth_445-449.pdf?AWSAccessKeyId=AKIAIWOWYYGZ2Y53UL3A&Expires=1543078437&Signature=4syUnsK4PEgFajiE36%2FDYSVQWo0%3D&response-content-disposition=inline%3B filename%3DON_THE_THERMAL_DEG (Accessed: 24 November 2018).

Cisneros, F. H. and Kokini, J. L. (2002) 'Effect of extrusion operating parameters on air bubble entrapment', *Journal of Food Process Engineering*, 25(4), pp. 251–283. doi: 10.1111/j.1745-4530.2002.tb00566.x.

Collins English Dictionary. (2018) *Ready-to-eat definition and meaning | Collins English Dictionary*. Available at: https://www.collinsdictionary.com/dictionary/english/ready-to-eat (Accessed: 11 November 2018).

Cosgrove, D. J. (2005) 'Growth of the plant cell wall', *Nature Reviews Molecular Cell Biology*. Nature Publishing Group, 6(11), pp. 850–861. doi: 10.1038/nrm1746.

Cuissinat, C. and Navard, P. (2006) 'Swelling and Dissolution of Cellulose Part II: Free Floating Cotton and Wood Fibres in NaOH–Water–Additives Systems', *Macromolecular Symposia*. Wiley-Blackwell, 244(1), pp. 19–30. doi: 10.1002/masy.200651202.

Czaja, W., Romanovicz, D. and Brown, R. M. (2004) 'Structural investigations of microbial cellulose produced in stationary and agitated culture', *Cellulose*. Kluwer Academic Publishers, 11(3/4), pp. 403–411. doi: 10.1023/b:cell.0000046412.11983.61.

Dahl, W. J. Whiting, S. J., Healey, A., Zello, G. A. and Hildebrandt, S. L. (2003) 'Increased stool frequency occurs when finely processed pea hull fiber is added to usual foods consumed by elderly residents in long-term care', *Journal of the American Dietetic Association*. Elsevier, 103(9), pp. 1199–1202. doi: 10.1016/S0002-8223(03)00977-5.

Dahl, W. J., Foster, L. M. and Tyler, R. T. (2012) 'Review of the health benefits of peas (Pisum sativum L.)', *British Journal of Nutrition*. Cambridge University Press, 108(S1), pp. S3–S10. doi: 10.1017/S0007114512000852.

Debet, M. R. and Gidley, M. J. (2007) 'Why do gelatinized starch granules not dissolve completely? Roles for amylose, protein, and lipid in granule "ghost" integrity', *Journal of Agricultural and Food Chemistry*. American Chemical Society, 55(12), pp. 4752–4760. doi: 10.1021/jf070004o.

Deffenbaugh, L. B. and Walker, C. E. (1989) 'Comparison of Starch Pasting in the Brabender Viscoamylograph and the Rapid Visco-Analyzer', *Cereal Chemistry*, 66(6), pp. 493–499.

Díaz-Calderón, P. MacNaughtan, B., Hill, S., Foster, T., Enrione, J. and Mitchell, J. (2018) 'Changes in gelatinisation and pasting properties of various starches (wheat, maize and waxy maize) by the addition of bacterial cellulose fibrils', *Food Hydrocolloids*. Elsevier, 80, pp. 274–280. doi: 10.1016/J.FOODHYD.2018.02.023.

Djilas, S., Čanadanović-Brunet, J. and Ćetković, G. (2009) 'By-products of fruits processing as a source of phytochemicals', *Chemical Industry and Chemical Engineering Quarterly*, 15(4), pp. 191–202. doi: 10.2298/CICEQ0904191D.

Doherty, R. D. Hughes, D. A., Humphreys, F. J., Jonas, J. J., Jensen, D. J., Kassner, M. E., King, W. E., McNelly, T. R. and McQueen, H. J. (1997) 'Current issues in recrystallization: a review', *Materials Science and Engineering: A*. Elsevier, 238(2), pp. 219–274. doi: 10.1016/S0921-5093(97)00424-3.

Drewnowski, A. and Specter, S. (2004) 'Poverty and obesity: the role of energy density and energy costs', *The American Journal of Clinical Nutrition*. Oxford University Press, 79(1), pp. 6–16. doi: 10.1093/ajcn/79.1.6.

Dufresne, A., Cavaille, J.-Y. and Vignon, M. R. (1997) 'Mechanical behavior of sheets prepared from sugar beet cellulose microfibrils', *Journal of Applied Polymer Science*. Wiley-Blackwell, 64(6), pp. 1185–1194. doi: 10.1002/(SICI)1097-4628(19970509)64:6<1185::AID-APP19>3.0.CO;2-V.

Duncan, J. (2008) *Principles and applications of thermal analysis, Chapter 4: Principles and applications of mechanical thermal analysis*. Ed Gabbott, P. Oxford. pp 119-163.

Dyer, W. J. and Morton, M. L. J. (1956) 'Fisheries Research Board Canada', *Fisheries Research Board Canada*, 13(129).

Emsland Group. (2018) *Potato flakes.* Available: https://www.emsland-group.de/product-solutions/food-innovation/natural-raw-materials/potato-flakes (Accessed: 18 June 2019).

Engelen, L. Van Der Bilt, A., Schipper, M. and Bosman, F. (2005) 'Oral Size

Perception of Particles: Effect of Size, Type, Viscosity and Method', *Journal of Texture Studies*, 36, pp. 373–386. Available at: https://onlinelibrary.wiley.com/doi/pdf/10.1111/j.1745-4603.2005.00022.x (Accessed: 7 December 2018).

Enrione, J. I., Diaz, P. C., Matiacevich, S. B. and Hill, S. E. (2012) 'Mechanical and Structural Stability of an Extruded Starch-protein-polyol Food System', *Journal of Food Research*, 1(2), pp. 224–232.

European Commission. (2015). *Paris agreement.* Available: https://ec.europa.eu/clima/policies/international/negotiations/paris_en. (Accessed: 05 June 2019).

European Commission. (2018) *Nutrition claims - European Commission*. Available at: https://ec.europa.eu/food/safety/labelling_nutrition/claims/nutrition_claims_en (Accessed: 29 October 2018).

Euvrard, S., Kanitakis, J., D'Incan, M., Lefrançois, N., Mornex, J. F. and Pouteil-Noble, C. (1996) 'Porokératoses et greffe d'organe', *Nouvelles Dermatologiques*. NRC Research Press Ottawa, Canada , 15(3), p. 208. doi: 10.1139/o59-099.

Evans, I. D. and Haisman, D. R. (1980) 'Rheology of gelatinised starch suspensions', Journal of Texture Studies, 10 (1979), pp. 347-370.

Fadda, S. Cincotti, A., Concas, A., Pisu, M. and Cao, G. (2009) 'Modelling breakage and reagglomeration during fine dry grinding in ball milling devices', *Powder Technology*, 194(3), pp. 207–216. doi: 10.1016/j.powtec.2009.04.009.

FAO. (1981) *Food Loss Prevention in Perishable Crops - Food and Agriculture Organization of the United Nations*. 1st edn. Food and Agricultural Organization of the United Nations. Available at: https://books.google.co.uk/books/about/Food_Loss_Prevention_in_Perishable_Crops.html?id=ty0mjwEACAAJ&redir_esc=y (Accessed: 30 October 2018).

FAO. (2002) *Chapter 2. Food security: concepts and measurement*. Available at: http://www.fao.org/docrep/005/y4671e/y4671e06.htm (Accessed: 15 February 2019).

FAO. (2008) *International Year of the Potato 2008*. Available at: www.potato2008.org (Accessed: 3 January 2019).

FAO. (2013) *Chapter 3. Feeding the world*. Statistical yearbook of the Food and Argicultural Organisation of the United Nations. Available at: www.fao.org/3/i3107e/i3107e03.pdf (Accessed: 11 June 2019).

FDA. (2008) *Chemical Contaminants - Acrylamide: Information on Diet, Food Storage, and Food Preparation*. Center for Food Safety and Applied Nutrition. Available at: https://www.fda.gov/food/foodborneillnesscontaminants/chemicalcontaminants/ucm151000.htm (Accessed: 15 February 2019).

Ferrer, A., Quintana, E., Filpponen, I., Solala, I., Vidal, T., Rodríguez, A. and Laine, J. (2012) 'Effect of residual lignin and heteropolysaccharides in

Justified text looks so strange like this. I suggest left justification **ONLY**

nanofibrillar cellulose and nanopaper from wood fibers', *Cellulose*. Springer Netherlands, 19(6), pp. 2179–2193. doi: 10.1007/s10570-012-9788-z.

Filipovic, N., Djuric, M. and Gyura, J. (2007) 'The effect of the type and quantity of sugar-beet fibers on bread characteristics', *Journal of Food Engineering*, 78(3), pp. 1047–1053. doi: 10.1016/j.jfoodeng.2005.12.050.

Fishwick, M. J. and Wright, A. J. (1977) 'Comparison of methods for the extraction of plant lipids', *Phytochemistry*, 16(10), pp. 1507–1510. doi: 10.1016/0031-9422(77)84011-9.

Flogan, C. and Dahl, W. (2010) 'Effects of Fiber-Fortified Foods on Children With Constipation', *ICAN: Infant, Child, & Adolescent Nutrition*. SAGE PublicationsSage CA: Los Angeles, CA, 2(5), pp. 312–317. doi: 10.1177/1941406410383980.

Flutto, L. (2003) 'PECTIN | Properties and Determination', *Encyclopedia of Food Sciences and Nutrition*. Academic Press, pp. 4440–4449. doi: 10.1016/B0-12-227055-X/00901-9.

Folch, J., Lees, M. and Slone Stanley, G. H. (1957) 'A simple method for the isolation and purification of total lipides from animal tissues.', *The Journal of Biological chemistry*, 226(1), pp. 497–509. Available at: http://www.ncbi.nlm.nih.gov/pubmed/13428781 (Accessed: 15 February 2019).

Foley, J. (2014) *The future of food: Feeding the world Billion*, *National Geographic* . Available at: https://www.nationalgeographic.com/foodfeatures/feeding-9-billion/ (Accessed: 30 October 2018).

FoodExecutive. (2017) *Global savory snacks market trend grows*. Available at: https://www.foodexecutive.com/en/marketing/2199-savory-snacks-market.html (Accessed: 30 October 2018).

Foster, T. J. Ablett, S., McCann, M. and Gidley, M. J. (1996) 'Mobility-resolved 13C-NMR spectroscopy of primary plant cell walls', *Biopolymers*. John Wiley & Sons, Ltd, 39(1), pp. 51–66. doi: 10.1002/(SICI)1097-0282(199607)39:1<51::AID-BIP6>3.0.CO;2-U.

Foster, T. J. (2013) 'Design of Foods Using Naturally Structured Materials', in *Formulation Engineering of Foods*. Chichester, UK: John Wiley & Sons, Ltd, pp. 44–58. doi: 10.1002/9781118597651.ch3.

Fry, S. C. (1989) *The Structure and Functions of Xyloglucan*, *Journal of Experimental Botany*. Available at: https://academic.oup.com/jxb/article-abstract/40/1/1/546699 (Accessed: 6 November 2018).

Fukuoka, M., Ohta, K. and Watanabe, H. (2002) 'Determination of the terminal extent of starch gelatinization in a limited water system by DSC', *Journal of Food Engineering*. Elsevier, 53(1), pp. 39–42. doi: 10.1016/S0260-8774(01)00137-6.

Garcia de Rodriguez, N. L., Thielemans, W. and Dufresne, A. (2006) 'Sisal cellulose whiskers reinforced polyvinyl acetate nanocomposites', *Cellulose*, 13(3), pp. 261–270. doi: 10.1007/s10570-005-9039-7.

Garrote, G., Domínguez, H. and Parajó, J. C. (2001) *Kinetic modelling of corncob autohydrolysis*, *Process Biochemistry*. Available at: www.elsevier.com/locate/procbio (Accessed: 29 October 2018).

Gdala, J., Buraczewska, L. and Grala, W. (1992) 'The chemical composition of different types and varieties of pea and the digestion of their protein in pigs', *Journal of Animal and Feed Sciences*. The Kielanowski Institute of Animal Physiology and Nutrition, Polish Academy of Sciences, Jabłonna, Poland, 1(1), pp. 71–79. doi: 10.22358/jafs/69896/1992.

de Gennaro, S., Birch, G. G., Parke, S. A. and Stancher, B. (2000) 'Studies on the physicochemical properties of inulin and inulin oligomers', *Food Chemistry*, 68(2), pp. 179–183. doi: 10.1016/S0308-8146(99)00173-9.

George, J. and Sabapathi, S. N. (2015) 'Cellulose nanocrystals: synthesis, functional properties, and applications.', *Nanotechnology, science and applications*. Dove Press, 8, pp. 45–54. doi: 10.2147/NSA.S64386.

Gilbert, H. J. (2010) 'The Biochemistry and Structural Biology of Plant Cell Wall Deconstruction', *Plant Physiology*, 153(2), pp. 444–455. doi: 10.1104/pp.110.156646.

Gilbert, L. (1998) 'The Consumer Market for Functional Foods', *Journal of Nutraceuticals, Functional & Medical Foods*. Taylor & Francis Group , 1(3), pp. 5–21. doi: 10.1300/J133v01n03_02.

Gimeno, E., Moraru, C. I. and Kokini, J. L. (2004) 'Effect of Xanthan Gum and CMC on the Structure and Texture of Corn Flour Pellets Expanded by Microwave Heating', *Cereal Chemistry Journal*. Wiley-Blackwell, 81(1), pp. 100–107. doi: 10.1094/CCHEM.2004.81.1.100.

Girotto, F. and Alibardi, L. (2015) 'Food waste generation and industrial uses: A review', *Waste Management*. Pergamon, 45, pp. 32–41. doi: 10.1016/J.WASMAN.2015.06.008.

Godfray, H. C. J., Beddington, J. R., Crute, I. R., Haddad, L., Lawrence, D., Muir, J. F., Pretty, J., Robinson, S., Thomas, S. M. and Toulmin, C. (2010) 'Food security: the challenge of feeding 9 billion people.', *Science (New York, N.Y.)*. American Association for the Advancement of Science, 327(5967), pp. 812–8. doi: 10.1126/science.1185383.

Gómez, M. Ronda, F., Bianco, C., Caballero, P. A. and Apesteguía, A. (2003) 'Effect of dietary fibre on dough rheology and bread quality', *European Food Research and Technology*. Springer-Verlag, 216(1), pp. 51–56. doi: 10.1007/s00217-002-0632-9.

Gould, J., Garcia-Garcia, G. and Wolf, B. (2016) 'Pickering particles prepared from food waste', *Materials*, 9(9), pp. 1–14. doi: 10.3390/ma9090791.

Grolleaud, M. (2002) *Post-harvest losses: discovering the full story. Overview of the phenomenon of losses during the Post-harvest System: Chapter 1 - Losses and waste: Do we know about what is it about?* Available at: http://www.fao.org/docrep/004/AC301S/ac301s02.htm#Datos inciertos y metodología (Accessed: 30 October 2018).

Guhados, G., Wan, W. and Hutter, J. L. (2005) 'Measurement of the elastic

modulus of single bacterial cellulose fibers using atomic force microscopy', *Langmuir*. American Chemical Society , 21(14), pp. 6642–6646. doi: 10.1021/la0504311.

Gustavsson, J. Cederberg, C., Sonesson, U., Van Otterdijk, R. and Meybeck, A. (2011) *Global food losses and food waste. Extent, Causes and Prevention.* Available at: http://www.fao.org/docrep/014/mb060e/mb060e00.pdf (Accessed: 30 October 2018).

Habibi, Y., Lucia, L. A. and Rojas, O. J. (2010) 'Cellulose Nanocrystals: Chemistry, Self-Assembly, and Applications', *Chemical Reviews*. American Chemical Society, 110(6), pp. 3479–3500. doi: 10.1021/cr900339w.

Habibi, Y. and Vignon, M. R. (2008) 'Optimization of cellouronic acid synthesis by TEMPO-mediated oxidation of cellulose III from sugar beet pulp', *Cellulose*. Springer Netherlands, 15(1), pp. 177–185. doi: 10.1007/s10570-007-9179-z.

Hall, M. B. (2009) 'Determination of starch, including maltooligosaccharides, in animal feeds: comparison of methods and a method recommended for AOAC collaborative study.', *Journal of AOAC International*, 92(1), pp. 42–9. Available at: http://www.ncbi.nlm.nih.gov/pubmed/19382561 (Accessed: 29 October 2018).

Hänsch, R. and Mendel, R. R. (2009) 'Physiological functions of mineral micronutrients (Cu, Zn, Mn, Fe, Ni, Mo, B, Cl)', *Current Opinion in Plant Biology*. Elsevier Current Trends, 12(3), pp. 259–266. doi: 10.1016/J.PBI.2009.05.006.

Harper, J. M. (1988) 'Effects of Extrusion Processing on Nutrients', in *Nutritional Evaluation of Food Processing*. Dordrecht: Springer Netherlands, pp. 365–391. doi: 10.1007/978-94-011-7030-7_14.

Hassan, B. Chatha, S. A. S., Hussain, A. I., Zia, K. M. and Akhtar, N. (2018) 'Recent advances on polysaccharides, lipids and protein based edible films and coatings: A review', *International Journal of Biological Macromolecules*. Elsevier B.V., 109, pp. 1095–1107. doi: 10.1016/j.ijbiomac.2017.11.097.

Hatfield, R. D. Grabber, J., Ralph, J. and Brei, K. (1999) 'Using the Acetyl Bromide Assay To Determine Lignin Concentrations in Herbaceous Plants: Some Cautionary Notes', *Journal of Agricultural and Food Chemistry*. American Chemical Society, 47(2), pp. 628–632. doi: 10.1021/JF9808776.

Hatfield, R. and Fukushima, R. S. (2005) 'Can Lignin Be Accurately Measured? Methods for Determining Lignin', *Crop Science*, 45(3), pp. 832–839. doi: 10.2135/cropsci2004.0238.

Hayes, M. H. B., Mylotte, R. and Swift, R. S. (2017) 'Humin: Its Composition and Importance in Soil Organic Matter', *Advances in Agronomy*. Academic Press, 143, pp. 47–138. doi: 10.1016/bs.argon.2017.01.001.

He, S. Quin, Y., Walid, E., Li, L., Cui, J. and Ma, Y. (2014) 'Effect of ball-milling on the physicochemical properties of maize starch', *Biotechnology Reports*. Elsevier, 3, pp. 54–59. doi: 10.1016/j.btre.2014.06.004.

Henriksson, M. Henriksson, G,. Berglund, L. A. and Lindström, T. (2007) 'An environmentally friendly method for enzyme-assisted preparation of

microfibrillated cellulose (MFC) nanofibers', *European Polymer Journal*. Pergamon, 43(8), pp. 3434–3441. doi: 10.1016/j.europolymj.2007.05.038.

Hermans, P. H. and Weidinger, A. (1946) 'On the Recrystallization of Amorphous Cellulose', *Journal of the American Chemical Society*. American Chemical Society, 68(12), pp. 2547–2552. doi: 10.1021/ja01216a037.

Herrick, F. W. Casebier, R. L., Hamilton, J. and Sandberg, K. R. (1983) 'Microfibrillated Cellulose: Morphology and accessibility', *Journal of Applied Polymer Science.* Applied Polymer Symposium*. 3, pp.797-813.*

Hess, K., Kiessig, H. and Gundermann, J. (1941) 'X-ray and electron microscopic', *Journal of Physical Chemistry.*Available at: https://www.degruyter.com/view/j/zpch.1941.49.issue-1/zpch-1941-4908/zpch-1941-4908.xml (Accessed: 24 November 2018).

Heux, L., Dinand, E. and Vignon, M. R. (1999) 'Structural aspects in ultrathin cellulose microfibrils followed by 13C CP-MAS NMR', *Carbohydrate Polymers*. Elsevier, 40(2), pp. 115–124. doi: 10.1016/S0144-8617(99)00051-X.

Hill, S. (2014) 'Protein assessment'. Nottingham.

Hiltunen, S., Heiskanen, I. and Backfolk, K. (2018) 'Effect of hydrothermal treatment of microfibrillated cellulose on rheological properties and formation of hydrolysis products', *Cellulose*, 25, pp. 4653–4662. doi: 10.1007/s10570-018-1884-2.

Holland, S., Tuck, C. and Foster, T. (2018) 'Selective recrystallization of cellulose composite powders and microstructure creation through 3D binder jetting', *Carbohydrate Polymers*. Elsevier, 200, pp. 229–238. doi: 10.1016/j.carbpol.2018.07.064.

Holtan, S. Rosenberg Read, M., Øvrebø, H. H. and Nygård Vold, I. M. (2017) 'Microfibrillated cellulose'. Borregaard AS. Available at: http://www.freepatentsonline.com/y2017/0121908.html (Accessed: 20 November 2018).

Howsmon, J. A. and Marchessault, R. H. (1959) 'The ball-milling of cellulose fibers and recrystallization effects', *Journal of Applied Polymer Science*. Wiley-Blackwell, 1(3), pp. 313–322. doi: 10.1002/app.1959.070010308.

Huang, Z.-M., Zhang, Y., Kotaki, M. and Ramakrishna, S. (2003) 'A review on polymer nanofibers by electrospinning and their applications in nanocomposites', *Composites Science and Technology*. Elsevier, 63(15), pp. 2223–2253. doi: 10.1016/S0266-3538(03)00178-7.

Huber, E. Francio, D. L., Biasi, V. Mezzomo, N. and Ferreira, S. R. S. (2016) 'Characterization of vegetable fiber and its use in chicken burger formulation', *Journal of Food Science and Technology*. Springer India, 53(7), pp. 3043–3052. doi: 10.1007/s13197-016-2276-y.

Hult, E.-L., Iversen, T. and Sugiyama, J. (2003) 'Characterization of the supermolecular structure of cellulose in wood pulp fibres', *Cellulose*. Kluwer Academic Publishers, 10(2), pp. 103–110. doi: 10.1023/A:1024080700873.

Hunter, R. E. and Dweltz, N. E. (1979) 'Structure of Cellulose II', *Journal of*

Applied Polymer Science, 23, pp. 249–259. Available at: https://onlinelibrary.wiley.com/doi/pdf/10.1002/app.1979.070230123 (Accessed: 31 January 2019).

Hurkman, W. J. and Tanaka, C. K. (1986) 'Solubilization of plant membrane proteins for analysis by two-dimensional gel electrophoresis.', *Plant Physiology*, 81(3), pp. 802–6. Available at: http://www.ncbi.nlm.nih.gov/pubmed/16664906 (Accessed: 29 October 2018).

Ibbett, R. Gaddipati, S., Davies, S., Hill, S. and Tucker, G. (2011) 'The mechanisms of hydrothermal deconstruction of lignocellulose: New insights from thermal–analytical and complementary studies', *Bioresource Technology*. Elsevier, 102(19), pp. 9272–9278. doi: 10.1016/J.BIORTECH.2011.06.044.

Ibbett, R. Phillips, J., Gray, D. and Foster, T. (2019) ' Enzyme digestion of pea haulum pulp as an approach for up-grading for improved textural and nutritional qualities for food and feed applications'. Under review.

Innventia. (2019) *About Innventia*. Available at: http://www.innventia.com/en/ (Accessed: 15 February 2019).

International Fiber Corporation. (2018) *International Fiber Corporation – Food Ingredients Applications*. Available at: http://www.ifcfiber.com/applications/food/food.php (Accessed: 29 October 2018).

Iotti, M. Gregersen, Ø, W., Moe, S. and Lenes, M. (2011) 'Rheological Studies of Microfibrillar Cellulose Water Dispersions', *Journal of Polymers and the Environment*. Springer US, 19(1), pp. 137–145. doi: 10.1007/s10924-010-0248-2.

Isaacson, T. Damasceno, C. M. B., Saravanan, R. S., He, Y., Catalá, C., Saladié, M. and Rose, J. K. C. (2006) 'Sample extraction techniques for enhanced proteomic analysis of plant tissues.', *Nature Protocols*, 1(2), pp. 769–74. doi: 10.1038/nprot.2006.102.

Iwamoto, S., Abe, K. and Yano, H. (2008) 'The Effect of Hemicelluloses on Wood Pulp Nanofibrillation and Nanofiber Network Characteristics', *Biomacromolecules*, 9(3), pp. 1022–1026. doi: 10.1021/bm701157n.

Iwamoto, S., Nakagaito, A. N. and Yano, H. (2007) 'Nano-fibrillation of pulp fibers for the processing of transparent nanocomposites', *Applied Physics A*. Springer-Verlag, 89(2), pp. 461–466. doi: 10.1007/s00339-007-4175-6.

Jane, J.-L. (1996) *Structure of starch granules*, *Żywność. Technologia. Jakość*. Available at: http://wydawnictwo.pttz.org/wp-content/uploads/2017/12/01_Jane.pdf (Accessed: 12 October 2018).

Jarvis, M. C. (1994) 'Solid-state NMR study of leaf cell walls of oil palm', *Phytochemistry*. Pergamon, 35(2), pp. 485–487. doi: 10.1016/S0031-9422(00)94787-3.

Jarvis, M. C. and Apperley, D. C. (1995) 'Chain conformation in concentrated pectic gels: evidence from 13C NMR', *Carbohydrate Research*. Elsevier, 275(1), pp. 131–145. doi: 10.1016/0008-6215(95)00033-P.

Jayakody, L. and Hoover, R. (2008) 'Effect of annealing on the molecular structure and physicochemical properties of starches from different botanical origins – A review', *Carbohydrate Polymers*. Elsevier, 74(3), pp. 691–703. doi: 10.1016/j.carbpol.2008.04.032.

Jenkins, P. J. and Donald, A. M. (1998) 'Gelatinisation of starch: a combined SAXS/WAXS/DSC and SANS study', *Carbohydrate Research*. Elsevier, 308(1–2), pp. 133–147. doi: 10.1016/S0008-6215(98)00079-2.

Kajiwara, K. and Miyamoto, T. (2004) 'Progress in structural characterization of functional polysaccharides', in Dumitriu, S. (ed.) *Polysaccharides structural diversity and functional versatility*. 2nd edn. New York: Marcel Dekker, pp. 1–40.

Kalichevsky, M. T. Jaroszkiewicz, E. M., Ablett, S., Blanshard, J. M. V. and Lillford, P. L. (1992) 'The glass transition of amylopectin measured by DSC, DMTA and NMR', *Carbohydrate Polymers*. Elsevier, 18(2), pp. 77–88. doi: 10.1016/0144-8617(92)90129-E.

Kanmani, P. Dhivya, E., Aravind, J. and Kumaresan, K. (2014) 'Extraction and Analysis of Pectin from Citrus Peels: Augmenting the Yield from Citrus limon Using Statistical Experimental Design', *Iranica Journal of Energy and Environment*, 5(3), pp. 303–312. doi: 10.5829/idosi.ijee.2014.05.03.10.

Karkle, E. L., Alavi, S. and Dogan, H. (2012) 'Cellular architecture and its relationship with mechanical properties in expanded extrudates containing apple pomace', *Food Research International*, 46(1), pp. 10–21. doi: 10.1016/j.foodres.2011.11.003.

Kerr, S. (2016) *Sugar Transport in Plants: Phloem | Biology 1520*. Available at: http://bio1520.biology.gatech.edu/nutrition-transport-and-homeostasis/plant-transport-processes-ii/ (Accessed: 29 October 2018).

Kim, C.-W. Kim, D-S., Kang, S., Marquez, M and Joo, Y. L. (2006) 'Structural studies of electrospun cellulose nanofibers', *Polymer*. Elsevier, 47(14), pp. 5097–5107. doi: 10.1016/j.polymer.2006.05.033.

Kim, S. H., Lee, C. M. and Kafle, K. (2013) 'Characterization of crystalline cellulose in biomass: Basic principles, applications, and limitations of XRD, NMR, IR, Raman, and SFG', *Korean Journal of Chemical Engineering*. Springer US, 30(12), pp. 2127–2141. doi: 10.1007/s11814-013-0162-0.

Kimura, M., Hatakeyama, T. and Nakano, J. (1974) 'DSC study on recrystallization of amorphous cellulose with water', *Journal of Applied Polymer Science*. Wiley-Blackwell, 18(10), pp. 3069–3076. doi: 10.1002/app.1974.070181015.

Klemm, D. Philipp, B., Heinze, T., Heinze, U. and Wagenknecht, W. (1998) *Comprehensive Cellulose Chemistry. Volume 1. Fundamentals and Analytical Methods*. 1st edn. Weinheim, Germany : American Chemical Society. doi: 10.1021/JA9857514.

Knudson, K. E. (1997) 'Carbohydrate and lignin contents of plant materials used in animal feeding', *Animal Feed Science Technology*, 67(4), pp. 319–338. Available at: www.megazyme.com (Accessed: 29 October 2018).

Kocherbitov, V. Ulvenlund, S., Kober, M., Jarring, K. and Arnebrant, T. (2008)

‘Hydration of Microcrystalline Cellulose and Milled Cellulose Studied by Sorption Calorimetry’. *Journal of Physical Chemistry B*, 112(12), pp. 3728-3734. American Chemical Society. doi: 10.1021/JP711554C.

Kumar, P., Barrett, D. M., Delwiche, M. J. and Stroeve, P. (2009) ‘Methods for pretreatment of lignocellulosic biomass for efficient hydrolysis and biofuel production’, *Industrial and Engineering Chemistry Research*. American Chemical Society, 48(8), pp. 3713–3729. doi: 10.1021/ie801542g.

Lad, M., Todd, T., Morris, G. A., MacNaughtan, W., Sworn, G. and Foster, T. J. (2013) 'On the origin of sharp peaks in the X-ray diffraction patterns of xanthan powders', *Food Chemistry.* 139 (1-4), pp. 1146-1151. doi:10.1016/j.foodchem.2013.01.096

Lancaster, J. E. Lister, C. E., Reay, P. F. and Triggs, M. (1997) ‘Influence of Pigment Composition on Skin Color in a Wide Range of Fruit and Vegetables’, *Journal of the American Society for Horticultural Science*. [American Society for Horticultural Science], 122(4), pp. 594–598. Available at: http://journal.ashspublications.org/content/122/4/594.short (Accessed: 29 October 2018).

Langan, P., Nishiyama, Y. and Chanzy, H. (2001) ‘X-ray structure of mercerized cellulose II at 1 Å resolution’, *Biomacromolecules*. American Chemical Society , 2(2), pp. 410–416. doi: 10.1021/bm005612q.

Langley-Evans, S. (2009) *Nutrition A Lifespan Approach*. 1st edn. Wiley-Blackwell.

Larsson, K. and Bengtsson, S. (1983) ‘“Metodbeskrivning Nr. 22”’, *Statens lantbrukskemiska laboratorium*, pp. 1–9.

Lasseuguette, E., Roux, D. and Nishiyama, Y. (2008) ‘Rheological properties of microfibrillar suspension of TEMPO-oxidized pulp’, *Cellulose*. Springer Netherlands, 15(3), pp. 425–433. doi: 10.1007/s10570-007-9184-2.

Lavoine, N. Desloges , I., Dufresne, A. and Bras, J. (2012) ‘Microfibrillated cellulose – Its barrier properties and applications in cellulosic materials: A review’, *Carbohydrate Polymers*, 90(2), pp. 735–764. doi: 10.1016/j.carbpol.2012.05.026.

Li, D. and Xia, Y. (2004) ‘Electrospinning of Nanofibers: Reinventing the Wheel?’, *Advanced Materials*, 16(14), pp. 1151–1170. doi: 10.1002/adma.200400719.

Liang, X.-H., Gu, L.-Z. and Ding, E.-Y. (1993) ‘Recrystallization behavior of cellulose and lignocellulose from Pinus massoniana’, *Wood Science and Technology*. Springer-Verlag, 27(6), pp. 461–467. doi: 10.1007/BF00193869.

Lichtenthaler, H. K. and Buschmann, C. (2001) *Current Protocols in Food Analytical Chemistry (CPFA)*. New York: John Wiley and Sons. Available at: https://www.botanik.kit.edu/molbio/download/425 Lichtenthaler und Buschmann 2001 Chl determ CurrProtFoodAnalChem 4-3-1.pdf (Accessed: 29 October 2018).

Liew, S. Q., Chin, N. L. and Yusof, Y. A. (2014) ‘Extraction and

Characterization of Pectin from Passion Fruit Peels', *Agriculture and Agricultural Science Procedia*. Elsevier, 2, pp. 231–236. doi: 10.1016/j.aaspro.2014.11.033.

Lima, M. A. da Silva, H. Kp., Bragatto, J., Rezende, C. A, Bernardinelli, O. D., Deazevedo, E. R., Gomez, L. D., McQueen-Mason, S. J., Labate, C. A. and Polikarpov, I. (2013) 'Effects of pretreatment on morphology, chemical composition and enzymatic digestibility of eucalyptus bark: a potentially valuable source of fermentable sugars for biofuel production - part 1.', *Biotechnology for Biofuels*. BioMed Central, 6(1), p. 75. doi: 10.1186/1754-6834-6-75.

Lin, Z. Huang, H., Zhang, H., Zhang, L., Yan. L. and Chen, J. (2010) 'Ball Milling Pretreatment of Corn Stover for Enhancing the Efficiency of Enzymatic Hydrolysis', *Applied Biochemistry and Biotechnology*. Humana Press Inc, 162(7), pp. 1872–1880. doi: 10.1007/s12010-010-8965-5.

Linder, S. (1974) 'A Proposal for the Use of Standardized Methods for Chlorophyll Determinations in Ecological and Eco-physiological Investigations', *Physiologia Plantarum*. Wiley/Blackwell (10.1111), 32(2), pp. 154–156. doi: 10.1111/j.1399-3054.1974.tb03743.x.

Lindner, H. and Kleinebudde, P. (1994) 'Use of Powdered Cellulose for the Production of Pellets by Extrusion/Spheronization', *Journal of Pharmacy and Pharmacology*. Wiley/Blackwell (10.1111), 46(1), pp. 2–7. doi: 10.1111/j.2042-7158.1994.tb03710.x.

Lipinski, B. Hanson, C., Lomax, J., Kitinoja, L., Waite, R. and Searchinger, T. (2013) *Installment 2 of Creating a Sustainable Food Future; Reducing Food Loss and Waste*. Available at: http://www.worldresourcesreport.org. (Accessed: 30 October 2018).

Lisińska, G. and Leszczyński, W. (1989) *Potato science and technology*. Elsevier Applied Science. Available at: https://books.google.co.uk/books/about/Potato_Science_and_Technology.html?id=WYT1S7qhn4sC&redir_esc=y (Accessed: 22 November 2018).

Liu, P., Yu, L., Liu, H., Chen, L. and Li, L. (2009) 'Glass transition temperature of starch studied by a high-speed DSC', *Carbohydrate Polymers*, 77(1), pp. 250–253. doi: 10.1016/j.carbpol.2008.12.027.

Loix, C., Huybrechts, M., Vangronsveld, J., Gielen, M., Keunen, E and Cuypers, A. (2017) 'Reciprocal Interactions between Cadmium-Induced Cell Wall Responses and Oxidative Stress in Plants', *Frontiers in Plant Science*. Frontiers, 8, p. 1867. doi: 10.3389/fpls.2017.01867.

Lu, Z. Fan, L., Zheng, H., Lu, Q., Liao, Y. and Huang, B. (2013) 'Preparation, characterization and optimization of nanocellulose whiskers by simultaneously ultrasonic wave and microwave assisted', *Bioresource Technology*. Elsevier, 146, pp. 82–88. doi: 10.1016/j.biortech.2013.07.047.

Lund, S. and Håkansson, J. (1986) 'Nutritional and growth studies with pea-crop meals and peas for growing—Finishing pigs', *Animal Feed Science and Technology*. Elsevier, 16(1–2), pp. 119–128. doi: 10.1016/0377-8401(86)90055-6.

Luque de Castro, M. D. and Priego-Capote, F. (2007) 'Ultrasound-assisted

crystallization (sonocrystallization)', *Ultrasonics Sonochemistry*. Elsevier, 14(6), pp. 717–724. doi: 10.1016/J.ULTSONCH.2006.12.004.

Lynch, A. J. and Rowland, C. A. (2005) *The history of grinding*. Society for Mining, Metallurgy, and Exploration.

Mæhre, H. K. Dalheim, L., Edvinsen, G. K., Elvevoll, E. O. and Jensen, I-J. (2018) 'Protein Determination-Method Matters.', *Foods (Basel, Switzerland)*. Multidisciplinary Digital Publishing Institute (MDPI), 7(1), pp. 1-11. doi: 10.3390/foods7010005.

Manard, K. and Menard, N. (2002) *Dynamic mechanical analysis in the analysis of polymers and rubbers*, *Encylopedia of Polymer Science and Technology*. John Wiley and Sons. doi: 10.1002/0471440264.pst102.pub2.

Martí-Henneberg, C. Capdevila, F., Arija, V., Pérez, S., Cucó, B., Vizmanos, B. and Fernández-Ballart, J. (1999) 'Energy density of the diet, food volume and energy intake by age and sex in a healthy population', *European Journal of Clinical Nutrition*. Nature Publishing Group, 53(6), pp. 421–428. doi: 10.1038/sj.ejcn.1600770.

McCleary, B. V. and Gibson, T.S. Mugford, D. C. (1992) *Measurement of total starch in cereal products by amyloglucosidase-alpha-amylase method: collaborative study*, *Journal of AOAC International (USA)*. AOAC International. Available at: http://agris.fao.org/agris-search/search.do?recordID=US9747129 (Accessed: 29 October 2018).

McClements, D. J. (2003) *Analysis of Ash and Minerals*, *Analysis of Food Products*. doi: 10.1017/CBO9781107415324.004.

McKendry, P. (2002) 'Energy production from biomass (part 1): overview of biomass', *Bioresource Technology*. Elsevier, 83(1), pp. 37–46. doi: 10.1016/S0960-8524(01)00118-3.

Mena Garza, M. N. (2015) *Redesign of biscuit manufacture*. The University of Nottingham.

Merriam-Webster (2018) *Fibrillation | Definition of Fibrillation*. Available at: https://www.merriam-webster.com/dictionary/fibrillation (Accessed: 22 November 2018).

Meyer, Y. Grosset, J., Chartier, Y. and Cleyet-Marel, J-C. (1988) 'Preparation by two-dimensional electrophoresis of proteins for antibody production: Antibodies against proteins whose synthesis is reduced by auxin in tobacco mesophyll protoplasts', *Electrophoresis*, 9(11), pp. 704–712. doi: 10.1002/elps.1150091105.

Mihranyan, A. and Strømme, M. (2004) 'Capillary condensation of moisture in fractal pores of native cellulose powders', *Chemical Physics Letters*. North-Holland, 393(4–6), pp. 389–392. doi: 10.1016/j.cplett.2004.06.043.

Mijnsbrugge, K. V., Meyermans, H. M., Montagu, M. V., Bauw, G. and Boerjan, W. (2000) 'Wood formation in poplar: identification, characterization, and seasonal variation of xylem proteins', *Planta*. Springer, 210(4), pp. 589–598. doi: 10.2307/23385966.

Mishra, V. (2013) *Extruded Snack Food*. Available at:

https://www.slideshare.net/vinitaPuranik/extruded-snack-food (Accessed: 11 November 2018).

Mitra, S. K. Walters, B. T., Clouse, S. D. and Goshe, M. B. (2009) 'An Efficient Organic Solvent Based Extraction Method for the Proteomic Analysis of Arabidopsis Plasma Membranes', *Journal of Proteome Research*, 8(6), pp. 2752–2767. doi: 10.1021/pr801044y.

Modenbach, A. A. and Nokes, S. E. (2014) 'Effects of Sodium Hydroxide Pretreatment on Structural Components of Biomass Repository Citation'. doi: 10.13031/trans.57.10046.

Moraru, C. I. and Kokini, J. L. (2003) 'Nucleation and Expansion During Extrusion and Microwave Heating of Cereal Foods', *Comprehensive Reviews in Food Science and Food Safety*. Wiley/Blackwell, 2(4), pp. 147–165. doi: 10.1111/j.1541-4337.2003.tb00020.x.

Moreira-Vilar, F. C. Siqueira-Soares, R. de C*.,* Finger-Teixeira, A., Oliveira, D. M de., Ferro, A. P., da Rocha, D. J., Ferrarese, M de. L. L., dos Santos, W. D. and Ferrarese-Filho, O. (2014) 'The Acetyl Bromide Method Is Faster, Simpler and Presents Best Recovery of Lignin in Different Herbaceous Tissues than Klason and Thioglycolic Acid Methods', *PLoS ONE*. Edited by M. Reigosa. Public Library of Science, 9(10), p. e110000. doi: 10.1371/journal.pone.0110000.

Morris, C. and Morris, G. A. (2012) 'The effect of inulin and fructo-oligosaccharide supplementation on the textural, rheological and sensory properties of bread and their role in weight management: A review', *Food Chemistry*, 133(2), pp. 237–248. doi: 10.1016/j.foodchem.2012.01.027.

Morris, K. (1972) *Lipid extraction procedures. In: Work, T.S and Work, E laboratory techniques in biochemistry and molecular biology.* Amsterdam.

Mossé, J. (1990) *Nitrogen to protein conversion factor for ten cereals and six legumes or oilseeds. A reappraisal of its definition and determination. Variation according to species and to seed protein content. Food Chemistry, 38(1), pp. 18-24.*

Muhd Julkapli, N., Akil, H. M. and Ahmad, Z. (2011) 'Preparation, properties and applications of chitosan-based biocomposites/blend materials: A review', *Composite Interfaces*, 18(6), pp. 449–507. doi: 10.1163/156855411X610232.

Nemoto, S. Ueno, A., Watthanaphanit, A., Hieda, J. and Saito, N. (2017) 'Crystallinity and surface state of cellulose in wet ball-milling process', *Journal of Applied Polymer Science*. John Wiley & Sons, Ltd, 134(22), pp 44903-44910. doi: 10.1002/app.44903.

Nor, N. Carr, A., Hardacre, A. and Brennan, C. (2013) 'The Development of Expanded Snack Product Made from Pumpkin Flour-Corn Grits: Effect of Extrusion Conditions and Formulations on Physical Characteristics and Microstructure', *Foods*. Multidisciplinary Digital Publishing Institute, 2(2), pp. 160–169. doi: 10.3390/foods2020160.

Norman, A. G. (1937) ‘The hemicelluloses: Extraction and preparation.’, *The Biochemical journal*. Portland Press Ltd, 31(9), pp. 1579–85. Available at: http://www.ncbi.nlm.nih.gov/pubmed/16746493 (Accessed: 29 October 2018).

Norman, A. G. and Shrikhande, J. G. (1935) ‘The hemicelluloses: The association of hemicelluloses with lignin.’, *The Biochemical journal*. Portland Press Ltd, 29(10), pp. 2259–66. Available at: http://www.ncbi.nlm.nih.gov/pubmed/16745902 (Accessed: 29 October 2018).

Oksman, K. Matthew, A. P., Bondeson, D. and Kvien, I. (2006) ‘Manufacturing process of cellulose whiskers/polylactic acid nanocomposites’, *Composites Science and Technology*, 66(15), pp. 2776–2784. doi: 10.1016/j.compscitech.2006.03.002.

Ozer, E. A. Ibanoglu, S., Ainsworth, P. and Yagmur, P. (2004) ‘Expansion characteristics of a nutritious extruded snack food using response surface methodology’, *European Food Research and Technology*. Springer-Verlag, 218(5), pp. 474–479. doi: 10.1007/s00217-004-0884-7.

Pääkkö, M. Ankerfors, M., Kosonen, H., Nykänen, A., Ahola, S., O' Sterberg, M., Ruokolainen, J., Laine, J., Larsson, P. T., Ikkala, M. and Lindströ, T. (2007) ‘Enzymatic Hydrolysis Combined with Mechanical Shearing and High-Pressure Homogenization for Nanoscale Cellulose Fibrils and Strong Gels’, *Biomacromolecules*, 8(6), pp. 1934–1941. doi: 10.1021/bm061215p.

Paes, S. S. (2008) *Understanding the mechanical properties of biopolymer films*. The University of Nottingham thesis.

Paes, S. S., Sun, S., MacNaughtan, W., Ibbett, R., Ganster, J., Foster, T. J. and Mitchell, J. R. (2010) ‘The glass transition and crystallization of ball milled cellulose’, *Cellulose*. Springer Netherlands, 17(4), pp. 693–709. doi: 10.1007/s10570-010-9425-7.

Pagán, J., Ibarz, A., Liorca, M., Pagán, A. and Barbosa-Cánovas, G. V. (2001) ‘Extraction and characterization of pectin from stored peach pomace’, *Food Research International*. Elsevier, 34(7), pp. 605–612. doi: 10.1016/S0963-9969(01)00078-3.

Park, I. M. Ibáñez, A. M., Zhong, F. and Shoemaker, C. F. (2007) ‘Gelatinization and pasting properties of waxy and non-waxy rice starches’, *Starch/Staerke*. Wiley-Blackwell, 59(8), pp. 388–396. doi: 10.1002/star.200600570.

Peng, F. Peng, P., Xu, F. and Sun, R-C. (2012) ‘Fractional purification and bioconversion of hemicelluloses’, *Biotechnology Advances*, 30(4), pp. 879–903. doi: 10.1016/j.biotechadv.2012.01.018.

Pereira, H. (2007) ‘The chemical composition of cork’, *Biology, Production and Uses*. Elsevier Science B.V., pp. 55–99. doi: 10.1016/B978-044452967-1/50005-4.

Peressini, D. Foschia, M., Tubaro, F. and Sensidoni, A. (2015) ‘Impact of soluble dietary fibre on the characteristics of extruded snacks’, *Food Hydrocolloids*. Elsevier, 43, pp. 73–81. doi: 10.1016/j.foodhyd.2014.04.036.

Peressini, D. and Sensidoni, A. (2009) 'Effect of soluble dietary fibre addition on rheological and breadmaking properties of wheat doughs', *Journal of Cereal Science*, 49(2), pp. 190–201. doi: 10.1016/j.jcs.2008.09.007.

Petersson, L., Kvien, I. and Oksman, K. (2007) 'Structure and thermal properties of poly(lactic acid)/cellulose whiskers nanocomposite materials', *Composites Science and Technology*. Elsevier, 67(11–12), pp. 2535–2544. doi: 10.1016/j.compscitech.2006.12.012.

Pickett, K. E. Kelly, S., Brunner, E., Lobstein, T. and Wilkinson, R. G. (2005) 'Wider income gaps, wider waistbands? An ecological study of obesity and income inequality.', *Journal of epidemiology and community health*. BMJ Publishing Group Ltd, 59(8), pp. 670–4. doi: 10.1136/jech.2004.028795.

Piernas, C. and Popkin, B. M. (2010a) 'Snacking Increased among U.S. Adults between 1977 and 2006', *The Journal of Nutrition*. Oxford University Press, 140(2), pp. 325–332. doi: 10.3945/jn.109.112763.

Piernas, C. and Popkin, B. M. (2010b) 'Trends In Snacking Among U.S. Children', *Health Affairs*. Health Affairs , 29(3), pp. 398–404. doi: 10.1377/hlthaff.2009.0666.

Pratt, C. D. (1970) *Twenty Years of Confectionery and Chocolate Progress*. Edited by C. . Pratt et al. Westport Connecticut: Avi Publishing Co. Available at: http://www.amazon.de/dp/0870550675.

Preece, I. A. (1944) 'Some hemicellulose extraction methods.', *The Biochemical journal*. Portland Press Ltd, 38(5), pp. 402–8. Available at: http://www.ncbi.nlm.nih.gov/pubmed/16747823 (Accessed: 29 October 2018).

Pretty, J. N., Morison, J. I. L. and Hine, R. E. (2003) 'Reducing food poverty by increasing agricultural sustainability in developing countries', *Agriculture, Ecosystems and Environment*, 95(1), pp. 217–234. doi: 10.1016/S0167-8809(02)00087-7.

Public Health England. (2016) *Government Dietary Recommendations Government recommendations for energy and nutrients for males and females aged 1-18 years and 19+ years*. Available at: www.gov.uk/phe (Accessed: 30 October 2018).

Quiroga Ledezma, C. C. (2018) 'Starch Interactions With Native and Added Food Components', *Starch in Food*. Woodhead Publishing, pp. 769–801. doi: 10.1016/B978-0-08-100868-3.00020-2.

Raschip, I. E., Yakimets, I., Martin, C., Paes, S. S., Vasile, C. and Mitchell, J. R. (2008) 'Effect of water content on thermal and dynamic mechanical properties of xanthan powder: A comparison between standard and novel techniques', *Powder Technology*, 182(3), pp. 436–443. doi: 10.1016/j.powtec.2007.07.010.

Rattihallik, V. (2010) *Water binding properties of cellulosic materials*. University of Nottingham.

Raven, P. H., Evert, R. F. and Eichorn, S. E. (1999) *Biology of Plants*. 6th edn. Edited by F. and Company. New York.

Redgwell, R. Trovato, V., Merinat, S., Curti, D., Hediger, S. and Manez, A. (2003) 'Dietary fibre in cocoa shell: characterisation of component polysaccharides', *Food Chemistry*. Elsevier, 81(1), pp. 103–112. doi: 10.1016/S0308-8146(02)00385-0.

Reichert, R. D. and MacKenzie, S. L. (1982) 'Composition of peas (Pisum sativum) varying widely in protein content', *Journal of Agricultural and Food Chemistry*. American Chemical Society, 30(2), pp. 312–317. doi: 10.1021/jf00110a024.

Reidpath, D. D., Burns, C., Garrard, J., Mahoney, M. and Townsend, M. (2002) 'An ecological study of the relationship between social and environmental determinants of obesity', *Health & Place*. Pergamon, 8(2), pp. 141–145. doi: 10.1016/S1353-8292(01)00028-4.

Reyniers, S., De Brier, N., Matthijs, S., Brijs, K. and Delcour, J. A. (2018) 'Impact of physical and enzymatic cell wall opening on the release of pre-gelatinized starch and viscosity forming potential of potato flakes', *Carbohydrate Polymers*, 194, pp. 401–410. doi: 10.1016/j.carbpol.2018.04.057.

Robertson, J. B. and Van Soest, P. J. (1981) 'The Detergent System of Analysis', in James, W. P. T. and Theander, O. (eds) *The Analysis of Dietary Fibre in Food*. New York, pp. 123–158.

Rolle, R. (2006) *Postharvest Management of Fruit and Vegetables in the Asia-Pacific Region*. Available at: www.apo-tokyo.org (Accessed: 12 November 2018).

Ros-Freixedes, R. and Estany, J. (2014) 'On the Compositional Analysis of Fatty Acids in Pork', *Journal of Agricultural, Biological, and Environmental Statistics*, 19(1), pp. 136–155. doi: 10.1007/s13253-013-0162-x.

Ros, J. M., Schols, H. A. and Voragen, A. G. J. (1996) 'Extraction, characterisation, and enzymatic degradation of lemon peel pectins', *Carbohydrate Research*. Elsevier, 282(2), pp. 271–284. doi: 10.1016/0008-6215(95)00389-4.

Rosenthal, A. J. (2015) 'Instrumental characterisation of textural properties of solid and semi-solid food', *Modifying Food Texture*. Woodhead Publishing, pp. 89–105. doi: 10.1016/B978-1-78242-334-8.00004-3.

Royal botanic gardens kew science. (2003) *Pisum sativum L. | Plants of the World Online | Kew Science*. Available at: http://powo.science.kew.org/taxon/urn:lsid:ipni.org:names:60454055-2#distribution-map (Accessed: 29 October 2018).

Royall, P. G. Huang, C-Y., Tang, S-W. J., Duncan, J., Van-de-Velde, G. and Brown, M. B. (2005) 'The development of DMA for the detection of amorphous content in pharmaceutical powdered materials', *International Journal of Pharmaceutics*, 301(1–2), pp. 181–191. doi: 10.1016/j.ijpharm.2005.05.015.

Ruan, W. H. Zhang, M. Q., Rong, M. Z. and Friedrich, K. (2004) *Mechanical Properties of Nanocomposites from Ball Milling Grafted Nano-Silica/Polypropylene Block Copolymer*, *Polymers & Polymer Composites*. Available at:

https://pdfs.semanticscholar.org/a219/70b171641b026fbf6852bcbfdea0cffddc9b.pdf (Accessed: 22 November 2018).

Sachez, T., Dufour, D., Moreno, I. X. and Ceballos, H. N. (2010) 'Comparison of Pasting and Gel Stabilities of Waxy and Normal Starches from Potato, Maize, and Rice with Those of a Novel Waxy Cassava Starch under Thermal, Chemical, and Mechanical Stress', *Journal Agricultural and Food Chem*istry 58, p. 5093. doi: 10.1021/jf1001606.

Saha, D. and Bhattacharya, S. (2010) 'Hydrocolloids as thickening and gelling agents in food: a critical review.', *Journal of Food Science and Technology*. Springer, 47(6), pp. 587–97. doi: 10.1007/s13197-010-0162-6.

Saheb, D. N. and Jog, J. P. (1999) 'Natural fiber polymer composites: A review', *Advances in Polymer Technology*. Wiley-Blackwell, 18(4), pp. 351–363. doi: 10.1002/(SICI)1098-2329(199924)18:4<351:AID-ADV6>3.0.CO;2-X.

Saito, A. (1967) 'Fisheries Research Board of Canada', *Kagaku To Seibutsu*, 5(8), pp. 466–466. doi: 10.1271/kagakutoseibutsu1962.5.466.

Saito, T. Yoshiharu, N., Putaux, J -L., Vignon, M. and Isogai, A. (2006) 'Homogeneous Suspensions of Individualized Microfibrils from TEMPO-Catalyzed Oxidation of Native Cellulose'. American Chemical Society. doi: 10.1021/BM060154S.

Saito, T., Hirota, M., Tamura, N., Kimura, S., Fukuzumi, H., Leux, L. and Isogai, A. (2009) 'Individualization of Nano-Sized Plant Cellulose Fibrils by Direct Surface Carboxylation Using TEMPO Catalyst under Neutral Conditions', *Biomacromolecules*. American Chemical Society, 10(7), pp. 1992–1996. doi: 10.1021/bm900414t.

Sandarani, M. (2017) 'A Review: Different Extraction Techniques of Pectin', *Journal of Pharmacognosy & Natural Products*. OMICS International, 03(03), pp. 1–5. doi: 10.4172/2472-0992.1000143.

Santoni, V., Bellini, C. and Caboche, M. (1994) 'Use of two-dimensional protein-pattern analysis for the characterization of Arabidopsis thaliana mutants', *Planta*. Springer-Verlag, 192(4), pp. 557–566. doi: 10.1007/BF00203594.

Sato, N. and Tsuzuki, M. (2011) 'Isolation and Identification of Chloroplast Lipids', in *Methods in Molecular Biology (Clifton, N.J.)*, pp. 95–104. doi: 10.1007/978-1-60761-925-3_9.

Schubert, H. (1993) 'Instantization of powdered food products', *Chemie Ingenieur Technik*, 1(33), pp. 28–45. Available at: https://www.researchgate.net/publication/282054092_Instantization_of_powdered_food_products (Accessed: 22 November 2018).

Schwartzberg, H. G., Wu, J. P. C., Nussinovitch, A. and Mugerwa, J. (1995) 'Modelling deformation and flow during vapor-induced puffing', *Journal of Food Engineering*. Elsevier, 25(3), pp. 329–372. doi: 10.1016/0260-8774(94)00015-2.

Serk, H. (2015) 'Cellular Aspects of Lignin Biosynthesis in Xylem Vessels of Zinnia and Arabidopsis'. Available at:

https://www.semanticscholar.org/paper/Cellular-Aspects-of-Lignin-Biosynthesis-in-Xylem-of-Serk/031476f6235082c9fb0c0a0522315c10c20f3ce2 (Accessed: 8 November 2018).

Shogren, R. L. (1992) 'Effect of moisture content on the melting and subsequent physical aging of cornstarch', *Carbohydrate Polymers*. Elsevier, 19(2), pp. 83–90. doi: 10.1016/0144-8617(92)90117-9.

Singh, N., Singh, J., Kaur, L., Singh Sodhi, N. and Singh Gill, B. (2003) 'Morphological, thermal and rheological properties of starches from different botanical sources', *Food Chemistry*. Elsevier, 81(2), pp. 219–231. doi: 10.1016/S0308-8146(02)00416-8.

Siqueira, G. Oksman, K., Tadokoro, S. and Matthew, A. P. (2016) 'Re-dispersible carrot nanofibers with high mechanical properties and reinforcing capacity for use in composite materials', *Composites Science and Technology*. Elsevier, 123, pp. 49–56. doi: 10.1016/j.compscitech.2015.12.001.

Siró, I. and Plackett, D. (2010) 'Microfibrillated cellulose and new nanocomposite materials: a review', *Cellulose*. Springer Netherlands, 17(3), pp. 459–494. doi: 10.1007/s10570-010-9405-y.

Sivam, A. S., Sun-Waterhouse, D., Quek, S. and Perera, C. O. (2010) 'Properties of bread dough with added fiber polysaccharides and phenolic antioxidants: a review.', *Journal of food science*. Wiley-Blackwell, 75(8), pp. R163-74. doi: 10.1111/j.1750-3841.2010.01815.x.

Sluiter, A., Hames, B., Ruiz, R., Scarlata, C., Sluiter, J., Templeton, D. and Crocker, D. (2008) *Determination of Structural Carbohydrates and Lignin in Biomass: Laboratory Analytical Procedure (LAP) (Revised July 2011)*. Available at: http://www.nrel.gov/biomass/analytical_procedures.html (Accessed: 29 October 2018).

van der Sman, R. G. M., Vollebregt, H. M., Meinders, M. B. J. and Beri, A. (2018) 'Effects of filler ingredients on the structure and texture of starchy, extruded snacks', *Food Structure*, 18, pp. 1–13. doi: 10.1016/j.foostr.2018.10.001.

van der Sman, R. G. M. and Broeze, J. (2013) 'Structuring of indirectly expanded snacks based on potato ingredients: A review', *Journal of Food Engineering*. Elsevier, 114(4), pp. 413–425. doi: 10.1016/J.JFOODENG.2012.09.001.

Sobue, H. and Fukuhara, S. (1960) 'No Title', *Kogyo Kagaku Zasshz*, 520(63).

Solala, I. Volperts, A., Andersone, A., Dizhbite, T., Mironova-Ulmane, N., Vehniäinen, A., Pere, J. and Vuorinen, T. (2012) 'Mechanoradical formation and its effects on birch kraft pulp during the preparation of nanofibrillated cellulose with Masuko refining', *Holzforschung*, 66(4), pp.477-483. doi: 10.1515/hf.2011.183.

Spence, K. L., Venditti, R. A., Rojas, O. J., Habibi, Y. and Pawlak, J. J. (2010) 'The effect of chemical composition on microfibrillar cellulose films from wood pulps: water interactions and physical properties for packaging

applications', *Cellulose*. Springer Netherlands, 17(4), pp. 835–848. doi: 10.1007/s10570-010-9424-8.

Stuart, T. (2009) *Waste : uncovering the global food scandal*. W.W. Norton & Co. Available at: https://www.slideshare.net/bellajohnson12/waste-uncovering-the-global-food-scandal-download-pdf-69084052.

Stubberud, L., Arwidsson, H. G., Larsson, A. and Graffner, C. (1996) 'Water solid interactions II. Effect of moisture sorption and glass transition temperature on compactibility of microcrystalline cellulose alone or in binary mixtures with polyvinyl pyrrolidone', *International Journal of Pharmaceutics*. Elsevier, 134(1–2), pp. 79–88. doi: 10.1016/0378-5173(95)04439-6.

Sullo, A. and Foster, T. J. (2010) 'Characterisation of Starch / Cellulose blends', *Annual transactions of the Nordic Rheology Society,* 18, pp. 1–8. Available at: http://citeseerx.ist.psu.edu/viewdoc/download?doi=10.1.1.660.6042&rep=rep1&type=pdf (Accessed: 22 October 2018).

Suopajärvi, T., Liimatainen, H. and Niinimäki, J. (2010) 'Fragment analysis of different size-reduced lignocellulosic pulps by hydrodynamic fractionation', *Cellulose*, 19, pp. 237–248. doi: 10.1007/s10570-011-9615-y.

Swatloski, R. P., Rogers, R. D. and Holbrey, J. D. (2002) 'Dissolution and processing of cellulose using ionic liquids'. Available at: https://patents.google.com/patent/WO2003029329A2 (Accessed: 29 October 2018).

Syntsya, A., Copikova, J. and Brus, J. (2000) '13C CP/MAS NMR Spectra of Pectins: a Peak - Fitting Analysis in the C -6 Region', *Czech Journal of Food Science*, 21(1), pp. 1–12.

Szcześniak, L., Rachocki, A. and Tritt-Goc, J. (2008) 'Glass transition temperature and thermal decomposition of cellulose powder', *Cellulose*. Springer Netherlands, 15(3), pp. 445–451. doi: 10.1007/s10570-007-9192-2.

Taggart, P. and Mitchell, J, R. (2009) 'Starch', in Phillips, G. O. and Williams, P. A. (eds) *Handbook of hydrocolloids*. 2nd edn. Cambridge: Woodhead Publishing Limited, pp. 108–142.

Talbott, L. D. and Ray, P. M. (1992) 'Molecular size and separability features of pea cell wall polysaccharides : implications for models of primary wall structure.', *Plant Physiology*. American Society of Plant Biologists, 98(1), pp. 357–68. doi: 10.1104/PP.98.1.357.

Thakur, B. R., Singh, R. K., Handa, A. K. and Rao, R. A. (1997) 'Chemistry and uses of pectin — A review', *Critical Reviews in Food Science and Nutrition*. Taylor & Francis Group , 37(1), pp. 47–73. doi: 10.1080/10408399709527767.

The Green Pea Company. (2019) *The Green Pea Company*. Available at: http://greenpeaco.com/ (Accessed: 12 February 2019).

The World Bank. (2017) *Population growth (annual %)* | *Data*. Available at: https://data.worldbank.org/indicator/SP.POP.GROW (Accessed: 30 October 2018).

Thiex, N., Novotny, L. and Crawford, A. (2012) 'Determination of ash in animal feed: AOAC Official Method 942.05 revisited', *Journal of AOAC International*, 95(5), pp. 1392–1397. doi: 10.5740/jaoacint.12-129.

Torcello-Gómez, A., Gedi, M. A., Ibbett, R., Nawaz Husain, K., Briars, R. and Gray, D. (2019) 'Chloroplast-rich material from the physical fractionation of pea vine (Pisum sativum) postharvest field residue (Haulm)', *Food Chemistry*, 272, pp. 18–25. doi: 10.1016/j.foodchem.2018.08.018.

Treviño, J., Centeno, C. and Caballero, R. (1987) 'The chemical composition of pea plant parts as related to harvesting time', *Animal Feed Science and Technology*. Elsevier, 16(4), pp. 305–309. doi: 10.1016/0377-8401(87)90019-8.

Turbak, A. F., Snyder, F. W. and Sandberg, K. R. (1982) 'Microfibrillated cellulose, a new cellulose product: properties, uses, and commercial potential', *Journal of Applied Polymer Science: Applied Polymer Symposium; (United States)*, 37. Available at: https://www.osti.gov/biblio/5062478-microfibrillated-cellulose-new-cellulose-product-properties-uses-commercial-potential (Accessed: 22 November 2018).

Unites States Department of Agriculture. (2018) *microcrystalline cellulose - Agricultural Marketing Service (AMS) Search Results*. Available at: https://search.usa.gov/search?utf8=✓&affiliate=usda-ams&query=microcrystalline+cellulose&commit=Search (Accessed: 20 November 2018).

UPM. (2019) *UPM about*. Available at: https://www.upm.com/ (Accessed: 15 February 2019).

USDA. (1973) 'Energy value of foods', *Journal of Chemical Education*. Available at: https://pubs.acs.org/doi/pdf/10.1021/ed053p80?src=recsys (Accessed: 24 October 2018).

Utz, K. (1986) 'The interocclusal tactile fine sensitivity of the natural teeth as studied by aluminium oxide particles', *Deut Zahnarztl*, 41, pp. 313–315.

Vermeire, A., Keleb, E. I., Kiekens, F., Van Driessche, I., Hoste, S., Remon, J. P. and Vervaet, C. (2005) 'Tablets Prepared by Single-Step Granulation/Tabletting: Interparticulate Binding Mechanism and Stability', *Pharmaceutical Development and Technology*. Taylor & Francis, 10(3), pp. 397–403. doi: 10.1081/PDT-65690.

Vittadini, E., Dickinson, L. and Chinachoti, P. (2001) '1H and 2H NMR mobility in cellulose', *Carbohydrate Polymers*. Elsevier, 46(1), pp. 49–57. doi: 10.1016/S0144-8617(00)00282-4.

Voragen, A. G. J., Coenen, G-J., Verhoef, R. P. and Schols, H. A. (2009) 'Pectin, a versatile polysaccharide present in plant cell walls', *Structural Chemistry*. Springer US, 20(2), pp. 263–275. doi: 10.1007/s11224-009-9442-z.

Wada, M., Okano, T., Sugiyama, J. and Horii, F. (1995) 'Characterization of tension and normally lignified wood cellulose inPopulus maximowiczii', *Cellulose*, 2(4), pp. 223–233. doi: 10.1007/BF00811814.

Wang, D. (2003) *Wood Chemistry Class, Structure and Properties of*

Hemicellulose, *Http://Web.Nchu.Edu.Tw/Pweb/Users/Taiwanfir/Lesson/10393.Pdf*. Available at: http://web.nchu.edu.tw/pweb/users/taiwanfir/lesson/10393.pdf (Accessed: 6 November 2018).

Wang, S.-S., Han, Y-H., Chen, J-L., Zhang, D-C., Shi, X-X., Ye, Y-X., Chen, D-L. and Li, M. (2018) 'Insights into Bacterial Cellulose Biosynthesis from Different Carbon Sources and the Associated Biochemical Transformation Pathways in Komagataeibacter sp. W1', *Polymers*, Multidisciplinary Digital Publishing Institute, 10(9), p. 963. doi: 10.3390/polym10090963.

Wang, W., Vignani, R., Scali, M. and Cresti, M. (2006) 'A universal and rapid protocol for protein extraction from recalcitrant plant tissues for proteomic analysis', *Electrophoresis*, 27(13), pp. 2782–2786. doi: 10.1002/elps.200500722.

Wang, W., Ma, X., Xu, Y., Cao, Y., Jiang, Z., Ding, T., Ye, X. and Liu, D. (2015) 'Ultrasound-assisted heating extraction of pectin from grapefruit peel: Optimization and comparison with the conventional method', *Food Chemistry*, 178, pp. 106–114. doi: 10.1016/j.foodchem.2015.01.080.

Wen, J.-L., Xiao, L-P., Sun, Y-C., Sun, S-N., Xu, F., Sun, R-C. and Zhang, X-L. (2011) 'Comparative study of alkali-soluble hemicelluloses isolated from bamboo (Bambusa rigida)', *Carbohydrate Research*. Elsevier, 346(1), pp. 111–120. doi: 10.1016/J.CARRES.2010.10.006.

Whistler, R. L., BeMiller, J. N. and Paschall, E. F. (1984) *Starch : chemistry and technology*. Academic Press.

Williams, J. and Davies, K. (2013) 'Chips and manufacture thereof'. Available at: https://patents.google.com/patent/WO2013171264A1 (Accessed: 14 October 2018).

Williams, K. M., Fox, P. and Marshall, T. (1995) 'a Comparison of Protein Assays for the Determination of the Protein Concentration of Beer', *Journal of the Institute of Brewing*. Wiley-Blackwell, 101(5), pp. 365–369. doi: 10.1002/j.2050-0416.1995.tb00874.x.

Wills, K., Emery, T., Thompson, I. and Giles, R. (1988) 'Alumina trihydrate use in toothpaste', *Manufacturing Chemist*, 10, pp. 41–45.

Winkworth-Smith, C. (2014) *Cellulose composite structures – by design*. University of Nottingham.

Wüstenberg, T. (ed.) (2014) *Cellulose and Cellulose Derivatives in the Food Industry*. Weinheim, Germany: Wiley-VCH Verlag GmbH & Co. KGaA. doi: 10.1002/9783527682935.

Xu, C. and Ferdosian, F. (2017) *Conversion of Lignin into Bio-Based Chemicals and Materials*. Berlin, Heidelberg: Springer Berlin Heidelberg (Green Chemistry and Sustainable Technology). doi: 10.1007/978-3-662-54959-9.

Yan, J., Hu, J., Yang, R., Zhang, Z. and Zhao, W. (2018) 'Innovative Nanofibrillated Cellulose from Rice Straw as Dietary Fiber for Enhanced Health Benefits Prepared by a Green and Scale Production Method', *ACS Sustainable Chemistry & Engineering*. American Chemical Society, 6(3), pp.

3481–3492. doi: 10.1021/acssuschemeng.7b03765.

Yang, H., Yan, R., Chin, T., Liang, D. T., Chen, H. and Zheng, C. (2004) 'Thermogravimetric analysis - Fourier transform infrared analysis of palm oil waste pyrolysis', *Energy and Fuels*. American Chemical Society , 18(6), pp. 1814–1821. doi: 10.1021/ef030193m.

Yang, H., Yan, R., Chen, H., Lee, D. H. and Zheng, C. (2007) 'Characteristics of hemicellulose, cellulose and lignin pyrolysis', *Fuel*. Elsevier, 86(12–13), pp. 1781–1788. doi: 10.1016/J.FUEL.2006.12.013.

York, W. S., Darvill, A. G., McNeil, M., Stevenson, T. T. and Albersheim, P. (1986) 'Isolation and characterization of plant cell walls and cell wall components', *Methods in Enzymology*. Academic Press, 118, pp. 3–40. doi: 10.1016/0076-6879(86)18062-1.

Yu, Y. and Wu, H. (2011) 'Effect of ball milling on the hydrolysis of microcrystalline cellulose in hot-compressed water', *AIChE Journal*. Wiley-Blackwell, 57(3), pp. 793–800. doi: 10.1002/aic.12288.

Zhao, H., Kwak, J., Wang, Y., Franz, J. A., White, J. and Holladay, J. E. (2006) 'Effects of Crystallinity on Dilute Acid Hydrolysis of Cellulose by Cellulose Ball-Milling Study'. *Energy fuels*, 20(2), pp.807-811. American Chemical Society . doi: 10.1021/EF050319A.

Zhao, H.-P., Feng, X.-Q. and Gao, H. (2007) 'Ultrasonic technique for extracting nanofibers from nature materials', *Applied Physics Letters*. American Institute of Physics, 90(7), p. 073112. doi: 10.1063/1.2450666.

Zimmermann, T., Bordeanu, N. and Strub, E. (2010) 'Properties of nanofibrillated cellulose from different raw materials and its reinforcement potential', *Carbohydrate Polymers*. Elsevier, 79(4), pp. 1086–1093. doi: 10.1016/j.carbpol.2009.10.045.

Zizza, C., Siega-Riz, A. M. and Popkin, B. M. (2001) 'Significant Increase in Young Adults' Snacking between 1977–1978 and 1994–1996 Represents a Cause for Concern!', *Preventive Medicine*. Academic Press, 32(4), pp. 303–310. doi: 10.1006/PMED.2000.0817.

Chapter 9 Appendix

Enzyme digestion of pea haulm pulp as a route to modify textural, rheological and nutritional properties for food applications

Roger N Ibbett*, Randa M Darwish, Hoi Man Lo, Jade B Phillips, David A Gray, Tim J Foster

* corresponding author (roger.ibbett@nottingham.ac.uk)

School of Biosciences, Division of Food Science, University of Nottingham, Sutton Bonington Campus. Loughborough, LE125RD, UK

Acknowledgements

This work was supported by the UK Engineering and Physical Sciences Research Council, through the Circular Economy programme , grant no EP/P008771/1.

Keywords

Pea-haulm; pulp; viscosity; enzyme; digestion; modelling; properties

Abstract

The pulp generated from the juicing of pea haulm is a green agricultural residue which represents an un-utilised but challenging nutritional resource, where there is a need for additional processing to improve acceptability for food or feed products. As a route to improve acceptability, the effects of enzyme digestion on the compositional and material characteristics of haulm pulp have been studied using different techniques, including novel real-time monitoring of viscosity of pulp slurries and suspensions. Kinetic modelling of suspension rheology has provided unique insights into the action of digestive enzymes on particle content, size and shape, important for the handling of wet ingredients and also for optimising sensory and nutritional attributes. The efficiency of different commercial enzymes has been evaluated and comparisons have also been made with the digestion of a broccoli stalk agricultural by-product. Particular consideration has been given to the fibrous nature of haulm pulp, as a model for similar process residues, especially the extent of recalcitrance of this fraction, which consists of cellulosic and lignocellulosic components. After extended digestion this most highly recalcitrant fraction remained as a final residue, but may have material applications, for example as a fiber feedstock in paper or packaging.

Introduction

The harvesting of many agricultural crops leads to the generation of green residues, consisting of stems, leaves and other plant structures. Such residues may contain useful macro- and micro-nutritional components (Galanakis 2012, Anal A 2017), but may have complex morphological and chemical organisation which may limit their value as food products for humans or in animal feed applications (Elleuch *et al*. 2011). In addition, materials from stem and other supporting structures may contain vascular and other fibrous tissues, which may require significant processing and formulation to improve their sensory and textural characteristics (McKee and Latner 2000). Green crop residues therefore represent an un-tapped but challenging nutritional resource, where further development effort would be justified to establish process routes for commercialisation as food or feed products. Also, different harvesting and logistical regimes might be required for utilisation of such residues, also incorporating alternative technologies at farm or factory level. Additionally, an assessment of any existing uses of such green residues would be required, to ascertain the acceptability of diversion of agricultural materials for new products (Henriksen and Breland 1999).

One green residue of recurring interest is that produced as a consequence of industrial harvesting of vine peas (Morrison and Pirie 1961). Modern harvesters take up the entire pea plant and separate the peas from the remainder of the green plant material. The peas are transported immediately for freezing and the green residue (haulm) is allowed to fall back onto the soil. The logistics and technical mechanism of harvesting could therefore be modified to allow collection of an amount of the haulm from the harvester rear outlet, which would be partly comminuted and homogenised as desired

for any further processing. Previous work has shown that there is great potential in the physical juicing of such haulm material, to generate a liquor feedstock for protein extraction (Aletor *et al*. 2002), or for production of wet or dry food ingredients rich in micro-nutrients (Gaynor and Hickey 1999). However, whilst the routes for processing of haulm juice are relatively straight forward, its production leads to generation of a less amenable residue consisting of the pressed haulm pulp. Work is therefore required to investigate if such pulp material could also have beneficial human or animal nutritional applications (Anandan *et al*. 2012). The haulm pulp is rich in both soluble and insoluble dietary fibre, together with smaller amounts of digestible carbohydrates, protein and important micro-nutrients (Torcello-Gómez *et al*. 2018). However, as described above, this fibrous fraction is likely to be unacceptable from a textural perspective for human sensory demand, but may also be difficult to manipulate from a mechanical perspective in a food processing environment.

This current study has focussed on the application of enzyme digestion as a means improving textural quality and nutritional accessibility of pea haulm pulp. Enzyme digestion is widely used in the food industry for hydrolysis of specific biopolymer bonds within a fruit or vegetable feedstock, designed to increase fluidity and solubility and/or to increase nutritional accessibility of specific functional components (Nagodawithana and Reed 1993). Haulm pulp is expected to consist mainly of cell-wall polymeric material, derived from all anatomical components of the plant remaining after separation of the peas, consisting of main and branched stems, tendrils and petioles, leaves and pods, where the majority of intra-cellular contents have been physically removed by pressing, including the chloroplast organelles and the cell sap. The material therefore serves as a useful model for the

development of methodologies for enzyme digestion and processing of other mixed green residues which might be available as by-products from agri-food operations (Gurmessa *et al* 2016).

In this study the effect of enzyme digestion on the compositional and material characteristics of haulm pulp were investigated using a variety of techniques, including a novel approach for real-time monitoring of rheological and microstructural properties of pulp suspensions. The rheology or flow of pulp suspensions provides a unique measure of the action of digestive enzymes on particle content, size and shape, which has a direct influence on the handling of wet ingredients and also on sensory and nutritional attributes. Rheological models for pulp suspension behaviour have been adapted from those developed for the polymer and paper industries, which have been used to evaluate the efficiency of comparative commercial enzymes and to compare with the digestion of broccoli stalk material, as a contrasting agricultural by-product. Particular consideration has been given to the fibrous nature of haulm pulp, as an exemplar for similar materials, especially the extent of recalcitrance of this fraction, which consists of cellulosic and lignocellulosic components.

Materials and Methods

Samples

Fresh pea haulm was collected from the Green Pea Company Ltd (www.greenpeaco.com), during commercial harvesting operations in the UK. The haulm was retrieved directly from the outlet of the harvester and immediately bagged for transport and further processing. A preliminary wash was carried out to remove any soil or stone contaminants, followed by hydro-extraction to remove entrained moisture. This course-cut material was pressed using a commercial twin-screw juicer (Angel 7500, www.Juicers.co.uk), which separated the green intra-cellular liquor contents from the cell-wall pulp residue. The fibrous residue was further washed and hydro-extracted before freezing at -18^{o}C for storage before experiments. Fresh broccoli stalks were obtained by manual cutting of broccoli heads purchased from a local supermarket. The cutting simulated the operation where florets would be separated from the stalks either in the kitchen or in a factory environment. Samples were again frozen at -18^{o}C for storage before experiments.

Both haulm pulp and broccoli stalk feedstocks were further mixed and blended with controlled amounts of water using a domestic food blender (BLX51, Kenwood UK Ltd). A fixed blending time of 2 minutes at a 5 wt% solids content was used to reduce visible particle dimensions to the order of 1-4 mm. Additional blending achieved little further reduction in particle dimensions, so the texture of the 2 minute blended suspension was considered to be a consistent starting state, against which the effect of enzymatic treatment could be assessed.

Three comparative commercial enzymes were selected for this study, from a consideration of the composition of the broccoli stalk and haulm pulp feedstocks. Depol 692L is a broad spectrum carbohydrase, including pectinase, with activities according the manufacturer of 800u/g cellulase, and 535 u/g pectinase (endogalacturonase) (Biocatalysts Ltd). Cellulase 13L is a cellulase with related β-glucanase and β-glucosidase side activities, with activity according to the manufacturer of 1500 u/g (Biocatalysts Ltd). Cellic CTec-2 is a mixture cellulase and hemicellulase enzymes, formulated for the digestion of lignocellulosic biomass, with cellulase activity determined as 203 FPU/g and β-glucosidase activity as 4900 CPU/g (Novozymes A/S) (Rodrigues *et al*. 2015). All three products were supplied as liquid concentrates. All were quoted as having optimum activity around 50-60ºC and around pH4-6.

Characterisation

Sample composition

Moisture contents of materials were determined by gravimetry. The proximate compositions of the initial feedstocks were determined using standard methods. A total acid hydrolysis protocol was applied to convert all polysaccharides to monomeric form, both for starting biomass material and where required for solid residues following treatments (Ibbett *et al*. 2014). Analysis of monomeric sugars was performed by high-pressure ion chromatography with pulsed amphoteric detection (HPAEC-PAD), using a PA20 column (Dionex UK). A combined program was operated initially with 10 mM NaOH as the mobile phase, running under isocratic conditions at 0.4 ml/min for 20 minutes, to separate neutral sugars, then under gradient

conditions up to 20% of 0.5 M NaOH / 0.5 M sodium acetate over 25 minutes, for detection of galacturonic acid (Currie and Perry 2006). Corrections were made for hydrolysis losses (Garna *et al*. 2006). Lignin was determined using a standard acetyl bromide assay (Sluiter *et al*. 2008). Protein was estimated from a determination of elemental nitrogen, with a multiplication factor of 6.25. Sugar monomer concentrations in liquor fractions produced following enzyme digestion were also analysed directly by HPAEC-PAD.

Enzyme digestions for kinetic studies

Small scale digestions were carried out using 25 ml of haulm pulp blends in 50 ml plastic falcon tubes, formulated at 3.2% insoluble solids content, including approximately 0.1 M sodium citrate buffer adjusted to pH5. The tubes were dosed with the appropriate amounts of enzyme, sealed and shaken horizontally at 150 rpm in an orbital incubator at 50^{o}C, which were then removed at appropriate time intervals up to 24 hours, followed by rapid chilling to halt the enzyme reactions. The tubes containing the digestates were centrifuged and aliquots of the supernatant liquors were separated and frozen in preparation for analysis of liberated sugars. The remainder of the samples were vacuum filtered through Whatman No 1 paper, with repeated washing with chilled water, before drying at ambient temperature. The solubilisation of material resulting from digestion was determined by calculation of weight loss, taking into account ambient moisture contents. Appropriate control samples were also prepared and analysed.

Bulk flow properties digestates

A single digestion was carried out using a thermostat controlled kitchen mixer (Thermomix Inc.). Volumes of 1000 ml of pulp or stalk blends were formulated at 5% total solids content with a concentration of 0.1 M citrate buffer at pH 5. The suspensions were mixed at 200 rpm, equilibrated at 50^{o}C, before dosing with 1% Depol 692 enzyme concentrate on weight of solid, with 50 ml samples taken out at 6 time intervals up to 180 minutes for the haulm pulp and 60 minutes for the broccoli stalks. The samples were immediately transferred for measurement of bulk flow characteristics, as described below, and then retrieved and chilled, then vacuum filtered and washed, then dried and weighed to determine the relative solubilisation of material, as described above.

The bulk flow properties of the haulm pulp and broccoli stalk digestates taken from the Thermomix were measured using a Bostwick consistometer (www.camlab.co.uk). Portions of 50 ml of the suspensions were sampled after different digestion time periods, which were transferred into the end reservoir of the device. The spring loaded gate was opened and the material allowed to flow along the trough, with measurement of the distance reached at 30 seconds. For some samples two distance measurements were taken, where a liquor (serum) separated from the suspension which flowed for a greater distance than the remaining mass (residue).

Viscosity measurements during enzyme digestion

The viscosities of haulm pulp and broccoli stalk blends were measured during enzyme digestion using a Rapid Visco Analyser device (RVA) (Newport Instruments Inc.). This consisted of a thermostatted sample pot,

stirred using a twin bladed propeller, where the circulation created by the stirrer enables measurement of liquors containing solid particles, which would potentially settle or migrate using more conventional rheometer geometries. Haulm and stalk blends were initially formulated at 5 wt% solids content in 0.1 M citrate buffer at pH 5, as described above, with further dilutions to between 3 and 3.5 wt% to give an initial experimental viscosity in the range 3000-7000 cP. An initial 10 minute mixing period was programmed for temperature stabilisation at 50^{o}C, after which an aliquot of enzyme concentrate was added and the run was commenced. Data was collected every four seconds, up to 360 minutes. Experiments were carried out with different enzymes and differing doses, also with controls with no enzyme addition. A further experiment was carried out where the viscosities of haulm pulp suspensions were determined at different solids contents without enzyme addition, by averaging of RVA datapoints over a 10 minute period, at 50^{o}C.

Microscopy and Image analysis

Samples of haulm-pulp digestates were diluted by quantitative water addition which were imaged under macro conditions using back-illumination through clear petri dishes. The lengths of visible particles were measured using tools within Image-J software (NIH open access, https://imagej.nih.gov/ij/). Approximately 100 particles from each dispersion were counted using a systematic grid, to provide both average particle length and also length distributions. Micro observation of selected dispersions was carried out under transmitted light conditions using a conventional compound microscope.

Results and Discussion

Bulk Flow behaviour

Both broccoli stalk and haulm pulp blends initially showed separate flow behaviour of an exuded liquor phase and a liquor entrained particulate phase through the Bostwick Consistometer, from figure 1a, with flow of both components travelling further as digestion time increased. Ultimately a single phase was observed at longer digestion times, where the reduction in particle size due to digestion allowed full entrainment of the liquor and particulate material. The haulm pulp blend exhibited much slower flow compared to the broccoli, due to its fibrous texture as discussed later, where flow was only moderately enhanced even at extended digestion times. Only around 15% of the haulm pulp was solubilised by the Depol 692 enzyme, after 3 hours digestion, from figure 1b, despite the broad range hydrolytic activity of the enzyme product for cell wall polysaccharides. The compositional data for haulm pulp and broccoli stalks are summarised in table 1, with basic anatomical data also summarised for the haulm pulp. As can be seen, the glucose content of the haulm pulp is relatively high, mainly derived from cellulose, with most starch in the haulm material previously removed into the juice fraction (Torcello-Gómez *et al*. 2018). The high xylose content of the haulm pulp is due to the presence of hemicellulose biopolymers, which are associated with cellulose in the cell wall (Talbot and Ray 1992). Also a significant proportion of lignin is seen in the pulp, indicating the presence of secondary cell wall structures as expected in vascular and other sclerenchyma tissues, which is an indication of greater recalcitrance towards enzyme digestion and lower nutritional accessibility (Hatfield *et al*. 1999). In contrast figure 1b reveals that over 50% of the broccoli-stalk blend was solubilised after only 1 hour digestion using the

Depol 692 product. This is consistent with the higher pectin content of this material, indicated from the presence of galacturonic acid, together with the higher proportions of arabinose and galactose, which contribute to the side branches along the pectin chain (Houben *et al*. 2011). Also the lower lignin content in broccoli stalks indicates lower extent of secondary cell wall structures and lower overall recalcitrance (Müller *et al*. 1993).

Figure 1

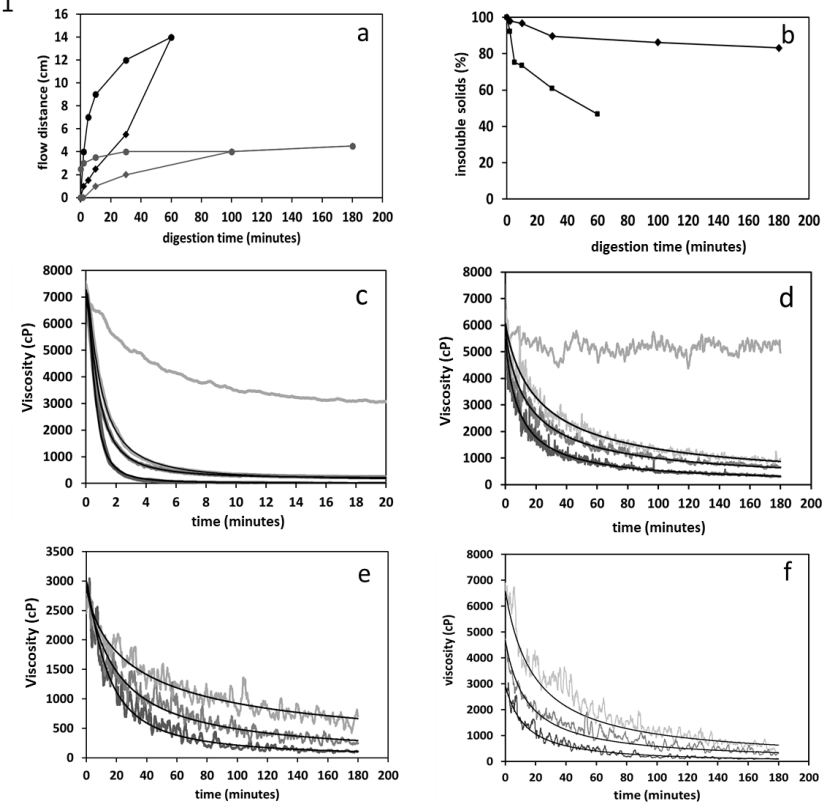


Figure 1 a: Bostwick flow distance of agri-residues digested at 5% initial solids content using Depol 692 enzyme at 1 wt%-solids dose, measured at time intervals; broccoli stalks, exuded liquor phase (⧫), broccoli stalks entrained particulate phase (●); pea haulm pulp, exuded liquor phase (⧫), pea haulm pulp, entrained particulate phase (●). b: Insoluble solids content of agri-residues digested at 5% initial solids content using 1wt%-solids Depol 692 enzyme, measured at time intervals; broccoli stalks (■); haulm pulp (⧫). c: Real-time RVA viscosity of broccoli stalks digested with Depol 692 enzyme at 0.25 wt%-solid (—), 0.5% (—), 1% (—), upper curve with no enzyme, smooth lines fit to equation (8). d: Real-time RVA viscosity of pea haulm pulp dosed with Depol 692 at 0.25 wt%-solid (—), 0.5% (—), 1% (—), upper curve with now enzyme, smoothed lines fit to equation (8) e: Real-time RVA viscosity of haulm pulp dosed with Cellic CTec-2 at 1 wt%-solid (—), 1.25% (—), 2.5% (—), smooth lines fit to equation (8). f: RVA profiles for pea-haulm pulp digested using 2.5 wt% CTec-2, with blends made up to solids contents giving initial viscosities of 7000 cP (—), 4500 cP (—), 3000 cP (—).

Table 1 composition of broccoli-stem and haulm-pulp agri-residue materials, and also haulm pulp solid residue recovered following 48 hours digestion at 2.5 wt% Cellic CT-2 enzyme.

component	broccoli stem (g/100g)	haulm pulp (g/100g)	haulm pulp post digest residue (g/100g)
glucose	21.4 ± 1.4*	34.5 ± 0.81	32.6 ± 1.2
xylose	1.9 ± 0.24	16.2 ± 0.32	16.9 ± 0.36
arabinose	8.0 ± 0.37	2.0 ± 0.05	1.2 ± 0.15
galactose	4.6 ± 0.04	1.9 ± 0.06	1.0 ± 0.07
galacturonic acid	20.7 ± 2.5	17.4 ± 2.1	16.7 ± 1.4
lignin	6.0 ± 0.33	14.7 ± 1.0	19.6 ± 0.91
protein (Nx6.25)	2.9 ± 0.07	12.5 ± 0.52	10.2 ± 1.2
anatomical structure		%-total	
stem		38 (38)#	
tendrils and petioles		16 (15)	
leaf		17 (16)	
pod		29 (31)	

* errors based on duplicate measurements. # values in brackets are on dry basis

Real-time viscosity behaviour

The measurement of the viscosities of broccoli and haulm-pulp by the Rapid Visco Analyser (RVA) technique enabled a comparison of the efficacies of the selected enzyme products under realistic real-time processing conditions. Examples of viscosity vs. time profiles measured by RVA are shown in figure 1c-f, with data overlaid in each graph for different enzyme doses. The reaction half-lives and also normalised viscosities at 3 hours digestion time are summarised in table 2. For both broccoli stalks and haulm pulp the rate of viscosity reduction increased with increasing amount of enzyme, implying that under these dosage conditions the active sites on the substrate were initially unsaturated, so additional enzyme resulted in a greater contribution of reacting material. The data revealed that for the same

Depol 692 and Cellulase 13L doses, broccoli was far more easily digested than haulm pulp, especially noting the x10 shorter time axis for broccoli stalks in figure 1c, compared to haulm pulp in figure 1d. Additionally some reduction in viscosity for the broccoli occurred without enzyme addition, suggesting an extent of natural enzyme action. Negligible viscosity reduction was observed for the haulm pulp without enzyme, consistent with the recalcitrance of this material. The RVA time profile for haulm pulp digested using the alternative Cellic CTec-2 product is shown in figure 1e, where although the overall reaction time was still much longer than for broccoli, a significant increase in rate and extent of digestibility was observed with increasing enzyme dosage, in table 2. This suggests that an enzyme cocktail optimised for digestion of lignocellulosic structures may be helpful for processing of this fibrous agricultural residue.

Table 2 Kinetics of viscosity reduction of blends of agricultural residues due to enzyme digestion as determined by real-time RVA measurements

	enzyme	dosage	time for half viscosity ($t_{1/2}$)	viscosity at 180 min	fitted parameters from kinetic model (equation 7)		
		(wt% on solid)	(min)	(% of initial)	D (g/g.min)	n	R^2
broccoli stalks	Depol 692	0.25	1.0	2.2	1500	1.45	0.98
		0.5	0.8	2.2	1667	1.6	0.99
		1	0.6	<0.1	3400	2.0	0.92
	Cellulase 13L	1	1.6	2.2	5.4	0.88	0.99
		2.5	1.5	0.5	16.3	1.11	0.99
		5	1.2	0.1	23.5	1.25	0.99
haulm pulp	Depol 692	0.25	25.0	15	1.5	0.88	0.95
		0.5	20.1	11	1.45	0.90	0.97
		1	9.7	5.2	1.87	0.92	0.99
	Cellulase 13L	1	17.0	19	0.002	0.55	0.96
		2.5	14.7	13	0.008	0.62	0.97
		5	12.8	11	0.023	0.72	0.99
	Cellic CTec-2	0.5	43.8	24	7.3	0.76	0.92
		1.25	20.4	10	62	1.0	0.94
		2.5	13.3	3.5	70	1.0	0.96

Enzyme digestion kinetics

The kinetics of enzyme digestion of biomass and crop residues have been reported extensively in relation to production of biofuels (Pihlajaniemi *et al*. 2016). For systems where enzyme accessibility is limited and where a high degree of conversion is desired it has been useful to apply models which account for the reducing amount of reactant over time and which incorporate parameters for diffusivity constraints through the material matrix. The model developed by Chastril has been successfully used by previous workers (Chrastril 1988; Carillo *et al*. 2005), according to equation (1), where P_t and are the P_∞ are the yields from enzyme digestion at time t and at infinite time, D is a rate constant including both reaction and physical/diffusional contributions, with units of 1/time x concentration, E is the enzyme concentration, n is dimensionless a parameter describing the structural diffusional constraint.

$$P_t = P_\infty(1 - e^{-EDt})^n \quad (1)$$

This model was used to describe the solubilisation of haulm pulp over time, at the three dosage concentrations of Cellic-CT2 enzyme used in the RVA experiments, where the extent of reaction was determined from the total solubilised mass and also from the concentration of liberated glucose. The overlayed experimental curves are shown in figure 2a and 2b, with the model data displayed as continuous lines, with the fitted model parameters summarised in table 3. Fitting was carried out using the Solver™ tool in Excel™ (Microsoft Inc.), by non-linear minimisation of the sum of errors

between experimental and model data, with the parameter for enzyme concentration as a known input.

Table 3 Modelled kinetic parameters for digestion of haulm pulp using Cellic CTec-2 enzyme, from equation (1)

dosage	From total solubilisation				from glucose liberation			
E	P_∞	D	n	R^2	P_∞	D	n	R^2
(wt%-substrate)	(%-total mass)	(g/g·min)			(%-total mass)	(g/g·min)		
0.5	14	1.12	0.6	0.96	11	0.051	0.35	0.98
1.25	21	0.32	0.6	0.98	14	0.012	0.25	0.99
2.5	33	0.128	0.5	0.98	18.5	0.0017	0.18	0.97

The model analysis revealed that the final amount of solubilised material from the haulm pulp (P_∞) increased significantly with increased enzyme dosage, from table 3, although this only reached a value of 33% of the total mass at the highest dose of 2.5 wt%-substrate. The liberation of glucose accounted only for a proportion of solubilisation, up to 18% of the total mass, with a greater proportion of other material solubilised at higher overall digestion. By inference from the sugar analysis of digestate residues, from table 1, this included both hemicellulose and pectin components, which would be liberated as a result of the overall deconstruction of the cell wall structure. The modelled rate constant D for the mass-loss data actually reduced with increasing enzyme dose, so at a low dose although the digestibility limit was lower, as indicated by P_∞, this limit was reached more quickly so the enzyme activity was apparently higher. At a higher enzyme dose a greater amount of substrate was digested, although this asymptote was reached over a longer time, so apparently the enzyme activity was lower. These findings suggest that at low dosage adsorption of the available enzyme may only take place on near-surface sites within the tissue substrate, accessed with low diffusional resistance. At higher dosage adsorption of the

available enzyme may extend to more inner sites, which would be accessed by more tortuous routes, representing greater diffusional resistance. The overall diffusional characteristics of the substrate were also indicated from the fitted parameter n, where for this haulm-pulp material n = 0.5-0.6, representing a structure with high diffusional resistance, where n = 1 for low resistance geometries (Chrastil 1988). The model parameters determined from the concentration of liberated glucose revealed a similar trend in diffusional rate constant (D), but with lower geometrical parameter n=0.2-0.35, indicating even higher diffusional constraint. This may be an indication of the inaccessibility of the cellulose fibrils within the cell wall, which are embedded the hemicellulose and lignin composite matrix.

Figure 2

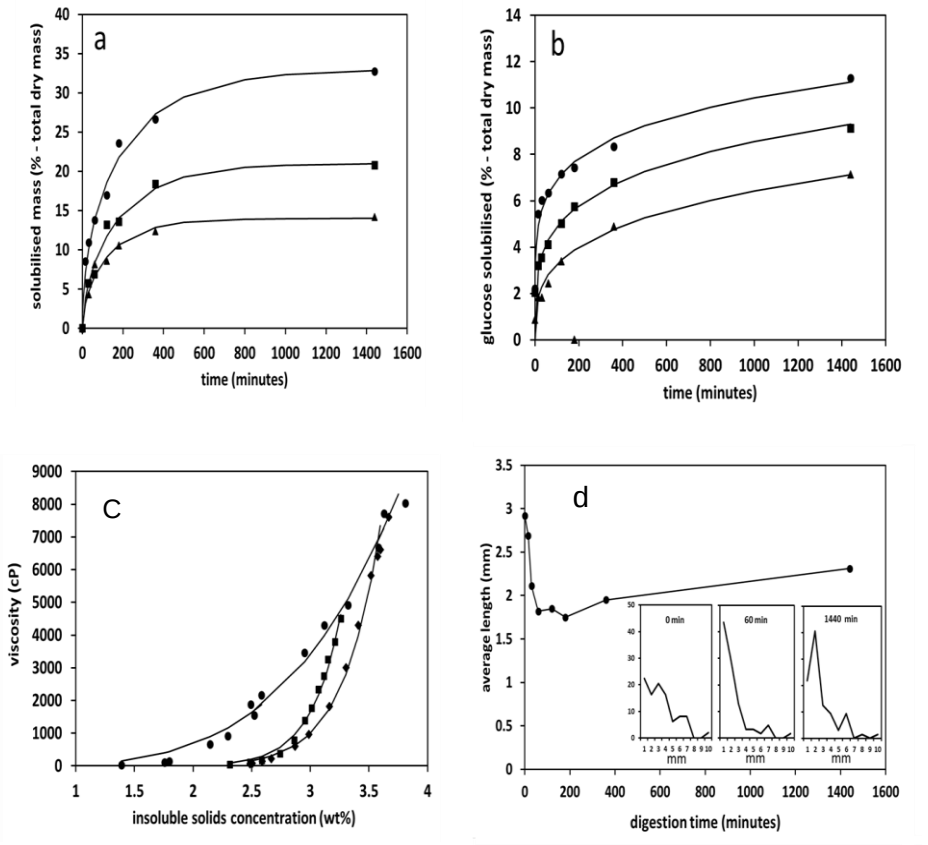


Figure 2 a: total mass solubilised following digestion of pea haulm pulp using Cellic CTec-2, 0.5 wt%-solid (▲), 1.25% (■), 2.5% (●). b: glucose solubilised following digestion of pea haulm pulp using Cellic CTec-2, 0.5 wt%-solid (▲), 1.25% (■), 2.5% (●). c: Relationship between RVA viscosity and insoluble solids concentration of pea haulm pulp mixtures; Physical blends without enzyme (●), Blend undergoing digestion with 2.5 wt% CTec-2 enzyme, with initial viscosity of 4500 cP (■), and 7000 cP (♦). d: dimensions of particles of pea haulm-pulp blends digested using 2.5 wt%-solid CTec-2. Length average particle length (●). Inserts are length distributions at different digestion times of 0, 60 and 1440 minutes.

Correlation of digestibility with viscosity

The overall digestibility kinetics appear consistent with the RVA-viscosity profiles of the haulm-pulp blends in figure 1, where the breakdown of particulate material resulting from digestion leads to a decrease in the resistance to shear-flow. Concentration of insoluble solids (or consistency) and fibre length are key properties of wood and plant fibre suspensions,

where both empirical and fundamental approaches have been applied to understand relationships with viscosity and flow (Derakhshandeh *et al*. 2011; Tatsumi *et al*. 2002). The crowding number (N) is a useful concept, which defines the number of fibres present in the volume swept out by the length of a fibre, according to equation (2), where C_v is the volume proportion of fibres in the suspension, including water of swelling, L is the length average fibre length, and d is the fibre diameter (Kerekes 2006). From this it is apparent that a greater crowding number leads to greater potential for fibre-fibre contact and a higher resistance to shear and flow in a suspension. This provides a starting point for appreciating the influence of enzyme digestion on texture and flow of blends of fibrous vegetable materials, where breakdown and solubilisation of tissue structure will reduce both volume proportion and also will reduce particle dimensions.

$$N = \frac{2}{3} C_v \left(\frac{L}{d}\right)^2 \quad (2)$$

By combining results using the same time basis it is possible to correlate the change in RVA measured viscosity during digestion with the extent of solubilisation of the haulm-pulp material. Two composite datasets are shown in figure 2c, for digestion with a dose of 2.5 wt%-substrate of Cellic CTec-2 enzyme with two starting concentrations of insoluble solids, made up at 3.3 and 3.7 wt%, which gave respective initial viscosities of approximately 4500 and 7000 cP. The curves show a steep fall in viscosity as material is digested and the solids concentration is reduced, where both curves could be extrapolated to the x-axis at a solids concentration in the blend of around 2.4 wt%. This represents the move towards a dilute regime, where N≤1 and

according to theory particle-particle interactions are by chance. Reworking equation (2), for N=1, with an estimation of C_v, then the axial ratio of the particles (L/d) at a consistency of 2.4 wt% would be around 6.6. In contrast, a further dataset is displayed in figure 2c, where the viscosities of blends of the haulm-fibre were been measured at different insoluble solids concentrations with no added enzyme. The resulting curve intersects with initial values for the two curves with digesting enzyme, but shows a more gradual decline, tending the x-axis at around 1.5 wt%, which corresponds to a higher fibre axial ratio around 8.5, from equation (2). This analysis suggests that the more rapid fall in viscosity under enzyme digestion conditions is due to a reduction in average fibre length due particle breakup rather than simply a reduction in solids content, where both factors contribute to the overall rheological characteristics of the blend.

Material basis for viscosity and texture

Cellulase and other polysaccharide digesting enzymes have large molecular dimensions and therefore tend to preferentially act at particle surfaces and the more accessible defects and void spaces within plant tissue structures (Zhu *et al*. 2008). Digestion may therefore lead to mechanically weakened points within the tissue, which provides a mechanism for breakup of longer fibres due to flexing during agitation, reducing the crowding number without significantly reducing the total insoluble solids. This inference is partly supported by fibre length measurements from microscopy. Overall, the haulm pulp consists of a wide range of sizes and shapes of particles, from figure 3a, but with a predominance of high aspect ratio fibres, originating from the vascular tissues of the stem and tendrils. By microscopy the

average axial ratio (L/d) for the initial pulp particles was estimated at around 15, so from equation (2) this gives an alternative estimation of starting crowding number for a consistency of 3.7 g/g of around N=8, which is a regime where forced particle-particle collisions occur (Kerekes 2006). As described, in the absence of digestion the measured viscosity tends to the x-axis at a consistency of 1.5 wt%, which for L/d = 15 corresponds to a crowding number N=2.1, which again implies a move towards the dilute regime. Following the previous arguments, in the presence of Cellic CTec-2 enzyme this apparent dilute state is reached at a higher insoluble solids content of 2.4 wt%, where for same crowding number N=2.1, it would be predicted from equation (2) that the axial ratio (L/d) would be reduced from 15 to around 9.6, due to particle breakup. This is consistent with the graphical microscopy data in figure 2d, which shows an initial fall in average fibre length in the early stages of digestion of the pulp with CTec-2 enzyme, also indicated from the fibre length distributions. However, at longer digestion times the average length appears to increase slightly, where the distribution at 1440 minutes digestion time suggests a complete dissolution of some of the very smallest particles, increasing the overall average. The images in figure 3b-e confirm that a proportion of fibrous material is retained even at these long digestion times. The net effect on viscosity is therefore a complex combination of both solids content and length factors.

Figure 3

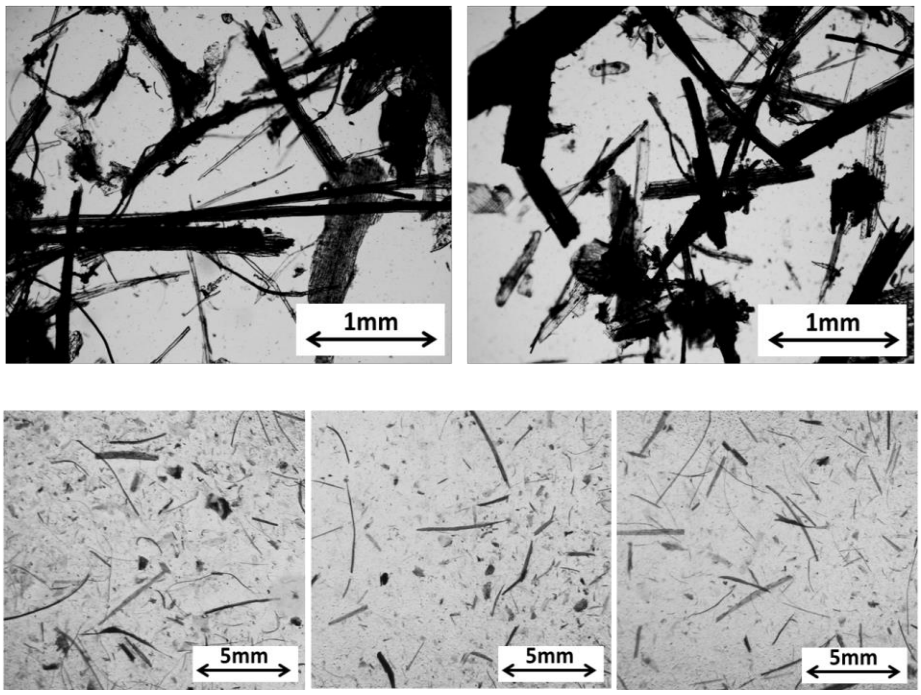


Figure 3 Images of particles in pea haulm pulp blends digested using 2.5 wt%-solid CTec-2; using macro camera configuration, a: before digestion, b: after 1440 minutes; using transmitted light microscopy configuration, c: before digestion, d: after 60 minutes, e: after 1440 minutes.

As a further approach to describe the characteristics of fibre suspensions, various studies have suggested versions of an empirical power law to describe the relationship between yield stress or viscosity (η) and the parameters of fibre aspect ratio (R) and insoluble solids concentration (Cn). This generic relation is shown in equation (3), where A, b and y are empirical parameters (Tatsumi *et al*. 2002; Derakhshandeh *et al*. 2011). Applying this equation to the experimental dataset in figure 2c in the absence of digesting enzyme (constant R), a fit was achieved with AR^b=42 and y=4.1. Other workers have found a power law relation around y=3 for wood pulp fibres (Derakhshandeh *et al*. 2011). In the presence of digesting enzyme R will be dependent on Cn, so an approach would be to modify equation (3) to give a

new equation (4), where R_i is now the initial average fibre aspect ratio, where the exponent (b.Cn) will change as Cn is reduced. Good fits were obtained for both digestion curves in figure 5 with R_i=15 and y=4, where for the initial viscosity of 7000 cP, A=0.020 and b=0.79 and for the initial viscosity of 4500 cP, A=0.006 and b=1.0.

$$\eta = A.R^{b}.Cn^{y} \quad (3)$$

$$\eta = A.R_i^{(b.Cn)}.Cn^{y} \quad (4)$$

Enzyme digestion kinetics from viscosity profiles

The viscosity reduction due to the breakup of fibres on the microscopic scale might be considered analogous to the scission of polymer chains on a molecular scale. For cellulose hydrolysis an equation has been derived for the extent of reaction (P_t) involving random bond scissions, according to equation (5), where M_o is the length of the macromolecular chain at time zero and M_t is the length of the chain at reaction time t (Ekenstam 1936; Emsley and Heywood 1997). By analogy, for fibres on a microscopic scale then M is replaced by the fibre length L, so equation (6) can be used to model the enzyme kinetics relating to fibre breakup. Furthermore, the fitting of the digestion profiles using equation (4) suggests that for a unitary value for Cn the viscosity may be simply proportional to fibre aspect ratio (if b=1), where some evidence for this relationship is also found for wood fibres that in a

suspension (Silveira *et al*. 2002). In this case M can be further replaced with viscosity (η), so the adaptation of equation (6) in combination with the earlier enzyme kinetic equation (1) gives equation (7), which can be used to model the experimental viscosity profiles from the RVA experiments, where other parameters are defined as before.

$$P_t = \frac{1}{M_0} - \frac{1}{M_t} \quad (5)$$

$$\left(P_t = \frac{1}{L_0} - \frac{1}{L_t}\right) \quad (6)$$

$$\eta_t = \frac{1}{(1-e^{-EDt})^n - \frac{1}{\eta_0}} \quad (7)$$

Values of D and n were determined from the fitting of equation (7) to the experimental data using Microsoft Excel™ and Solver™, summarised in table 2, with the fitted curves superimposed as continuous lines over the experimental RVA profiles in figure 1. The model has obvious limitations in that it only describes viscosity changes due to reduction in fibre length, ignoring reduction of insoluble solids through solubilisation. For the broccoli stalk data this is clearly inappropriate, as a large amount of the plant material is solubilised over the course of the 3 hour RVA digestion. The model may be more realistic for the haulm pulp data, where solubilisation is less efficient, especially over shorter timescales up to 60 minutes, from figure 2a. From the fitting exercise the diffusion-structural parameter (n) is mostly less than

1 for the haulm-pulp profiles, from table 3, which indicates some diffusional resistance to the reaction, although the values are higher than determined directly from the solubilisation kinetics, from table 3. This could be an indication of a tendency towards a sequential process, where the molecular scale disruption of the polysaccharide structure due to enzyme hydrolysis is followed by the eventual micro-scale fracture of tissue particles and the reduction of fibre length. However, the high diffusional structural parameters determined for broccoli stalk again suggest that this model is inappropriate for materials undergoing extensive solubilisation, and where particles are not fibrous in nature.

The diffusional kinetic parameter (D) for the haulm pulp increases with increasing enzyme dosage, which is contrary to the data from the solubilisation kinetics, where overall accessibility is believed to be reduced as the enzyme seeks inner reactive sites. Possibly the microscale fracture of fibre particles is enhanced as the hydrolysis reaction extends to inner reactive sites, so that the loss of fibre length correlates more directly with the amount of enzyme applied.

Potential and limitations of enzyme digestion

The results have demonstrated that lignin containing green crop residues such a haulm pulp can be partially digested by application of mixed hydrolysing enzymes. A proportion of cellulase activity appears to be helpful in deconstructing the lignocellulosic cell wall structures, with the Cellic CTec-2 product demonstrating the ability to solubilise cellulose derived glucan from the cell wall, as well as other cell wall polysaccharides. However, a

wider range of trials would be required to select a fully optimal enzyme cocktail and dosing regime, which is beyond the scope of this paper. However, from this work it would be expected that even for an optimal product the solubilisation of materials such as haulm pulp would be limited in extent and also slow to develop, requiring a digestion time of at least several hours. A positive finding is that enzyme digestion can lead to a useful reduction in the measured viscosity of suspensions, due to the break-up of high aspect ratio particles and the consequent reduction of particle-particle interactions. However, the limited digestion means that a significant proportion of solid particles will be retained in suspension, with dimensions similar to the starting material, so it is unlikely that enzyme digestion alone would lead to an acceptable food or drink product such as a smoothie or soup. Furthermore, for constant dosing and digestion times the final viscosity of digestates and hence the concentration of residual particles is likely to be raised in line with the initial concentration of the suspension, as shown in figure 1f. This will further limit the range of concentrations and other processing conditions for an acceptable sensory texture. Supplementary mechanical processing may be required to alleviate such issues, where further work might investigate the benefit of simultaneous enzyme digestion during wet-milling treatments.

Enzyme treatment of haulm pulp may be beneficial as a technique for enhancement of nutritional accessibility for feed applications, possibly augmenting an ensiling activity, where textural issues are not as significant and where partial digestion might usefully increase bio-accessibility. The liberation of additional glucan and other sugars would also enhance primary juice yields if an enzyme digestion treatment was applied to the whole haulm

material. Following digestion it is assumed that the most recalcitrant fibrous particles would remain as a solid residue, where the compositional data for the residue following 48 hours digestion in table 1 indicates an increased lignin content, suggesting a greater proportion of lignified secondary cell wall material. The fibres in such a final residue might have useful mechanical strength and dimensions for materials applications, such as paper and packaging.

Conclusions

In this study a fibrous pea haulm pulp material was shown to be partially digestible using polysaccharide hydrolysing enzymes with inclusion of a proportion of cellulase activity. A useful reduction in the measured viscosity of suspensions was achieved, measured in real time, due in some extent to the break-up of high aspect ratio particles and the consequent reduction of particle-particle interactions. Models for understanding of this phenomenon were explored which may be helpful in developing protocols both for in increasing fluid flow for processing and for the improvement of sensory texture. However, the limited digestion of the haulm pulp meant that a significant proportion of solid particles were retained in suspension, with dimensions similar to the starting material, so further mechanical or other processing would be required to produce an acceptable food or drink ingredient. The liberation of additional glucan and other sugars would be likely to enhance primary juice yields if an enzyme digestion treatment was applied to the whole haulm material prior to pressing. Enzyme digestion of haulm pulp may also be useful for enhancement of nutritional value for ruminant or other feed applications. Following digestion it was found that

more highly lignified fibrous particles remained as a solid residue, which alternatively might have useful dimensions and mechanical properties for materials applications.

References

Aletor, O., Oshodi, A., Ipinmoroti., K., (2002). Chemical composition of common leafy vegetables and functional properties of their leaf protein concentrates. Food Chemistry, 78, 63–68

Anandan, S., Zoltanb, H., Khana, A., Ravia, D., Blümmel, M., (2012). Feeding value of sweet sorghum bagasse and leaf residues after juice extraction for bio-ethanol production fed to sheep as complete rations in diverse physical forms. Animal Feed Science and Technology, 175, 131–136.

Anal, K., A., (ed) (2017) Food Processing By-Products and their Utilization. John Wiley and Sons Ltd, Online ISBN:9781118432921, DOI:10.1002/9781118432921

Carrillo, F., Lis, M.J., Colom, X., Lopez-Mesas, M., Valldeperas, J., 2005. Effect of alkali pretreatment on cellulase hydrolysis of wheat straw: Kinetic study. Process Biochemistry, 40, 3360–3364.

Chrastil, J., (1988) Enzymic produc formation curves with the normal or diffusion limited reaction mechanism and in the presence of substrate inhibitors. International Journal of Biochemistry, 20(7), 683-693.

Currie, H., Perry. H., (2006). Resolution of complex monosaccharide mixtures from plant cell wall isolates by high pH anion exchange chromatography. Journal of Chromatography A, 1128, 90–96.

Derakhshandeh, B., Kerekes, R., Hatzikiriakos, S., Bennington, C., (2011). Rheology of pulp fibre suspensions: A critical review. Chemical Engineering Science, 66, 3460–3470.

Ekenstam, A. (1936) The behaviour of cellulose in mineral acid solutions: Kinetic study of the decomposition of cellulose in acid solutions. Berichte 69, 553.

Elleuch, M., Bedigian, D., Roiseux, O, Besbes, S., Blecker, C., Attia, H. (2011) Dietary fibre and fibre-rich by-products of food processing: Characterisation, technological functionality and commercial applications: A review. Food Chemistry, 124, 411–421.

Emsley, A., Heywood, R., (1997) On the kinetics of degradation of cellulose. Cellulose, 4, 1–5

Galanakis, C. M., (2012). Recovery of high added-value components from food wastes: Conventional, emerging technologies and commercialized applications. Trends in Food Science & Technology, 26, 68-87.

Garna, H., Mabon, N., Nott, K., Wathelet, B., Paquot, M., (2006). Kinetic of the hydrolysis of pectin galacturonic acid chains and quantification by ionic chromatography. Food Chemistry, 96, 477–484.

Gurmessa K., Tolemariam, T., Tolera, A., Beyene, F., (2016) Production and Utilization of Crop Residues in Horro and Guduru Districts, Western Ethiopia. Food Science and Quality Management, 48, 77-84.

Hatfield, R., Ralph, J., Grabber, J., (1999). Cell wall structural foundations: Molecular basis for improving forage digestabilities. Crop Science 39(1), 27-37.

Henriksen, T., Breland, T., (1999). Evaluation of criteria for describing crop residue degradability in

a model of carbon and nitrogen turnover in soil. Soil Biology and Biochemistry, 31, 1135-1149.

Houben, K., Jolie, R., Fraeye, I., Van Loey, A., Hendrickx M., (2011). Comparative study of the cell wall composition of broccoli, carrot, and tomato: Structural characterization of the extractable pectins

and hemicelluloses. Carbohydrate Research, 346, 1105–1111.

Ibbett, R., Gaddipati, S., Greetham, D., Hill, S., Tucker, G., (2014). The kinetics of inhibitor production resulting from hydrothermal deconstruction of wheat straw studied using a pressurised microwave reactor. Biotechnology for Biofuels, 7, 45-58

Kerekes, R., (2006) Rheology of fibre suspensions in papermaking: An overview of recent research. Nordic Pulp and Paper Research Journal, 21(5), 100-114.

McKee, L., Latner T., (2000). Underutilized sources of dietary fiber: A review. Plant Foods for Human Nutrition, 55, 285–304.

Morrison J., Pirie, N., (1961). The large-scale production of protein from leaf extracts. Journal of the Sciences of Food and Agriculture, 12, 1-6

Müller, S., Jardine, W., Evans ,B., Viëtor, R., Snape, C., Jarvis, M., (1999). Cell wall composition of vascular and parenchyma tissues in broccoli stems. Journal of the Science of Food and Agriculture, 83, 1289–129.

Nagodawithana, T., Reed, G., (eds.) (1993) Enzymes in Food Processing 3rd Edition, Academic Press Inc. San Diego, USA.

Pihlajaniemi, V., Sipponen, M., Kallioinen, A., Nyyssölä, A., Laakso, S., Rate-constraining changes in surface properties, porosity and hydrolysis kinetics of lignocellulose in the course of enzymatic saccharification. Biotechnology for Biofuels, 9:18-30.

Rodrigues, A., Haven, M., Lindedam, J., Felby, C., Gama, M., (2015). Celluclast and Cellic®CTec2: Saccharification/fermentation of wheatstraw, solid–liquid partition and potential of enzyme recycling byalkaline washing. Enzyme and Microbial Technology, 79, 70–77.

Silveira, M., Ferreira, A., Lobo, L., (2002). The Viscosity of Aqueous Suspensions of Cellulose Fibers Part 1. Influence of Consistency and Fiber Length. Silva Lusitana, 10(2), 171 – 178.

Sluiter, A., Hames, B., Ruiz, R., Scarlata, C., Sluiter, J., Templeton, D., Crocker D., (2008). Determination of Structural Carbohydrates and Lignin in Biomass. Technical Report NREL/TP-510-42618.Issue Date: 4/25/2008

Talbott, L., Ray, P., (1992). Molecular Size and Separability Features of Pea Cell Wall Polysaccharides. Plant Physiology, 98, 357-36.

Tatsumi, D., Ishioka, S., Matsumoto, T., (2002). Effect of Fiber Concentration and Axial Ratio on the Rheological Properties of Cellulose Fiber Suspensions. Journal of Society of Rheology, Japan, 30(1), 27-32.

Torcello-Gómez, A., Gedi, M., Ibbett, R., Husain, K., Briars, R., Gray, D., (2018). Chloroplast-Rich Material from The Physical Fractionation of Pea Vine (Pisum sativum) Postharvest Field Residue (Haulm). Journal of Food Chemistry. Accepted manuscript available online: 6-AUG-2018 DOI, 10.1016/ j.foodchem. 2018.08.018

Zhu, L.., O'Dwyer, J., Chang, V., Granda, C., Holtzapple, M., (2008) Structural features affecting biomass enzymatic digestibility. Bioresource Technology, 99, 3817–3828.